# Development of novel therapeutic approaches to promote the healing of chronic wounds

Zauri kronikoen orbaintzea sustatzeko baliabide terapeutiko berrien garapena

**Itxaso García Orue**

Vitoria-Gasteiz 2018

Laboratory of Pharmaceutics,

NanoBioCel Group

School of Pharmacy

University of the Basque Country (UPV/EHU)

*What if I fall?*

*Oh, but my darling, what if you fly?*

Erin Hanson

***ACKNOWLEDGEMENT FOR THE FINANCIAL SUPPORT***

*Itxaso García gratefully acknowledges the support provided by the Basque Government for the fellowship grant. This project has been funded by the Spanish Ministry of Economy and Competitiveness (INNPACTO, IPT-2012-0602-300000, 2012). In addition, it has been partially supported by the Basque Government (Consolidated Groups, IT-428-10 and IT-528-10 and ELKARTEK 2015, Nanoplatform, KK-2015/0000036).*

***ACKNOWLEDGMENT TO THE EDITORIALS***

*Authors would like to thank the editorials for granting permission to reuse their previously published articles in this thesis. The links to the final published versions are the following:*

*Garcia-Orue et al. J. Drug Deliv. Sci.Technol. 42, 2-17 (2017)*
*https://www.sciencedirect.com/science/article/pii/S177322471630627X*

*Garcia-Orue et al. Eur. J. Pharm. Biopharm. 108, 310-316 (2016)*
*https://www.sciencedirect.com/science/article/pii/S0939641116301308*

*Garcia-Orue et al. Int. J. Pharm. 523,556-566 (2017)*
*https://www.sciencedirect.com/science/article/pii/S0378517316310584*

*Garcia-Orue et al. Application of Nanobiomaterials. Nanomaterial in soft tissue engineering, Vol. 5, Ch 2, 31-55 (2016)*
*https://www.sciencedirect.com/science/article/pii/B9780323428651000027*

*The last two experimental works have been sent to the following journals:*

*Composite nanofibrous membranes of PLGA/*Aloe vera *containing lipid nanoparticles for wound dressing applications (Chapter 3) has been sent to the International Journal of Pharmaceutics.*

*Development of a gelatin/chitosan bilayer hydrofilm for wound healing (Chapter 4) has been sent to the European Journal of Pharmaceutics and Biopharmaceutics.*

***ACKNOWLEDGMENTS TO THE RESEARCH GROUPS***

*The thesis has been carried out in the NanoBioCel group of the School of Pharmacy (EHU/UPV). In addition, we would like to thank to the groups that have collaborate in this project:*

- *Department of Chemical Engineering and Pharmaceutical Technology, School of Pharmacy, Institute of Biomedical Technologies (ITB), Center for Biomedical Research of the Canary Islands (CIBICAN), University of La Laguna, Tenerife, Spain*
- *BIOMAT Research Group, Chemical and Environmental Engineering Department, Engineering College of Gipuzkoa, University of the Basque Country (UPV/EHU), Plaza de Europa 1, 20018 Donostia-San Sebastián, Spain*
- *Plastic & Reconstructive Surgery Research, Division of Musculoskeletal & Dermatological Sciences, School of Biological Sciences, University of Manchester, Manchester, UK.*

## GLOSSARY / GLOSARIOA

**ADSC:** adipose derived stem cells / gantzetik eratorritako zelula amak

**AV:** *Aloe vera* extract / *Aloe veraren* extraktua

**b-FGF:** basic fibroblast growth factor / fibroblastoen hazkuntza faktore basikoa

**CCK-8:** cell counting kit 8 / zelulak kontatzeko kit 8

**CFU:** colony forming unit / kolonia formatzaile unitatea

**CPH:** (1,6bis(pcarboxyphenoxy) hexane / (1,6-bis(p-karboxifenoxi)hexanoa

**CPTEG:** 1,6-bis(p-carboxyphenoxy)-3,6-dioxaoctane / 1,6-bis(p-karboxifenoxi)-3,6-dioxaoktanoa

**DAB:** 3,3'-Diaminobenzidine / 3.3'-diaminobenzidina

**DDS:** drug delivery system / farmakoak askatzeko sistema

**DLS:** dynamic light scattering / argi dispertsio dinamikoa

**DMEM:** Dulbeccos's modified Eagle's medium / Dulbeccok eraldatutako Eagleren ingurunea

**DMSO:** dimethyl sulfoxide / dimetil sulfoxidoa

**DSC:** differential scanning calorimetry / ekorketazko kalorimetria diferentziala

**ECM:** extracellular matrix / matrize extrazelularra

**EDTA:** ethylenediaminetetraacetic acid / azido etilendiaminotetraazetikoa

**EE:** encapsulation efficacy / kapsularatze eraginkortasuna

**EGF:** epidermal growth factor / hazkuntza faktore epidermikoa

**ELISA:** enzyme-Linked Immunosorbent assay / entzimei lotutako immunoxurgapen saiakuntza

**FCS:** foetal calf serum / zekor fetuaren seruma

**FBS:** foetal bovine serum / behi fetuen seruma

**FDA:** food and drug administration / farmako eta elikagaien administrazioa

**FGF-1:** fibrobast growth factor -1 /fibroblastoen hazkuntza faktore -1

**FTIR:** Fourier-transform infrared spectroscopy / Fourieren transformatu bidezko espek-troskopio infragorria

**GAG:** glycosaminoglycan /glukosaminoglikanoa

**GF:** growth factor / hazkuntza faktorea

**GRAS:** generally recognized as safe / orokorrean seguru bezala onartua

**H&E:** hematoxylin eosine / hematoxilina eosina

**IGF-I:** insulin like growth factor -I / intsulinaren antzeko hazkuntza faktorea -I

**LDH:** lactate deshydrogenase / laktato deshidrogenasa

**LPS:** lipopolysaccharide / lipopolisakaridoa

**MMP:** matrix metalloproteinase / matrizearen proteinasa metalikoak

**MP:** microparticle / mikropartikula

**NLC:** nanostructured lipid carriers / nanoegituratutako eramaile lipidikoak

**NP:** nanoparticle /nanopartikula

**P3HT:** poly(3-hexylthiphene / poli(3hexiltifenea)

**PBS:** phosphate buffered saline / gatz fosfato tanpoia

**PCL:** poly(ε-caprolactone) /poli(ε-kaprolaktona)

**PCNA:** proliferating cell nuclear antigen / ugaritzen daduen zelulen nukleoko antigenoa

**PDGF:** platelet derived growth factor / plaketetatik erratorritako hazkuntza faktorea

**PDI:** polydispersity index / polidispertsioaren indizea

**PEG:** polyethylene glicol / polietilenglikola

**PELA:** poly(ethylene glycol-co-lactic acid) / poli(etilenglikol-ko- azido laktikoa)

**PEtU/PDM:** poly(ether)urethane-polydimethyl-siloxane / polieter-uretano-polidimetilsiloxanoa

**PGA:** poly(glycolic acid) / azido poliglikolikoa

**PGIcNAc:** poly-N-acetyl glucosamine / poli-N-azetil glukosamina

**pHEMA:** poly-2-hydroxyethylmethacrylate / poli-2-hidroxietilmetakrilatoa

**pHPMA:** poly-2-hydroxypropylmethacrylate / poli-2hidroxipropilmetakrilatoa

**PLA:** poly(lactic acid) / azido polilaktikoa

**PLGA:** poly(lactic-co-glycolic) acid / azido poli(laktiko-ko-glikolikoa)

**PLLCL:** poly(L-lactic acid-co-ε-caprolactone) / azido poli(L-laktikoa-ko-ε-kaprolaktona)

**PPADT:** poly-(1,4-phenyleneacetone dimethylene thioketal) / poli-(1,4-fenileneazetona dimetilene tioketala

**PRP:** platelet rich plasma / plaketetan aberatsa den plasma

**PU:** polyurethane / poliuretanoa

**PVA:** polyvinyl alcohol/ alkohol polibinilikoa

**rhEGF:** recombinant human epidermal growth factor / giza hazkuntza faktore epidermal errekonbinantea

**ROS:** reactive oxygen species / oxigeno espezie erreaktiboak

**SD:** standard deviation / desbideraketa estandarra

**SDF-1α:** stromal-cell derived factor-1α / zelula estromaletatik erratorritako faktorea -1α

**SEM:** scanning electron microscope / ekorketazko mikroskopio elektronikoa

**SLN:** solid lipid nanoparticles / nanopartikula solido lipidikoak

**STZ:** streptozotocin / estreptozotozina

**TEM:** transmission electron microscope / transmisioko mikroskopio elektronikoa

**$T_g$:** glass transition temperature / beira-trantsiziozko tenperatura

**TGFβ1:** transforming growth factor β1 / hazkuntza faktore eraldatzaile β1

**TNF-α:** tumor necrosis factor α / tumoreen nekrosi faktorea α

**UV:** ultra violet / ultra morea

**VEGF:** vascular endothelial growth factor / hazkuntza faktore endotelial baskularra

**VIP:** vasoactive intestinal peptide / hesteko peptido basoaktiboa

**WVPR:** water vapour permeability rate / ur-lurrunaren iragazkortasun abiadura

**WVTR:** water vapour transmission rate / ur-lurrunaren transmisio abiadura

**α-SMA:** α smooth muscle actin / muskulu leunaren α aktina

## INDEX

# ENGLISH VERSION

# Introduction

# Nanotechnology-based delivery systems to release growth factors and other endogenous molecules for chronic wound healing

I. Garcia-Orue[a,b], J.L. Pedraz[a,b], R.M. Hernandez[a,b], M. Igartua[a,b,*]

a NanoBioCel Group, Laboratory of Pharmaceutics, School of Pharmacy, University of the Basque Country (UPV/EHU).

b Biomedical Research Networking Center in Bioengineering, Biomaterials and Nanomedicine (CIBER-BBN).

*Corresponding author: M. Igartua

## ABSTRACT

The topical administration of growth factors (GFs) and other endogenous molecules (insulin, insulin like GF-1, stromal-cell derived factor, LL37, vasoactive intestinal peptide, heparin, melatonin, lipocalin, serpin-A1 and β-stradiol) have proven to enhance chronic wound healing. However, their low stability *in vivo* makes necessary to improve their administration in terms of dose, delivery system and security. In that regard, novel drug delivery systems (DDSs) have been used to address this problem, since they are able to release drugs in a localized and controlled manner, protecting them from the proteases present in wound bed. Among them, DDSs based in nanotechnology can be highlighted such as, polymeric or lipid micro- and nanoparticles, lipid nanoparticles and nanofibrous membranes. The aim of this review is to provide an overview of nanotechonology based DDSs for the controlled release of endogenous molecules. In addition, an insight about the role of GFs in wound healing and the most common biomaterials used in DDSs are also given. Those formulations present numerous advantages, such as protection of the drug, good biocompatibility, controlled or sustained release, high drug-loading and good mechanical properties. Overall, the controlled release of GFs incorporated into nanotechnology based DDSs has demonstrated a great potential for chronic wound healing.

**Published in:** Journal of Drug Delivery Science and Technology 4(2017) 2-17, doi: https://doi.org/10.1016/j.jddst.2017.03.002

Chronic wounds are becoming a challenging clinical problem despite of being a very common pathology. In fact, in 2012 in USA approximately 6.5 million people suffered from chronic wounds, and $25 billion were spent on wound-related complications. In Europe, wound management cost an average of 6000-10000 € per patient and year, associated to nursing time, hospitalisation, dressing changes and wound infections [1,2]. Moreover, it is believed that 1-2% of the population will experience chronic wounds during their lifetime, because their incidence is growing due to the rise of high-risk population, such as, diabetic, obese, smokers or elderly people [3-5].

Current therapies cannot guarantee an effective healing, and thereby, healing time extends for large periods and recurrence is frequent. Therefore, developing a treatment able to heal the injuries effectively and in a short period of time has become a mayor need. In that regard, significant efforts have been made in the search of new treatments and in the improvement of the current ones, such as, the administration of growth factors (GFs) and other active endogenous compounds. A promising strategy to improve GF treatment is to develop new drug delivery systems (DDSs) to release GF in a local and controlled way [6].

The aim of this review is to provide a general overview of novel DDSs based in nanotechnology for the controlled release of GFs and other endogenous molecules for wound healing, specifically of polymeric micro- and nanoparticles (MP/NPs), lipid nanoparticles and nanofibrous structures. In addition, the review also gives an insight about the most common biomaterials used in DDSs.

## 1. The role of growth factors and other endogenous molecules in wound healing

Physiologically, wounds heal in an orderly and efficient manner characterised by 4 distinct but overlapping phases, comprising haemostasis, inflammation, proliferation and remodelling, as depicted in Fig. 1 [7]. This complex process needs to be tightly regulated to create a balanced molecular environment that enables healing. The regulation relies on several GFs

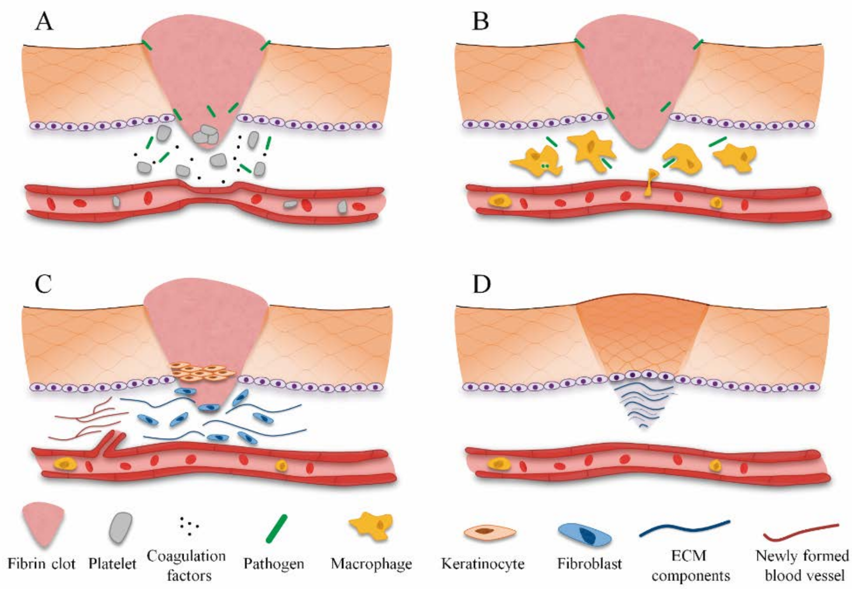


**Fig. 1.** Wound healing process. (A) Haemostasis. Right after skin injury, a short vasoconstriction occurs to prevent bleeding, and thereafter platelets are activated leading to coagulation and fibrin clot formation. (B) Inflammation. In this phase neutrophils, macrophages and lymphocytes infiltrate into the wound, with the aim of avoiding wound infection and removing damage tissue. (C) Proliferative phase. In response to chemotactic signals produced in the previous phases, fibroblasts and keratinocytes migrate to the wound bed and profusely proliferate. Moreover, fibroblasts release proteins to form a new extracellular matrix (ECM) that replaces the fibrin clot; and neo-angioenesis occurs to provide the necessary nutrients and oxygen to the wound. (D) Remodelling phase. This phase consists in the development of the new epithelium or scar tissue. For that purpose, the composition and the organisation of the provisional ECM changes to resemble that of the normal skin [1-5].

and cytokines that compose a complex signaling network that alters the growth, differentiation and metabolism of targeted cells [8,9]. The effect of GFs is executed by their binding to specific receptors which lead to the activation of a cascade of molecular events [10,11].

Nevertheless, in some cases wounds fail to progress through normal stages of healing, delaying the restoration of skin integrity and frequently relapsing, such is the case of vascular, diabetic and pressure ulcers [3,12,13]. The pathophysiology of chronic wounds exhibits some differences in comparison to normal wound healing. Their most notable characteristic the continuous inflammatory state of chronic wounds, due to an uncontrolled inflammatory positive feedback loop. Therefore, neutrophils are present during all the healing process, releasing large amounts of degradative matrix metallic proteinases (MMPs) which favor wound matrix degradation. Moreover, the proteolytic microenvironment induces the degradation of GFs, and thus their function is inhibited, altering the regulation of the process. In addition, fibroblasts present an impaired migration and a reduced ability to answer to GF stimuli, which contribute to delay healing. Finally, chronic wounds are more susceptible to infection due to the long healing periods [5,6].

A promising strategy for the treatment of chronic wounds is the exogenous administration of GFs, since their levels are decreased due to the proteolytic environment [8]. In fact, some GFs have been commercialised for wound healing applications, such as, PDGF (Regranex®), EGF (Heberprot-P, Regen-D™ and Easyef®) and bFGF (FIBLAST®) [6]. In addition, in order to mimic the physiological combination of GFs and chemokines, platelets rich plasma (PRP) has been studied for wound healing. PRP is an autologous concentration of human platelets in a small volume of plasma that contains several GFs and other biologically active proteins important for wound healing [14].

Unfortunately, due to their protein nature, GFs have a very short stability *in vivo* that leads to a frequent administration. To overcome that limitation, GFs have been incorporated in DDSs that protect them

**Table 1.** Summary of the main activities and sources of GFs and other endogenous molecules involved in wound healing**.**

| GF | Source | Activity | Ref. |
|---|---|---|---|
| FGF-1 (fibroblast GF-1) | Endothelial cells and macropaghes | Induces the release of collagenase and plasminogen activator<br>Stimulates fibroblast proliferation and differentiation<br>Promotes endothelial cell and keratinocyte migration and proliferation<br>Stimulates macrophage migration by the induction of cytokine production | [15-17] |
| b-FGF (basic fibroblast GF) | Chondrocytes, fibroblasts, endothelial cells, keratinocytes, macrophages, mast cells and smooth muscle cells | Regulates the synthesis and deposition of various extracellular matrix (ECM) components<br>Promotes fibroblasts and endothelial cell migration and proliferation<br>Increases keratinocyte migration during reepithelisation | [10,15,16] |
| EGF (epidermal GF) | Fibroblasts, macrophages and platelets | Promotes keratinocyte and fibroblast migration and proliferation<br>Stimulates the production of proteins such as fibronectin<br>Increases the expression of keratins K6 and K16, involved in the proliferative signaling phatway | [6,10,14,18] |
| VEGF (vascular endothelial GF) | Endothelial cells, fibroblasts, keratinocytes, macrophages, neutrophils, platelets and smooth muscle cells | Promotes endothelial cell migration, proliferation and differentiation (potent angiogenic factor)<br>Induces vascular permeability<br>Induces lymphangiogenesis | [6,10,16,19] |
| PDGF (platelet derived GF) | Endothelial cells, fibroblasts keratinocytes, macrophages and platelets | Is chemotactic for neutrophils, macrophages, fibroblasts and smooth muscle cells<br>Stimulates macrophages to produce and release GFs<br>Is involved in recruiting pericytes to capillaries, increasing their structural integrity<br>Enhances fibroblasts proliferation and induces the myofibroblast phenotype in them<br>Stimulates fibroblasts to produce ECM proteins and to contract collagen matrix | [8,10,11] |

| GF | **Source** | **Activity** | **Ref.** |
|---|---|---|---|
| IGF-I (insulin-like GF-I) | Fibroblasts, hepatocytes, macrophages, neutrophils and skeletal muscle cells | Increases keratinocyte migration and proliferation<br>Stimulates fibroblast proliferation | [6,8,10,11,20] |
| Insulin | Pancreatic β-cells | Stimulates keratinocyte migration, proliferation and differentiation<br>Stimulate fibroblasts proliferation and ECM proteins production<br>Modulates the release of inflammatory cytokines | [21] |
| SDF-1α (stromal-cell derived factor -1α) | Dermal fibroblasts and endothelial cells | Inhibits microvascular endothelial cell apoptosis<br>Enhances endothelial proliferation and tube formation<br>Stimulates bone marrow stem cell activation, mobilisation and retention to injury site | [11,22,23] |
| LL37 | Dendritic cells, keratinocytes, lymphocytes, macrophages, mast cells neutrophils and NK cells | Is the first defense against pathogens: antibacterial, antibiofilm, antiviral and antifungal activity<br>Is chemotactic for monocytes, neutrophils, dendritic cells, macrophages, fibroblasts and keratinocytes<br>Balances the production and release of pro- and anti-inflammatory cytokines<br>Promotes keratinocyte and endothelial progenitor cells migration and proliferation | [24] |
| VIP (vasoactive intestinal peptide) | CNS neurons, lung, and small intestine cells | Stimulates the synthesis of TGF-α<br>Promotes angiogenesis<br>Promotes fibroblasts and keratinocyte proliferation | [20,25-27] |
| Desulphated Heparin | Basophils and mast cells | Regulates the inflammatory phase by binding to pro- and anti-inflammatory agents<br>Stimulates proliferation of fibroblasts, smooth muscle cells and keratinocytes<br>Interacts with multiple GF promoting their wound healing effects | [9] |

| GF | Source | Activity | Ref. |
|---|---|---|---|
| Melatonin | Pineal gland | Releases inflammatory mediators<br>Is involved in angiogenesis and cell proliferation and migration<br>Stimulates the accumulation of collagen and glycosaminoglycans (GAGs) at the wound site | [28] |
| Lipocalin-2 | Glial cells | Promotes keratinocyte migration | [29, 30] |
| Serpin-A1 | Primarily in the liver but also in intestinal epithelial cells, macrophages, monocytes and neutrophils | Inhibits elastase activity<br>Presents potent anti-inflammatory activity | [31, 32] |
| β-stradiol | Ovary | Limits the local accumulation of granulocytes and macrophages following vascular injury<br>Endorses re-epithelisation<br>Stimulates the secretion of TGF-β1 by fibroblasts<br>Increases collagen deposition | [33, 34] |

from proteases presents in the wound bed, and the same has been done with some other endogenous molecules that regulate wound healing. In the Table 1, there are summarised the GFs and the other active molecules used in DDSs, their sources and their main wound healing activities.

## 2. Biomaterials for the development of nanotechnology based DDSs for wound healing

A wide variety of biomaterials have been used for developing novel DDSs, and all of them are expected to meet a series of characteristics, such as, good stability, biocompatibility and biodegradability, high drug-loading, good mechanical properties, controlled or sustained release and drug protection [6,35].

Polymers, either natural or synthetic, have been widely used for the development of nanofibers, micro- and nanoparticles (MP/NP) and the advantages and limitations of the most used ones are listed in Table 2. Natural polymers include alginate, gelatin, fibrin, chitosan, collagen, hyaluronic acid, etc. They have been broadly used because they have a great biocompatibility due to their similarity to macromolecules recognised by the human body. Moreover, some of them are involved in the repair of damaged tissue and have cell-binding sites and biomolecular signatures, which give an added value to their use in DDSs for wound healing [36]. Nevertheless, they show some sub-optimal characteristics, including, batch to batch differentiation, susceptibility to cross-contamination, immunogenicity, presence of immunogenic/pathogenic sections and high price. In addition, regarding the possibility of developing nanofibrous membranes, their poor mechanical properties hinder the electrospinning process and the handling of the obtained nanofibers [35].

For that purpose, synthetic polymers exhibit better mechanical properties, being more easily electrospinnable. The rest of the advantages of synthetic polymers over naturals are reliability, easily controlled physicochemical properties, lower price, well-defined structures and degradation kinetics [37]. However, they lack good cell-recognition sites and have poor affinity for cell attachment. Among the most used synthetic polymers there are polylactic acid (PLA), poly(ε-caprolactone) (PCL), polyglicolic acid (PGA) and their combinations (PLGA and PLLCL) [35,38].

An approach to improve polymers´ characteristics is to develop DDSs that include both synthetic and natural polymers, in order to obtain a formulation that can take advantage of the strengths, bioactivities and degradation rates of all the components [39].

Lipids used to develop lipid nanoparticles need to exhibit similar characteristics as polymers, namely, biocompatibility and biodegradability, controlled release, targeted drug delivery, high drug loading and drug protection. In addition, they partially fluidize skin lipids and increase drug partitioning, thereby facilitating drug transport [40]. Depending on the DDS type, different lipids are used in their development. For instance, liposomes are typically composed of phospholipids, cholesterol and an aqueous medium. Phospholipids are the major components of liposomes and they are fluid at skin temperature. Among them, natural phosphatidylcholines are the most used ones due to toxicological and price concerns. Cholesterol is added to impart rigidity to the lipid bilayer, however it can reduce the encapsulation efficiency of hydrophilic drugs and can impact negatively in the permeation through the skin [40,41]. On the other hand, solid lipid nanoparticles (SLNs) are prepared using various solid lipids, such as, mono-, di- and triglycerides, fatty acids, waxes, and steroids. Moreover, numerous surfactants are used to enhance sterical stabilisation, including phospholipids, poloxamers and polysorbates [42]. Finally, nanostructured lipid carriers (NLCs), besides of a solid lipid, contain a lipid liquid at room temperature, usually up to 30% of the content [43].

## 3. Nanotechnology-based delivery systems for wound healing

### *3.1 Polymeric micro and nanoparticles*

The encapsulation of peptides and proteins in polymeric colloidal systems has been widely used to overcome some of the

**Table 2.** Advantages and limitations of the most used polymers for the development of nanotechnology based DDSs for wound healing.

| Natural polymers | | | | | | |
|---|---|---|---|---|---|---|
| Polymer | Degradation | Mechnical prop. | Physicochemical properties | Advantages | Limitations | Ref. |
| Collagen | Enzymatic | Weak | Hydrophilic | Integrin biding sites, low antigenicity, stimulates wound healing | High cost, hard processing, chances of contamination, contraindicated in 3 degree skin burns and sensitive/allergic patients. | [35, 39] |
| Gelatin | Enzymatic | Weak | Hydrophilic | Low cost, integrin biding sites, no antigenicity, allows chemical modifications | Need fixing to prevent dissolving or congealing with temperature | [35, 44,45] |
| Fibrin | Enzymatic | Weak | Hydrophilic | Participates in wound healing as provisional matrix, involved in blood clotting | Instable, poor mechanical stiffness, hard processing | [35, 44] |
| Chitosan | Enzymatic | Weak | Hydrophilic | Non antigenic, biologically renewable, antimicrobial effects, participate in wound healing: blood clotting and granulation tissue formation | Limited supply, long processing time | [35, 39,46,47] |
| Alginate | Enzymatic | Weak | Hydrophilic | Resistance to acid, can absorb large amount of water | High cost, drug loss by leaching | [35, 39,47] |
| Silk fibroin | Enzymatic | Strong | Hydrophilic | Reduce aggregation, adhesiveness, absorption of exudates, low immunogenicity, controllable degradation rate | High cost, over hydration | [35, 39,47,48] |
| Hyaluronic acid | Enzymatic | Weak | Hydrophilic | Easily functionalised, easily controllable | High cost | [35] |

| Synthetic polymers | | | | | | |
|---|---|---|---|---|---|---|
| Polymer | Degradation | Mech-nical prop. | Physico-chemical properties | Advantages | Limitations | Ref. |
| PGA | Hydrolytic | Strong | Hydrophilic | Predictable bioabsorption | Fast degrading (2-4 weeks), sharp increases in localised pH | [35, 39,44,49] |
| PLA | Hydrolytic (Slow Rates) | Strong | Hydrophobic | Good bioresorbable, wound healing activity due to degradation products | Poor wetting, systemic or local reaction due to acidic degradation products, poor stiffness. | [35, 44] |
| PLGA | Hydrolytic | Strong | Variable | Rapid endo-lysosomal escape, high mechanical strength, wound healing activity due to degradation products compatibility with other polymers | Systemic or local reaction due to acidic degradation products, lack of cell recognition motifs | [35, 39,50] |
| PCL | Hydrolytic (Slow Rates) | Highly elastic | Hydrophobic | Relatively low cost, long term release | Systemic or local reactions, lack of cell recognition motifs | [35, 39,44,50] |
| PLLCL | Hydrolytic | Strong | Hydrophobic | Great solvent flexibility elasticity, maintained PLA ultimate tensile strength | Systemic or local reaction due to acidic degradation products, lack of cell recognition motifs | [35, 39,44,50] |
| PU | Hydrolytic | Weak | Variable | High loading capacity | Slower degradation | [35 |

issues related to the administration of proteins for wound healing. For instance, *in vivo* half-life is highly improved after encapsulation, due to the protective effect of the MPs and NPs against the proteases present in the wound bed. In addition, they provide a controlled release of the encapsulated compound, avoiding the need of frequent administration, and in some cases, allowing a reduction of the dose. That, jointly with the ability to enable a local administration, improves treatment efficacy, avoiding the secondary effects caused by high doses or systemic exposure [6,51,52]. At the end of this section, Table 3 provides a summary of the polymeric MP/NPs used for wound healing applications.

bFGF has been extensively incorporated into MPs for wound healing. For instance, in a study conducted by Liu *et al.* alginate microspheres loaded with bFGF were incorporated into a carboxymethyl chitosan-polyvinil alcohol (PVA) composite hydrogel. The resulting formulation achieved a faster wound recovery rate with higher reepithelisation and regeneration of the dermis than the hydrogel and the hydrogel loaded with free bFGF [53]. In addition, Place *et al.* developed a formulation to deliver bFGF based in polyelectrolyte complex NPs containing cationic polysaccharides (chitosan and N,N,N-trimethyl chitosan) and anionic GAGs (heparin and chondroitin sulfate). Those NPs were designed to mimic aggrecan, a proteoglycan that serves as reservoir for GFs physiologically. Therefore, the bFGF, besides of being stabilised against proteases, was presented in a biomimetic context that favored it interaction with the surrounding tissue. *In vitro* experiments demonstrated the capability of the formulations to improve bFGF administration, since they enhanced proliferation and metabolic activity of marrow stromal cells in comparison to bFGF alone and bFGF bound to aggrecan [54].

Li and colleagues encapsulated bFGF into gelatin MPs because the electrostatic binding between them can enhance the protective effect. The particles were loaded into a porous collagen/cellulose nanocrystals scaffold, which proved to enhance angiogenesis *in vitro* and *in vivo* [55]. Wound dressings containing bFGF loaded gelatin microspheres were further studied by Park *et al.*, who incorporated them into a porous chitosan scaffold. The efficacy of the dressing was proved *in vivo* in pressure ulcers inflicted to aged mice, and the results showed a higher wound closure rate. Moreover, those animals presented lower protease levels due to chitosan, and thus higher exogenous or endogenous bFGF levels [56]. In another study, Kawai and colleagues incorporated bFGF containing gelatin MPs into a bilayer commercial artificial dermis (Pelnac™) composed of an inner collagen sponge and an outer silicon layer. The formulation efficacy was assessed in two animal models, a full thickness excisionals wound in guinea pigs and a pressure-induced decubitus ulcer in genetically diabetic mice. In both cases, the formulation accelerated fibroblast proliferation and capillary formation. Moreover, diabetic mice receiving bFGF containing gelatin MP showed an enhanced resistance against infection [57,58].

Huang and collaborators developed another bilayer wound dressing, enclosing bFGF containing gelatin MPs into a bilayer scaffold composed of a gelatin sponge inner layer, which porous structure serves as a host for proliferation cells, and an elastomeric polyurethane (PU) membrane external layer, which improves the mechanical properties of the scaffold. The application of the dressing into full thickness wounds in York pigs led to a faster wound closure and better skin remodeling [59]. Ulubayram *et al.* replaced the bFGF with EGF in the gelatin MPs of the bilayer dressing and they evaluated *in vivo* in an excisional wound model in rabbits. In the higher dose tested, a greater area reduction was observed in wounds treated with the dressing than in wounds treated with EGF solution. Moreover, the histological findings showed that the newly formed tissue had almost the structure of native skin [60]. Later, they analysed the efficacy of the gelatin sponge loaded with EGF containing MPs in excisional wounds in normal and streptozotocin (STZ)-induced diabetic rats. Wound closure was specially enhanced in non diabetic rats although a slight improvement was observed in diabetic rats. In regard to histological analyses, the effect of the dressing was significantly different between normal and diabetic rats, but overall it improved granulation tissue formation and reepithelisation [61]. In addition, Zhou and colleagues encapsulated EGF in other natural polymer, concretely in chitosan. The chitosan NPs containing EGF were incorporated into a fibrin gel that exhibited a sustained release of the factor, maintaining its ability to stimulate fibroblast proliferation for at least 7 days [62]. EGF has also been encapsulated in synthetic MPs such as PLGA, achieving an improved growth rate of fibroblasts *in vitro* [63]. In another study, EGF loaded into PLGA NPs exhibited an accelerated wound closure in full thickness wounds inflicted to diabetic rats, because the EGF released from the particles promoted the highest level of fibroblast proliferation [64]. In a posterior study conducted by our research group, EGF was loaded into PLGA-alginate MPs. Alginate was added with the aim of improving the encapsulation efficiency by increasing the viscosity of the internal aqueous phase and thus limiting the diffusion of the GF from the MPs. *In vitro*, the MPs demonstrated that the EGF remained active after the encapsulation process. Moreover *in vivo*, they induced a faster and more effective wound healing, in terms of wound closure, reepithelisation and resolution of the inflammatory process, after a single intralesional injection into full thickness wounds inflicted to STZ-induced diabetic rats [65].

Additionally, PLGA has been used to encapsulate other active compounds, such as FGF-1, LL37 and insulin. FGF-1 loaded MPs were embedded into a fibrin gel and they improved fibroblast proliferation *in vitro* [66]. On the other hand, LL37 loaded MPs were applied in full thickness wounds, where they produced an improvement in granulation tissue formation, reepithelisation, collagen deposition and neoangiogenesis as shown in Fig. 2 [67]. Regarding to the encapsulation of insulin in PLGA (Fig. 3), it showed an enhancement in wound closure in a keratinocyte migration assay [68]. Later, the insulin loaded MPs were incorporated into alginate or alginate-polyethylene glycol (PEG) sponges, which did not alter their bioactivity [69].

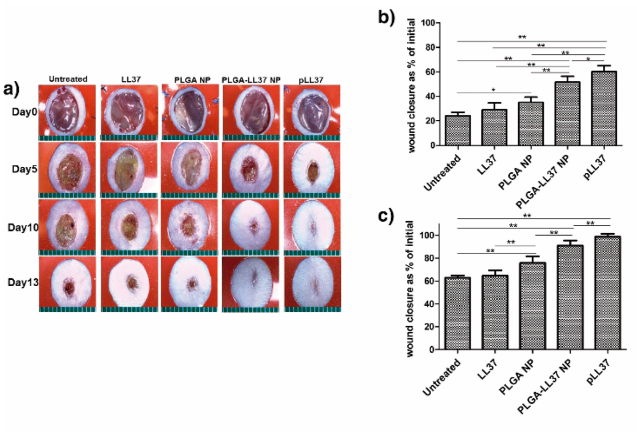


**Fig. 2.** PLGA-LL37 NPs accelerate wound healing. (A) Representative images of wounds of five tested groups: Untreated, LL37, PLGA-NP, PLGA-LL37 NP and pLL37 (positive units). Ruler units in mm. (B) Wound area at day 5 (n = 13) and (c) day 10 (n = 10) (mean ± SD). Reproduced and adapted with permission from Chereddy et. al.[6] (©2014).

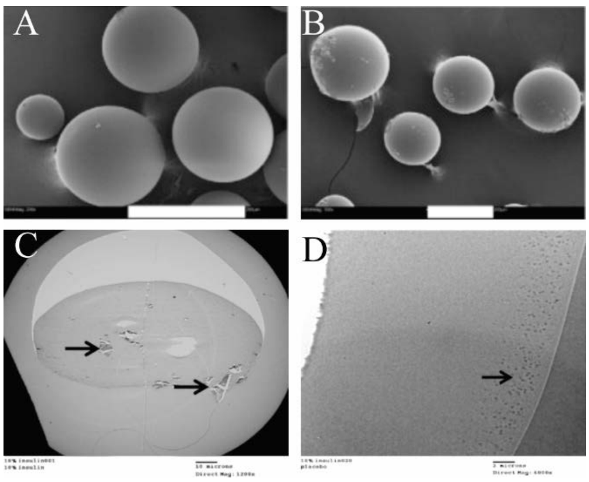


**Fig. 3.** PLGA MPs containing insulin crystals. Shape and surface morphology of MPs with (A) 0% and (B) 10% insulin crystal loadings. White size bar represents 200 µm. (C) Cross sectional images of PLGA microspheres with 10% w/w crystalline insulin entrapment. Black arrows point to insulin crystals embedded into the inside, and extending out from the surface of PLGA microspheres. Size bars represent 10 µm. (D) The highly porous outer region the PLGA microsphere highlighted by a black arrow.  Size bars represent 2 µm. Reproduced and adapted with permission from Hrynyk et al. [7] (©2010).

Subsequently, those dressings demonstrated their efficacy *in vivo* in a burn injury in rats, achieving a faster and more regenerative healing by increasing the rate of disintegration of dead tissue, reducing oxidative stress, stimulating collagen deposition and enhancing angiogenesis [70].

The incorporation of VEGF in NPs has proven to improve angiogenesis *in vitro* and *in vivo*. On one hand, *in vitro*, in a study where endothelial cells were incubated with the release medium of VEGF loaded fibrin NPs incorporated in chitosan-hyaluronic acid sponges [71]. On the other hand, *in vivo*, analysing the effect of subcutaneous implants of calcium alginate MPs loaded with VEGF [72]. Moreover, VEGF showed an improvement of wound healing after the application of VEGF loaded PLGA NPs into full thickness excisional wounds in diabetic and non-diabetic mice. Wound healing was enhanced in both animal models, in terms of collagen deposition, granulation tissue formation, angiogenesis and reepithelisation, due to the combined effect of VEGF and the lactate released from PLGA degradation [73].

Losi *et al.* went a step further and encapsulated two GFs (bFGF and VEGF) in PLGA NPa, since both of them play key roles in wound healing. The nanoparticles were loaded in a bilayer scaffold composed of a fibrin layer that acted as a DDS and a poly(ether)urethane-polydimethylsiloxane (PEtU/PDM) layer that provided mechanical resistance. An *in vivo* wound healing assay in diabetic mice showed that the formulation improved wound healing in comparison to the administration of free GFs and the empty scaffold, although similar results were obtained loading directly the GFs into the dressings [74]. In another study, VEGF was encapsulated together with EGF. In this case, GFs were entrapped in chitosan MPs loaded into a dextran-based hydrogel as illustrated in Fig 4. The DDS achieved a faster wound healing in heat induced wounds, in comparison to a more frequent administration of the free GFs, demonstrating the ability of microparticulate delivery systems to improve GF dosage [75].

In addition, numerous GFs and cytokines can be jointly encapsulated in MPs and NPs using platelets lysate or platelet rich plasma (PRP). Fontana *et al.* loaded platelet lysate into porous silicon MPs, achieving promising results in a wound model *ex vivo*: a greater proliferative effect than the positive control (platelet lysate as in particles) and an effective, but short lasting acidophilia of the collagen fibres, sign of ongoing regeneration [76]. A strategy to achieve a more sustained release of the GFs from PRP or plasma lysate is to produce NPs containing heparin, since it binds to them acting as a GF reservoir. In that regard, fragmin-protamine MP/NPs containing PRP were developed, since protamine forms water insoluble complexes with the low molecular weight heparin (fragmin). Those particles provided a faster wound closure and an enhanced angiogenesis in split thickness skin graft donor site wounds in rats [77]. Those results were in agreement with the ones obtained by La and colleagues, who also observed a faster wound closure and an improved angiogenesis in large wounds inflicted to athymic mice; after the administration of PRP into PLGA NPs conjugated with heparin and incorporated into a fibrin gel [78].

Heparin, besides of stabilizing GFs has anti-inflammatory activity and it can be useful in burn wounds. For that purpose, Lakshmi and collaborators developed a DDS consisting of chitosan MPs loaded with desulphated heparin embedded into a collagen matrix. The DDSs were effective to regulate inflammatory events in burn wounds in rats, thereby achieving a faster wound closure and granulation tissue formation [79].

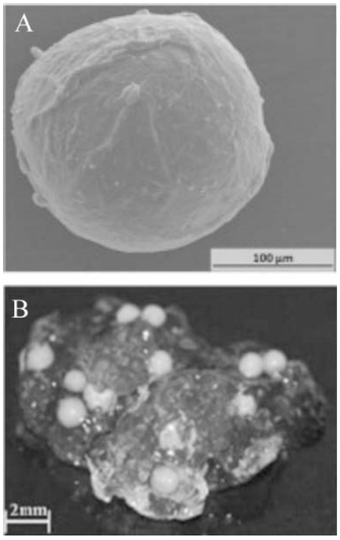


**Fig. 4.** Chitosan MPs containing EGF and VEGF, loaded into a dextran-based hydrogel. (A) SEM images of the chitosan MPs 400x. (B) Images of dextran hydrogel with microparticles incorporated. Reproduced and adapted with permission from Ribeiro et al. [8] (©2013).

Chitosan NPs can be produced due to electrostatic interactions with a negatively charged lipid such as lecithin, as the ones produced in a study by Blazevic and colleagues. Those chitosan/lecithin NPs were loaded with melatonin, and their efficacy was demonstrated by their ability to promote wound healing *in vitro* [80].

In some cases, DDSs have been developed using more unusual polymers, in order to take advantage of their characteristics. In that regard, Petersen and collaborators developed MPs composed of amphyphilic polyanhydrides (1,6bis(pcarboxyphenoxy) hexane (CPH) and 1,6-bis(p-carboxyphenoxy)-3,6-dioxaoctane (CPTEG)), that unlike some other synthetic polymers exhibit both bulk and surface erosion properties and present a less acidic degradation products. Therefore, they can reduce the risk of moisture induced aggregation and produce a more protein-friendly environment. The MPs produced with those polymers were able to release lipocalin-2 in a sustained manner that increased cell migration rate more than the administration of the protein alone [29].

In addition, some polymers are used due to their ability to target the encapsulated drug to the action site. Taking that into account, NPs composed of poly-(1,4-phenyleneacetone dimethylene thioketal) (PPADT), a ROS (reactive oxygen species) responsive polymer, have been developed to release SDF-1α. Labeled NPs showed an effective release and targeting of the protein to wound bed, since PPADT mainly depolymerise and release the SDF-1α there, due to the elevated ROS levels of the wound. Moreover, a faster wound closure and an enhanced vascularisation were observed in mice wounds treated with the NPs [81].

On the other hand, some polymers need to be functionalised in order to develop a suitable DDS for wound dressing. In that regard, Wang and colleagues developed a formulation based on *in situ* generated MPs loaded with VIP due to dopamine functionalisation. For that purpose they functionalised PCL nanofibers with dopamine. Then, VIP was absorbed into the nanofibers due to the adhesive properties of the dopamine. Finally, VIP loaded MPs were produced *in situ*, immersing and

**Table 3**. Summary of different MP/NPs developed to release GFs and other active compounds and their main outcomes

| DDSs | GF | Results | Ref. |
|---|---|---|---|
| Alginate MPs incorporated to a carboxymethyl chitosan-PVA hydrogel | bFGF | The formulation achieved a faster wound recovery rate with a higher reepithelisation and regeneration of the dermis in a full thickness burn wound in rats. | [53] |
| Aggrecan mimetic polyelectrolyte complex NPs | bFGF | The formulation maintained bFGF activity *in vitro*, in metabolic and proliferation activity assays. | [54] |
| Gelatin MPs into a porous collagen/cellulose nanocrystals scaffold | bFGF | An increment of cell proliferation in endothelial cells was achieved with the DDS. And after being subcutaneously implanted into rats it enhanced angiogenesis *in vivo*. | [55] |
| Gelatin MP in a porous chitosan scaffold | bFGF | Until day 7 the scaffold and the scaffold with bFGF accelerated wound closure in pressure ulcer in aged mice models. And with the bFGF scaffold the levels of proteases decreased by day 10. | [56] |
| Gelatin MPs into an artificial dermis (Pelnac®) | bFGF | A prolonged *in vivo* retention of the bFGF into the artificial dermis was achieved with the MPs. In both, a full thickness excisional wound model in guinea pigs and a pressure induced decubitus ulcer model in *db/db* mice, the treated group presented a higher fibroblast proliferation and capillary formation in a dose-dependent way. | [57,58] |
| Gelatin MPs loaded into a bilayer scaffold (gelatin sponge and PU membrane) | bFGF | The scaffolds led to a faster wound closure and better wound remodeling in a full thickness skin wound in York pigs. | [59] |
| Gelatin MPs in a bilayer dressing (gelatin sponge + PU layer) | EGF | With the higher dose tested the formulation achieved a greater area reduction in a full thickness excisional wound in rabbits. The histological findings showed that the newly formed tissue was almost as normal skin. | [60] |
| Gelatin MPs in gelatin sponges | EGF | The formulation was analysed in a full thickness wound model in diabetic and non-diabetic rats. The wound closure was especially improved in non diabetic rats treated with the formulation. In both diabetic and non-diabetic rats, the formulation improved the histological scores (reepithelisation, granulation tissue and neovascularisation). | [61] |

| DDSs | GF | Results | Ref. |
|---|---|---|---|
| Chitosan NPs loaded in a fibrin gel | EGF | The formulation presented biologic adhesiveness properties and it showed a more sustained release than the NP or the gel alone. In addition, the EGF maintains it ability to stimulate the proliferation of fibroblast after the encapsulation process. | [62] |
| PLGA MPs | EGF | The MPs improved growth rate of fibroblast *in vitro*. | [63] |
| PLGA NPs | EGF | In a diabetic rat wound model, the NPs accelerated wound closure in comparison to free EGF. | [64] |
| PLGA-Alginate MPs | EGF | In a full thickness wound model in diabetic rats, the formulation achieved a faster and more effective wound healing in terms of wound closure, reepithelisation and resolution of the inflammatory process. | [65] |
| PLGA MPs embedded in fibrin scaffolds | FGF-1 | The scaffold enhanced fibroblasts proliferation *in vitro*. | [66] |
| PLGA NPs | LL37 | The treatment improved *in vivo* wound healing in NMRI mice in terms of granulation tissue formation, reepithelisation, collagen deposition and neoangiogenesis. | [67] |
| PLGA MPs | Insulin | The formulation achieved a faster wound closure in vitro in a scratch assay in keratinocytes. | [68] |
| PLGA MPs into alginate or alginate – PEG sponge dressings | Insulin | The application of the dressings in burn injuries in rats achieved a faster and more regenerative healing: faster closure, higher rate of disintegration of dead tissue, decreased oxidative stress, and enhanced collagen deposition and maturation. | [69, 70] |
| Fibrin NPs loaded in chitosan-hyaluronic acid sponges | VEGF | The formulation improved capillary like tubule formation (angiogenesis) *in vitro*. | [71] |
| Calcium alginate MPs | VEGF | The subcutaneous implantation of the MPs enhanced angiogenesis, in a extension of 0.6-0.8 mm in the surrounding tissue. | [72] |
| PLGA NPs | VEGF | *In vitro* the NPs improved proliferation and migration of keratinocytes and up regulated VEGFR-2 expression. *In vivo* they enhanced granulation tissue formation, collagen content, reepithelisation and angiogenesis, in both diabetic and non diabetic mice wound models. | [73] |

| DDSs | GF | Results | Ref. |
|---|---|---|---|
| PLGA NPs loaded in PETu/PDM)/fibrin based scaffolds | VEGF and bFGF | The administration of the DDS improved wound healing in a full thickness wound model in diabetic mice, in comparison to the administration of the free GFs, but not in comparison to the administration of the GFs directly into the scaffolds. | [74] |
| Chitosan MPs loaded in a dextran-based hydrogel | EGF and VEGF | After the application of the hydrogel to heat induced wounds in rats, they achieved a faster wound healing in comparison to a more frequent administration of the free GFs. | [75] |
| Porous silicon (Psi) MPs | Platelet lysate | The formulation improved *in vitro* wound closure and *ex vivo* it enhanced wound regeneration, as proved by the proliferative effect and acidophilia observed. | [76] |
| Fragmin-protamine MP/NPs | PRP | The treatment promotes reepithelisation and angiogenesis in a split thickness skin graft donor site wound model conducted in rats. | [77] |
| Heparin conjugated PLGA NPs in a fibrin gel | PRP | The wounds treated with the formulation achieved a faster wound closure and an enhanced angiogenesis in athymic mice. | [78] |
| Chitosan MPs embedded into a collagen matrix | Desulphated heparin | The treatment applied in burn wound injuries was able to accelerate wound closure, by an earlier reduction of the inflammation and an acceleration of the granulation tissue formation. | [79] |
| Lecithin/chitosan NPs | Melatonin | In an i*n vitro* scratch assay in HaCaT cells the formulation improved cell migration. | [80] |
| Amphyphilic polyanhidride MPs based on CPH and CPTEG | Lipocalin-2 | The formulation increased cell migration more than the administration of the protein alone, due to sustained release. | [29] |
| PPADT NPs (a ROS reactive nanomaterial) | SDF-1α | The NPs showed and effective release and targeting to the wounds, due to the high ROS content in the wound bed. In addition, the wounds treated with the NPs showed a faster wound closure and an enhanced vascularisation in a mice wound model. | [81] |
| In situ generated PCL MPs into PCL nanosheets | VIP | The developed DDS significantly promoted wound healing favouring granulation tissue formation and angiogenesis in a mice excisional wound model. | [25] |

and removing the nanofibers from acetone, so the partially dissolved PCL precipitated, forming MPs. *In vivo* wound healing studies revealed that the resulting DDS significantly promoted wound healing favoring granulation tissue formation and angiogenesis [25].

### *3.2 Lipid nanoparticles*

As summarised in Table 4, lipid nanoparticles are a suitable DDS to release GFs and other endogenous molecules for wound healing. Among them, liposomes have been thoroughly studied since their discovery in the 1960 [82]. Liposomes are spherical vesicles composed of a bilayer lipidic membrane [83]. Besides of the characteristics given by the lipids (biocompatilibity and biodegradability) they present some beneficial properties due to the their structure: (i) the ability to encapsulate hydrophilic compounds into the aqueous compartiment and hydrophobic compounds in the bilayer, (ii) the capacity to allow a sustained release, and (iii) the increase of drug accumulation in the skin due to their mimic of the epidermis composition. Despite their benefits, liposomes have shown several limitations, such as, low stability that may cause uncontrolled release of the entrapped drugs, low encapsulation efficiency and sedimentation, aggregation or fusion during storage [84,85].

In 1988, Brown and collaborators loaded for the first time a GF, concretely EGF, into a liposome for wound healing application. The EGF was encapsulated into a multilamellar lecithin liposome and topically applied into 5 cm incisions inflicted to rats. The liposomes prolonged the exposure of the EGF, producing a 200% increase in wound tensile strength and an increased collagen formation and fibroblast proliferation in comparison to the application of EGF in solution [86]. Later, another research group developed a different multilamellar liposome formulation loaded with EGF. The formulation efficacy was assessed *in vivo* in second-degree burns against free EGF and empty liposomes, and it showed the fastest wound healing in terms of collagen formation, wound contraction, fibroblast proliferation and recovery of the epithelium [87]. In order to facilitate the administration of the liposomes, they were embedded into a chitosan gel, which ensured a good moist healing environment. This formulation was also evaluated in second-degree burns in rats achieving similar results to that of the liposomes, which demonstrated the suitability of incorporating the liposomes into the chitosan gel [88].

In a different study, Pierre *et al.* hypothesised that after the topical administration of IGF-I loaded liposomes, wound healing would be as enhanced as after the systemic administration of higher doses of IGF plus Growth Hormone (GH). That hypothesis was demonstrated assessing wound reephitelisation in a wound healing study performed in rats [89].

In a study published by Xiang and colleagues, the drug loading capacitiy of the liposomes was studied. In that regard, they analysed the suitability of 4 methods to encapsulate bFGF into liposomes. All of them presented similar advantages such as, easy preparation method and mild conditions; but they differed in terms of entrapment rate, bioactivity and physical stability. Among them, the pH gradient method was determined to be the most suitable; and therefore *in vivo* efficacy of the liposomes was assessed using that entrapment method. The formulation was able to promote wound healing and to accelerate dermal proliferation and tissue collagen generation in second-degree burns generated in rats [90]. Lastly, a liposome formulation containing SDF-1 and dispersed into an acellular commercial dermis (Alloderm®) was developed. Spiking the decelullarised dermis with liposomes resulted in a promising strategy for wound healing, rather than spiking directly free SDF-1, since the former exhibited a more persistent cell proliferation in the dermis, an increased granulation tissue thickness and an improved wound closure in a full thicknes wound inflicted to diabetic mice [91].

In order to overcome the limitations of the liposomes, a new lipid nanoparticle generation was developed, solid lipid nanoparticles (SLN). SLNs are nanoparticles composed of lipids that are solid at room temperature stabilised by a shell of surfactants [92]. In comparison to liposomes they present a higher flexibility modulating the release and a better protection of the incorporated drugs, because their solid state reduced the exchange of the hydrophilic drugs with the external water phase [93,94]. However, SLNs have a limited stability; since the number of imperfections in the crystal lattice is reduced during storage, leading to drug expulsion [40]. To address that problem, lipid nanoparticles with an amorphous matrix were developed using blends of solid and liquid lipids [95,96]. Furthermore, those nanostructured lipid carriers (NLC) presented a higher drug loading capacity and a lower water content in the final dispersion than SLNs [94]. Despite the limitations of SLNs, both of them exhibit numerous advantages for wound healing, some of them shared with liposomes: (i) they allow a controlled release, (ii) they increase skin hydration effect, due to their adhesiveness and occlusivity, (iii) their small size ensures a close contact with the skin, and (iv) they enable a topical administration, reducing systemic exposure [95].

Taking that into account, our research group encapsulated EGF into NLCs and SLNs. The resulting formulations maintained the EGF bioactivity after the manufacturing process and even after the gamma sterilisation process. Then, the efficacy of the formulation was assessed in a full thickness excisional wound model in diabetic mice (*db/db* mice). Both formulations presented very similar improvement in wound healing in comparison to a higher dose of free EGF, in terms of wound closure, reepithelisation and restoration of the inflammatory process. However, the advantages of NLCs, such as the higher encapsulating efficiency and the lack of organic solvent in their preparation, made them a better option for wound healing [97]. Therefore, the subsequent *in vivo* wound healing study in a porcine model was carried out using only EGF loaded NLCs (Fig. 5). Although pigs are more complicated to handle due to their large size, they mimic better the wound healing process of humans and they allow creating bigger wounds, as in this case, where the wound area was of 30 $cm^2$. The results obtained were in agreement with the previous ones, since the NLCs also improved wound closure and healing quality in comparison to a higher dose of free EGF

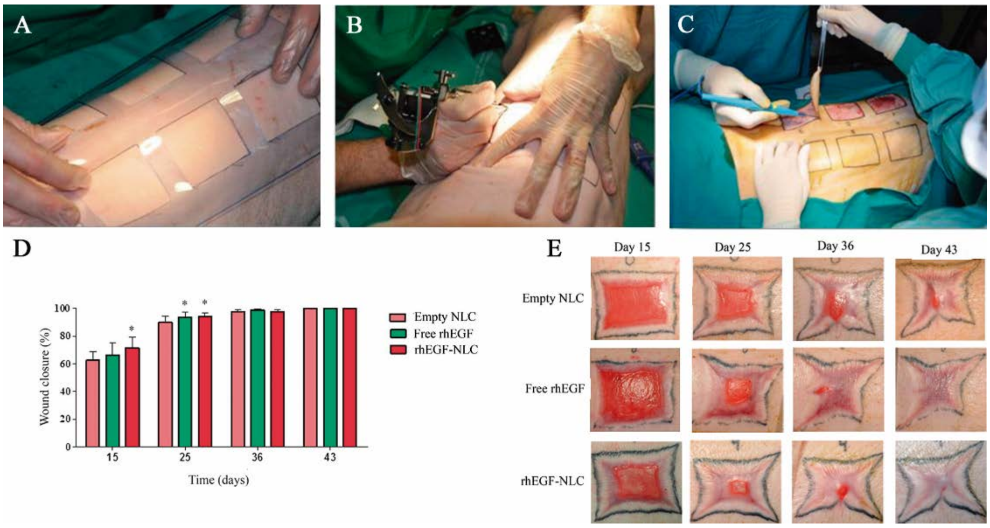


**Fig. 5.** *In vivo* wound porcine model for the administration of rhEGF loaded NLCs. (A-C) surgical procedure for wound creation: (A) Plastic frame used to standardise the wound area. (B) Tattooing of the wound perimeter. (C) Surgical procedure to create full-thickness wounds using monopolar diathermy. (D) Graphical representation of wound closure from the second week to the end of the study. Data shown as means ± S.D. Statistical significance *p < 0.05 greater than empty NLC. (E) Wound images obtained from each experimental group. Reproduced and adapted with permission from Gainza et al. [9] (©2014).

[98]. Finally, in order to facilitate the topical administration of both EGF loaded SLNs and NLCs, they were embedded into either semi-solid hydrogels (based on Noveon AA-1 and Pluronic F-27) or a fibrin based scaffold. All the formulations showed the ability to maintain a sustained released of EGF for at least 48 h, presented minimal penetration from the intact skin surface to the *stratum corneum*¸ and had similar uptake of EGF into damaged skin. However, fibrin formulations were perceived as advantageous due to their biocompatibility, shelf-life, and the ability of fibrin to act as a haemostatic mediator and as a matrix for tissue repair [99].

In view of the promising results obtained by encapsulating EGF into NLCs, in a new study we decided to load the antimicrobial peptide LL37 into NLCs. The encapsulation process did not alter the bioactivity of the drug, since it maintained its antibacterial activity against *E. coli* and its anti-inflammatory activity by reversing the macrophage activation caused by lipopolysaccharide (LPS). A full thickness excisional wound model in *db/db* diabetic mice was utilised to evaluate the efficacy of the formulation and an improved healing was observed in wounds treated with the developed DDS in terms of wound closure, reepithelisation and restoration of the inflammatory process [100]. LL37 has also been loaded into SLNs. For instance, in a study by Fumakia *et al.*, LL37 and serpin-1 were loaded into SLNs, and the resulting formulation had antibacterial activity against *E. coli* and *S. aureus;* promoted *in vitro* wound closure in fibroblast and keratinocytes and reversed inflammatory activity of macrophages against LPS [31].

### *3.3 Nanofibrous structures*

The unique architectural structure of the nanofibrous meshes makes them a promising approach as wound dressings, as summarised in Table 5. Nanofibers are usually produced by electrospinning, a technique that uses electrostatic forces to draw the nanofiber mats from a droplet [101]. These mats consist of biodegradable non-woven, ultra-fine polymeric fibers, whose diameter is in a range from several micrometers to a few nanometers [35,102]. Nanofiber dressings offer a high surface to volume ratio and a high interconnected porosity, which allow gas permeation and thus cell respiration, the removal of exudates and the retainment of moisture preventing wound desiccation and dehydration [103]. Furthermore, nanofibrous membranes are very appealing in tissue engineering due to their structural similarity to native ECM, which encourages cell migration and proliferation and support tissue formation [44,104].

In regard to drug delivery, nanofibrous dressings exhibit a high drug-loading capacity and moreover, they provide an excellent protection from the environmental harms. In addition, these formulations present a remarkable controlled and sustained release of drugs, extending their therapeutic activity for even longer periods of time [35]. Using the electrospinning technique, drugs can be incorporated to the nanofibrous mats by three different approaches: (i) directly loaded by blending

**Table 4.** Summary of different lipid particles developed to release GFs and other active compounds and their main outcomes.

| DDSs | GF | Results | Ref. |
|---|---|---|---|
| Lecithin multilamellar liposomes | EGF | In comparison to the application of free EGF, the formulation prolonged local exposure to EGF in 5 cm incisions inflicted to rats. Therefore the formulation increased wound tensile strength, collagen formation and fibroblast proliferation. | [86] |
| Cholesterol and DPPC multilamellar liposomes | EGF | The formulation efficacy was assessed in a second degree burn injury in rats, and it achieved the fastest wound healing among all analysed groups, in terms of collagen formation, wound contraction, cell proliferation and recovery of epithelium. | [87] |
| Cholesterol and DPPC multilamellar liposomes in a chitosan gel | EGF | After the application of the treatments in a second degree burn injury in rats, the developed formulation achieved a faster reepithelisation rate than EGF loaded directly into the chitosan gel and EGF loaded liposomes. On the other hand, fibroblast proliferation was similar in the animals treated with EGF liposomes loaded into the chitosan gel or applied directly. | [88] |
| Liposomes | IGF- I | The topical application of liposomes achieved similar wound reepithelisation as higher doses of a combination of GH plus IGF or IGF-liposomes administered systemically in a scald injury rat model. | [89] |
| Soybean lecithin and cholesterol liposomes | bFGF | The formulation was applied in a second degree burn wounds in rats, and the medium dose applied achieved a more completed wound repair in terms of morphological observation, dermal cell proliferation and TGF-β1 expression. On the contrary wound healing time and collagen deposition were similarly promoted by the medium and the high dose applied. | [90] |
| DSPC, DSPA and cholesterol liposomes distributed in an acellular dermis (Alloderm) | SDF-1 | The liposomes maintained the activity of SDF-1 *in vitro*, and when applied to a diabetic murine excisional wound they promoted long-term cell proliferation in the dermis, they enhanced granulation tissue thickness and they accelerated slightly wound closure in comparison to the administration of free SDF-1. | [91] |

| DDSs | GF | Results | Ref. |
|---|---|---|---|
| SLN (precirol) and NLC (precirol and mygliol) | EGF | Both formulations improved healing in comparison to free EGF in a diabetic mice wound model, in terms of wound closure, reepithelisation and restoration of the inflammatory process.<br>Due to higher encapsulation efficiency and the lack of organic solvent in its production, NLCs efficacy was assessed in a pig wound healing model. In it, the NLCs improved wound closure and wound healing quality in comparison to a higher dose of free rhEGF. | [97, 98] |
| SLN and NLC embedded in semi-solid hydrogels (Noveon AA-1 or Pluronic F-27) or fibrin based solid scaffold. | EGF | All the formulations were similar in terms of EGF release, uptake of EGF into damaged skin and minimal penetration in the intact skin. | [99] |
| NLC (precirol and mygliol) | LL37 | The NLCs presented antibacterial activity and anti-inflammatory activity *in vitro*, and *in vivo* were able to improve wound closure, reepithelisation and restoration of the inflammatory process in a full thickness excisional wound model in diabetic mice. | [10 0] |
| SLN (gliyceryl monoestearate + α-phosphatidylcholine) | LL37 and Serpin-1 | The formulation presented antibacterial activity against *E. coli* and *S. aureus*, it promoted wound closure in an *in vitro* scratch assay, it protected monolayer culture integrity from LPS and it showed anti-inflammatory activity against LPS. | [31] |

or emulsifying the active compound into the electrospinning solution; (ii) by coaxial electrospinning, a technique in which two immiscible components are simultaneously electrospun through separate feeding capillary channels to generate nanofibers composed of a core-shell structure; and (iii) immobilising the drugs on the surface of the nanofibers through weak interactions (hydrogen bonding or electrostatic, van de Waals or hydrophobic interaction) or covalent bindings that produce chemical surface-modifications in the nanofibers [105].

The three methods mentioned above have been used to generate nanofibers loaded with GFs and other endogenous molecules for wound healing. Among direct loading, our research group emulsified EGF and *Aloe vera* with PLGA to obtain nanofibrous membranes with the combined beneficial effect of both EGF and *Aloe vera*. *In vitro,* the nanofibers showed a promotion of fibroblast proliferation and antimicrobial activity against *S. aureus* and *S. epidermidis*; and *in vivo,* they accelerated significantly wound closure and reepithelisation in a full thickness wound model in diabetic mice [106]. The electrospinnning of emulsions has also been used to encapsulate EGF in PCL/hyaluronan nanofibers and bFGF in poly(ethylene glycol)-poly(DL-lactide) (PELA) nanofibers, with the aim of increasing the encapsulation efficiency and alleviate the initial burst release. Both formulations developed with this strategy were able to improve wound healing *in vivo* [107,108].

Direct blending of hydro- and lipophilic compounds into the respective hydro- and lipophilic electrospun solutions has also been done to obtain wound dressings. Among hydrophilic nanofibers, Bertoncelj *et al.,* developed a chitosan/PEO membrane loaded with PRP that stimulated cell proliferation, changed cell morphology and limited cell mobility *in vitro* [109]. On the other hand, the lipophilic compound β-estradiol was loaded in a PU/dextran composite nanofiber to develop a post-menopausal wound dressing, which was able to accelerate wound closure *in vivo* in partial thickness wounds [34].

In order to obtain a more controlled release, nanofibers can be also directly loaded with NPs containing GFs. In that regard, Lai *et al.* developed a dual mesh, composed of collagen and hyaluronic acid separate nanofibers that mimics physiological delivery of EGF, bFGF, VEGF and PDGF. For that purpose, EGF and bFGF were directly loaded into the nanofibers to obtain a rapid release; and VEGF and PDGF were loaded into gelatin NPs prior to being electrospun to obtain a gradual and a slow release profile. After confirming the expected release behavior *in vitro*, the nanofibrous dressing were applied in full thickness wounds in STZ-induced diabetic rats with promising results, as depicted in Fig. 6 [110]. On the other hand, Xie *et al.* developed chitosan-PEO nanofibers with the aim of obtaining a fast release of VEGF and a slow release of PDGF-BB, for which PDGF-BB was loaded in PLGA NPs before electrospinning. *In vitro* release confirmed that the sought profile was obtained, and afterwards the dressing efficacy was assessed *in vivo* against a commercial dressing (Hydrofera Blue®). The results showed that the developed formulation accelerated wound healing both in early and later stages [111].

Schneider and colleagues developed a silk fibroin electrospun mesh loaded directly with EGF. It showed an initial burst release convenient for a fast activation of the keratinocytes, as demonstrated by the improvement in wound closure and reepithelisation obtained in a human skin equivalent wound model *in vitro* [48]. Nevertheless, in a subsequent *in vivo* wound healing study, where the efficacy of the direct loaded nanofibers was compared to a coated formulation, a slightly faster wound closure rate and epidermal differentiation was observed with the coated formulation [112]. In another study, the direct EGF loading was compared with coaxial electrospinning in PLLCL and gelatin nanofibers. The result showed a more promising outcome with coaxial electrospinning, since it more sustained release led to an improvement of proliferation and differentiation of adipose derived stem cells (ADSC) [113].

Another interesting aproach was based on Poly (3-hexylthiphene) (P3HT), a polymer that after light stimulation converts optical energy into electrical causing the photocurrent effect, which has shown

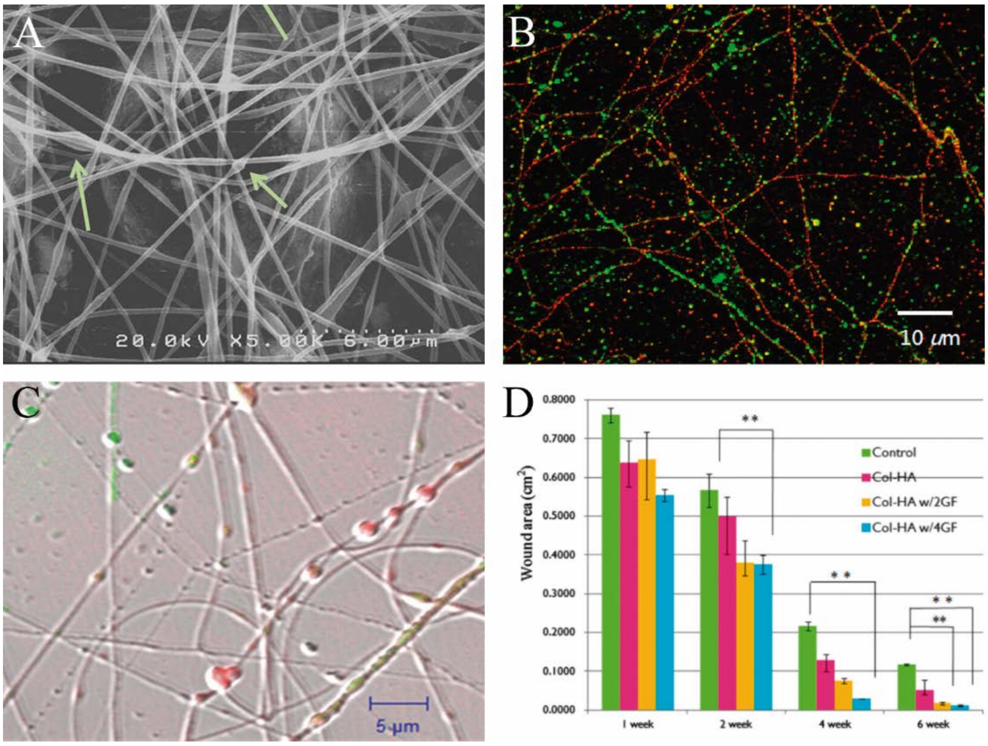


**Fig. 6.** Composite collagen-hyaluronic acid nanofibers containing free GFs (bFGF and EGF) and GFs loaded into gelatin NSs (VEGF and PDGF). (A) SEM images of the morphology of nanofibers. (Arrows indicate gelatin NPs; the scale bar 6 µm). (B) Fluorescent images by confocal microscopy of nanofibers, collagen dyed in red and hyaluronic acid dyed in green. (C) Fluorescent images by confocal microscopy of collagen nanofibers with fluorescein(red) loaded gelatin NSs and hyaluronic acid nanofibers with rhodamine b (green) loaded gelatin NSs. (D) Wound area at different times of untreated wounds and wounds treated with collagen-hyaluronic acid nanofibers, collagen-hyaluronic acid nanofibers containing bFGF and EGF and collagen-hyaluronic acid nanofibers containing bFGF, EGF, VEGF and PDGF. (⁄⁄p < 0.01, ⁄P < 0.05). Reproduced and adapted with permission from Lai et al. [111] (©2014).

promising results in skin regeneration. In order to improve its biocompatibility, coaxial electrospinning was used to encapsulate EGF and P3HT in the core of a gelatin/PLLCL nanofibrous mesh. The formulation improved fibroblast proliferation and wound closure *in vitro,* and it was able to induce ADSC differentiation into keratinocytes under light stimulation [114].

In order to achieve a longer therapeutic effect, EGF can be immobilised to the nanofibers by covalent binding with the amine groups exposed on their surface. In that regard, Tigli and colleagues developed a PCL and PCL/gelatin scaffold with EGF covalently immobilised on it surface. That immobilisation resulted in an earlier spreading and faster proliferation of fibroblast seeded on top [115]. Similar results were obtained after binding EGF covalently to the surface of PCL/collagen nanofibers, as an acceleration in keratinocyte spreading and proliferation was observed. In addition, the keratinocytes seeded on top of the nanofibers exhibited superior differentiation ability, evidenced by a higher loricrin expression [116].

Choi *et al.*, developed another DDS based on the covalent conjugation of EGF to the nanofibers. In this case, EGF was immobilised on the surface of PEG/PCL block copolymers and it efficacy in wound healing was compared to that of nanofibers plus EGF solution. The dressing containing conjugated EGF showed superior therapeutic activity in both *in vitro* and *in vivo* wound healing studies, due to the greater protection of the GF. A higher enhancement of keratinocyte specific gene expression was observed *in vitro,* and an accelerated wound closure and an improvement of EGFR expression *in vivo* [117]. Taking into account the promising results obtained by immobilising EGF in PEG/PCL block copolymer, a coaxial electrospun composed of PEG/PCL was developed. It was loaded with EGF and bFGF, the first one immobilised in the surface and the second one encapsulated in the core. The formulation exhibited an initial burst release of bFGF and no negligible release of EGF; and in comparison to nanofibers with the single GFs, it accelerated wound closure achieving more mature wounds on day 7 in burn wounds inflicted to STZ-induced diabetic mice [118].

As demonstrated by Song and colleagues, there are more ways to covalently conjugate active compounds to nanofibers surface. In that regard, they conjugated Cys-KR12 (an antimicrobial peptide motif originated from LL37) to silk fibroin nanofibers, using EDC/NHS and thiol-maleimide click chemistry. The conjugation process did not affect the bioactivity of the Cys-KR12, since *in vitro* studies confirmed that it exhibited antimicrobial and proliferative activities and suppressed LPS induced inflammation [119].

In a study by Patel *et al.*, bFGF and laminin were immobilised in the surface of PLLA using a strategy based on the capacity of heparin to associate with endogenous molecules, thereby PLLA was functionalised with heparin and subsequently bFGF and laminin were conjugated. The resulting formulation was able to enhance wound healing *in vitro* in a scratch assay, especially when the nanofibers were oriented perpendicularly to the gap [120].

## 4. Conclusions and future perspectives

In recent years the incidence of chronic wounds is increasing alarmingly, as the risk population grows. Furthermore, due to the lack of efficient treatments, chronic wounds are becoming a clinical and economical burden. In comparison with the physiological healing process, a series of abnormalities occur during chronic healing, such as the decrease of the levels of GFs and other molecules that are involved in healing regulation. Therefore, the exogenous administration of GFs is a promising approach for the treatment of wound healing, although their low stability *in vivo* limits their clinical application. An attempt to cope with this is the development of novel DDSs containing GFs, including polymeric MP/NP, lipid nanoparticles, nanofibrous structures and their combinations. Those formulations, besides of protecting the encapsulated drug, present numerous advantages. Among others they offer good biocompatibility, controlled or sustained release, high drug-loading and good mechanical properties. In addition, depending on the polymer and DDS used,

**Table 5.** Summary of different nanofibrous membranes developed to release GFs and other active compounds and their main outcomes.

| **DDSs** | **GF** | **Loading method** | **Results** | **Ref.** |
|---|---|---|---|---|
| PLGA and *Aloe vera* nanofibers | EGF | Direct loading, by emulsification | *In vitro* it improved fibroblast proliferation and showed antimicrobial activity. *In vivo* it accelerated wound closure and reepithelisation in a diabetic mice wound model. | [106] |
| PCL and hyaluronan nanofibers | EGF | Direct loading, by emulsification | The formulation enhanced keratinocyte and fibroblast proliferation and infiltration *in vitro*. And it enhanced the regeneration of a fully functional skin, *in vivo*. | [107] |
| PELA nanofibers | bFGF | Direct loading, by emulsification | The formulation enhanced fibroblast adhesion, proliferation and ECM secretion *in vitro*. And when applied to wounds inflicted to diabetic rats, it improved wound closure, achieving a complete reepithelisation and regeneration of skin appendages in 2 weeks. | [108] |
| Chitosan and PEO nanofibers | PRP | Direct loading, by blending | The formulation stimulates cell proliferation, changed cell morphology and limited cell mobility. | [109] |
| PU and dextran nanofibers | β-estradiol | Direct loading, by blending | The formulation accelerated wound area reduction in an *in vivo* partial thickness wound healing in rats. | [34] |
| Collagen and hyaluronic acid dual nanofibers | VEGF, bFGF, PDGF and EGF | Direct loading. bFGF and EGF directly and VEGF and PDGF loaded into gelatin NPs | The DDS increased endothelial cell growth rate and allowed a better network. In wounds inflicted to diabetic rats it accelerated wound closure, increased collagen deposition and enhanced maturation of vessels. | [110] |

| DDSs | GF | Loading method | Results | Ref. |
|---|---|---|---|---|
| Chitosan and PEO nanofibers | VEGF and PDGF-BB | Direct loading, VEGF directly and PDGF-BB in PLGA NPs. | In comparison to commercial Hydrofera Blue®, the formulation accelerated wound healing in rats, in both early (promoted angiogenesis, increased reepithelisation, controlled granulation tissue formation) and later stages (quicker collagen deposition and earlier remodelling). | [111] |
| Silk nanofibers | EGF | Direct loading, by blending | The nanofibers promoted wound closure and reepithelisation, in an *in vitro* human skin equivalent wound model. | [48] |
| Silk nanofibers | EGF and silver sulfadiazine | Comparison between direct loading and surface immobilisation | Mice treated with the drug coated formulation presented a slightly faster wound closure and an increased epidermal differentiation into hair follicles and sebaceous glands, in comparison to mice treated with the direct loading formulation. | [112] |
| PLLCL and gelatin nanofibers | EGF, insulin, hydrocortisone and retinoic acid | Comparison between direct loading and coaxial electrospinning | Due to a more sustained release, the coaxial electrospinning formulation led to a higher cell proliferation and differentiation. | [113] |
| Gelatin/PLLCL and P3HT (a photosensitive polymer) nanofibers | EGF | Coaxial electrospinning, the core was composed of EGF and P3HT | The formulation improved fibroblast proliferation and wound closure *in vitro* and was able to induce ADSC differentiation into keratinocytes under light stimulation due to the ability of P3HT to convert optical energy into electrical. | [114] |
| PCL and PCL/gelatin nanofibers | EGF | Surface immobilisation | The immobilisation of EGF on the nanofibers surface led to an earlier spreading and faster proliferation of the fibroblasts seeded on its top. | [115] |

| DDSs | GF | Loading method | Results | Ref. |
|---|---|---|---|---|
| PCL and PCL/collagen nanofibers | EGF | Surface immobilisation | The formulation enhanced keratinocyte spreading, proliferation and differentiation ability. | [116] |
| PEG and PCL nanofibers | EGF | Surface immobilisation | The application of the DDS into a burn wound inflicted to diabetic mice led to a superior wound closure and enhanced EGFR expression. In addition, *in vitro* it enhanced keratinocyte-specific gene expression. | [117] |
| PCL/PEG nanofibers | bFGF and EGF | EGF immobilised on the surface and bFGF loaded by coaxial electrospinning | The formulation showed a binary release profile with an initial burst of bFGF and negligible release of EGF, and was able to accelerate wound closure and enhance wound maturation in a burn wound model in diabetic mice. | [118] |
| Silk fibroin nanofibers | Cys-KR12 | Surface immobilisation | The encapsulated factor maintained its antimicrobial and proliferative activities, its ability to promote keratinocyte differentiation and to suppress LPS induced inflammation. | [119] |
| PLLA nanofibers functionalised with heparitn | Laminin and bFGF | Surface immobilisation | The formulation enhanced wound healing *in vitro* in a scratch assay, especially when the nanofibers were oriented perpendicularly to the scratch. | [120] |

specific properties can be obtained, such as, drug targeting or an environment that simulates native ECM.

Overall, the controlled release of GFs incorporated into nanotechnology based DDSs has demonstrated a great potential for the treatment of chronic wounds and skin regeneration. However, up to date, the research on DDSs releasing GFs for wound healing is still at the preclinical phase, and further studies are needed in order to advance to the clinical phase. Among the preclinical studies needed, there are tolerance and toxicity assays in animal models, and efficacy assays in larger animal models, such as, porcine models.

Since most of the summarised DDSs are developed as topical delivery systems, a critical issue that need to be studied before their approval is the systemic absorption of the encapsulated drug. In addition, the suitability of the polymers is another key issue that need to be proved, because some of the polymers used for the development of these DDSs are not approved for clinical use.

Although there are not clinical trials or marketed products based in nanotechnology to release GFs or other endogenous molecules for wound healing application, there are two marketed products based in nanotechnology for wound healing. On the one hand, there is Altrazeal®, a crystalline white powder consisting of nanoparticles of freeze dried poly-2-hydroxyethyl-methacrylate (pHEMA) and poly-2-hydroxypropylmethacrylate (pHPMA). Due to nanoflex technology, in contact with the wound exudates the particles hydrate and aggregate becoming a moist and flexible film [121]. On the other hand, there is Talymed® and advanced matrix composed of shortened nanofibers of poly-N-acetyl glucosamine (pGIcNAc) [122]. In addition, there is a clinical trial currently recruiting participants, to evaluate the safety and performance of SPINNER, a portable electrospinning device that produces *in-situ* nanofiber dressings [123].

## 5. Acknowledgments

I. Garcia-Orue thanks the Basque Government for the fellowship grant. This project has been funded by the Spanish Ministry of Economy and competitiveness (INNPACTO, IPT-2012-0602-300000, 2012). In addition, it has been partially by the Basque Government (ELKARTEK 2015, Nanoplatform, KK-2015/0000036).

## 6. References

[1] V.W. Wong, G.C. Gurtner, Tissue engineering for the management of chronic wounds: current concepts and future perspectives, Exp. Dermatol. 21 (2012) 729-734. doi: 10.1111/j.1600-0625.2012.01542.x.

[2] J. Posnett, F. Gottrup, H. Lundgren, G. Saal, The resource impact of wounds on health-care providers in Europe, J. Wound Care 18 (2009)154.doi:10.12968/jowc.2009.18.4.41607.

[3] C.K. Sen, G.M. Gordillo, S. Roy, R. Kirsner, L. Lambert, T.K. Hunt, F. Gottrup, G.C. Gurtner, M.T. Longaker, Human skin wounds: a major and snowballing threat to public health and the economy, Wound Repair Regen. 17 (2009) 763-771. doi: 10.1111/j.1524-475X.2009.00543.x.

[4] A.J. Whittam, Z.N. Maan, D. Duscher, V.W. Wong, J.A. Barrera, M. Januszyk, G.C. Gurtner, Challenges and opportunities in drug delivery for wound healing, Adv. Wound Care (New Rochelle) 5 (2016) 79-88. doi: //dx.doi.org/10.1089%2Fwound.2014.0600.

[5] N.B. Menke, K.R. Ward, T.M. Witten, D.G. Bonchev, R.F. Diegelmann, Impaired wound healing, Clin. Dermatol. 25 (2007) 19-25. doi: //dx.doi.org/10.1016/j.clindermatol.2006.12.05.

[6] G. Gainza, S. Villullas, J.L. Pedraz, R.M. Hernandez, M. Igartua, Advances in drug delivery systems (DDSs) to release growth factors for wound healing and skin regeneration, Nanomedicine 11 (2015) 1551-1573. doi: //dx.doi.org/10.1016/j.nano.2015.03.002.

[7] R.F. Diegelmann, M.C. Evans, Wound healing: an overview of acute, fibrotic and delayed healing, Front. Biosci. 9 (2004) 283-289. doi: //dx.doi.org/10.2741/.

[8] S. Barrientos, H. Brem, O. Stojadinovic, M. Tomic-Canic, Clinical application of growth factors and cytokines in wound healing, Wound Repair Regen. 22 (2014) 569-578. doi: 10.1111/wrr.12205.

[9] P. Olczyk, L. Mencner, K. Komosinska-Vassev, Diverse roles of heparan sulfate and heparin in wound repair, Biomed. Res. Int. 2015(2015)549417.doi: 10.1155/2015/549417.

[10] S. Barrientos, O. Stojadinovic, M.S. Golinko, H. Brem, M. Tomic Canic, Growth factors and cytokines in wound healing, Wound Repair Regen 16 (2008) 585-601. doi: 10.1111 /j.1524-475X.2008.00410.x.

[11] S. Werner, R. Grose, Regulation of wound healing by growth factors and cytokines, Physiol. Rev. 83 (2003) 835-870. doi: 10.1152/phy srev.00031.2002.

[12] P.S. Briquez, J.A. Hubbell, M.M. Martino, Extracellular matrix-inspired growth factor delivery systems for skin wound healing, Adv. Wound Care (New Rochelle) 4 (2015) 479-489. doi: 10.1089/wound.2014.0603.

[13] T. Velnar, T. Bailey, V. Smrkolj, The wound healing process: an overview of the

cell-ular and molecular mechanisms, J. Int. Med. Res. 37 (2009) 1528-1542. doi: 10.1177 /147323000903700531.

[14] A. Lubkowska, B. Dolegowska, G. Banfi, Growth factor content in PRP and their applicability in medicine, J. Biol. Regul. Homeost. Agents 26 (2012) 22S.

[15] M. Zakrzewska, E. Marcinkowska, A. Wiedlocha, FGF-1: from biology through engineering to potential medical applications, Crit. Rev. Clin. Lab. Sci. 45 (2008) 91-135. doi: 10.1080/10408360701713120.

[16] M.G. Tonnesen, X. Feng, R.A.F. Clark, Angiogenesis in wound healing, J. Investig. Dermatol. Symp. Proc. 5 (2000) 40-46. doi: //dx.doi.org/10.1046/j.1087-0024.2000.00014.x.

[17] X. Li, C. Wang, J. Xiao, W.L. McKeehan, F. Wang, Fibroblast growth factors, old kids on the new block, Semin. Cell Dev. Biol. 53 (2016)155-167.doi: //dx.doi.org/10.1016/j.sem cdb.2015.12.014.

[18] J. Hardwicke, D. Schmaljohann, D. Boyce, D. Thomas, Epidermal growth factor therapy and wound healing — past, present and future perspectives, The Surgeon 6 (2008) 172-177. doi: //dx.doi.org/10.1016/S1479-666X (08)80114-X.

[19] K.E. Johnson, T.A. Wilgus, Vascular endothelial growth factor and angiogenesis in the regulation of cutaneous wound repair, Adv. Wound. Care. (New Rochelle) 3 (2014) 647-661. doi: 10.1089/wound.2013.0517.

[20] M.A. Seeger, A.S. Paller, The roles of growth factors in keratinocyte migration, Adv. Wound. Care. (New Rochelle) 4 (2015) 213-224. doi: 10.1089/wound.2014.0540.

[21] T. Emanuelli, A. Burgeiro, E. Carvalho, Effects of insulin on the skin: possible healing benefits for diabetic foot ulcers, Arch. Dermatol. Res. 308 (2016) 677-694. doi: 10.1007/ s00403-016-1686-z.

[22] T.K. Ho, X. Shiwen, D. Abraham, J. Tsui, D. Baker, Stromal-Cell-Derived Factor-1 (SDF-1)/CXCL12 as potential target of therapeutic angiogenesis in critical leg ischaemia, Cardiol. Res. Pract. 2012 (2012) 143209. doi: 10.1155/2012/143209 [doi].

[23] T.T. Lau, D.A. Wang, Stromal cell-derived factor-1 (SDF-1): homing factor for engineered regenerative medicine, Expert Opin. Biol. Ther. 11 (2011) 189-197. doi: 10.1517/ 14712598.2011.546338.

[24] D. Vandamme, B. Landuyt, W. Luyten, L. Schoofs, A comprehensive summary of LL-37, the factotum human cathelicidin peptide, Cell. Immunol. 280 (2012) 22-35. doi: 10.1016/j. cellimm.2012.11.009.

[25] Y. Wang, Z. Chen, G. Luo, W. He, K. Xu, R. Xu, Q. Lei, J. Tan, J. Wu, M. Xing, In-situ-generated vasoactive intestinal peptide loaded microspheres in mussel-inspired polycaprolactone nanosheets creating spatiotemporal releasing microenvironment to promote wound healing and angiogenesis, ACS Appl. Mater. Interfaces 8 (2016) 7411-7421. doi: 10.1021/ acsami.5b11332.

[26] J. Chéret, N. Lebonvallet, V. Buhé, J.L. Carre, L. Misery, C. Le Gall-Ianotto, Influence of sensory neuropeptides on human cutaneous wound healing process, J. Dermatol. Sci. 74

(2014)193-203.doi: //dx.doi.org/10.1016/j.jdermsci.2014.02.001.

[27] W. Jiang, H. Wang, Y.S. Li, W. Luo, Role of vasoactive intestinal peptide in osteoarthritis, J. Biomed. Sci. 23 (2016) 1. doi: 10.1186/s12929-016-0280-1 [doi].

[28] J. Drobnik, Wound healing and the effect of pineal gland and melatonin, J. Exp. Integr. Med. 2 (2012) 3-14. doi: 10.5455/jeim.040112.ir.009.

[29] L.K. Petersen, A.S. Determan, C. Westgate, L. Bendickson, M. Nilsen-Hamilton, B. Narasimhan, Lipocalin-2-loaded amphiphilic polyanhydride microparticles accelerate cell migration, J. Biomater. Sci. Polym. Ed. 22 (2011)1237-1252.doi: 10.1163/092050610X502776.

[30] K. Suk, Lipocalin-2 as a therapeutic target for brain injury: An astrocentric perspective, Prog. Neurobiol. 144 (2016) 158-172. doi: //dx.doi.org/10.1016/j.pneurobio.2016.08.001.

[31] M. Fumakia, E.A. Ho, Nanoparticles encapsulated with LL37 and serpin A1 promotes wound healing and synergistically enhances antibacterial activity, Mol. Pharm. 13 (2016) 2318-2331. doi: 10.1021/acs.molpharmaceut.6b00099.

[32] C.A.B. Kandregula, G. Smilin Bell Aseervatham, G.T. Bentley, R. Kandasamy, Alpha-1 antitrypsin: associated diseases and therapeutic uses, Clin. Chim. Acta 459 (2016) 109-116.doi: //dx.doi.org/10.1016/j.cca.2016.05.028.

[33] S.C. Gilliver, G.S. Ashcroft, Sex steroids and cutaneous wound healing: the contrasting influences of estrogens and androgens, Climacteric 10 (2007) 276-288. doi: 10.1080/13697130701456630.

[34] A.R. Unnithan, A.R.K. Sasikala, P. Murugesan, M. Gurusamy, D. Wu, C.H. Park, C.S. Kim, Electrospun polyurethane-dextran nanofiber mats loaded with estradiol for post-menopausal wound dressing, Int. J. Biol. Macromol. 77 (2015) 1-8. doi: //dx.doi.org/10.1016/j.ijbiomac.2015.02.044.

[35] T. Garg, G. Rath, A.K. Goyal, Biomaterials-based nanofiber scaffold: targeted and controlled carrier for cell and drug delivery, J. Drug Target. 23 (2015) 202-221. doi: 10.3109/1061186X.2014.992899.

[36] J.M. Dang, K.W. Leong, Natural polymers for gene delivery and tissue engineering, Adv. Drug Deliv. Rev. 58 (2006) 487-499. doi: //dx.doi.org/10.1016/j.addr.2006.03.001.

[37] T. Garg, G. Rath, A.K. Goyal, Comprehensive review on additives of topical dosage forms for drug delivery, Drug Deliv. 22 (2015) 969-987.doi: 10.3109/10717544.2013.879355.

[38] W. Li, C.T. Laurencin, E.J. Caterson, R.S. Tuan, F.K. Ko, Electrospun nanofibrous structure: A novel scaffold for tissue engineering, J. Biomed. Mater. Res. 60 (2002) 613-621. doi: 10.1002/jbm.10167.

[39] J. Gunn, M. Zhang, Polyblend nanofibers for biomedical applications: perspectives and challenges, Trends Biotechnol. 28 (2010) 189-197.doi: //dx.doi.org/10.1016/j.tibtech.2009.12.006.

[40] S. Jain, N. Patel, M.K. Shah, P. Khatri, N. Vora, Recent advances in lipid-based vesicles

and particulate carriers for topical and transdermal application, J. Pharm. Sci. (2016). doi: //dx.doi.org/10.1016/j.xphs.2016.10.001.

[41] S.B. Kulkarni, G.V. Betageri, M. Singh, Factors affecting microencapsulation of drugs in liposomes, J. Microencapsul. 12 (1995) 229-246. doi: 10.3109/02652049509010292.

[42] M. Geszke-Moritz, M. Moritz, Solid lipid nanoparticles as attractive drug vehicles: Composition, properties and therapeutic strategies, Materials Science and Engineering: C 68 (2016)982-994.doi: //dx.doi.org/10.1016/j.msec.2016.05.119.

[43] S. Doktorovova, E.B. Souto, Nanostructured lipid carrier-based hydrogel formulations for drug delivery: a comprehensive review, Expert. Opin. Drug Deliv. 6 (2009) 165-176. doi: 10.1517/17425240802712590.

[44] C.P. Barnes, S.A. Sell, E.D. Boland, D.G. Simpson, G.L. Bowlin, Nanofiber technology: Designing the next generation of tissue engineering scaffolds, Adv. Drug Deliv. Rev. 59 (2007)1413-1433.doi: //dx.doi.org/10.1016/j.addr.2007.04.022.

[45] K. Su, C. Wang, Recent advances in the use of gelatin in biomedical research, Biotechnol. Lett. 37 (2015) 2139-2145. doi: 10.1007/s10529-015-1907-0.

[46] T. Dai, M. Tanaka, Y.Y. Huang, M.R. Hamblin, Chitosan preparations for wounds and burns: antimicrobial and wound-healing effects, Expert Rev. Anti Infect. Ther. 9 (2011) 857-879. doi: 10.1586/eri.11.59.

[47] G.D. Mogoşanu, A.M. Grumezescu, Natural and synthetic polymers for wounds and burns dressing, Int. J. Pharm. 463 (2014) 127-136.doi: //dx.doi.org/10.1016/j.ijpharm.2013.12.015.

[48] A. Schneider, X.Y. Wang, D.L. Kaplan, J.A. Garlick, C. Egles, Biofunctionalized electrospun silk mats as a topical bioactive dressing for accelerated wound healing, Acta Biomater. 5 (2009) 2570-2578. doi: //dx.doi.org/10.1016/j.actbio.2008.12.013.

[49] K.K. Chereddy, G. Vandermeulen, V. Préat, PLGA based drug delivery systems - promising carriers for wound healing activity, Wound Repair Regen. (2016). doi: 10.1111/wrr.12404.

[50] B.J. Kim, H. Cheong, E. Choi, S. Yun, B. Choi, K. Park, I.S. Kim, D. Park, H.J. Cha, Accelerated skin wound healing using electrospun nanofibrous mats blended with mussel adhesive protein and polycaprolactone, J. Biomed. Mater. Res. A 105 (2017) 218-225. doi: 10.1002/jbm.a.35903.

[51] Z. Değim, Use of microparticulate systems to accelerate skin wound healing, J. Drug Target. 16 (2008) 437-448. doi: 10.1080/10611860802088572.

[52] M. Ye, S. Kim, K. Park, Issues in long-term protein delivery using biodegradable microparticles, J. Control Release 146 (2010) 241-260. doi: //dx.doi.org/10.1016/j.jconrel.2010.05.011.

[53] Q. Liu, Y. Huang, Y. Lan, Q. Zuo, C. Li, Y. Zhang, R. Guo, W. Xue, Acceleration of skin regeneration in full-thickness burns by incorporation of bFGF-loaded alginate microspheres into a CMCS–PVA hydrogel, J. Tissue

Eng. Regen. Med. (2015). doi: 10.1002/term.2057.

[54] L.W. Place, M. Sekyi, M.J. Kipper, Aggrecan-mimetic, glycosaminoglycan-containing nanoparticles for growth factor stabilization and delivery, Biomacromolecules 15 (2014) 680-689. doi: 10.1021/bm401736c.

[55] W. Li, Y. Lan, R. Guo, Y. Zhang, W. Xue, Y. Zhang, *In vitro* and *in vivo* evaluation of a novel collagen/cellulose nanocrystals scaffold for achieving the sustained release of basic fibroblast growth factor, J. Biomater. Appl. 29 (2015)882-893.doi: 10.1177/0885328214547091.

[56] C.J. Park, S.G. Clark, C.A. Lichtensteiger, R.D. Jamison, A.J.W. Johnson, Accelerated wound closure of pressure ulcers in aged mice by chitosan scaffolds with and without bFGF, Acta Biomater. 5 (2009) 1926-1936. doi: //dx.doi.org/10.1016/j.actbio.2009.03.002.

[57] K. Kawai, S. Suzuki, Y. Tabata, Y. Ikada, Y. Nishimura, Accelerated tissue regeneration through incorporation of basic fibroblast growth factor-impregnated gelatin microspheres into artificial dermis, Biomaterials 21 (2000)489-499.doi: //dx.doi.org/10.1016/S0142-9612(99)00207-0.

[58] K. Kawai, S. Suzuki, Y. Tabata, Y. Nishimura, Accelerated wound healing through the incorporation of basic fibroblast growth factor-impregnated gelatin microspheres into artificial dermis using a pressure-induced decubitus ulcer model in genetically diabetic mice, Br. J. Plast. Surg. 58 (2005) 1115-1123. doi: //dx.doi.org/10.1016/j.bjps.2005.04.010.

[59] S. Huang, T. Deng, H. Wu, F. Chen, Y. Jin, Wound dressings containing bFGF-impregnated microspheres, J. Microencapsul. 23 (2006)277-290.doi: 10.1080/02652040500435170.

[60] K. Ulubayram, A.N. Cakar, P. Korkusuz, C. Ertan, N. Hasirci, EGF containing gelatin-based wound dressings, Biomaterials 22 (2001) 1345-1356. doi: //dx.doi.org/10.1016/S0142-9612(00)00287-8.

[61] S. Dogan, S. Demirer, I. Kepenekci, B. Erkek, A. Kiziltay, N. Hasirci, S. Müftüoğlu, A. Nazikoğlu, N. Renda, U.D. Dincer, A. Elhan, E. Kuterdem, Epidermal growth factor-containing wound closure enhances wound healing in non-diabetic and diabetic rats, Int. Wound J. 6 (2009) 107-115. doi: 10.1111/j.1742-481X.2009.00584.x.

[62] W. Zhou, M. Zhao, Y. Zhao, Y. Mou, A fibrin gel loaded with chitosan nanoparticles for local delivery of rhEGF: preparation and in vitro release studies, J. Mater. Sci. Mater. Med. 22 (2011) 1221. doi: 10.1007/s10856-011-4304-9.

[63] X. Dong, J. Xu, W. Wang, H. Luo, X. Liang, L. Zhang, H. Wang, P. Wang, J. Chang, Repair effect of diabetic ulcers with recombinant human epidermal growth factor loaded by sustained-release microspheres, Sci. China C Life Sci. 51 (2008) 1039-1044. doi: 10.1007/s11427-008-0126-5.

[64] Y. Chu, D. Yu, P. Wang, J. Xu, D. Li, M. Ding, Nanotechnology promotes the full-thickness diabetic wound healing effect of recombinant human epidermal growth factor in diabetic

rats, Wound Repair Regen. 18 (2010) 499-505. doi: 10.1111/j.1524-475X.2010.00612.x.

[65] G. Gainza, J.J. Aguirre, J.L. Pedraz, R.M. Hernández, M. Igartua, rhEGF-loaded PLGA-Alginate microspheres enhance the healing of full-thickness excisional wounds in diabetised Wistar rats, Eur. J. Pharm. Sci. 50 (2013) 243-252.doi: //dx.doi.org/10.1016/j.ejps.2013.07.003.

[66] S.M. Royce, M. Askari, K.G. Marra, Incorporation of polymer microspheres within fibrin scaffolds for the controlled delivery of FGF-1, J. Biomater. Sci. Polym. Ed. 15 (2004) 1327-1336. doi: 10.1163/1568562041960016.

[67] K.K. Chereddy, C. Her, M. Comune, C. Moia, A. Lopes, P.E. Porporato, J. Vanacker, M.C. Lam, L. Steinstraesser, P. Sonveaux, H. Zhu, L.S. Ferreira, G. Vandermeulen, V. Préat, PLGA nanoparticles loaded with host defense peptide LL37 promote wound healing, J. Control Release 194 (2014) 138-147. doi: //dx.doi.org/10.1016/j.jconrel.2014.08.016.

[68] M. Hrynyk, M. Martins-Green, A.E. Barron, R.J. Neufeld, Sustained prolonged topical delivery of bioactive human insulin for potential treatment of cutaneous wounds, Int. J. Pharm. 398 (2010) 146-154. doi: //dx.doi.org/10.1016/j.ijpharm.2010.07.052.

[69] M. Hrynyk, M. Martins-Green, A.E. Barron, R.J. Neufeld, Alginate-PEG sponge architecture and role in the design of insulin release dressings, Biomacromolecules 13 (2012) 1478-1485. doi: 10.1021/bm300186k.

[70] S. Dhall, J. Silva, Y. Liu, M. Hrynyk, M. Garcia, A. Chan, J. Lyubovitsky, R. Neufeld, M. Martins-Green, Release of insulin from PLGA–alginate dressing stimulates regenerative healing of burn wounds in rats, Clin. Sci. 129 (2015) 1115-1129. doi: 10.1042/CS20150393.

[71] A. Mohandas, B.S. Anisha, K.P. Chennazhi, R. Jayakumar, Chitosan–hyaluronic acid/VEGF loaded fibrin nanoparticles composite sponges for enhancing angiogenesis in wounds, Colloids and Surfaces B: Biointerfaces 127 (2015) 105-113. doi: //dx.doi.org/10.1016/j.colsurfb.2015.01.024.

[72] Y.M. Elcin, V. Dixit, G. Gitnick, Extensive in vivo angiogenesis following controlled release of human vascular endothelial cell growth factor: implications for tissue engineering and wound healing, Artif. Organs 25 (2001) 558-565. doi: aor6830 [pii].

[73] K.K. Chereddy, A. Lopes, S. Koussoroplis, V. Payen, C. Moia, H. Zhu, P. Sonveaux, P. Carmeliet, A. des Rieux, G. Vandermeulen, V. Préat, Combined effects of PLGA and vascular endothelial growth factor promote the healing of non-diabetic and diabetic wounds, Nanomedicine 11 (2015) 1975-1984. doi: //dx.doi.org/10.1016/j.nano.2015.07.006.

[74] P. Losi, E. Briganti, C. Errico, A. Lisella, E. Sanguinetti, F. Chiellini, G. Soldani, Fibrin-based scaffold incorporating VEGF- and bFGF-loaded nanoparticles stimulates wound healing in diabetic mice, Acta Biomater. 9 (2013)7814-7821.doi: //dx.doi.org/10.1016/j.actbio.2013.04.019.

[75] M.P. Ribeiro, P.I. Morgado, S.P. Miguel, P. Coutinho, I.J. Correia, Dextran-based hydrogel containing chitosan microparticles loaded with growth factors to be used in wound

healing, Mater. Sci. Eng. C Mater. Biol. Appl. 33 (2013) 2958-2966. doi: //dx.doi.org/10.1016/j.msec.2013.03.025.

[76] F. Fontana, M. Mori, F. Riva, E. MÃ¤kilÃ¤, D. Liu, J. Salonen, G. Nicoletti, J. Hirvonen, C. Caramella, H. Santos, Platelet lysate-modified porous silicon microparticles for enhanced cell proliferation in wound healing applications, ACS Appl. Mater. Interfaces 8 (2016) 988-996. doi: 10.1021/acsami.5b10950.

[77] Y. Takabayashi, M. Ishihara, Y. Sumi, M. Takikawa, S. Nakamura, T. Kiyosawa, Platelet-rich plasma-containing fragmin-protamine micro-nanoparticles promote epithelialization and angiogenesis in split-thickness skin graft donor sites, J. Surg. Res. 193 (2015) 483-491. doi: //dx.doi.org/10.1016/j.jss.2014.08.011.

[78] W. La, H.S. Yang, Heparin-conjugated poly(lactic-co-glycolic acid) nanospheres enhance large-wound healing by delivering growth factors in platelet-rich plasma, Artif. Organs 39 (2015) 388-394. doi: 10.1111/aor.12389.

[79] T.S.R. Lakshmi, N. Shanmugasundaram, S. Shanmuganathan, M. Babu, Efficacy of desulfated heparin mitigating inflammation in rat burn wound model, J. Biomed. Mater. Res. B Appl. Biomater. 97B (2011) 215-223. doi: 10.1002/jbm.b.31797.

[80] F. Blažević, T. Milekić, M.D. Romić, M. Juretić, I. Pepić, J. Filipović-Grčić, J. Lovrić, A. Hafner, Nanoparticle-mediated interplay of chitosan and melatonin for improved wound epithelialisation, Carbohydr. Polym. 146 (2016) 445-454. doi: //dx.doi.org/10.1016/j.carbpol.2016.03.074.

[81] T. Tang, H. Jiang, Y. Yu, F. He, S. Ji, Y. Liu, Z. Wang, S. Xiao, C. Tang, G. Wang, Z. Xia, A new method of wound treatment: targeted therapy of skin wounds with reactive oxygen species-responsive nanoparticles containing SDF-1α, Int. J. Nanomedicine 10 (2015) 6571-6585. doi: 10.2147/IJN.S88384.

[82] T.M. Allen, P.R. Cullis, Liposomal drug delivery systems: From concept to clinical applications, Adv. Drug Deliv. Rev. 65 (2013) 36-48.doi: //dx.doi.org/10.1016/j.addr.2012.09.037.

[83] D.B. Yarosh, Liposomes in investigative dermatology, Photodermatol. Photoimmunol. Photomed. 17 (2001) 203-212. doi: 10.1111/j.1600-0781.2001.170501.x.

[84] M. Toh, G.N.C. Chiu, Liposomes as sterile preparations and limitations of sterilisation techniques in liposomal manufacturing, Asian Journal of Pharmaceutical Sciences 8 (2013) 88-95.doi: //dx.doi.org/10.1016/j.ajps.2013.07.011.

[85] Y. Rahimpour, H. Hamishehkar, Liposomes in cosmeceutics, Expert Opin. Drug Deliv. 9 (2012) 443-455. doi: 10.1517/17425247.2012.666968.

[86] G.L. Brown, L.J. Curtsinger, M. White, R.O. Mitchell, J. Pietsch, R. Nordquist, A. Fraunhofer, G.S. Schultz, Acceleration of tensile strenght of incisions treated with EGF and TGF-beta, Ann. Surg. 208 (1988) 788-794.

[87] C. Alemdaroğlu, Z. Degim, N. Celebi, M. Şengezer, M. Alömeroglu, A. Nacar, Investigation of epidermal growth factor containing lip-

osome formulation effects on burn wound healing, J. Biomed. Mater. Res. A 85A (2008) 271-283. doi: 10.1002/jbm.a.31588.

[88] Z. Değim, N. Çelebi, C. Alemdaroğlu, M. Deveci, S. Öztürk, C. Özoğul, Evaluation of chitosan gel containing liposome-loaded epidermal growth factor on burn wound healing, Int. Wound J. 8 (2011) 343-354. doi: 10.1111/j.1742-481X.2011.00795.x.

[89] E.J. Pierre, J.R. Perez-polo, A.T. Mitchell, S. Matin, H.L. Foyt, D.n. Hernfon, Insuline-like growth factor-I liposomal gene transfer and systemic growth hormone stimulate wound healing, J. Burn Care Rehabil. 18 (1997) 287-291.

[90] Q. Xiang, J. Xiao, H. Zhang, X. Zhang, M. Lu, H. Zhang, Z. Su, W. Zhao, C. Lin, Y. Huang, X. Li, Preparation and characterisation of bFGF-encapsulated liposomes and evaluation of wound-healing activities in the rat, Burns 37 (2011) 886-895. doi: //dx.doi.org/10.1016/j.burns.2011.01.018.

[91] M.A.P. Olekson, R. Faulknor, A. Bandekar, M. Sempkowski, H.C. Hsia, F. Berthiaume, SDF-1 liposomes promote sustained cell proliferation in mouse diabetic wounds, Wound Repair Regen. 23 (2015) 711-723. doi: 10.1111/wrr.12334.

[92] M. Schäfer-Korting, W. Mehnert, H. Korting, Lipid nanoparticles for improved topical application of drugs for skin diseases, Adv. Drug Deliv. Rev. 59 (2007) 427-443. doi: //dx.doi.org/10.1016/j.addr.2007.04.006.

[93] R.H. Müller, R.D. Petersen, A. Hommoss, J. Pardeike, Nanostructured lipid carriers (NLC) in cosmetic dermal products, Adv. Drug Deliv. Rev. 59 (2007) 522-530. doi: //dx.doi.org/10.1016/j.addr.2007.04.012.

[94] R.H. Müller, M. Radtke, S.A. Wissing, Solid lipid nanoparticles (SLN) and nanostructured lipid carriers (NLC) in cosmetic and dermatological preparations, Adv. Drug Deliv. Rev. 54, Supplement (2002) S155. doi: //dx.doi.org/10.1016/S0169-409X(02)00118-7.

[95] J. Pardeike, A. Hommoss, R.H. Müller, Lipid nanoparticles (SLN, NLC) in cosmetic and pharmaceutical dermal products, Int. J. Pharm. 366 (2009) 170-184. doi: //dx.doi.org/10.1016/j.ijpharm.2008.10.003.

[96] S. Das, W.K. Ng, R.B.H. Tan, Are nanostructured lipid carriers (NLCs) better than solid lipid nanoparticles (SLNs): development, characterizations and comparative evaluations of clotrimazole-loaded SLNs and NLCs?, Eur. J. Pharm. Sci. 47 (2012) 139-151. doi: //dx.doi.org/10.1016/j.ejps.2012.05.010.

[97] G. Gainza, M. Pastor, J.J. Aguirre, S. Villullas, J.L. Pedraz, R.M. Hernandez, M. Igartua, A novel strategy for the treatment of chronic wounds based on the topical administration of rhEGF-loaded lipid nanoparticles: In vitro bioactivity and in vivo effectiveness in healing-impaired db/db mice, J. Control Release 185 (2014) 51-61. doi: //dx.doi.org/10.1016/j.jconrel.2014.04.032.

[98] G. Gainza, D.C. Bonafonte, B. Moreno, J.J. Aguirre, F.B. Gutierrez, S. Villullas, J.L. Pedraz, M. Igartua, R.M. Hernandez, The topical administration of rhEGF-loaded nanostructured lipid carriers (rhEGF-NLC) improves healing in a porcine full-thickness excisional wound model, J. Control Release 197 (2015)

41-47. doi: //dx.doi.org/10.1016/j.jconrel.2014 .10.033.

[99] G. Gainza, W.S. Chu, R.H. Guy, J.L. Pedraz, R.M. Hernandez, B. Delgado-Charro, M. Igartua, Development and in vitro evaluation of lipid nanoparticle-based dressings for topical treatment of chronic wounds, Int. J. Pharm. 490 (2015) 404-411. doi: //dx.doi.org/ 10.1016/j.ijpharm.2015.05.075.

[100] I. Garcia-Orue, G. Gainza, C. Girbau, R. Alonso, J.J. Aguirre, J.L. Pedraz, M. Igartua, R.M. Hernandez, LL37 loaded nanostructured lipid carriers (NLC): A new strategy for the topical treatment of chronic wounds, Eur. J. Pharm. Biopharm. (2016). doi: //dx.doi.org/10. 1016/j.ejpb.2016.04.006.

[101] K.C. Gupta, A. Haider, Y. Choi, I. Kang, Nanofibrous scaffolds in biomedical applications, Biomater. Res. 18 (2014) 5. doi: 10.1186/2055-7124-18-5.

[102] M. Abrigo, S.L. McArthur, P. Kingshott, Electrospun nanofibers as dressings for chronic wound care: advances, challenges, and future prospects, Macromol. Biosci. 14 (2014) 772-792. doi: 10.1002/mabi.201300561.

[103] L. Pachuau, Recent developments in novel drug delivery systems for wound healing, Expert. Opin. Drug Deliv. 12 (2015) 1895-1909. doi: 10.1517/17425247.2015.1070143.

[104] N. Bhattarai, D. Edmondson, O. Veiseh, F.A. Matsen, M. Zhang, Electrospun chitosan-based nanofibers and their cellular compatibility, Biomaterials 26 (2005) 6176-6184. doi: //dx.doi.org/10.1016/j.biomaterials. 2005.03.027.

[105] J.S. Choi, H.S. Kim, H.S. Yoo, Electrospinning strategies of drug-incorporated nanofibrous mats for wound recovery, Drug Deliv. Transl. Res. 5 (2015) 137-145. doi: 10.1007/s13346-013-0148-9.

[106] I. Garcia-Orue, G. Gainza, F.B. Gutierrez, J.J. Aguirre, C. Evora, J.L. Pedraz, R.M. Hernandez, A. Delgado, M. Igartua, Novel nanofibrous dressings containing rhEGF and Aloe vera for wound healing applications, Int. J. Pharm. (2016). doi: //dx.doi.org/10.1016 /j.ijpharm.2016.11.006.

[107] Z. Wang, Y. Qian, L. Li, L. Pan, L.W. Njunge, L. Dong, L. Yang, Evaluation of emulsion electrospun polycaprolactone/hyaluronan/epidermal growth factor nanofibrous scaffolds for wound healing, J. Biomater. Appl. 30 (2016) 686-698. doi: 10.1177/ 0885328215586907.

[108] Y. Yang, T. Xia, W. Zhi, L. Wei, J. Weng, C. Zhang, X. Li, Promotion of skin regeneration in diabetic rats by electrospun core-sheath fibers loaded with basic fibroblast growth factor, Biomaterials 32 (2011) 4243-4254. doi: //dx.doi.org/10.1016/j.biomaterials.2011.02.042.

[109] V. Bertoncelj, J. Pelipenko, J. Kristl, M. Jeras, M. Cukjati, P. Kocbek, Development and bioevaluation of nanofibers with blood-derived growth factors for dermal wound healing, Eur. J. Pharm. Biopharm. 88 (2014) 64-74. doi: //dx.doi.org/10.1016/j.ejpb.2014.06.001.

[110] H. Lai, C. Kuan, H. Wu, J. Tsai, T. Chen, D. Hsieh, T. Wang, Tailored design of electrospun composite nanofibers with staged release of multiple angiogenic growth factors for

chronic wound healing, Acta Biomater. 10 (2014)4156-4166.doi: //dx.doi.org/10.1016/j.actbio.2014.05.001.

[111] Z. Xie, C.B. Paras, H. Weng, P. Punnakitikashem, L. Su, K. Vu, L. Tang, J. Yang, K.T. Nguyen, Dual growth factor releasing multi-functional nanofibers for wound healing, Acta Biomater. 9 (2013) 9351-9359. doi: //dx.doi.org/10.1016/j.actbio.2013.07.030.

[112] E.S. Gil, B. Panilaitis, E. Bellas, D.L. Kaplan, Functionalized silk biomaterials for wound healing, Adv. Healthc. Mater. 2 (2013) 206-217. doi: 10.1002/adhm.201200192.

[113] G. Jin, M.P. Prabhakaran, D. Kai, S. Ramakrishna, Controlled release of multiple epidermal induction factors through core–shell nanofibers for skin regeneration, Eur. J. Pharm. Biopharm. 85 (2013) 689-698. doi: //dx.doi.org/10.1016/j.ejpb.2013.06.002.

[114] G. Jin, M.P. Prabhakaran, S. Ramakrishna, Photosensitive and biomimetic core-shell nanofibrous scaffolds as wound dressing, Photochem. Photobiol. 90 (2014) 673-681. doi: 10.1111/php.12238.

[115] R.S. Tigli, N.M. Kazaroglu, B. Mavis, M. Gumusderelioglu, Cellular behavior on epidermal growth factor (EGF)-immobilized PCL/gelatin nanofibrous scaffolds, J. Biomater. Sci. Polym. Ed. 22 (2011) 207-223. doi: 10.1163/092050609X12591500475424.

[116] M. Gümüşderelioğlu, S. Dalkıranoğlu, R.S.T. Aydın, S. Çakmak, A novel dermal substitute based on biofunctionalized electrospun PCL nanofibrous matrix, J. Biomed. Mater. Res. A 98A (2011) 461-472. doi: 10.1002/jbm.a.33143.

[117] J.S. Choi, K.W. Leong, H.S. Yoo, *In vivo* wound healing of diabetic ulcers using electrospun nanofibers immobilized with human epidermal growth factor (EGF), Biomaterials 29 (2008) 587-596. doi: //dx.doi.org/10.1016/j.biomaterials.2007.10.012.

[118] J.S. Choi, S.H. Choi, H.S. Yoo, Coaxial electrospun nanofibers for treatment of diabetic ulcers with binary release of multiple growth factors, J. Mater. Chem. 21 (2011) 5258-5267. doi: 10.1039/C0JM03706K.

[119] D.W. Song, S.H. Kim, H.H. Kim, K.H. Lee, C.S. Ki, Y.H. Park, Multi-biofunction of antimicrobial peptide-immobilized silk fibroin nanofiber membrane: Implications for wound healing, Acta Biomater. 39 (2016) 146-155. doi: //dx.doi.org/10.1016/j.actbio.2016.05.008.

[120] S. Patel, K. Kurpinski, R. Quigley, H. Gao, B.S. Hsiao, M. Poo, S. Li, Bioactive nanofibers: synergistic effects of nanotopography and chemical signaling on cell guidance, Nano Lett. 7 (2007) 2122-2128. doi: 10.1021/nl071182z.

[121] R.H. Fitzgerald, M. Bharara, J.L. Mills, D.G. Armstrong, Use of a Nanoflex powder dressing for wound management following debridement for necrotising fasciitis in the diabetic foot, International Wound Journal 6 (2009) 133-139. doi: 10.1111/j.1742-481X.2009.00596.x.

[122] T.J. Kelechi, M. Mueller, C.S. Hankin, A. Bronstone, J. Samies, P.A. Bonham, A randomized, investigator-blinded, controlled pilot study to evaluate the safety and efficacy of a poly-N-acetyl glucosamine–derived membrane

material in patients with venous leg ulcers, J. Am. Acad. Dermatol. 66 (2012) e215. doi: //dx.doi.org/10.1016/j.jaad.2011.01.031.

[123] Bethesda (MD): National Library of Medicine (US). [Internet]. NCT02680106, Evaluation of the SPINNER Device for the Application of Wound Dressing: Treatment of Split Skin Graft Donor Sites (SPINNER01); 2016. Available from:https://clinicaltrials.gov/ct2/show/NCT02680106?term=spinner&rank=1 (Accessed 2017/02/10/).

# Objectives

As stated in the introduction, current therapies cannot provide an effective healing for chronic wounds, which are becoming a health burden. In addition, their incidence is growing; since the high-risk population, which comprises diabetic, obese, smokers or elderly people, is rising alarmingly. Therefore, the development of new therapies for delayed wound healing has gained importance in the last years. Among others, the administration of endogenous molecules involved in the healing process is one of the most promising new therapies. Nevertheless, due to their short stability *in vivo*, they need to be protected from the proteases of the wound bed by being encapsulated into carriers, such as lipid nanoparticles. Another alternative for wound healing is the use of nanofibrous membranes, since their unique structure present a high porosity and surface area to volume ratio, which enhances wound healing. Finally, another interesting strategy is the development of bilayer dressings, which combine the different properties and functions of each layer, *e.g.*, the dense upper layer has a protective function and the porous lower layer is designed to absorb wound exudates.

Taking all the previous described aspects into account, the aim of the current thesis was the development and characterisation of different therapeutic approaches for wound healing management. Concretely, the objectives of the present study were the following:

1. Development, characterisation and *in vivo* assessment of the efficacy of nanostructured lipid carriers (NLCs) containing the human peptide LL37.

2. Development, characterisation and *in vivo* assessment of the efficacy of electrospun nanofibrous dressings composed of PLGA and *Aloe vera* containing EGF.

3. Incorporation of NLCs to the PLGA/*Aloe vera* dressings in order to improve some of their features, such as the removal, handling, elasticity and occlusivity.

4. Development, characterisation and *ex vivo* assessment of the efficacy of a bilayer hydrofilm dressing composed of gelatin and chitosan.

# Experimental work

# CHAPTER 1

## LL37 loaded nanostructured lipid carriers (NLC): a new strategy for the topical treatment of chronic wounds

I. Garcia-Orue[a], G. Gainza[a,c], C. Girbau[d], R. Alonso[d], .J.J. Aguirre[e], J.L. Pedraz[a,b], M. Igartua[a,b] and R.M.Hernandez[a,b,*]

[a] NanoBioCel Group, Laboratory of Pharmaceutics, School of Pharmacy, University of the Basque Country (UPV/EHU).

[b] Biomedical Research Networking Centre in Bioengineering, Biomaterials and Nanomedicine (CIBER-BBN).

[c] Biopraxis Research AIE, Miñano, Vitoria-Gasteiz.

[d] Department of Immunology, Microbiology and Parasitology, School of Pharmacy, University of the Basque Country .

[e] Hospital Universitario de Álava (HUA) Txagorritxu, Vitoria-Gasteiz, 01009, Spain.

*Corresponding author: Prof. Rosa Maria Hernandez.

**ABSTRACT**

The LL37 is a human antimicrobial peptide which not only has a broad spectrum of antimicrobial activity, but it has also been proved to modulate wound healing by participating in angiogenesis, epithelial cell migration and proliferation, and immune response. In this work, LL37 has been encapsulated in nanostructured lipid carriers (NLCs), produced by the melt-emulsification method, in order to improve its effectiveness. The characterisation of the NLC-LL37 showed a mean size of 270 nm, a zeta potential of -26 mV and an encapsulation efficiency of 96.4%. The cytotoxicity assay performed in Human Foreskin Fibroblasts demonstrated that the NLC-LL37 did not affect cell viability. Moreover, the *in vitro* bioactivity assay evidenced that the peptide remained active after the encapsulation, since the NLC-LL37 reversed the activation of the macrophages induced by LPS in the same way as the LL37 in solution. In addition, the *in vitro* antimicrobial assay revealed the NLC-LL37 activity against *E. coli*. The effectiveness of the nanoparticles was assessed in a full thickness wound model in *db/db* mice. The data demonstrated that NLC-LL37 significantly improved healing compared to the same concentration of the LL37 solution in terms of wound closure, reepithelisation grade and restoration of the inflammatory process. Overall, these findings suggest a promising potential of the NLC-LL37 formulation for chronic wound healing.

**Published in:** European Journal of Pharmaceutics and Biopharmaceutics 108 (2016), 310-316. Doi: https://doi.org/10.1016/j.ejpb.2016.04.006

## 1. Introduction

The incidence of suffering non-healing chronic wounds has exponentially increased with aging of population together with the resultant comorbidities of diabetes, venous insufficiency and associated chronic diseases. It has been estimated that 1-2% of the population in the developed countries would experience a chronic wound in their lifetime, representing 2% of the European health budget according to the United Nations [1,2].

Cutaneous wound healing is an orderly and timely reparative process, designed to restore the skin barrier function and homeostasis. It is accomplished by regulated processes that overlap in space and time, including an initial inflammatory response, a proliferative phase and a final remodelling phase [3,4]. Chronic wounds fail to proceed in these subsequent phases, stagnating in a permanent inflammatory state in which the wound do not heal. This inflammation maintains a constant infiltration of macrophages and neutrophils, which produce an excessive amount of collagenases, proteases and reactive oxygen species that degrade healing mediators and hamper the formation of the extracellular matrix and new epithelia. In addition, these lesions usually get infected and remain open for extended periods of time, occasionally endangering the life of the patient [1,5].

Current advances in wound care have focused on finding new treatments for wound healing, such as the administration of healing mediators for wound repair. In this regard, one of the strategies that is gaining a notorious interest is the administration of the human antimicrobial peptide LL37. It should be noted that the downregulation of LL37 has been associated with an increased risk in suffering chronic ulcers [6].

The LL37 has been detected in an inactive preform (hCAP18) in several immune and dermal-epithelial cells. After a skin injury, hCAP18 is released to the extracellular environment due to cell degranulation, leading to its activation into the LL37 peptide [4,7]. It has been proven that this molecule modulates wound healing by activating angiogenesis [8,9] and epithelial cell migration and proliferation [10,11]. Furthermore, it has demonstrated a broad spectrum of antimicrobial, antiviral and antifungal activity [12-15].

In addition, the LL37 presents an immunomodulatory effect, since it is chemotactic to monocytes, neutrophils and dendritic cells [13]. The LL37 also shows the ability to neutralise the proinflamatory responses exerted by macrophages (very important in chronic wounds) by its union to lipopolysaccharide (LPS) [13,16].

The *in vivo* wound healing studies conducted to date, have required high doses and dosing frequencies of free LL37 because of the rapid degradation of the peptide [15,17] or gene therapy [18] to achieve improved healing. With the aim of overcoming these limitations, Chereddy and cols. encapsulated the LL37 peptide into PLGA nanoparticles obtaining a significantly improvement in the wound healing activity after intradermal administration [19]. In line with this approach, the encapsulation of LL37 into nanostructured lipid carriers (NLC) is presented as a promising alternative to optimise the administration of the LL37 in terms of dose, delivery pattern, and safety. The NLCs, besides of protecting the encapsulated peptide against the degradation of the proteases, can be administered through the topical route, thereby reducing the systemic effects due to a lower systemic bioavailability of the drug. Furthermore, the NLCs allow a sustained release of the drugs at the site of action and present an excellent biocompatibility, making them a suitable option for the topical treatment of chronic wounds [20-22].

Thus, the aim of our study is the development of a topical formulation based on LL37 loaded NLCs (NLC-LL37) for the treatment of chronic wounds. *In vitro* studies were carried out to determine the biocompatibility of the formulation and the activity against LPS of the encapsulated LL37. In addition, antimicrobial tests were undertaken in *E. coli* to analyse the efficacy of NLC-LL37 against bacteria. Finally, the wound healing activity of the NLC-LL37 was evaluated *in vivo* in a full thickness wound model in *db/db* mice.

## 2. Materials and methods

### *2.1 NLC-LL37 preparation*

The NLC-LL37 were prepared trough the melt emulsification method and following the procedure previously described by our group [23,24]. Briefly, a warm aqueous phase (heated at 40 °C, 1 min) containing 3 ml of water, 20 mg of Poloxamer 188 (Panreac, Spain) and 40 mg of Tween® 80 (Panreac, Spain) was added to a melted lipid phase containing 200 mg of the solid lipid Precirol® ATO 5 (Gattefossé Spain, Spain) and 20 mg of the liquid lipid Miglyol® 812N (Sasol Germany GmbH). Then, 50 µL of an 80 mg/mL LL37 (95.0% pure, Caslo ApS, DK) aqueous solution was added and immediately after, the mixture was emulsified for 15 s at 50 W (Branson® 250 sonifier, CT, USA). The resulting emulsion was stored at 4°C to allow the re-crystallisation of the lipid for the NLC formation. On the following day, the particles were collected using a 100 kDa molecular weight cut-off centrifugal filter unit (Amicon, "Ultracel-100k", Millipore, Spain) at 2,500 rpm for 10 minutes and washed three times with MillliQ water. Finally, the NLC suspension was freeze dried with the cryoprotectant trehalose (Sigma-Aldrich, Spain) in a final concentration of 15% (w/w) of the weighed lipid. The target loading of LL-37 in NLCLL37 was 2% (w/w).

### *2.2 Nanoparticle characterisation*

The mean particle size (Z-average diameter) and the polydispersity index (PDI) were measured by Dynamic Light Scattering (DLS), and the zeta potential was determined through Laser Doppler microelectrophoresis (Malvern® Zetasizer Nano ZS, Model Zen 3600; Malvern instruments Ltd., UK). The measurement medium for zeta potential was water (pH 5.6), and the measured electrophoretic mobility was converted into zeta potential through the Smoluchowski approximation. Each assay was performed in triplicate after nanoparticles lyophilisation. Nanoparticle morphology was examined by transmission electron microscopy (TEM, Philips EM208S).

The encapsulation efficiency (EE) of the NLC-LL37 was assessed indirectly by measuring the free LL37 (non-encapsulated) in the supernatant obtained after the filtration/centrifugation process described in Section 2.1. The amount of free LL37 was quantified using a commercially available ELISA kit for LL37 (human LL37 ELISA kit, Hycult® biotech, Netherlands). The EE (%) was determined using the following equation (1):

$$EE(\%)=\frac{\text{Teoric amount -Free amount}}{\text{Teoric amount of LL37}}\times 100 \quad (1)$$

### *2.3* In vitro *cell culture studies*

#### *2.3.1 Cell culture*

Human Foreskin Fibroblasts (HFF) (ATCC, Manassas, USA) were cultured on Dulbeccos's modified Eagle's medium (DMEM) (ATCC, Manassas, USA) supplemented with 15% (v/v) fetal bovine serum (FBS), 1% (v/v) L-glutamine and 1% (v/v) penicillin-streptomycin.

The RAW 264.7 cell line (Murine Macrophages; ATCC, Manassas, USA) was cultured on a specific growth medium DMEM/F-12, GlutaMAX™ Supplement (Gibco®, Life Technologies, Spain) supplemented with 10% (v/v) FBS and 1% (v/v) penicillin-streptomycin.

The cell lines were maintained at 37°C in a humidified incubator with a 5% $CO_2$ atmosphere. The cell passages were performed every 2-3 days depending on the cell line.

#### *2.3.2 Cell viability studies*

The effect of the NLC-LL37 on cell viability was assayed using HFF cells. 1000 cells/well were seeded into 96-well culture plates and incubated 24 h to allow cell attachment. Then, the medium was replaced by serial concentrations of NLC-LL37 (corresponding to 5000-50 ng of LL37/mL) and empty NLCs resuspended in 1% serum-supplemented-DMEM. After 48 h of incubation, the cell viability was measured by adding 10 µL of CCK-8 reagent (Sigma-Aldrich, Saint Louise, USA) to the wells. The mixture was incubated for 4 h and the absorbance was then read at 450 nm and at 650 nm as the reference wavelength. The absorbance was directly proportional to the number of living cells in the culture.

### *2.3.3 Inhibition of macrophages activation induced by LPS*

This assay was conducted in the RAW 264.7 cell line. $10^5$ cells/well were seeded into a 96-well culture plate and incubated for 24 h to allow cell attachment. Then, the medium was replaced by the following samples (all of them were resuspended in 1% serum-supplemented DMEM/F-12 containing 20 ng/ml of LPS prior to their incorporation into the cell culture): (i) 5000 ng/ml of free LL37, (ii) the NLC-LL37 concentration equivalent to 5000 ng/ml of LL37 and (iii) the same concentration of empty NLC. As negative control 1% serum-supplemented medium was used and as positive control 1% serum-supplemented medium with 20 ng/ml of LPS.

After 6 h of incubation, the supernatant of the wells was collected to quantify the TNF-α released from the macrophages using a commercially available ELISA kit (Murine TNF-α ELISA Development kit, PeproTech, USA). The results were displayed as the percentage of absorbance value of each group compared to those obtained in the negative control.

### *2.4 Antimicrobial assay*

In order to test the antimicrobial activity of the formulations, *Escherichia coli* ATCC 25922 was grown overnight at 37°C in Mueller Hinton broth (Conda, Pronadisa, Spain). Then, the bacterial suspension was diluted to $10^5$ CFU/ml. Free LL37 (20 µg/ml), NLC-LL37 (the concentration corresponding to 20 µg/ml LL37) and empty NLC (the same nanoparticle concentrations as the previous group) were incubated with 1 ml of this bacterial suspension at 37°C with gentle agitation. In addition, 1 ml of the bacterial suspension alone was also incubated, to use it as control.

At 4 h of incubation, aliquots were taken from each suspension, diluted in PBS and 100 µl were inoculated in Mueller Hinton agar plates (Conda/Pronadisa, Spain). The plates were incubated for 24 h at 37°C and subsequently, the colony forming units were determined as the total number of colonies grown on each plate. Three independent experiments were performed. The antibacterial effect was assessed as the percentage of death cells compared to the control.

## *2.5* In vivo *wound healing study*

### *2.5.1. Animals*

For the *in vivo* experiment, 16 eight week-old male *db/db* (BKS.Cg-*m*+/+Lepr$^{db}$/J) mice were used (Janvier laboratories, France). Every experiment was conducted according to the protocols approved by the Institutional Ethical Committee for Animal Experimentation of the University of the Basque Country (Procedure number: CEBA/243/ 2012/HERNANDEZ MARTIN). Animals were housed in individual cages that were maintained on a 12 h light-dark cycle, and were given standard rodent chow and water *ad libitum*.

### *2.5.2 Wound healing assay*

The wound healing assay was performed adapting the procedure described by Michaels *et al.* [25]. Human main healing mechanism is through granulation tissue formation and re-epithelisation, while mice's one is through wound contraction. In order to mimic human healing process and avoid mice's main process, two silicone rings of 1 cm in diameter were sutured on each side of the midline using a 3-0 nylon suture (Aragó, Spain), after anesthetising the mice and removing their dorsal hair. Then, two full thickness wounds of 8 mm in diameter and extending through the *panniculus carnosus* were created using a punch biopsy tool (Acu-Punch, Acuderm, USA). After the administration of the treatments, the wounds were covered with one layer of petrolatum gauze (Tegaderm® 3M) and two layers of adhesive.

The mice were divided in 4 groups (n=4): (i) untreated control, (ii) 6 µg of free LL37, (iii) 6 µg of LL37 encapsulated into NLC-LL37 and (iv) 2 µg of LL37 encapsulated into NLC-LL37. Treatments, previously resuspended in 10 µL of MilliQ water, were administered topically allowing them to spread over the wound bed, on day 1 and 4 after the wound induction. On day 8, the mice were sacrificed through $CO_2$ inhalation.

### *2.5.3 Evaluation of wound healing*

The effectiveness of the treatments was evaluated by measuring the wound area ($px^2$) on days 1, 4 and 8 after the surgery.

Those days, photographs of the wounds were taken using a digital camera (Lumix FS16, Panasonic®, Spain), and the wound area was assessed with an image analysis programme (ImageJ®, Biophotonics Facility, University of McMaster, Canada). The wound closure was expressed as the percentage of the initial wound area.

*2.5.4 Histological analysis of healing*

After the sacrifice of the mice, the wound and surrounding tissue (~1 cm) were excised and fixed in 3.7 % paraformaldehyde for 24 h. Then the tissues were bisected, embedded in paraffin, and sectioned in 5 µm thick layers. Samples were processed by H&E staining for wound healing evaluation and by Masson trichrome staining for collagen deposition evaluation.

The re-epithelisation process was assessed following the scale established by Sinha *et al., 2003* [26]. The score of each wound was determined semi-quantitatively giving to each wound a value within a range from 0 to 4: 0, reepithelisation at the margin of the wound; 1, reepithelisation covering less than half of the wound; 2, reepithelisation covering more than half of the wound; 3, reepithelisation covering the entire wound with irregular thickness, and 4, reepithelisation covering the entire wound with normal thickness.

The resolution of the inflammatory process and wound maturity was determined according to the scale described by Cotran *et al*., 2000 [27]: 1, acute inflammation, with the formation of fibrin clot and migration of leucocytes and polynuclear neutrophils; 2, diffuse acute inflammation, with the predominance of granulation tissue formation and angiogenesis and with barely presence of pyogenic membrane; 3, chronic inflammation, with the presence of granulation tissue and with fibroblast proliferation and 4, resolution and healing, disappearance of chronic inflammation, although occasionally round cells can be found.

The deposition of collagen was determined following the scale described by Gal *et al, 2006.* [28]: 0, absent of collagen; 1, mild content of collagen; 2, moderate content of collagen and 3, marked content of collagen.

*2.5.5 Immunohistochemistry*

In order to assess neoangiogenesis in the wound bed, immunohistochemical studies were performed using a specific monoclonal anti-CD31 antibody (JC70 clon, 760-4378, Ventana-Roche). 5 µm thick tissue slides were incubated with the primary antibody for 36 min at 37 °C, and subsequently the layers were treated with Ultraview Universal DAB detection kit (760-500, Ventana-Roche) to visualize the antigen. Afterwards, the number of blood vessels was counted per field.

*2.6 Statistical analyses*

All of the data are expressed as the mean ± standard deviation. Based on the result of the normality test and the Levene test for the homogeneity of variances, the means were compared through one-way ANOVA, with the subsequent application of Student-Newman-Keuls post-hoc; or through Mann-Whitney U test. All the statistical calculations were performed using SPSS 22.0.01 (SPSS®, INC., Chicago, IL, USA).

## 3. Results and discussion

3.*1 Nanoparticle characterisation*

As illustrated in Table 1 the NLC-LL37 and the empty NLC showed similar mean size, however, the NLC-LL37 exhibited a slightly higher size: 273.6 ± 27.64 nm and 220.6 ± 5.48 nm, respectively. The polydispersity index (PDI) was below 0.4 in both formulations, indicating a stable polydisperse system. The analysis of the zeta potential revealed that both formulations presented a similar surface charge of about -31 mV in the case of NLC-LL37

**Table 1**.Characterisation of NLCs: Mean size, PDI, zeta potential, EE and peptide loading. Data are shown as the means ± SD.

| | Size (nm) | PDI | Zeta Potential (mV) | EE % | Peptide loading (µg LL37/mg NLC) |
|---|---|---|---|---|---|
| NLC-LL37 | 273.6±27.64 | 0.3 ±0.06 | -31.63±1.94 | 96.40±0.41 | 16.76 ± 0.07 |
| Empty NLC | 220.6 ± 5.48 | 0.27 ±0.03 | -26.10 ±0.53 | | |

and about -26 mV in the case of empty NLCs. In addition, the NLC-LL37 presented high encapsulation efficiency (96.40 ± 0.41 %) and a peptide loading of 16.76 ± 0.07 µg LL37/mg nanoparticle.

According to the TEM photographs of the nanoparticles, they showed a similar size to that obtained with DLS (Fig. 1).

*3.2* In vitro *cell culture studies*

*3.2.1 Cell viability*

In order to evaluate the cytotoxicity of the NLCs, HFF cells were incubated for 48 h in the presence of the particles, and then the cell viability was determined using a CCK-8 assay. As shown in Fig. 2, neither the NLC-LL37 nor the empty NLC did affect the cell viability, demonstrating the absence of toxicity of the formulations.

*3.2.2 Inhibition of macrophage activation*

With the aim of determining whether the encapsulation process affects the bioactivity of the peptide, the ability of the LL37 binding the LPS endotoxin was determined.

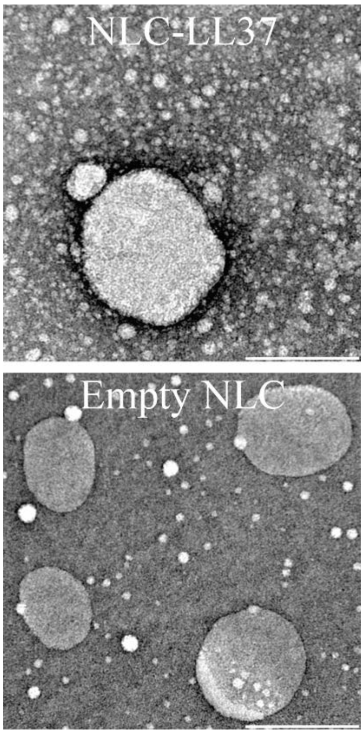


**Fig. 1.** TEM photographs of NLC-LL37 and empty NLCs. The scale bar indicates 200 nm.

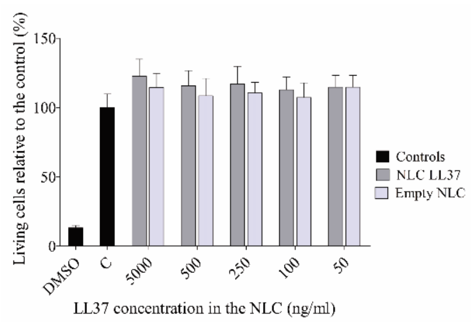


**Fig. 2.** Cell viability after NLC treatment. The results are given as the mean % of living cells relative to the control ± SD. Controls are C (cells without any addition) and DMSO (cells after addition of DMSO).

To quantify the binding ability, the TNF-α released from the RAW 267.4 macrophage cell line was measured, because the union between the LL37 and the LPS inhibits the activation of the macrophages, and therefore its cytokine release, including the TNF-α.

As depicted in Fig. 3, the peptide remains active after the encapsulation, since the level of TNF-α released from the macrophages after the incubation with LPS decreased similar to when they were treated with NLC-LL37 or with the free peptide. However, after the administration of empty NLCs, reversal of the TNF-α production was not observed, which indicated that the inhibition of the macrophages was due to the effect of the LL37 on the LPS, as described previously [14,15].

Nevertheless, as shown by Rosenfeld *et al*., the union between the LL37 and the LPS is not enough to neutralise the activation of the macrophages. To achieve the neutralisation, it is necessary to dissociate the LPS aggregates and to compete with them for the CD14 receptor in the macrophages. Therefore, it is remarkable that the encapsulation process did not affect the bioactivity of the LL37, since the encapsulated peptide maintained the capacity to bind both the LPS, trough electrostatic and hydrophobic interactions, and the CD14, through a selective union [16].

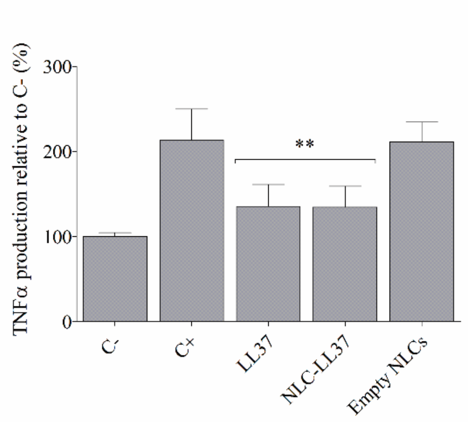


**Fig. 3.** Inhibition of the activation of the macrophages. The results are given as the mean % of TNF-α production relative to the control ± SD. ** significantly greater than empty NLC and C+ ($p<0.01$). Controls are C- (cells without any addition) and C+ (cells after the addition of LPS).

### *3.3 Antimicrobial assay*

Antimicrobial activity was tested against *E. coli*, because it is one of the most common bacteria in infected wounds [29]. Briefly, free LL37, NLC-LL37 and empty NLC were incubated with *E. coli* and samples were taken at determinate times. The samples were inoculated in an agar plate, incubated for 24 h and the grown colonies counted. The results showed that the free LL37 killed the 100% of the bacteria in the first 4 h, whereas the percentage of killed cells was lower with the NLC-LL37, 72.63 ± 13.37 %. Nevertheless, the NLC-LL37 exhibited a significantly greater antimicrobial effect tan the empty NLC, as depicted in Fig. 4.

The enhanced antimicrobial effect of the free LL37 might be due to the availability of the total peptide dose since the beginning of the study, whereas the available dose of the NLC-LL37 was lower at the beginning of the incubation time due to the

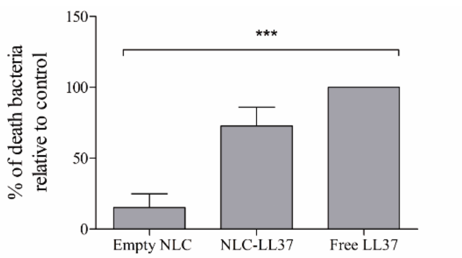


**Fig. 4.** Antimicrobial assay. The results are given as the mean percentage of death bacteria relative to the control ± SD. *** between the three groups (p<0.001).

sustained release of the formulation. Thereby, the NLC-LL37 were not able to kill the 100% of the *E. coli* at the beginning, and the subsequent exponential growth of the remaining bacteria hampered the ability of the NLC-LL37 to cause the death of every cells. However, this is an *in vitro* assay that does not completely resemble the clinical practice, where bacteria are proliferating constantly in the wound, which makes more necessary a sustained release of the peptide rather than a high initial dose.

*3.4* In vivo *wound healing assay*

The effectiveness of the treatments was assessed by calculating the wound closure. For that, the wounds areas ($px^2$) were measured from photographs taken on days 1, 4 and 8 after the surgery, and the wound closure was determined subtracting final areas to the initial areas.

The differences among groups were more pronounced on day 8, even though in both days there were significant differences. As shown in Fig. 5A, the biggest wound area reduction was found in the group treated with the high dose of NLC-LL37. On day 8 the wound area reduction was significantly greater than all the other groups. However, on day 4, this group only showed a significantly greater wound closure compared to the control group. Those results are in agreement with the qualitative area reduction observed in the macroscopic images of the wounds shown in Fig. 5B, since a higher reduction of the area can be seen in the wounds that received the high dose of NLC-LL37.

Regarding to the groups treated with the low dose of NLC-LL37 and with the free LL37, they presented a very similar wound closure, although the former had a slightly superior area reduction. Moreover, an improvement in wound closure was obtained compared to the control group, although significant differences were only found on day 8.

Besides of wound closure, the treatment effectiveness was also evaluated through histological analysis. Wound samples were collected on day 8 and stained with H&E prior to the assessment of the reepithelisation grade and the resolution of the inflammation.

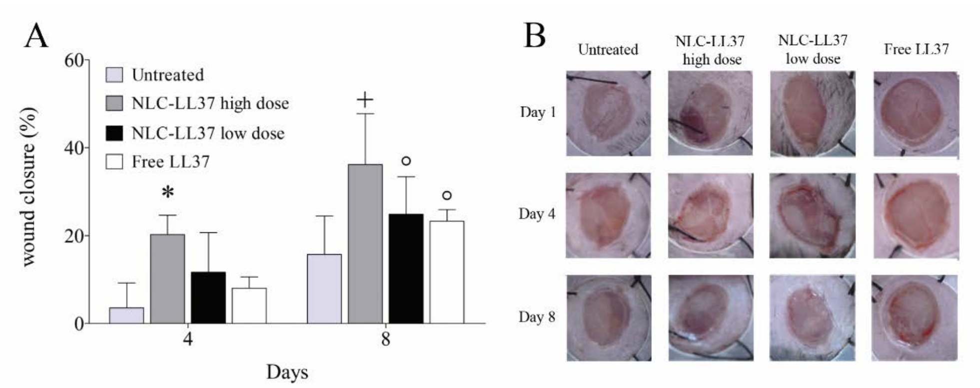


**Fig 5.** *In vivo* wound closure. (A) Wound closure represented as the percentage of reduction of the initial area. * Significantly greater than untreated group ($p<0.05$); ○ significantly greater than untreated group ($p>0.05$), + significantly greater than the rest of the groups ($p<0.05$). (B) Wound images.

The reepithelisation is the main healing process in humans, whereas in rodents the main process is wound contraction. However, reepithelisation is an important healing process in this animal model, since the *db/db* mice have impaired the wound contraction process, according to Fang *et al*., because of the extreme obesity of the animals reduces the looseness of the skin [30,31]. Furthermore, the wound contraction is more impaired by the silicone splint sutured around the wounds [25], which makes the reepithelisation an important healing process in this animal model.

The results obtained in the analysis of the reepithelisation (Fig. 6A) showed that the wounds treated with the high dose of NLC-LL37 presented a significantly higher grade of reepithelisation, with new epithelium covering more than a half of the wound, around 2, according to the scale described by Sinha *et al.* [26]. Conversely, the wounds treated with free LL37 and those of the control group had reepithelisation covering less than a half of the wound (~1), and the wounds treated with the low dose of NLC-LL37 had reepithelisation only in the margin of the wounds (~0). These results are consistent with those obtained in wound closure, since the high dose of NLC-LL37 improved the wound healing compared to a lower dose of the NLC-LL37 and the same dose of free LL37.

The analysis of the resolution of the inflammation was conducted following the criteria established by Cotran *et al.* [27]. As shown in Fig. 6B, the groups treated with the high dose of NLC-LL37 and with the free LL37 presented an accelerated inflammation recovery, as the wounds exhibited a predominance of granulation tissue formation and angiogenesis, with barely presence of pyogenic membrane and neutrophils (grade 2). However, the wounds of the control group and of the group treated with the low dose of NLC-LL37 were characterised by the formation of the fibrin clot and the migration of macrophages and polynuclear neutrophils that form the pyogenic membrane (grade 1). The permanent neutrophil infiltration showed in the last groups, is characteristic of chronic wounds and it is involved in delayed wound healing, since neutrophils release an excessive amount of proteases that degrade the extracellular matrix [32].

It may be noteworthy to mention that even if the group treated with the high dose of NLC-LL37 and the group treated with the free LL37 presented a diffuse acute inflammation grade (grade ~2), the former showed a slightly higher value, thus, a slightly improvement in wound maturation.

During early wound healing, fibroblasts of granulation tissue synthesise type III collagen, which is gradually replaced by type I collagen to recover uninjured skin phenotype. Bearing in mind that collagen, and mostly type I collagen, constitutes about the 80% of the dry weight of the normal skin, collagen deposition in wounds is indicative of wound maturation [33].

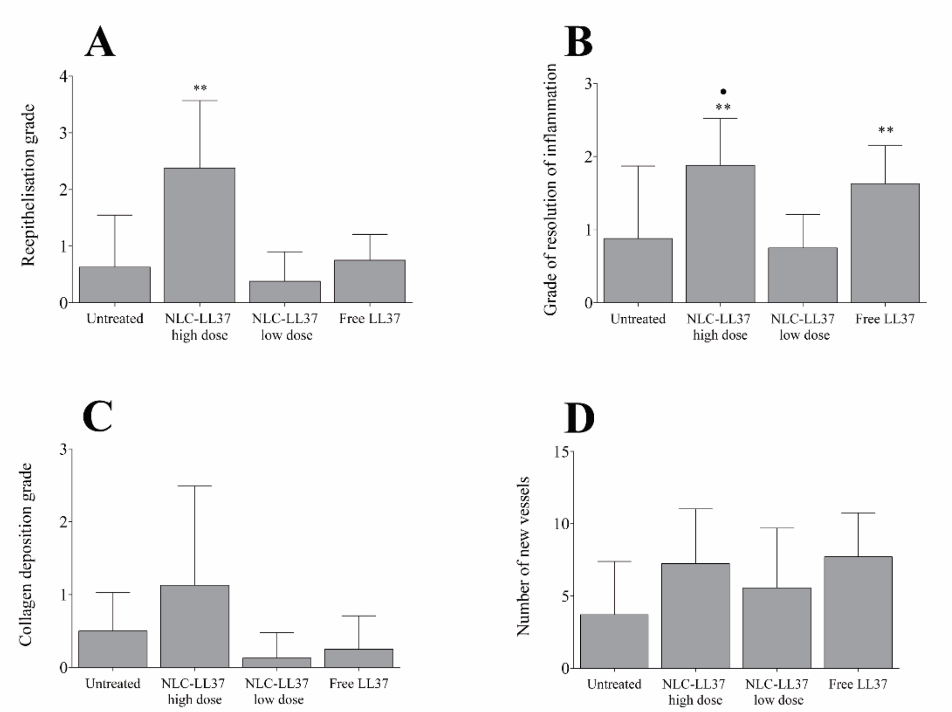


**Fig. 6.** Histological analysis. (A) Reepithelisation grade. ** Significantly greater than the rest of the groups (p>0.01). (B) Grade of resolution of inflammation. ** Significantly greater than NLC-LL37 low dose (p<0.01); ● significantly greater than untreated group (p<0.05). (C) Collagen deposition. (D) Number of new vessels in immunohistochemically stained tissue slides. All the results are shown as mean ±SD.

Accordingly, Masson Trichrome staining revealed that the high dose of NLC-LL37 slightly improved wound maturation, as it enhanced collagen deposition compared to the rest of the treatments, as depicted in Fig. 6C. In untreated wounds, in the wounds that received the low dose of NLC-LL37 and in the wounds that received free LL37 there was a lack of collagen deposition (grade 0 according to the criteria set by Gal *et al.* [28]), since most of the wounds did not show collagen and only a few of them showed a mild deposition. The group treated with the highest dose of NLC-LL37 presented a mild deposition of collagen (grade 1), however, one wound exhibited a marked deposition of collagen and another one, a moderate deposition. Nevertheless, the differences in collagen deposition did not achieve statistical significance, possibly due to the great variability found within the groups. That wide variability was previously described by Trousdale *et al.* (2009) analysing wound healing in *db/db* mice [34].

The angiogenic process was evaluated by counting the newly formed blood vessels in tissue slides that were immunohistochemically stained with antiCD31 monoclonal antibody. Although the results did not reach statistical significance, the wounds treated with free LL37 and with the high dose of NLC-LL37 presented a tendency to show higher number of vessels compared to the untreated wounds. In fact, two of the wounds showed more than 10 new vessels in each group, whereas none of the wounds in the untreated group showed more than 8 vessels. Furthermore, the group treated with the low dose of NLC-LL37 presented a slightly augmented microvascular density (one wound with more than 10 vessels) compared to the untreated group, as illustrated in Fig. 6D.

Overall, these results indicate that topically administered NLC-LL37 can improve wound healing in terms of wound closure, reepithelisation and resolution of the inflammation in a full thickness wound compared to the administration of the free peptide. The enhanced activity of the encapsulated peptide can be explained by the protective effect of the NLCs, which protect the LL37 against both, chemical degradation and degradation caused by the proteases present in the wound bed.

Moreover, the NLCs allow a controlled release profile, and thus extend the duration of the LL37 effect [20,21]. That is why, the NLC-LL37 formulation can reduce the high dosing frequency needed when the peptide is administered freely.

Previous studies have demonstrated the usefulness of encapsulating LL37 in nanoparticles [19], however in this study the nanoparticles encapsulating LL37 have been administered through the topical route for the first time, which presents several advantages. First of all, the lipidic nature of the NLCs creates an occlusive layer that increases skin hydration favouring the penetration of the encapsulated LL37 [21,35]. Moreover, the topical administration is an easy, comfortable and safe route for the patient.

## 4. Conclusion

In the current study NLCs loaded with 2% of LL37 have been developed. The nanoparticles exhibited a mean size of 270 nm, showed lack of cytotoxicity and the encapsulated LL37 maintained its bioactivity, as it was evidenced by the immunomodulatory and the antimicrobial *in vitro* assays.

The *in vivo* full thickness wound healing assay conducted in *db/db* mice, demonstrated that the administration of 6 µg of LL37 into NLC-LL37 topically improved wound healing compared to the administration of the free LL37. Taking into account all these findings, it can be concluded that the topical administration of NLC-LL37 might present an interesting strategy for the treatment of chronic wounds.

## 5. Acknowledgments

I. García-Orue thanks the Basque Government for the fellowship grant. The authors thank for technical and human support provided by SGIker of UPV/EHU and European funding (ERDF and ESF). This project has been funded by the Spanish Ministry of Economy and competitiveness (INNPACTO, IPT-2012-0602-300000, 2012). In addition, it has been partially supported by the Basque government (Consolidated Groups, IT-407-07 and IT-528-10) and the University of the Basque Country UPV/EHU (UFI11/32).

## 6. References

[1] C.K. Sen, G.M. Gordillo, S. Roy, R. Kirsner, L. Lambert, T.K. Hunt, F. Gottrup, G.C. Gurtner, M.T. Longaker, Human skin wounds: A major and snowballing threat to public health and the economy, Wound Repair and Regeneration 17 (2009) 763-771.

[2] V.W. Wong, G.C. Gurtner, Tissue engineering for the management of chronic wounds: current concepts and future perspectives, Exp. Dermatol. 21 (2012) 729-734.

[3] P. Martin, Wound Healing--Aiming for Perfect Skin Regeneration, Science 276 (1997) 75-81.

[4] A.J. Singer, R.A. Clark, Cutaneous wound healing, N Engl J Med 341 (1999) 738-746.

[5] R.F. Diegelmann, M.C. Evans, Wound healing: an overview of acute, fibrotic and delayed healing., Front Biosci. 9 (2004) 283-289.

[6] J.D. Heilborn, M.F. Nilsson, O. Sørensen, M. Ståhle-Bäckdahl, G. Kratz, G. Weber, N. Borregaard, The Cathelicidin Anti-Microbial Peptide LL-37 is Involved in Re-Epithelialization of Human Skin Wounds and is Lacking in Chronic Ulcer Epithelium, J. Invest. Dermatol. 120 (2003) 379-389.

[7] M. Frohm, B. Agerberth, G. Ahangari, M. Ståhle-Bäckdahl, S. Lidén, H. Wigzell, G.H. Gudmundsson, The Expression of the Gene Coding for the Antibacterial Peptide LL-37 Is Induced in Human Keratinocytes during Inflammatory Disorders, Journal of Biological Chemistry 272 (1997) 15258-15263.

[8] R. Koczulla, G. von Degenfeld, C. Kupatt, F. Krötz, S. Zahler, T. Gloe, K. Issbrücker, P. Unterberger, M. Zaiou, C. Lebherz, A. Karl, P. Raake, A. Pfosser, P. Boekstegers, U. Welsch, P.S. Hiemstra, C. Vogelmeier, R.L. Gallo, M. Clauss, R. Bals, An angiogenic role for the human peptide antibiotic LL-37/hCAP-18., J Clin Invest 111 (2003) 1665-1672.

[9] S.B. Coffelt, S.L. Tomchuck, K.J. Zwezdaryk, E.S. Danka, A.B. Scandurro, Leucine Leucine-37 Uses Formyl Peptide Receptor–Like 1 to Activate Signal Transduction Pathways, Stimulate Oncogenic Gene Expression, and Enhance the Invasiveness of Ovarian Cancer Cells, Molecular Cancer Research 7 (2009) 907-915.

[10] K. Hase, L. Eckmann, J.D. Leopard, N. Varki, M.F. Kagnoff, Cell Differentiation Is a Key Determinant of Cathelicidin LL-37/Human Cationic Antimicrobial Protein 18 Expression by Human Colon Epithelium, Infection and Immunity 70 (2002) 953-063.

[11] R.C. Anderson, M. Rehders, P.L. Yu, Antimicrobial fragments of the pro-region of cathelicidins and other immune peptides, Biotechnol. Lett. 30 (2008) 813-818.

[12] D. Vandamme, B. Landuyt, W. Luyten, L. Schoofs, A comprehensive summary of LL-37, the factotum human cathelicidin peptide, Cell Immunol 280 (2012) 22-35.

[13] Y. Kai-Larsen, B. Agerberth, The role of the multifunctional peptide LL-37 in host defense, Front. Biosci 13 (2008) 3760-3767.

[14] J. Turner, Y. Cho, N. Dinh, A.J. Waring, R.I. Lehrer, Activities of LL-37, a Cathelin-Associated Antimicrobial Peptide of Human

Neutrophils, Antimicrobial Agents and Chemotherapy 42 (1998) 2206-2214.

[15] R. Ramos, J.P. Silva, A.C. Rodrigues, R. Costa, L. Guardão, F. Schmitt, R. Soares, M. Vilanova, L. Domingues, M. Gama, Wound healing activity of the human antimicrobial peptide LL37, Peptides 32 (2011) 1469-1476.

[16] Y. Rosenfeld, N. Papo, Y. Shai, Endotoxin (Lipopolysaccharide) Neutralization by Innate Immunity Host-Defense Peptides: peptide properties ad plausible modes of action, Journal of Biological Chemistry 281 (2006) 1636-1643.

[17] R.E. Hancock, Cationic peptides: effectors in innate immunity and novel antimicrobials, Lancet Infect Dis 1 (2001) 156-164.

[18] M. Carretero, M. Del Río, M. García, M.J. Escámez, I. Mirones, L. Rivas, C. Balague, J.L. Jorcano, F. Larcher, A cutaneous gene therapy approach to treat infection through keratinocyte-targeted overexpression of antimicrobial peptides., FASEB J. 18 (2004) 1931-1933.

[19] K.K. Chereddy, C. Her, M. Comune, C. Moia, A. Lopes, P.E. Porporato, J. Vanacker, M.C. Lam, L. Steinstraesser, P. Sonveaux, H. Zhu, L.S. Ferreira, G. Vandermeulen, V. Préat, PLGA nanoparticles loaded with host defense peptide LL37 promote wound healing, J Control Release 194 (2014) 138-147.

[20] M. Schäfer-Korting, W. Mehnert, H. Korting, Lipid nanoparticles for improved topical application of drugs for skin diseases, Adv. Drug Deliv. Rev. 59 (2007) 427-443.

[21] J. Pardeike, A. Hommoss, R.H. Müller, Lipid nanoparticles (SLN, NLC) in cosmetic and pharmaceutical dermal products, Int. J. Pharm. 366 (2009) 170-184.

[22] R.H. Müller, M. Radtke, S.A. Wissing, Solid lipid nanoparticles (SLN) and nanostructured lipid carriers (NLC) in cosmetic and dermatological preparations, Adv. Drug Deliv. Rev. 54, Supplement (2002) S131-S155.

[23] G. Gainza, M. Pastor, J.J. Aguirre, S. Villullas, J.L. Pedraz, R.M. Hernandez, M. Igartua, A novel strategy for the treatment of chronic wounds based on the topical administration of rhEGF-loaded lipid nanoparticles: In vitro bioactivity and in vivo effectiveness in healing-impaired db/db mice, J Control Release 185 (2014) 51-61.

[24] G. Gainza, D.C. Bonafonte, B. Moreno, J.J. Aguirre, F.B. Gutierrez, S. Villullas, J.L. Pedraz, M. Igartua, R.M. Hernandez, The topical administration of rhEGF-loaded nanostructured lipid carriers (rhEGF-NLC) improves healing in a porcine full-thickness excisional wound model, J Control Release 197 (2015) 41-47.

[25] J. Michaels, S.S. Churgin, K.M. Blechman, M.R. Greives, S. Aarabi, R.D. Galiano, G.C. Gurtner, db/db mice exhibit severe wound-healing impairments compared with other murine diabetic strains in a silicone-splinted excisional wound model, Wound Repair Regen 15 (2007) 665-670.

[26] U.K. Sinha, L.A. Gallagher, Effects of Steel Scalpel, Ultrasonic Scalpel, CO2 Laser, and Monopolar and Bipolar Electrosurgery on Wound Healing in Guinea Pig Oral Mucosa, Laryngoscope 113 (2003) 228-236.

[27] R. Cotran, G.K. Kumar, T. Collins, Reparación de los tejidos: proliferacion celular, fibrosis y curación de las heridas, in: R. Cotran, G.K. Kumar, T. Collins (Eds.), Patología Estructural Y Funcional, McGraw-Hill, Interamericana, Madrid, 2000, pp. 95-120.

[28] P. Gál, T. Toporcer, B. Vidinský, M. Mokrý, M. Novotný, R. Kilík, K. Smetana, T. Gál, J. Sabo, Early changes in the tensile stregnth and morphology of primary sutured skin wounds in rats, Folia Biol. (Praha) 52 (2006) 109-115.

[29] A.R. Siddiqui, J.M. Bernstein, Chronic wound infection: Facts and controversies, Clin. Dermatol. 28 (2010) 519-526.

[30] R.C. Fang, Z.B. Kryger, D.W. Buck II, M. De La Garza, R.D. Galiano, T.A. Mustoe, Limitations of the db/db mouse in translational wound healing research: Is the NONcNZO10 polygenic mouse model superior?, Wound Repair and Regeneration 18 (2010) 605-613.

[31] V.I. Tkalcevic, S. Cužic, M.J. Parnham, I. Pašalic, K. Brajša, Differential Evaluation of Excisional Non-occluded Wound Healing in db/db Mice, Toxicologic Pathology 37 (2009) 183-192.

[32] N.B. Menke, K.R. Ward, T.M. Witten, D.G. Bonchev, R.F. Diegelmann, Impaired wound healing, Clin. Dermatol. 25 (2007) 19-25.

[33] J. Li, J. Chen, R. Kirsner, Pathophysiology of acute wound healing, Clin. Dermatol. 25 (2007) 9-18.

[34] R.K. Trousdale, S. Jacobs, D.A. Simhaee, J.K. Wu, J.W. Lustbader, Wound Closure and Metabolic Parameter Variability in a db/db Mouse Model for Diabetic Ulcers, J. Surg. Res. 151 (2009) 100-107.

[35] R.H. Müller, R.D. Petersen, A. Hommoss, J. Pardeike, Nanostructured lipid carriers (NLC) in cosmetic dermal products, Adv. Drug Deliv. Rev. 59 (2007) 522-5

# CHAPTER 2

## Novel nanofibrous dressings containing rhEGF and Aloe vera for wound healing applications

I. García-Orue[a], G. Gainza[a], F.B. Gutierrez[b], J.J. Aguirre[b], C. Evora[c], J.L. Pedraz[a,d], R.M. Hernandez[a,d], A. Delgado[c]*, M. Igartua[a,d]**

[a] NanoBioCel Group, Laboratory of Pharmaceutics, School of Pharmacy, University of the Basque Country (UPV/EHU).

[b] Hospital Universitario de Álava (HUA) Txagorritxu, Vitoria-Gasteiz, 01009, Spain.

[c] Department of Chemical Engineering and Pharmaceutical Technology. School of Pharmacy. University of La Laguna, Tenerife, Spain.

[d] Biomedical Research Networking Centre in Bioengineering, Biomaterials and Nanomedicine (CIBER-BBN).

*Corresponding author: Dr. A. Delgado and Dr. M. Igartua

### ABSTRACT

Nanofibrous membranes produced by electrospinning possess a large surface area-to-volume ratio, which mimics the three-dimensional structure of the extracellular matrix. Thus, nanofibrous dressings are a promising alternative for chronic wound healing, since they can replace the natural ECM until it is repaired. Therefore, in this study we developed a PLGA nanofibrous membrane that contains recombinant human Epidermal Growth Factor (rhEGF) and *Aloe vera* (AV) extract. Both of them promote wound healing, as EGF is a wound healing mediator and AV stimulates the proliferation and activity of fibroblast. The obtained membranes were composed of uniform and randomly oriented fibers with an average diameter of 356.03 ± 112.05 nm, they presented a porosity of 87.92 ± 11.96 % and the amount of rhEGF was 9.76 ± 1.75 µg/mg. The *in vitro* viability assay demonstrated that the membranes containing rhEGF and AV improved fibroblast proliferation, revealing the beneficial effect of the combination. Furthermore, these membranes accelerated significantly wound closure and reepithelisation in an *in vivo* full thickness wound healing assay carried out in *db/db* mice. Overall, these findings demonstrated the potential of PLGA nanofibers containing rhEGF and AV for the treatment of chronic wounds.

**Published in:** International Journal of Pharmaceutics
523 issue 2 (2017), 556-566. Doi: https://doi.org/10.1016/j.ijpharm.2016.11.006

## 1. Introduction

Wound healing is a dynamic and complex process with the aim of restoring the normal anatomical structure and functionality of the skin (Diegelmann and Evans 2004). In order to achieve that objective, diverse immunological and biological systems participate in a coordinated way, through three distinct but overlapping phases, including an inflammatory response (which comprises hemostasis and inflammation), a proliferative phase (consisting of protein synthesis and wound contraction) and a remodelling phase (Monaco and Lawrence 2003; Morton and Phillips 2016; Schreml, et al. 2010). Nevertheless, some wounds fail to progress through healing in that timely and spatially organised manner. The disturbance of the healing can be caused by several factors, such as, infection, necrosis, tissue hypoxia, exudates and an excess of inflammatory cytokines. Therefore, wounds get stagnated in a permanent inflammatory stage, with an abnormally high level of proinflammatory cytokines and proteases, which lead to the deterioration of the extracellular matrix (ECM) and, thus, perpetuating a non healing state (Briquez, et al. 2015; Velnar, et al. 2009).

The treatment of chronic wounds has gained a huge impact in our society, due to the alarming increase of its prevalence in the last years. Moreover, the prevalence is expected to continue growing exponentially because of the increase of the high risk population, which includes elderly, diabetics and obese (Whittam, et al. 2016). Indeed, it has been estimated that 1-2% of the population of developed countries will suffer from chronic wounds during their lifetime, representing their associated cost the 2% of the European health budget according to the United Nations (Sen, et al. 2009). Current studies to overcome this clinical problem are focused on the development of wound dressings able to enhance wound healing. Among those, nonwoven nanofibrous membranes are of especial interest, since their unique architectural features mimic the three dimensional structure of the ECM (Choi, et al. 2015).

Nanofibers are usually produced by electrospinning, a simple, cost effective and versatile technique that uses an electric force to spin nanometric fibers from a polymeric solution (Abrigo, et al. 2014; Gainza, et al. 2015b). The nanofibers generated by this technique exhibit a high surface area-to-volume ratio and a high porosity, that enhance wound healing through diverse mechanisms. For example, they allow gas permeation, which promotes cell respiration; they retain moisture and they improve the removal of exudates (Pachuau 2015). The dressings should promote cell migration and proliferation, while preventing tissue ingrowth within the nanofibrous membrane, since they are designed to be removed once the wound has healed (Abrigo, et al. 2014). Furthermore, nanofibers can be loaded with active compounds to accelerate the wound healing, as it has been shown in numerous studies with the encapsulation of drugs such as, growth factors, Aloe vera extract, curcumin, metformin, ciprofloxacin and collagen, among others (Choi, et al. 2008; Kataria, et al. 2014; Lai, et al. 2014; Lee, et al. 2014; Merrell, et al. 2009; Uslu and Aytimur 2012). In addition, the encapsulation of drugs into nanofibers allows their topical administration, which present several advantages. Firstly, it improves patient compliance, permitting self administration; secondly, it maximises the therapeutic potential by the improvement of bioavailability and the maintenance of drug concentration in the wound site; and finally, it reduces the systemic drug toxicity (Pachuau 2015; Whittam, et al. 2016).

The nanofibrous membranes obtained through electrospinning have also been used in cell based therapies. The similarity of the membranes to the ECM allows cell penetration, differentiation and adhesion, making them a suitable approach for developing skin substitutes or stem cell therapy. Skin substitutes are scaffolds seeded with cells to resemble the native skin structure (Dickinson and Gerecht 2016). In order to ease cell-matrix interactions, scaffolds are often produced of collagen and other naturally occurring ECM proteins (Hodgkinson and Bayat 2011), as the skin substitute developed by Powell *et al.* where human dermal fibroblast and epidermal keratinocytes were seeded into a collagen electrospun scaffold (Powell, et al. 2008). In another study, Han *et al.* developed a scaffold based on other natural polymer (PHVB) that was seeded with hair follicular cells because their low immunogenicity is advantageous for allografts (Han, et al. 2007). On the other hand, a variety of stems cells; such as, adipose-derived stem cells (Gu, et al. 2014; Machula, et al. 2014), mesenchymal stem cells (Bhowmick, et al. 2016; Steffens, et al. 2014), unrestricted somatic stem cells (Bahrami, et al. 2016; Keshel, et al. 2014) and urine derived stem cells (Fu, et al. 2014); have been used to produce wound healing scaffolds anchored to electrospun membranes. Those stem cells have proven to improve wound healing due to their capacity to differentiate into endothelial cells and to express soluble factors and ECM proteins needed in wound healing.

*Aloe vera* extract (AV) is a compound that can benefit from the encapsulation in nanofibers for wound healing treatment. *Aloe vera* is an herbaceous succulent plant that belongs to Liliaceae family. Besides ist pharmacological activity, which includes anti-inflammatory, antiarthritis, antibacterial, antifungal and hypoglycaemic effects, it has been reported to promote wound healing (Choi and Chung 2003; Ha shemi, et al. 2015). The healing effect is mainly mediated by a compound called glucomannan that affects fibroblast growth factor and stimulates the activity and proliferation of the fibroblasts, which improves collagen production and secretion by those cells (Hashemi, et al. 2015).

Growth factors are also interesting compounds for encapsulating in nanofibrous wound dressings, since they are essential healing mediators for a successful tissue repair (Choi, et al. 2012). Among others, the Epidermal Growth Factor (EGF) is a key signalling molecule that stimulates keratinocyte and fibroblast proliferation and migration, hence improving wound healing (Bodnar 2013). Furthermore, its external administration in chronic wounds has been proven to promote wound healing (Choi, et al. 2008; Gainza, et al. 2015a). However, the clinical application of EGF is hampered by its short half-life, due to its degradation by the hidrolitic enzymes present in the wound bed. Therefore, the encapsulation in nanofibrous membranes can overcome this limitation, as these formulations protect the EGF form the environment, and thus enhance its stability (Pachuau 2015).

Nanofibrous membranes can be produced from natural or synthetic polymers. Natural polymers used in electrospinning include ECM components, such as, collagen, laminin, fibrin or elastin; and other polymers such as, chitosan, agarose, gelatine, pectin, silk, etc. The properties of those polymers (biocompatibility, non-toxicity, physcochemical properties and matrix-cell interactions) made them adequate for wound healing (Garg, et al. 2015). However, their weak mechanical properties and difficulty for electrospinning make necessary to reinforce them with synthetic polymers (Hodgkinson and Bayat 2011). Among the synthetic polymers used for electrospinning there are cellulose acetate, polylactic-co-glycolic acid (PLGA), poly(vinyl alcohol), poly(lactic acid), polystyrene, polyglycerol, polyglycolide, polyurethane, etc. Synthetic materials are stronger and cheaper, present a well defined structure and are more easily electrospinable (Garg, et al. 2015).

Taking that into account, in this study, PLGA was electrospinned to develop a nanofibrous dressing loaded with rhEGF and AV for the treatment of chronic wounds. The nanofibrous membranes were characterised to evaluate their suitability for wound dressing, and *in vitro* tests were undertaken to analyse the bioactivity of the encapsulated active compounds.

In addition, dressings' efficacy was assessed *in vivo*. Although pig dermis is probably the most similar to that of humans, rodent wound models are more common due to the difficulties in working with large animals (Seaton, et al. 2015). Nevertheless, rodent wound healing parallels worse human wound healing, because they heal primarily by contraction due to their loose skin. In order to avoid that difference, wounds are inflicted in specific anatomic sites as head, ears or tail, where skin is tighter. Another approach to address that problem is to adhere circular silicone splints beyond the wound margin to prevent wound contraction, which makes this model the most representative of open human wounds in rodents (Fang and Mustoe 2008).

To mimic the delayed wound healing in chronic wounds, rodent models with impaired healing conditions can be used, such as, ischemic (Elgharably, et al. 2014; Magin, et al. 2016) or diabetic models. Among diabetic models the most widely used are chemically induced diabetes secondary to streptozocin injections, since it destroys pancreatic β-cells developing a phenotype similar to type I diabetes (Inpanya, et al. 2012; Moura, et al. 2014); and genetically diabetic *db/db* mice (BKS.Cg-m +/+ Leprdb/J), which present a mutation of the leptin receptor and thus, possess a phenotype of type II diabetes (Guillemin, et al. 2016; Losi, et al. 2013). A study carried out by Michaels *et al*. demonstrated that wound healing was more impaired in the *db/db* mice than in the streptozocin model (Michaels, et al. 2007).

Accordingly, in this study the dressings were topically applied in a full-thickness excisional splinted wound model in *db/db* mice, and their efficacy was assessed in terms of wound closure, reepithelisation grade, recovery of the inflammatory stage and collagen deposition.

## 2. Materials and methods

### *2.1 Nanofiber preparation*

An emulsion (o/w) containing rhEGF, AV, and PLGA was electrospun to fabricate a PLGA-AV-EGF nanofibrous membrane. The organic phase of the emulsion was composed of 140 mg of PLGA 50:50 (Resomer RG504, Evonik, Germany) in 650 µL of hexafluoroisopropanol (HFIP, Fluka, Switzerland), and the aqueous phase was 350 µL of a polyvinyl alcohol (PVA) solution (0.5% w/v) containing 140 mg of Aloe vera powder (Agora Valencia SL., Spain) and 5 mg of rhEGF (Centre for Genetic Engineering and Biotechnology, Cuba). Both phases were vortexed at level 10 for 3 min to form the emulsion (Vortex-Genie 2, Scientific Industries Inc., USA). The resulting emulsion was loaded into a Luer-lock syringe (Norm-Ject) with an 18G needle attached to a pump (Harvard Apparatus, MA) providing a flow rate of 1 mL/h and it was electrospun horizontally on a rotating collector located at 12 cm from the needle, under 12 kV power supply. The collector rotating speed was set at 200 rpm.

The preparation of the PLGA-AV and the PLGA nanofibers only differ from the explained above in the composition of the aqueous phase, which lacked the rhEGF, and the rhEGF and the AV, respectively. The injected volume was normalized to obtain membranes with similar thickness.

The products used for producing the membranes were previously sterilised by gamma radiation and the syringe, the collector and the needle used for electrospinning were autoclaved. Moreover, the electrospinning process was carried out under aseptic conditions. Finally, before the *in vitro* and *in vivo* studies the membranes were sterilised by keeping them under UV light for 30 minutes.

*2.2. Nanofiber characterisation*

The nanofibrous membrane morphology, i.e. membrane quality and fiber diameter, was analysed using Scanning Electron Microscopy images (SEM, Jeol JSM-6300). Porosity (P) of the membranes was calculated through the following equation (Eq. 1), where $\rho_{real}$ and $\rho_{app}$ are the real and apparent densities, respectively:

$$P\ (\%) = \left(1 - \frac{\rho_{app}}{\rho_{real}}\right) \times 100 \qquad (1)$$

Real density was assessed by means of a helium pycnometer (Micromeritics, AccuPyc 1330, USA) and apparent density was calculated dividing the mass by the calculated volume (length × width × height). Membrane thickness was measured from photographs obtained by stereo microscopy (Leica M205 C, Leica LAS, Germany).

Monotonic tensile tests of the PLGA-AV-EGF, PLGA-AV and PLGA nanofibers were performed under displacement control on an Instron 5848 microtester, using a 5 N full scale load cell (Instron®, UK). The samples were loaded at a displacement rate of 0.01 mm/s up to rupture. The load-displacement curve was transformed in a stress-strain curve and the ultimate strength was determined to compare the mechanical properties of the different nanofibers. At least 5 samples of each membrane were tested and the results were presented as mean ± standard deviation.

Nanofibers degree of water uptake in an aqueous environment was evaluated *in* *vitro* to compare the behaviour of the three nanofibrous membranes. After weighing 1x1 cm nanofiber samples, they were soaked in 1 ml of PBS and incubated at 32 °C for 1 h. Then, they were removed and the excess of water dried. Finally, the nanofiber pieces were weighed to calculate the water uptake through the following equation (Eq. 2):

$$\text{Water uptake (\%)}=\frac{M\text{-}M_0}{M_0}\times 100 \qquad (2)$$

Where M represents the weight of the membrane after the immersion in PBS and $M_0$ represents the initial weight of the nanofibrous mesh.

The Water Vapour Permeability Rate (WVPR) through the membranes was determined modifying the method described by Li *et al.* (Li, et al. 2013). The mouth of a cup containing silica gel dessicant (1cm in diameter) was thoroughly covered with the test membrane, so that water vapor only can enter to the cup through the membrane. The cup was placed in a chamber at 30°C with a constant relative humidity of 75% for 24 hours. The change of the weight of the assembly before and after the exposure time was recorded and WVPR was calculated using the following equation (3):

$$\text{WVPR}=\frac{M_1\text{-}M_0}{A\times T} \qquad (3)$$

Where M0 is the weight of the assembly before the assay, M1 is its weight after the assay, A is the exposure area of the membrane and T is the exposure time.

The thermal behaviour of the nanofibers, the physical blend of the components and the components themselves were studied using Differential Scanning Calorimetry (DSC-50, Shimadzu, Japan). Each sample was sealed in an aluminium pan and heated from 25°C to 350°C at a heating rate of 10°C per minute.

To determine the amount of rhEGF loaded into the PLGA-AV-EGF nanofibers, a piece of 1x1 cm of the membrane was dissolved in 200 µL of dimethyl sulphoxide (DMSO) (Scharlau, Spain), vortexed until it became a clear solution and mixed with 800 µL of phosphate buffered saline (PBS) (Life technologies, California, USA). The amount of rhEGF in the dissolution was estimated using a commercially available Sandwich Enzyme-Linked Immunosorbent assay kit for human EGF (human EGF ELISA development kit, Peprotech, USA). The assay was performed following the manufacturer's instructions.

*2.3* In vitro *rhEGF release*

The release study was conducted on a Franz diffusion cell system. A piece of 1x1 cm of PLGA-AV-EGF nanofiber membrane (corresponding to 9.76 µg of rhEGF), humidified with 30 µl of PBS, was placed on the donor chamber, above a nylon filter with 0.45 µm pore size (Tecnokroma®, Spain). On the receptor chamber 5 ml of PBS were added and the system was maintained under stirring. At selected intervals, 1 ml of the receptor chamber was removed and replaced with fresh PBS. The amount of rhEGF released in the medium was determined by ELISA using the protocol described in 2.2 section. The assay was performed in triplicate and the results were expressed as the cumulative percentage of rhEGF released over time.

*2.4* In vitro *antibacterial assay*

The antimicrobial activity of the PLGA-AV membrane was tested using *Staphylococcus aureus* and *Staphylococcus epidermidis* as model microorganisms. Briefly, 100 µL of a $10^5$ CFU/mL suspension of each bacteria were spread on a Mueller Hinton agar plate. PLGA and PLGA-AV nanofibers were cut into 6 mm circular discs. 6 mm blank discs loaded with 10 µL of an AV aqueous solution (30 mg/mL) were used as controls. Samples and controls were place on the plates and incubated 36 h at 37ºC. Afterwards, plates were observed for the presence of inhibition zone around the samples.

*2.5.* In vitro *cell culture studies*

*2.5.1 Cell culture*

BalbC/3T3 A31 fibroblast (ATCC, USA) were cultured on Dulbecco's modified Eagle's medium (DMEM) (ATCC, USA) supplemented with 10% (v/v) foetal calf serum and 1% (v/v) penicillin-streptomycin and incubated at 37°C in a humidified incubator with a 5% $CO_2$ atmosphere.

### 2.5.2 Bioactivity assay

The effect of the released medium of PLGA-AV-EGF nanofibers, PLGA-AV nanofibers and PLGA nanofibers on cell viability was assayed in the fibroblasts. The cells were seeded in a 96-well plate at a density of 6000 cell/well, and cultured overnight to allow cell attachment.

The following samples were added to the wells: (i) complete culture medium as negative control, (ii) 20 ng/ml of free rhEGF, (iii) 20 ng/ml of rhEGF released from the PLGA-AV-EGF nanofibers, (iv) the release medium of the PLGA-AV nanofibers and (v) the release medium of the PLGA nanofibers. After 48 h of incubation, cell viability was evaluated using a CCK-8 kit (cell counting kit-8, Sigma-Aldrich, USA). Briefly, 10 µL of the CCK-8 reagent were added to the cells, and the mixture was incubated for 4 h. Then the absorbance was read at 450 nm and at 650 nm as the reference wavelength (Plate Reader Infinite M200, Tecan, Switzerland). The measured absorbance was directly proportional to the number of living cells in each well.

### 2.5.3 Adhesion assay

In order to evaluate the adhesion of the cells to the nanofibrous membranes, BalbC/3T3 A31 fibroblasts were cultured on top of the membranes and the attached cells counted. Briefly, 1x1 cm of PLGA, PLGA-AV and PLGA-AV-EGF nanofibers were cut and fixed to the bottom of 96 culture plate wells using 10 µl of fibrin as adhesive. The nanofibers were incubated for 30 min at 37 °C to allow the formation of the fibrin clot, and subsecuently, 15,000 cells were seeded in each well. Control wells were also seeded with 15,000 cells and incubated with complete culture medium.

Cells were incubated overnight at 37°C to allow cell attachment. Afterwards, the membranes were washed with PBS and the adhered cells were detached by incubating them for 10 min with 50 µl of trypsin-EDTA (Lonza, Switzerland). Finally, the trypsin was collected and the cells were counted using an automated cell counter (Automated Cell Counter TC20™, Bio-Rad, California, USA). The adhesion to the membranes was assesses as the percentage of counted cells compared to the control. Three independent experiments were performed.

In addition, SEM images were taken to observe cell adhesion. After overnight cell incubation, cells were fixed in a 2.5% glutaraldehyde solution followed by dehydration in graded ethanol series. Finally, images were taken using a SEM microscope (Hitachi S4800, Tokyo, Japan).

### *2.6.* In vivo *wound healing study*

#### *2.6.1 Animals*

For the *in vivo* study, 20 male *db/db* (BKS.Cg-m+/+Leprdb/J) mice (8 weeks old) were used (Janvier laboratories, France). All the experiment were conducted following the protocols approved by the Institutional Ethical Committee for Animal Experimentation of the University of the Basque Country (Procedure number: CEBA/243/2012/HERNANDEZ MARTIN). The mice were housed in individual cages under a 12 h light-dark cycle, and they were given free access to standard rodent chow and water.

#### *2.6.2 Wound healing assay*

The wound healing assay was performed according to the procedure described by Michaels *et al.* (Michaels, et al. 2007). After anesthetising the mice with isoflurane (Isoflo, Esteve, Spain) and removing their dorsal hair, two silicone rings of 1 cm diameter were sutured on each side of the midline using a 3-0 nylon suture (Aragó, Spain). The aim of the sutured silicone rings was to avoid wound healing through contraction, the main healing mechanism of mice, and hence mimic human main healing mechanisms, which are granulation tissue formation and re-epithelisation. Subsequently, a full thickness wound extending through the *panniculus carnosus* was created in the middle of each ring, using an 8 mm in diameter punch biopsy tool (Acu-Punch, Acuderm, USA). The treatments were administered after the wound induction, and finally, the wounds were covered with one layer of petrolatum gauze (Tegaderm®, 3M, Minnesota, USA) and two layers of adhesive gauze.

The mice were divided in 5 groups of 4 animal each (n=4): (i) untreated control,

(ii) 10 µg of free rhEGF in a final volume of 10 µL of PBS, (iii) 1x1 cm of PLGA-AV-EGF nanofibers, (iv) 1x1 cm of PLGA-AV nanofibers and (v) 1x1 cm of PLGA nanofibers. Treatments were changed on day 4 after wound induction.

The membranes were previously hydrated in PBS and topically applied on the wound bed. The free rhEGF, instead, was dissolved in 10 µL of PBS, administered topically and allowed to spread on the wound bed before aplying the dressings. On day 8, the mice were sacrificed through $CO_2$ inhalation.

*2.6.3 Evaluation of wound healing*

In order to evaluate the effectiveness of the treatments, the wound area ($px^2$) was measured on days 1, 4 and 8 post wound induction. Those days, wounds were photographed using a digital camera (Lumix FS16, Panasonic®, Japan), and their area was calculated using an image analysis programme (ImageJ®, Biophotonics Facility, Canada). The wound closure was expressed as the percentage of the initial wound area.

*2.6.4 Histological analysis of healing*

On day 8, after mice sacrifice, the wound and surrounding tissue (about 1x1 cm) were excised and fixed in 3.7% paraformaldehyde. After 24 h, the biopsies were bisected, embedded in paraffin, and sectioned in 5 µm thick layers. Finally, the tissue slices were processed by hematoxylin-eosin (H&E) staining for morphological evaluation and by Masson trichrome staining for collagen deposition evaluation.

The re-epithelisation process was determined following the scale established by Sinha *et al.* (Sinha and Gallagher 2003). Each wound received a value within a range from 0 to 4: 0, only the wound edges are re-epithelised; 1, less than the half of the wound is reepithelised; 2, more than half of the wound is reepithelised; 3, the entire wound is reepithelised with irregular thickness; and 4, the entire wound is reepithelised with normal thickness.

The resolution of the inflammatory process and wound maturity was assessed in accordance with the scale described by

Cotran *et al.* (Cotran, et al. 2000). Wounds were semi-quantitatively rated according to the following criteria: 0, absence of inflammation; 1, acute inflammation, comprising formation of the fibrin clot and the pyogenic membrane and the migration of leucocytes and polynuclear neutrophils; 2, diffuse acute inflammation, comprising the formation of granulation tissue, angiogenesis and almost non-existence of pyogenic membrane; 3, chronic inflammation, which consist on fibroblast proliferation and 4, resolution and healing, which consist on the disappearance of chronic inflammation, although occasionally round cells can be found.

The deposition of collagen was evaluated following the scale described by Gál *et al.* (Gál, et al. 2006): 0, absent of collagen; 1, mild content of collagen; 2, moderate content of collagen and 3, marked content of collagen.

### *2.7 Statistical analysis*

Data were expressed as the mean ± standard deviation (SD). Based on the result of the normality test, the means were compared through one-way ANOVA for multiple comparison or Mann-Whitney U test. Subsequently to the one-way ANOVA test, Bonferroni or Tamhane post-hoc were applied based on the Levene test for the homogeneity of variances. All the statistical calculations were performed using SPSS 22.0.01 (SPSS®, INC., Chicago, IL, USA).

## **3. Results**

### *3.1 Nanofiber characterisation*

The SEM photographs displayed in Fig. 1 showed that the membranes were composed of uniform and randomly oriented nanofibers. As shown in Table 1, they presented a high porosity above 79 %.

As expected, the thickness of the different membranes was similar, with a value of 45.92 ± 0.78 µm, 56.76 ± 1.23 µm and 59.17 ± 1.83 µm, for the PLGA-AV-EGF, the PLGA-AV and the PLGA nanofibers, respectively. However, the nanofibers diameter varies between the membranes, being 356.03 ± 112.05 nm in the PLGA-AV-EGF nanofibers, 486.99 ± 114.73 nm

**Table 1.** Nanofiber characterisation: membrane porosity (%), membrane thickness (µm), nanofibers diameter (nm), tensile strength (MPa), water uptake (%), WVPR ($g/m^2day$) and peptide loading ($\mu g/cm^2$). Data are expressed as the mean ± SD.

| Nanofiber composition | Membrane porosity (%) | Membrane thickness (µm) | Nanofiber diameter (nm) | Tensile strength (MPa) | Water uptake (%) | WVPR ($g/m^2day$) | Peptide loading ($\mu g/cm^2$) |
|---|---|---|---|---|---|---|---|
| PLGA | 79.50 ±7.42 | 59.17 ±1.83 | 561.61 ±124.28 | 3.06 ±0.35 | 218.17 ±45.03 | 1861.28 ±372.89 | - |
| PLGA-AV | 87.92 ±11.96 | 56.76 ±1.27 | 486.99 ±114.73 | 4.66 ±0.90 | 273.92 ±42.19 | 1690.09 ±190.25 | - |
| PLGA-AV-EGF | 87.52 ±6.62 | 45.92 ±0. 78 | 356.03 ±112.05 | 2.21 ±0.49 | 290.58 ±49.92 | 1907,39 ±228.82 | 9.76 ±1.75 |

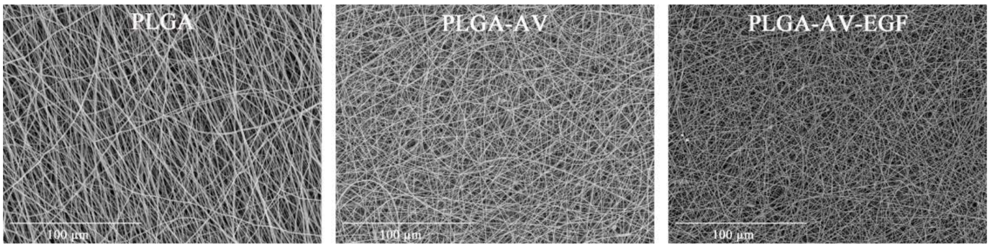


**Fig. 1.** SEM photographs of PLGA, PLGA-AV and PLGA-AV-EGF nanofibers. The scale bar in each image indicates 100 µm.

in the PLGA-AV nanofibers and 561.61 ± 124.28 nm in the PLGA nanofibers.

In order to confirm the integrity of the membranes, their mechanical properties were determined. The ultimate tensile strength of the PLGA, PLGA-AV and PLGA-AV-EGF nanofibers were 3.06 ± 0.35 MPa, 4.66 ± 0.90 MPa and 2.21 ± 0.49 MPa, respectively as illustrated in table 1.

The hydrophilicity of the membranes was determined quantifying their water uptake. The results showed that all the membranes presented a similar water uptake above 200 %; being 218.17 ± 45.03 % in PLGA nanofibers, 273.9 2± 42.19% in PLGA-AV nanofibers and 290.58 ± 49.92% in PLGA-AV-EGF nanofibers, as depicted in Table 1. The WVPR was also very similar in all the membranes, being 1861.28 ±372.89 $g/m^2day$, 1690.09 ± 190.25

g/m$^2$day and 1907.39 ± 228.82 g/m$^2$day for PLGA, PLGA-AV and PLGA-AV-EGF nanofibers respectively (Table 1).

Regarding the thermal behaviour, the glass transition temperature ($T_g$) of PLGA electrospun membrane was lower than that of the raw PLGA, being them 49.84 ± 0.23°C and 53.85 ± 0.16°C, respectively (Table 2). In addition, a minor decrease of PLGA $T_g$ was observed in the components physical blends, probably due to the presence of AV. It is noteworthy that the thermal peaks detected in the PLGA-AV and PLGA-AV-EGF electrospun membranes were the same of those observed in the PLGA-AV physical blend, while the corresponding peaks of rhEGF were not detected in any nanofiber or physical blend, probably because it was used in a very small proportion (Table 2).

The amount of rhEGF loaded in the PLGA-AV-EGF nanofibers was 9.76 ± 1.75 µg rhEGF/cm$^2$. The *in vitro* rhEGF release profile illustrated in Fig. 2 showed an initial burst release where about a 35% of the total drug was released within the first 8 hours; followed by a slower release phase up to 7 days. The total drug release of the study was about the 50% of the total drug content.

**Table 2.** DSC results. The endothermic DSC peaks of the nanofibers, their components blends and their components itself. The data are expressed as the mean ± SD.

| | Endothermic DSC peak (°C) | |
|---|---|---|
| PLGA | 53.85±0.16 | |
| Aloe vera | 67.94±0.33 | 155.82±0.37 |
| rhEGF | 63.68±4.11 | 199.10±0.19 |
| PLGA and Aloe vera blend | 52.04±0.83 | 68.89±0.56 |
| PLGA, Aloe vera and rhEGF blend | 52.28±0.5 | 69.01±1.42 |
| PLGA nanofibers | 49.84±0.23 | |
| PLGA-AV nanofibers | 51.46±1.04 | 70.30±3.76 |
| PLGA-AV-EGF nanofibers | 52.04±0.08 | 71.73±1.48 |

*3.2* In vitro *antibacterial assay*

The antibacterial effect of the AV present in the PLGA-AV nanofibers was assessed using the zone of inhibition test against *S. aureus* and *S. epidermidis*. As observed in Fig. 3, a bacterial growth inhibition zone appeared around AV controls and PLGA-AV nanofibers with both bacterias, although qualitatively the inhibition zone diameter around controls was bigger than the one of the PLGA-AV nanofibers. On the contrary, PLGA nanofibers did not show any inhibition of bacterial growth.

### *3.3* In vitro *bioactivity assay*

In order to assess whether the electrospinning process affect the bioactivity of the components, fibroblasts were incubated with the released medium of the membranes. After 48 h, cell proliferation was determined by a CCK-8 assay.

As depicted in Fig. 4, the highest cellular proliferation was observed when the cells were treated with the released me dium of PLGA-AV-EGF nanofibers, reaching a threefold increase in comparison to the control. Moreover, the cells treated with PLGA-AV nanofibers released medium also showed an increase in proliferation compared to the control, although it was smaller than the increment achieved with the previous one. On the other hand, PLGA nanofibers did not enhance cell growth.

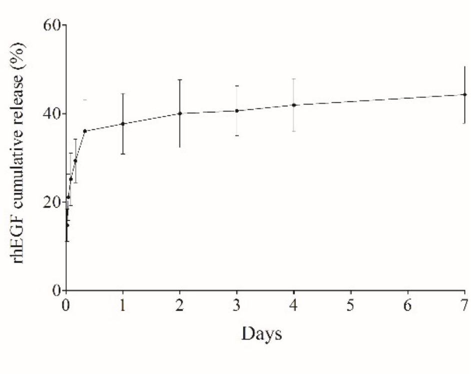


**Fig. 2.** rhEGF release profile. rhEGF cumulative *in vitro* release profile from PLGA-AV-EGF nanofibers. The assay was performed in triplicate and the results are given in terms of the mean ± SD of the cumulative percentage of rhEGF released over time.

### *3.4 Adhesion assay*

The adhesion ability of the cells to the nanofiborus membranes was evaluated seeding fibroblasts on top of the membranes. SEM images of those membranes showed cell adhesion onto the surface of the nanofibers (Fig. 5A). However, as showed in Fig. 5B, cells cannot attach well onto the membranes, since only a 16.85 ± 3.48 %, 17.99 ± 7.19 % and 24.73 ± 6.40 % of the cells got attached on to the PLGA-AV-EGF, PLGA-AV and PLGA nanofibers, respectively.

### *3.5* In vivo *wound healing assay*

The effectiveness of the membranes was evaluated in a full thickness splinted wound healing assay carried out in *db/db* mice by calculating the wound area closure. In that regard wounds areas ($px^2$) were measured from photographs taken on days 1, 4 and 8 post wounding, and the wound closure of each wound was calculated as the percentage of the initial area.

As shown in Fig. 6A the greatest wound area reduction was observed in the animals treated with the PLGA-AV-EGF nanofibers. The differences with the rest of the groups were found statistically significant both days, being these differences more pronounced on day 8. Those results were in agreement with the gross observa tion of the wounds depicted in Fig. 6B, where a higher reduction of the area was observed in the wounds treated with PLGA-AV-EGF nanofibers. Moreover, the mice that received the same dose of free rhEGF did not show any improvement of wound closure in comparison to control.

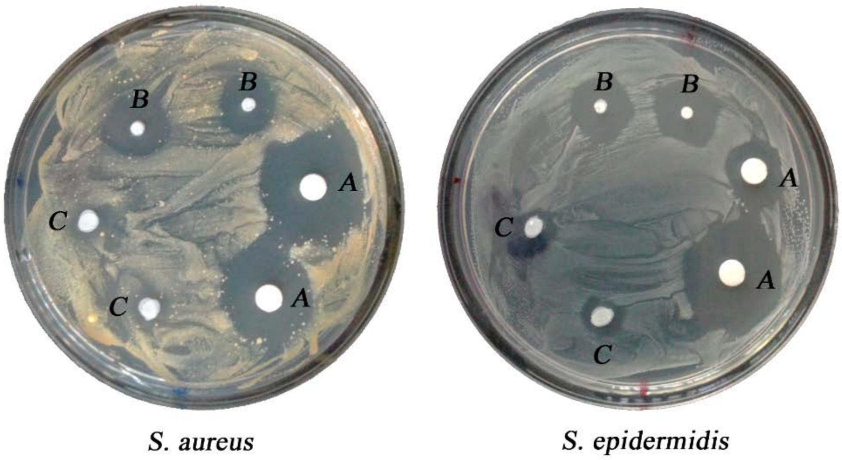


**Fig. 3.** *In vitro* antimicrobial assay. Images of the culture plates seeded with *S. aureus* and *S. epidermidis*. The inhibition zone caused by the samples can be observed: (A) free AV as control, (B) PLGA-AV nanofibers and (C) PLGA nanofibers.

Among the rest of the groups, no differences were observed on day 4. However, on day 8 the mice treated with PLGA-AV nanofibers presented a significantly higher wound closure compared to the rest of the groups.

Histological analyses were also made to assess the effectiveness of the developed formulations. For that purpose, wound biopsies were collected and stained either with H&E or Masson trichrome to evaluate reephitelisation, resolution of the inflammation and maturation of the wound, or collagen deposition, respectively. Fig. 7A shows a 10 fold magnification of histological sections (H&E stains) of wounds at day 8.

The evaluation of the reepithelisation was made following the criteria stablished by Sinha et al. (Sinha and Gallagher 2003). As depicted in Fig. 7B the results showed that the animals treated with PLGA-AV-EGF and PLGA-AV nanofibers presented a significantly higher grade of reepithelisation. In both cases, the mean reepithelisation value was around 3, which corresponds to wounds entirely covered with new epithelium of irregular thickness according to the previously mentioned

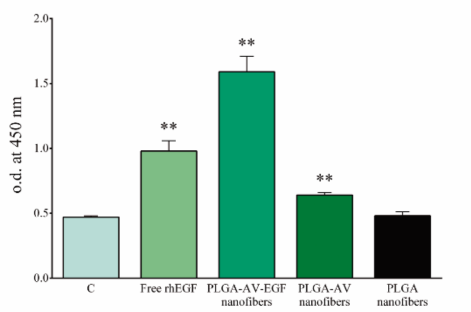


**Fig. 4.** Membranes bioactivity assay. The cell viability results are given as the mean O.D. values ± SD at 450 nm wavelength measured using the CCK-8 colourimetric assay.** $p<0.01$ comparing free rhEGF, PLGA-AV-EGF and PLGA-AV nanofibers with each other and the rest of the groups.

scale. Nevertheless, a great variability was observed in the group treated with PLGA-AV nanofibers (2.875 ± 0 991), since reepithelisation varied from covering less than the half of the wound (grade 1) to cover the entire wound with normal thickness (grade 4); while a much smaller variability was found in the group treated with PLGA-AV-EGF nanofibers (grade 2.875 ± 0.354), since every wound except one presented a value of 3.

The animals treated with PLGA nanofibers also showed a significant improvement of reepithelisation in comparison to the control (1.857 ± 0.9 and 0.875 ± 0.641, respectively), although the difference was smaller than the observed with the membranes containing active compounds.

The resolution of the inflammation was assessed according to the scale described by Cotran *et al.* (Cotran, et al. 2000). As illustrated in Fig. 7C, there were no significant differences among groups, although a slight tendency to accelerate the inflammation recovery was observed in the groups treated with PLGA-AV-EGF nanofibers and PLGA-AV nanofibers. In those groups the mean value of the inflammation resolution was around grade 3 (3 ± 0.926 and 2.875 ± 0.835, respectively), while in the remaining groups the mean value was around grade 2 (free rhEGF 2.25 ± 0.07, PLGA nanofibers 2.143 ± 0.9 and untreated control 1.75 ± 1.165), revealing a further maturation of the wounds belonging to the first groups, as they have advanced from the formation of the granulation tissue to fibroblast proliferation.

In addition, the groups treated with nanofibers containing active compounds were the only groups that achieved a complete disappearance of chronic inflammation (grade 4), precisely, 3 wounds reached a complete resolution and healing in the PLGA-AV-EGF nanofiber group and 2 wounds reached that grade in the PLGA-

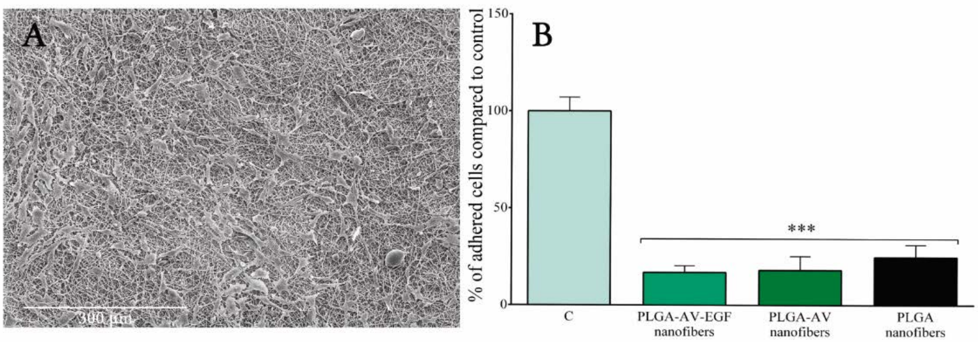


**Fig.5.** *In vitro* adhesion assay. (A) SEM image of the nanofibers with cells attached. The scale bar indicates 300 µm. (B) The cell adhesion results are given as the mean ± SD of the % of cells counted in comparison to the control. *** p<0.001 comparing PLGA-AV-EGF, PLGA-AV and PLGA nanofibers with the control group.

AV nanofiber group. Moreover, the rest of the groups presented wounds trapped in the acute inflammation phase (grade 1). That permanent migration of leucocytes and polynuclear neutrophils to the wound bed is typical of chronic wounds, due to the excessive amount of proteases released by neutrophils, which degrade the ECM delaying wound healing (Menke, et al. 2007).

In regard to collagen deposition (Fig. 7D), no differences were observed among groups. The greatest collagen deposition was observed in the animals treated with PLGA-AV-EGF nanofibers and PLGA nanofibers, since most of the wounds presented a mild deposition of collagen (grade 1 according to the criteria established by Gál *et al.* (Gál, et al. 2006)), and a few of them presented either a moderate content or absent of collagen, grade 2 and grade 0, respectively. Most of the wounds treated with PLGA-AV nanofibers and free rhEGF also showed mild content of collagen (grade 1), however, the rest of them did not present any collagen deposition (grade 0). Finally, in the control group a great variability was observed, since most of the wounds did not show any collagen (grade 0), whereas some of them presented a marked content of it (grade 3).

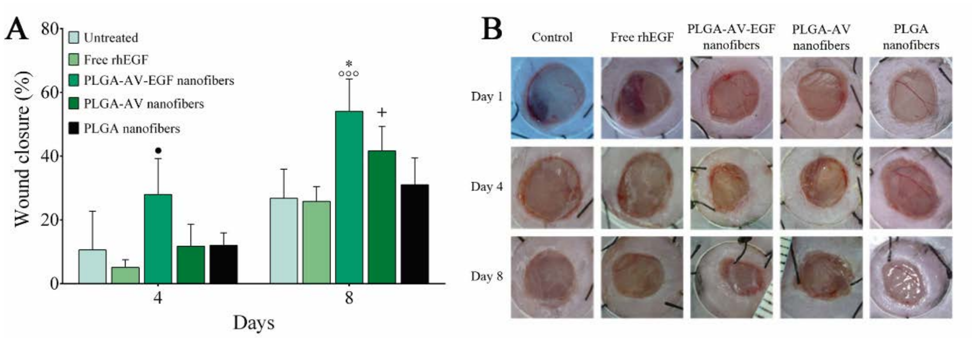


**Fig. 6.** *In vivo* wound closure. (A) Wound closure represented as the percentage of reduction of the initial area on days 4 and 8 after wound induction (n=8). ● $p<0.05$ comparing PLGA-AV-EGF nanofibers with the rest of the groups, on day 4. ○○○ $p<0.001$ comparing PLGA-AV-EGF nanofibers with free rhEGF, PLGA nanofibers and no treatment on day 8. * $p<0.05$ comparing PLGA-AV-EGF nanofibers with PLGA-AV nanofibers. + $p<0.05$ comparing PLGA-AV nanofibers with PLGA nanofibers, free rhEGF and untreated groups. (B) Wound images of each group on days 1, 4 and 8.

## 4. Discussion

The unique architectural features of nanofibrous membranes generated by electrospinning makes them a suitable option for developing novel wound dressings. Thus, the aim of this study was to develop a wound dressing loaded with rhEGF and composed of PLGA and the largest possible amount of *Aloe vera* extract. The produced membranes were composed of uniform and randomly oriented nanofibers and their high porosity allows cell respiration and gas permeation and prevents wound dehydration according to Abrigo *et al.* (Abrigo, et al. 2014).

The PLGA-AV-EGF and PLGA-AV nanofibers diameter was within the range of the collagen fibers of the ECM (50-500 nm). However, the PLGA nanofibers diameter was slightly above the upper limit.That mimicking of the ECM can promote the hemostasis of injured tissues due

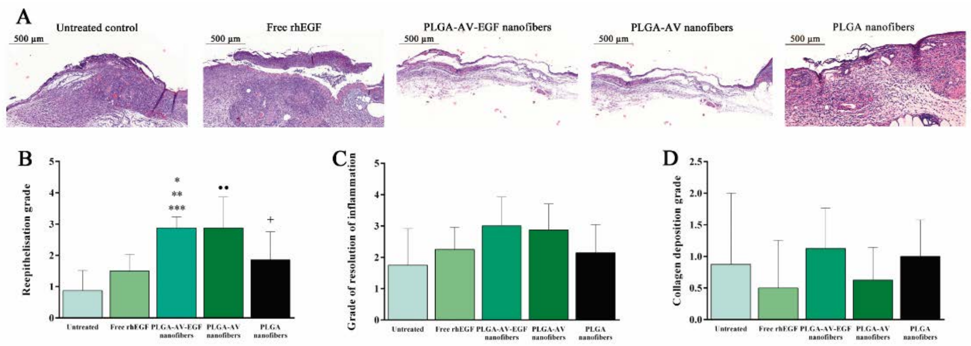


**Fig. 7.** Histological analysis of the wounds (n=8). (A) Histological images (H&E staining) of wounds at day 8, 10X magnification. (B) Reepithelisation grade of the wound on day 8. *** $p<0.001$ comparing PLGA-AV-EGF nanofiber treated group with untreated group. ** $p<0.01$ comparing PLGA-AV-EGF nanofiber treated group with the group treated with free rhEGF. *$p<0.05$ comparing PLGA-AV-EGF nanofiber treated group with the group treated with PLGA nanofibers. ●● $p<0.01$ comparing the group treated with PLGA-AV nanofibers with the group treated with free rhEGF and the untreated group. + $p<0.05$ comparing PLGA nanofiber treated group with untreated group. (C) Grade of resolution of the inflammation. (D) Collagen deposition on the wounds. Data are expressed as mean ±SD.

to the presence of small interstices and the high-surface area of the fibers (Abrigo, et al. 2014).

The mechanical properties of the membranes indicated that they were adequate for wound dressing application, since the obtained values were very similar to the human skin tensile strength, which ranged from 5.7 MPa to 12.6 MPa according to Jacquemoud *et al.* (Jacquemoud, et al. 2007). The slight differences found between the membranes tensile strenght lied in the different composition of the membranes, since the *Aloe vera* extract gave to the nanofibers more elasticity to endure tensile force rising the utilmate tensile strength of the PLGA-AV membrane, while the salts presents in the lyophilised rhEGF slightly decreased the PLGA-AV-EGF nanofibers tensile strength.

Although water uptake was similar in the three membranes, the PLGA nanofibers presented the lowest value. PLGA is a hydrophobic polymer and thus, its water uptake is low. However, the membranes containing AV were more hydrophilic and therefore, they were able to absorb more water. Those results were in agreement with the results obtained by Son et al. (Son, et al. 2013), who observed a higher degree of swelling when PLGA was electrospun with increasing gelatin concentrations rather than electrospun alone.

Wounds dressings require water vapour permeability to drain exudates, but they also need to retain moisture to help wound healing (Abrigo, et al. 2014; Natarajan, et al. 2000). In order to maintain that specific control of moisture, WVPR of commercial skin dressings have been reported to be in the range of 426-2047 $g/m^2$day (Tu, et al. 2015), therefore the developed dressings presented an adequate WVPR for wound healing application.

The results obtained in the analysis of the thermal behaviour showed that the electrospun PLGA presented a high degree of alignment and orientation of polymer chains, as suggested by the decrease of the $T_g$ of the PLGA membrane in comparison to the raw PLGA. Similar reduction in $T_g$ was observed previously (Fouad, et al. 2013). Moreover, the detection of the same thermal peaks in the PLGA-AV and

PLGA-AV-EGF electrospun membranes and the PLGA-AV physical blend reveals an immiscible blend morphology of this two components in the nanofibers.

The *in vitro* release of the EGF present in the PLGA-AV-EGF membrane exhibited a biphasic profile, with an initial burst release and a slower sustained phase. The burst release is related to the percentage of surface-associated protein, which is important to obtain a rapid activation of the keratinocytes of the wound edge (Schneider, et al. 2009). In the following sustained phase, only about the 50% of the total drug was released. Nevertheless, the release of the loaded drugs may be accelerated *in vivo*, driven by a faster polymer degradation caused by the enzymes present in the wound bed (Fredenberg, et al. 2011).

An important property of wound dressings is their ability to protect the wounds against microbial growth to prevent wound infections. According to the zone inhibition test, PLGA-AV membranes were able to inhibit bacterial growth, since AV presented antibacterial effect through numerous low molecular weight compounds, such as, α-bisabolol, lupeol, cinnamonic acid, salicylic acid and uric acid, which can kill bacteria by interfering with enzymatic processes (Ghayempour, et al. 2016; Tummalapalli, et al. 2016). Moreover, nanofibrous dressings can prevent bacterial growth into the wound creating a physical barrier, since the small pore size prevents the entry of microorganisms (Abrigo, et al. 2014).

The higher inhibition zone obtained by the free AV used as control might be due to the availability of the total AV dose since the beginning of the study, while the AV of the nanofibrous membranes needed to be release from the nanofibers in order to inhibit bacterial growth. Due to the lack of antibacterial activity of EGF, the antimicrobial activity of PLGA-AV-EGF membrane was not analysed, since the effect of the AV was already proven with the PLGA-AV membranes.

The bioactivity of the rhEGF and AV remained unchanged after the electrospinning process, since the extracts from the membranes maintained the ability to enhance fibroblast proliferation, as both of them have proven to do previously (Boudreau and Beland 2006; Gainza, et al. 2015a). Nevertheless, the most striking result from the bioactivity assay was the great promotion of cell proliferation by the PLGA-AV-EGF nanofibers, which revealed the beneficial effect of the combination of AV and rhEGF. Moreover, the effect in cell growth was caused exclusively by them, as highlighted by the lack of proliferation increment when cells were incubated with the PLGA nanofibers extract.

Since the membranes were designed to be changed during the treatment, cell adhesion or tissue ingrowth within the nanofibrous structure should be prevented in order to avoid pain and damage of the newly formed tissue after dressing removal. The low percentage of cells that got adhered onto the nanofibers proved their inability to attach cells, and therefore demonstrated their suitability as temporary wound dressings.

Wound healing was evaluated *in vivo* in a full thickness splinted model in *db/db* mice. Unlike in humans, reepithelisation does not play a major role in rodent wound healing models. However, in *db/db* mice this process gains importance due to a lack of wound contraction, making the healing process more similar to that of humans. Wound contraction is impaired because of the extreme obesity of the animals, which reduces the looseness of their skin (Fang, et al. 2010; Tkalcevic, et al. 2009). Moreover, the impairment of contraction is enhanced by the placement of silicone splints around the wounds, increasing the importance of reepithelisation (Michaels, et al. 2007). However, as we have observed in collagen deposition, the wound healing of these mice presented a wide variability as previously described by Trousdale *et al.* (Trousdale, et al. 2009).

Overall, the PLGA-AV-EGF nanofibers have shown that they can improve wound healing in terms of wound closure and reepithelisation, in comparison to free rhEGF. The enhanced wound healing activity of the nanofibers containing rhEGF can be partially explained by their protective effect against the proteases present in the wound bed, as shown by multiple in vivo studies carried out with EGF loaded nanofibers which did not contain Aloe vera, such as the study performed by Choi *et al.*, where PCL-PEG electrospun nanofibers were chemically conjugated with EGF (Choi, et al. 2008); or the study performed by Lai *et al.*, where a dual wound dressing composed of hialuronic acid fibers containing bFGF and gelatine nanoparticles loaded with VEGF and collagen fibers containing EGF and gelatine nanoparticles loaded with PDGF (Lai, et al. 2014), respectively. Moreover, the duration of the rhEGF in the wound is extended by the sustained release achieved with the electrospun membranes, and thus its effect is improved.

Although in a lesser extent than PLGA-AV-EGF nanofibers, the PLGA-AV nanofibers also showed an improvement of wound healing, since both Aloe vera and electrospun nanofibers themselves have been proven to enhance wound healing (Abrigo, et al. 2014; Hashemi, et al. 2015). The unique architecture of electrospun membranes, i.e. the high surface to volume area and the nanoporosity, allows water and gas permeability maintaining an adequate moisture of the wound and promoting cell respiration. Furthermore, the small size of the pores prevents the entry of microorganisms to the wound. Altogether, the electrospun membranes promote cell migration and proliferation to the wound bed, and thus enhance the release of wound healing mediators, such as, collagen, growth factors or angiogenic factors, and thereby facilitate the formation of granulation tissue and reepithelisation (Abrigo, et al. 2014; Shahverdi, et al. 2014). In addition, the improvement of re-epithelisation may be related to the chosen polymer; since the lactate, one of the degradation products of PLGA, has been proven to accelerate wound healing (Porporato, et al. 2012) .

*Aloe vera* has been used previously to develop nanofibrous dressings for tissue engineering in ratios of 1:3, 1:6 and 1:8 in comparison to the rest of the components (Bhaarathy, et al. 2014; Karuppuswamy, et al. 2014; Suganya, et al. 2014). However, in the current study the proportion of *Aloe vera* was considerably higher, since the ratio of Aloe vera, PLGA and rhEGF was 1:1:0.4. Therefore, it is the first time where nanofibers with that composition and such a large proportion of *Aloe vera* have been developed for wound dressing application. That use of *Aloe vera* highlights the novelty of the study, since it has shown to improve wound closure.

Accordingly, the improvement of wound closure was due to the combination of the three elements, the rhEGF, the *Aloe vera* extract and the PLGA nanofibers, since all of them promoted actively wound healing.

## 5. Conclusion

In the current study, an aqueous phase of *Aloe vera* was emulsified into PLGA and the emulsion was electrospun to develop a nanofibrous dressing loaded with rhEGF. The nanofibers contained the same amount of *Aloe vera* and PLGA (1:1), and to the best of our knowledge such a high concentration of *Aloe vera* for wound healing application in a nanofibrous dressing has not been studied so far.

The membranes were composed of uniform fibers of 356.03 ± 112.05 nm in diameter, presented a porosity of 87.52% and a thickness of 45.92 ± 0.78 µm. The electrospinning process did not affect the bioactivity of the active compounds as demonstrated by the *in vitro* bioactivity assay.

The *in vivo* full thickness wound healing assay carried out in *db/db* mice, showed an improvement in wound healing, in terms of wound closure and reephitelisation, when PLGA-AV-EGF nanofibers were applied on the wound. Accordingly, these results showed that the topical application of PLGA-AV-EGF nanofibers with a high concentration of *Aloe vera* might be a suitable strategy for the treatment of chronic wounds.

## 6. Acknowledgments

I. García-Orue thanks the Basque Government for the fellowship grant. The authors thank for technical and human support provided by SGIker of UPV/EHU and European funding (ERDF and ESF). This project has been funded by the Basque Government (ELKARTEK 2015, Nanoplatform, KK-2015/0000036). In addition, it has been partially supported by the University of the Basque Country

(UPV/EHU) (UFI 11/32). Authors also wish to thank the intellectual and technical assistance from the ICTS "NANBIOSIS", more specifically by the Drug Formulation Unit (U10) of the CIBER-BBN at the UPV/EHU.

## 7. References

Abrigo, M., McArthur, S.L., Kingshott, P., 2014. Electrospun Nanofibers as Dressings for Chronic Wound Care: Advances, Challenges, and Future Prospects. Macromol. Biosci., 14, 772-792. doi: 10.1002/mabi.201300561.

Bahrami, H., Keshel, S.H., Chari, A.J., Biazar, E., 2016. Human unrestricted somatic stem cells loaded in nanofibrous PCL scaffold and their healing effect on skin defects. Artif. Cells Nanomed. Biotechnol., 44, 1556-1560. doi: 10.3109/21691401.2015.1062390.

Bhaarathy, V., Venugopal, J., Gandhimathi, C., Ponpandian, N., Mangalaraj, D., Ramakrishna, S., 2014. Biologically improved nanofibrous scaffolds for cardiac tissue engineering. Mater. Sci. Eng. C. Mater. Biol. Appl., 44, 268-277. doi: http://dx.doi.org/10.1016/j.msec.2014. 08. 018.

Bhowmick, S., Scharnweber, D., Koul, V., 2016. Co-cultivation of keratinocyte-human mesenchymal stem cell (hMSC) on sericin loaded electrospun nanofibrous composite scaffold (cationic gelatin/hyaluronan/chondroitin sulfate) stimulates epithelial differentiation in hMSCs: In vitro study. Biomaterials, 88, 83-96. doi: http://dx.doi.org/10.1016/j.biomaterials.2016.02.034.

Bodnar, R.J., 2013. Epidermal Growth Factor and Epidermal Growth Factor Receptor: The Yin and Yang in the Treatment of Cutaneous Wounds and Cancer. Adv. Wound Care (New Rochelle), 2, 24-29. doi: 10.1089/wound .2011.0326.

Boudreau, M.D., Beland, F.A., 2006. An evaluation of the biological and toxicological properties of Aloe barbadensis (miller), Aloe vera. J. Environ. Sci. Health C Environ. Carcinog. Ecotoxicol. Rev., 24, 103-154. doi: 10.1080/ 10590500600614303.

Briquez, P.S., Hubbell, J.A., Martino, M.M., 2015. Extracellular Matrix-Inspired Growth Factor Delivery Systems for Skin Wound Healing. Adv. Wound Care (New Rochelle), 4, 479-489. doi: 10.1089/wound.2014.0603.

Choi, J.S., Kim, H.S., Yoo, H.S., 2015. Electrospinning strategies of drug-incorporated nanofibrous mats for wound recovery. Drug Deliv. Transl. Res., 5, 137-145. doi: 10.1007 /s13346-013-0148-9.

Choi, J.S., Leong, K.W., Yoo, H.S., 2008. In vivo wound healing of diabetic ulcers using electrospun nanofibers immobilized with human epidermal growth factor (EGF). Biomaterials, 29, 587-596. doi: http://dx.doi.org/ 10.1016/j.biomaterials.2007.10.012.

Choi, J.K., Jang, J., Jang, W., Kim, J., Bae, I., Bae, J., Park, Y., Kim, B.J., Lim, K., Park, J.W., 2012. The effect of epidermal growth factor (EGF) conjugated with low-molecular-weight protamine (LMWP) on wound healing of the skin. Biomaterials, 33, 8579-8590. doi:

http://dx.doi.org/10.1016/j.biomaterials.2012.07.061.

Choi, S., Chung, M., 2003. A review on the relationship between aloe vera components and their biologic effects. Semin. Integr. Med., 1, 53-62. doi: http://dx.doi.org/10.1016/S1543-1150(03)00005-X.

Cotran, R., Kumar, G.K., Collins, T., 2000. Reparación de los tejidos: proliferacion celular, fibrosis y curaicón de las heridasIn: Cotran, R., Kumar, G.K., Collins, T. (Eds.), Patología Estructural Y Funcional, McGraw-Hill, Interamericana, Madrid, pp. 95-120.

Dickinson, L.E., Gerecht, S., 2016. Engineered Biopolymeric Scaffolds for Chronic Wound Healing. Front. Physiol., 7, 341. doi: 10.3389/fphys.2016.00341.

Diegelmann, R.F., Evans, M.C., 2004. Wound healing: an overview of acute, fibrotic and delayed healing. Front. Biosci., 9, 283-289. doi: http://dx.doi.org/10.2741/.

Elgharably, H., Ganesh, K., Dickerson, J., Khanna, S., Abas, M., Ghatak, P.D., Dixit, S., Bergdall, V., Roy, S., Sen, C.K., 2014. A modified collagen gel dressing promotes angiogenesis in a preclinical swine model of chronic ischemic wounds. Adv. Wound Care (New Rochelle), 22, 720-729. doi: 10.1111/wrr.12229.

Fang, R.C., Kryger, Z.B., Buck II, D.W., De La Garza, M., Galiano, R.D., Mustoe, T.A., 2010. Limitations of the db/db mouse in translational wound healing research: Is the NONcNZO10 polygenic mouse model superior? Wound Repair Regen., 18, 605-613. doi: 10.1111/j.1524-475X.2010.00634.x.

Fang, R.C., Mustoe, T.A., 2008. Animal models of wound healing: uility in transgenic mice. J. Biomater. Sci. Polym. Ed., 19, 989-1005. doi: 10.1163/156856208784909327.

Fouad, H., Elsarnagawy, T., Almahjdi, F.N., Khalil, K.A., 2013. Preparation and in vitro thermo-mechanical characterization of electrospun PLGA nanofibers for soft and hard tissue replacement. Int. J. Electrochem. Sci., 8, 2293-2304.

Fredenberg, S., Wahlgren, M., Reslow, M., Axelsson, A., 2011. The mechanisms of drug release in poly(lactic-co-glycolic acid)-based drug delivery systems—A review. Int. J. Pharm., 415, 34-52. doi: http://dx.doi.org/10.1016/j.ijpharm.2011.05.049.

Fu, Y., Guan, J., Guo, S., Guo, F., Niu, X., Liu, Q., Zhang, C., Nie, H., Wang, Y., 2014. Human urine-derived stem cells in combination with polycaprolactone/gelatin nanofibrous membranes enhance wound healing by promoting angiogenesis. J. Transl. Med., 12, 274. doi: 10.1186/s12967-014-0274-2.

Gainza, G., Bonafonte, D.C., Moreno, B., Aguirre, J.J., Gutierrez, F.B., Villullas, S., Pedraz, J.L., Igartua, M., Hernandez, R.M., 2015a. The topical administration of rhEGF-loaded nanostructured lipid carriers (rhEGF-NLC) improves healing in a porcine full-thickness excisional wound model. J. Control Release, 197, 41-47. doi: http://dx.doi.org/10.1016/j.jconrel.2014.10.033.

Gainza, G., Villullas, S., Pedraz, J.L., Hernandez, R.M., Igartua, M., 2015b. Advances in drug delivery systems (DDSs) to release growth factors for wound healing and skin regeneration. Nanomedicine, 11, 1551-1573. doi: http://dx.doi.org/10.1016/j.nano.2015.03.002.

Gál, P., Toporcer, T., Vidinský, B., Mokrý, M., Novotný, M., Kilík, R., Smetana, K., Gál, T., Sabo, J., 2006. Early changes in the tensile stregnth and morphology of primary sutured skin wounds in rats. Folia Biol. (Praha), 52, 109-115.

Garg, T., Rath, G., Goyal, A.K., 2015. Biomaterials-based nanofiber scaffold: targeted and controlled carrier for cell and drug delivery. J. Drug Target., 23, 202-221. doi: 10.3109 /1061186X.2014.992899.

Ghayempour, S., Montazer, M., Mahmoudi Rad, M., 2016. Encapsulation of Aloe Vera extract into natural Tragacanth Gum as a novel green wound healing product. Int. J. Biol. Macromol., 93, Part A, 344-349. doi: http://dx.doi.org/10.1016/j.ijbiomac.2016.08.076.

Gu, J., Liu, N., Yang, X., Feng, Z., Qi, F., 2014. Adiposed-derived stem cells seeded on PLCL/P123 eletrospun nanofibrous scaffold enhance wound healing. Biomed. Mater., 9 (3), 035012. doi: 10.1088/1748-6041/9/3/035012.

Guillemin, Y., Le Broc, D., Ségalen, C., Kurkdjian, E., Gouze, J.N., 2016. Efficacy of a collagen-based dressing in an animal model of delayed wound healing. J. Wound Care, 25, 406-413. doi: 10.12968/jowc.2016.25.7.406.

Han, I., Shim, K.J., Kim, J.Y., Im, S.U., Sung, Y.K., Kim, M., Kang, I., Kim, J.C., 2007. Effect of Poly(3-hydroxybutyrate-co-3-hydroxyvalerate) Nanofiber Matrices Cocultured With Hair Follicular Epithelial and Dermal Cells for Biological Wound Dressing. Artif. Organs, 31, 801-808. doi: 10.1111/j.1525-1594.2007. 00466.x.

Hashemi, S.A., Madani, S.A., Abediankenari, S., 2015. The Review on Properties of Aloe Vera in Healing of Cutaneous Wounds. Biomed. Res. Int., 2015, 714216. doi: 10.1155/2015/714216.

Hodgkinson, T., Bayat, A., 2011. Dermal substitute-assisted healing: enhancing stem cell therapy with novel biomaterial design. Arch. Dermatol. Res., 303, 301-315. doi: 10.1007/s00403-011-1131-2.

Inpanya, P., Faikrua, A., Ounaroon, A., Sittichokechaiwut, A., Viyoch, J., 2012. Effects of the blended fibroin/aloe gel film on wound healing in streptozotocin-induced diabetic rats. Biomed. Mater., 7, 035008. doi: 10.1088/1748-6041/7/3/035008.

Jacquemoud, C., Bruyere-Garnier, K., Coret, M., 2007. Methodology to determine failure characteristics of planar soft tissues using a dynamic tensile test. J. Biomech., 40, 468-475. doi: http://dx.doi.org/10.1016/j.jbiomech .2005.12.010.

Karuppuswamy, P., Venugopal, J.R., Navaneethan, B., Laiva, A.L., Sridhar, S., Ramakrishna, S., 2014. Functionalized hybrid nanofibers to mimic native ECM for tissue engineering applications. Appl. Surf. Sci., 322, 162-168. doi: http://dx.doi.org/10.1016/j.apsusc.2014.10.074.

Kataria, K., Gupta, A., Rath, G., Mathur, R.B., Dhakate, S.R., 2014. In vivo wound healing performance of drug loaded electrospun composite nanofibers transdermal patch. Int. J.

Pharm., 469, 102-110. doi: http://dx.doi.org/10.1016/j.ijpharm.2014.04.047.

Keshel, S.H., Biazar, E., Rezaei Tavirani, M., Rahmati Roodsari, M., Ronaghi, A., Ebrahimi, M., Rad, H., Sahebalzamani, A., Rakhshan, A., Afsordeh, K., 2014. The healing effect of unrestricted somatic stem cells loaded in collagen-modified nanofibrous PHBV scaffold on full-thickness skin defects. Artif. Cells Nanomed. Biotechnol., 42, 210-216. doi: 10.3109/21691401.2013.800080.

Lai, H., Kuan, C., Wu, H., Tsai, J., Chen, T., Hsieh, D., Wang, T., 2014. Tailored design of electrospun composite nanofibers with staged release of multiple angiogenic growth factors for chronic wound healing. Acta Biomater., 10, 4156-4166. doi: http://dx.doi.org/10.1016/j.actbio.2014.05.001.

Lee, C., Hsieh, M., Chang, S., Lin, Y., Liu, S., Lin, T., Hung, K., Pang, J.S., Juang, J., 2014. Enhancement of Diabetic Wound Repair Using Biodegradable Nanofibrous Metformin-Eluting Membranes: in Vitro and in Vivo. ACS Appl. Mater. Interfaces, 6, 3979-3986. doi: 10.1021/am405329g.

Li, C., Fu, R., Yu, C., Li, Z., Guan, H., Hu, D., Zhao, D., Lu, L., 2013. Silver nanoparticle/chitosan oligosaccharide/poly(vinyl alcohol) nanofibers as wound dressings: a preclinical study. Int. J. Nanomedicine, 8, 4131-4145. doi: 10.2147/IJN.S51679 [doi].

Losi, P., Briganti, E., Errico, C., Lisella, A., Sanguinetti, E., Chiellini, F., Soldani, G., 2013. Fibrin-based scaffold incorporating VEGF- and bFGF-loaded nanoparticles stimulates wound healing in diabetic mice. Acta Biomater., 9, 7814-7821. doi: http://dx.doi.org/10.1016/j.actbio.2013.04.019.

Machula, H., Ensley, B., Kellar, R., 2014. Electrospun Tropoelastin for Delivery of Therapeutic Adipose-Derived Stem Cells to Full-Thickness Dermal Wounds. Adv. Wound Care (New Rochelle), 3, 367-375. doi: 10.1089/wound.2013.0513.

Magin, C.M., Neale, D.B., Drinker, M.C., Willenberg, B.J., Reddy, S.T., La Perle, K.M., Schultz, G.S., Brennan, A.B., 2016. Evaluation of a bilayered, micropatterned hydrogel dressing for full-thickness wound healing. Exp. Biol. Med. (Maywood), 241, 986-995. doi: 10.1177/1535370216640943.

Menke, N.B., Ward, K.R., Witten, T.M., Bonchev, D.G., Diegelmann, R.F., 2007. Impaired wound healing. Clin. Dermatol., 25, 19-25. doi: http://dx.doi.org/10.1016/j.clindermatol.2006.12.005.

Merrell, J.G., McLaughlin, S.W., Tie, L., Laurencin, C.T., Chen, A.F., Nair, L.S., 2009. Curcumin-loaded poly(epsilon-caprolactone) nanofibres: Diabetic wound dressing with anti-oxidant and anti-inflammatory properties. Clin. Exp. Pharmacol. Physiol., 36, 1149-1156. doi: 10.1111/j.1440-1681.2009.05216.x.

Michaels, J., Churgin, S.S., Blechman, K.M., Greives, M.R., Aarabi, S., Galiano, R.D., Gurtner, G.C., 2007. db/db mice exhibit severe wound-healing impairments compared with other murine diabetic strains in a silicone-splinted excisional wound model. Wound Repair Regen., 15, 665-670. doi: 10.1111/j.1524-475X.2007.00273.x.

Monaco, J.L., Lawrence, W.T., 2003. Acute wound healing: An overview. Clin. Plast. Surg., 30, 1-12. doi: http://dx.doi.org/10.1016/S0094-1298(02)00070-6.

Morton, L.M., Phillips, T.J., 2016. Wound healing and treating wounds: Differential diagnosis and evaluation of chronic wounds. J. Am. Acad. Dermatol., 74, 589-605. doi: http://dx.doi.org/10.1016/j.jaad.2015.08.068.

Moura, L.I.F., Dias, A.M.A., Suesca, E., Casadiegos, S., Leal, E.C., Fontanilla, M.R., Carvalho, L., de Sousa, H.C., Carvalho, E., 2014. Neurotensin-loaded collagen dressings reduce inflammation and improve wound healing in diabetic mice. Biochim. Biophys. Acta, 1842, 32-43. doi: http://dx.doi.org/10.1016/j.bbadis.2013.10.009.

Natarajan, S., Williamson, D., Stiltz, A.J., Harding, K., 2000. Advances in Wound Care and Healing Technology. Am. J. Clin. Dermatol., 1, 269-275. doi: 10.2165/00128071-200001050-00002.

Pachuau, L., 2015. Recent developments in novel drug delivery systems for wound healing. Expert. Opin. Drug Deliv., 12, 1895-1909. doi: 10.1517/17425247.2015.1070143.

Porporato, P.E., Payen, V.L., De Saedeleer, C.J., Préat, V., Thissen, P., Feron, O., Sonveaux, P., 2012. Lactate stimulates angiogenesis and accelerates the healing of superficial and ischemic wounds in mice . Angiogenesis, 15, 581-592. doi: 10.1007/s10456-012-9282-0.

Powell, H.M., Supp, D.M., Boyce, S.T., 2008. Influence of electrospun collagen on wound contraction of engineered skin substitutes. Biomaterials, 29, 834-843. doi: http://dx.doi.org/10.1016/j.biomaterials.2007.10.036.

Schneider, A., Wang, X.Y., Kaplan, D.L., Garlick, J.A., Egles, C., 2009. Biofunctionalized electrospun silk mats as a topical bioactive dressing for accelerated wound healing. Acta Biomater., 5, 2570-2578. doi: http://dx.doi.org/10.1016/j.actbio.2008.12.013.

Schreml, S., Szeimies, R., Prantl, L., Landthaler, M., Babilas, P., 2010. Wound healing in the 21st century. J. Am. Acad. Dermatol., 63, 866-881. doi: http://dx.doi.org/10.1016/j.jaad. 2009.10.048.

Seaton, M., Hocking, A., Gibran, N.S., 2015. Porcine Models of Cutaneous Wound Healing. ILAR Journal, 56, 127-138. doi: 10.1093/ilar/ilv016.

Sen, C.K., Gordillo, G.M., Roy, S., Kirsner, R., Lambert, L., Hunt, T.K., Gottrup, F., Gurtner, G.C., Longaker, M.T., 2009. Human skin wounds: A major and snowballing threat to public health and the economy. Wound Repair Regen., 17, 763-771. doi: 10.1111/j.1524-475X.2009.00543.x.

Shahverdi, S., Hajimiri, M., Esfandiari, M.A., Larijani, B., Atyabi, F., Rajabiani, A., Dehpour, A.R., Gharehaghaji, A.A., Dinarvand, R., 2014. Fabrication and structure analysis of poly(lactide-co-glycolic acid)/silk fibroin hybrid scaffold for wound dressing applications. Int. J. Pharm., 473, 345-355. doi: http://dx.doi.org/10.1016/j.ijpharm.2014.07.021.

Sinha, U.K., Gallagher, L.A., 2003. Effects of Steel Scalpel, Ultrasonic Scalpel, CO2 Laser, and Monopolar and Bipolar Electrosurgery on Wound Healing in Guinea Pig Oral Mucosa. Laryngoscope, 113, 228-236. doi: 10.1097/ 00005537-200302000-00007.

Son, S., Franco, R., Bae, S., Min, Y., Lee, B., 2013. Electrospun PLGA/gelatin fibrous tubes for the application of biodegradable intestinal stent in rat model. Journal of Biomedical Materials Research Part B: Applied Biomaterials, 101B, 1095-1105. doi: 10.1002/jbm.b.32923.

Steffens, D., Leonardi, D., Soster, P.R.d.L., Lersch, M., Rosa, A., Crestani, T., Scher, C., de Morais, M.G., Costa, J.A.V., Pranke, P., 2014. Development of a new nanofiber scaffold for use with stem cells in a third degree burn animal model. Burns, 40, 1650-1660. doi: http://dx.doi.org/10.1016/j.burns.2014.03.008.

Suganya, S., Venugopal, J., Ramakrishna, S., Lakshmi, B.S., Dev, V.R.G., 2014. Naturally derived biofunctional nanofibrous scaffold for skin tissue regeneration. Int. J. Biol. Macromol., 68, 135-143. doi: http://dx.doi.org/ 10.1016/j.ijbiomac.2014.04.031.

Tkalcevic, V.I., Cužic, S., Parnham, M.J., Pašalic, I., Brajša, K., 2009. Differential Evaluation of Excisional Non-occluded Wound Healing in db/db Mice. Toxico. Pathol., 37, 183-192. doi: 10.1177/0192623308329280.

Trousdale, R.K., Jacobs, S., Simhaee, D.A., Wu, J.K., Lustbader, J.W., 2009. Wound Closure and Metabolic Parameter Variability in a db/db Mouse Model for Diabetic Ulcers. J. Surg. Res., 151, 100-107. doi: http://dx.doi.org /10.1016/j.jss.2008.01.023.

Tu, Y., Zhou, M., Guo, Z., Li, Y., Hou, Y., Wang, D., Zhang, L., 2015. Preparation and characterization of thermosensitive artificial skin with a Sandwich structure. Mater Lett, 147, 4-7. doi: http://dx.doi.org/10.1016/ j.matlet.2015.01.163.

Tummalapalli, M., Berthet, M., Verrier, B., Deopura, B.L., Alam, M.S., Gupta, B., 2016. Composite wound dressings of pectin and gelatin with aloe vera and curcumin as bioactive agents. Int. J. Biol. Macromol., 82, 104-113. doi: http://dx.doi.org/10.1016/j.ijbiomac. 2015.10.087.

Uslu, I., Aytimur, A., 2012. Production and characterization of poly(vinyl alcohol)/poly(vinylpyrrolidone) iodine/poly (ethylene glycol) electrospun fibers with (hydroxypropyl)methyl cellulose and aloe vera as promising material for wound dressing. J. Appl. Polym. Sci., 124, 3520-3524. doi: 10.1002/app.35525.

Velnar, T., Bailey, T., Smrkolj, V., 2009. The Wound Healing Process: An Overview of the Cellular and Molecular Mechanisms. J. Int. Med. Res., 37, 1528-1542. doi: 10.1177/147323000903700531.

Whittam, A.J., Maan, Z.N., Duscher, D., Wong, V.W., Barrera, J.A., Januszyk, M., Gurtner, G.C., 2016. Challenges and Opportunities in Drug Delivery for Wound Healing. Adv. Wound Care (New Rochelle), 5, 79-88. doi: http://dx.doi.org/10.1089%2Fwound.2014 .060

# CHAPTER 3

## Composite nanofibrous membranes of PLGA/*Aloe vera* containing lipid nanoparticles for wound dressing applications

I. Garcia-Orue [a,b], G. Gainza[c], P. Garcia-Garcia[d], F.B. Gutierrez[e], J.J. Aguirre[e,d], R.M. Hernandez[a,b], A. Delgado[d*], M. Igartua[a,b*]

[a] NanoBioCel Group, Laboratory of Pharmaceutics, School of Pharmacy, University of the Basque Country (UPV/EHU).

[b] Biomedical Research Networking Centre in Bioengineering, Biomaterials and Nanomedicine (CIBER-BBN).

[c] Biopraxis Research AIE, Miñano, Vitoria-Gasteiz.

[d] Department of Chemical Engineering and Pharmaceutical Technology, School of Pharmacy, Institute of Biomedical Technologies (ITB), Center for Biomedical Research of the Canary Islands (CIBICAN), University of La Laguna, Tenerife.

[e] Hospital Universitario de Álava (HUA) Txagorritxu, Vitoria-Gasteiz, 01009, Spain.

*Corresponding author: A. Delgado and M. Igartua

**ABSTRACT**

Electrospun nanofibrous dressings present suitable characteristics to be used in wound healing, such as high porosity and high surface area-to-volume ratio. In this study, a wound dressing based in PLGA and *Aloe vera* containing lipid nanoparticles (NLCs) was developed. NLCs were added in order to add a lipid component that could avoid the adhesion of the dressing to the wound and improve its handling. Membranes with and without NLCs were composed of uniform fibers of about 1 µm in diameter. Their porosity was above 80% and their thickness was about 160 µm. Both dressings showed similar water uptake and water vapour transmision rate, of 370 % and 1100 g/m$^2$day, respectively. The formulation containing NLCs presented a higher ultimate tensile strength (2.61 ± 0.46 MPa). Both formulations were biocompatible *in vitro*. Furthermore, the cell adhesion assay demonstrated that both membranes had a low adherence profile, although it was lower with the dressing containing NLCs. Finally, their efficacy was evaluated in a full thickness wound healing assay conducted in *db/db* mice, where both enhanced healing similarly. Accordingly, the PLGA-AV-NLC membrane might be a promising strategy for the treatment of chronic wounds, since it improved handling in comparison to the formulation without NLCs.

**Sent to:** International Journal of Pharmaceutics.

## 1. Introduction

Electrospinning is a technique to obtain membranes composed of polymeric nanofibers, which uses electric force to elute nanofibers from a polymeric solution. Due to the electrostatic repulsion produced by the application of high voltage charges to the solution, the polymeric droplet is stretched and ejected to the collector. The final nanofibers are formed during the ejection process in which solvent is evaporated, allowing the arrival of solid nanofibers to the collector [1,2]. This process produces membranes composed of nonwoven polymeric nanofibers that mimic the three dimensional structure of extracellular matrix [3]. Their distinctive characteristics are high porosity and a high surface area-to-volume ratio. Those properties make them suitable to develop dressings for wound healing, as they allow gas permeation and thus cells breathing [4]. In addition, they help to regulate wound moisture, enhancing tissue regeneration [5], since they promote the removal of exudates from the wound bed, and they retain moisture to prevent wound desiccation [6]. Furthermore, the small size of the pores hinders the entrance of microorganisms, and thus wound infection [2].

Research to develop novel wound dressings has gained importance due to the great increase in chronic wound incidence; in fact, only in the US, chronic wounds annually affect 5.7 million people (around 2% of the population) and cost $20 billions [7]. A factor involved in that growth is the rise of diseases associated with wound chronicity, such as, diabetes, venous insufficiency and obesity [8,9]. Wounds occurring in patients suffering those diseases, usually fail to progress through the organized steps of physiological healing that comprises the following subsequent but overlapping phases: hemostasis, inflammation, proliferation and remodelling phase [10,11]. Chronic wounds remain stagnated into the inflammatory phase, with a constant infiltration of macrophages and neutrophils to the wound bed [12]. Those cells secrete a great amount of proinflammatory cytokines and proteases, that degrade healing mediators and extracellular matrix and hamper the formation of new epithelia, leading to a delay in healing [11,13].

In the current study, we developed a composite nanofibrous membrane of PLGA (poly lactic-co-glycolide acid) and *Aloe vera* extract containing lipid nanoparticles (nanostructured lipid carriers or NLC) [14]. PLGA is a synthetic polymer which has good biocompatibility and biodegradability [15]. In comparison to natural polymers, it presents some advantages, among which are lower price; well-defined structure and degradation kinetics; reliability [16]; better mechanical properties, that make them more easily electrospinable [17]; and the presence of lactate as a degradation product, which has proven to accelerate wound healing [18].

In order to improve the wound healing properties of the PLGA nanofibers, they were also composed of *Aloe vera,* which has been widely used in wound healing since ancient times [19], because it has shown to promote healing in addition to its anti-inflammatory, antifungal, antibacterial and hypoglycemic properties [20]. Due to the action of glucomannan, Aloe vera affects fibroblast growth factor (FGF), stimulating the activity and proliferation of fibroblasts, and thus, enhancing their collagen production and secretion, as well as the transversal connection among collagen chains [21,22]. In addition, Aloe vera contains some vitamins, amino acids and anthraquinones involved in the enhacement of wound healing due to their antioxidant activity [23]. Finally, it is noteworthy to mention that due to its antimicrobial activity, *Aloe vera* can help in the prevention of wound infection [21]. For all the above reasons, *Aloe vera* has been already used to develop nanofibrous wound dressings using different polymers, such as, silk fibroin, poly-lactic-co-ε-caprolactone, poly- caprolactone, PLGA, Poly(vinyl) alcohol or poly-L-lactic acid [14,24-28].

Traditionally, primary dressings have been impregnated in vaseline or paraffin to prevent adhesion to the wound surface. Nevertheless, the lipid component frequently was absorbed into the secondary dressing or in the wound, drying the primary dressing and increasing the risk of adherence to the wound [29,30]. In order to avoid that limitation, Urgotul™ was developed, a non-occlusive thin sheet composed of a polyester net impregnated with hydrocolloid particles dispersed in a petroleum jelly matrix. In contact with wound exudates the hydrocolloid particles hydrate, and jointly with the petroleum jelly, they form a lipido-colloid interphase that prevent wound adherence [31,32]. Considering this, in the present study, NLCs were incorporated to the PLGA/*Aloe vera* formulation in order to add a lipid component that could avoid adhesion to the wound. The NLCs were distributed in the PLGA nanofibrous structure during the electrospinning process, in order to avoid its diffusion to the secondary dressing and thus, decrease the risk of adherence. Furthermore, we hypothesise that the addition of the NLCs could improve some features of the dressing, such as, handling, elasticity and occlusivity. The fabricated nanofibrous PLGA-AV-NLC membranes were subjected to physical, mechanical and cytocompatibility evaluation. Their wound healing efficacy was assessed *in vivo* in a splinted full thickness wound model performed in diabetic *db/db* mice.

## 2. Material and methods

### *2.1 Nanofibers preparation*

PLGA-AV-NLC nanofibers were produced electrospinning an emulsion containing all the components. The organic phase was composed of 300 mg of PLGA (Resomer, LG824; Evonik, Germany) into 2.5 ml of hexafluoroisopropanol (HFIP, Fluka, Switzerland), and the aqueous phase was composed of 300 mg of *Aloe vera* extract (Agora Valencia SL:, Spain) and 30 mg of NLCs in 1.2 ml of a 0.5 % (w/v) PVA solution. To create the emulsion both phases were vortexed at level 10 for 3 min (Vortex-Genie 2, Scientific Industries Inc., USA). The resulting emulsion was loaded into a Luer-lock syringe (Norm-Ject) containing a 14 G needle and attached to a pump (Harvard Apparatus, MA) that provided a flow rate of 2.7 mL/h. The nanofibers were electrospun horizontally on a rotating collector (250 rpm) located at 8 cm from the needle, under 10 kV power supply. Similarly, PLGA-AV nanofibers were prepared without adding NLCs to the aqueous phase.

The NLCs incorporated into the nanofibers were prepared following the procedure described previously by our research group [33-35]. Briefly, an aqueous phase composed of 40 mg of Tween® 80 (Panreac, Spain) and 20 mg of Poloxamer 188 (Panreac, Spain) in 3 ml MilliQ water and a lipid phase composed of 200 mg of Precirol® ATO 5 (Gattefossé Spain, Spain) and 20 mg of Mygliol 812N (Sasol Germany GmbH), were heated separately until the lipid phase melted into a clear solution (40°C). Then, the aqueous phase was added to the lipid phase and the mixture was sonicated for 15 s at 50 W (Branson® 250 Sonifier, CT, USA). The resulting emulsion was stored at 4°C overnight to allow the re-crystallisation of the lipid.

It is noteworthy to mention that before the *in vitro* and *in vivo* studies the membranes were sterilised by keeping them under UV light for 30 min.

*2.2 Nanoparticle and nanofiber characterisation*

The mean particle size (Z-average diameter) and the polydispersity index (PDI) of the NLCs incorporated into the nanofibers were measured through Dynamic Light Scattering (DLS) and their zeta potential was determined by Laser Doppler micro-electrophoresis (Malvern® Zetasizer Nano ZS, Model Zen 3600; Malvern instruments Ltd., UK). The electrophoretic mobility was measured in water (pH 5.6) and it was converted into zeta potential through the Smoluchowski approximation.

The morphology of the nanofibrous membranes, namely, fiber diameter and membrane quality, was assessed using Scanning Electron Microscopy photographs (SEM, Jeol JSM-6300) and their thickness was measured using stereo microscopy photographs (Leica M205 C, Leica LAS, v3 software, Germany). Membrane's porosity (P) was calculated using the following equation (Eq. 1):

$$P\ (\%)=\left(1-\frac{\rho_{app}}{\rho_{real}}\right)\times 100 \qquad (1)$$

Where $\rho_{real}$ is the real density that was assessed by means of a helium pycnometer (Micromeritics, AccuPyc 1330, USA); and $\rho_{app}$ is the apparent density that was calculated dividing the weighed mass of the membranes by their volume (length × width × height).

The monotonic tensile tests of both dressings (PLGA-AV and PLGA-AV-NLC membranes) were performed under displacement control on a texture analyser, using a 5 N full scale load cell (Instron 5848 microtester, Instron®, UK). The samples were loaded at a displacement rate of 0.01 mm/s up to rupture. The load-displacement curve obtained from those tests was transformed into a stress-strain curve and the ultimate tensile strength was obtained from it. At least 5 samples were tested from each membrane and the results were shown as mean ± standard deviation (SD).

To determine the water uptake of the different nanofibrous membranes 1.3x1.3 cm pieces of the membranes were cut and weighed. Then, the samples were immersed in 1 ml of PBS and incubated at 32 °C for 72 h. After incubation, the excess of water was dried blotting them with filter paper and they were weighed again to calculate the water uptake using the following equation (Eq. 2):

$$\text{Water uptake (\%)} = \frac{M-M_0}{M_0} \times 100 \qquad (2)$$

Where $M_0$ and M are the mass of the membranes before and after 72 h incubation in PBS, respectively.

The Water Vapour Transmision Rate (WVTR) of the membranes was quantified following a modified procedure of the method described by Li *et al.* [36]. The mouth of a cup filled with silica gel dessicant (1 cm in diameter) was thoroughly sealed with a piece of the nanofibrous membrane, to make the membrane the only way water vapour could enter to the cup. The assembly was weighed and placed in a chamber with a constant relative humidity of 75% at 30 °C. After 24 h, the assembly was weighed again to calculate the WVTR through the following equation (Eq. 3):

$$\text{WVTR} = \frac{M_1-M_0}{A \times T} \qquad (3)$$

Where $M_0$ is the weight of the assembly at the beginning of the assay, $M_1$ is its weight after the incubation time, T is the exposure time (1 day) and A is the exposure area (0.79 $cm^2$).

The thermal behaviour of the nanofibrous membranes, the physical blend of their components and the components themselves was analysed using Differential Scanning Calorimetry (DSC-50, Shimadzu, Japan). 1-2 mg of each sample was weighed and sealed into an aluminium pan. Then, the samples were heated from 25°C to 350°C at a heating rate of 10°C per minute.

### *2.3* In vitro *cell culture studies*

#### *2.3.1 Cell culture*

The cell lines used in this study were HaCaT keratinocytes and BalbC/3T3 A31 fibroblasts (ATCC, Manassas, USA). The first one was cultured on Dulbecco's modified Eagle's medium (DMEM) (41965-039, Gibco®, Ma, USA) supplemented with 10% (v/v) foetal bovine serum (FBS) and 1% (v/v) penicillin-streptomycin. The fibroblasts were cultured on DMEM (30-2202, ATCC, Manassas, USA) supplemented with 10% (v/v) foetal calf serum (FCS) and 1% (v/v) penicillin-streptomycin. Cell lines were incubated in a humidified incubator at 37 °C with a 5% $CO_2$ atmosphere and cell passages were done every 2-3 days depending on the cell line.

#### *2.3.2 Cell viability studies*

The effect of the nanofibrous membranes on cell viability was assessed incubating their extracted medium with fibroblast and keratinocytes. The cells were seeded in a 96 well-plate, fibroblasts at a density of 6000 cell/well and keratinocytes at 12000 cell/well.

Cells were cultured overnight to allow cell attachment, and then, the following samples were added: (i) starving medium as negative control, (ii) medium incubated with a 1x1 cm piece of PLGA-AV membrane for 24 hours, (iii) medium incubated with a 1x1 cm piece of PLGA-AV-NLC membrane for 24 hours. The starving medium for the control and samples incubated with HaCaT cells, was DMEM containing 0.5% (v/v) of FBS and for the samples incubated with fibroblasts was DMEM with 0.2% (v/v) of FCS.

Cells were incubated with the samples for 48 h, and afterwards the viability was assessed using a CCK-8 kit (cell counting kit-8, Sigma-Aldrich, Saint Louise, USA). Briefly, 10 µL of the CCK-8 reagent was added to the cells. After 4 hours of incubation the absorbance of the mixture was read at 450 nm, using 650 nm as reference wavelength (Plate Reader Infinite M200, Tecan, Switzerland). The absorbance and the number of living cells in each well were directly proportional.

*2.3.3 Adhesion assay*

The ability of the cells to adhere to the nanofibrous membranes was evaluated by seeding cells on top of them and measuring the number of adhered cells after an incubation time. PLGA-AV and PLGA-AV-NLC membranes were cut in disks of 14 mm in diameter and fixed to the bottom of 24 well-plates using 10 µl of fibrin as adhesive. Membranes were incubated for 30 min to allow the formation of fibrin clot and then cells were seeded on top of them, fibroblasts at a density of 20,000 cells/well and keratinocytes at a density of 40,000 cells/well. Control wells were also seeded with the same cell density.

Cells were incubated overnight to allow their attachment to the membranes. Then, membranes were washed with PBS and cells were detached incubating them with trypsin for 10 minutes. After trypsin neutralization, cells were collected and centrifugated for 5 minutes at 100 rpm. Finally, cells were counted using an automated cell counter (Automated Cell Counter TC20™, Bio-Rad, California, USA). The adhesion to the membranes was expressed as the percentage of cells counted comparing to the control. Three independent studies were performed.

In addition, SEM images were taken to observe the adhered cells and their morphology. For this assay, membranes and cells were incubated as in the previous one. But, after overnight incubation, instead of detaching them, cells were fixed in a 2.5 % glutaraldehyde solution and dehydrated in graded ethanol series. Finally, microphotographs of the membranes were taken using a SEM microscope (Hitachi S4800, Tokyo, Japan).

### *2.4* In vivo *wound healing assay*

#### *2.4.1 Animals*

For the *in vivo* study 24 male *db/db* mice (BKS.Cg-m$^{+/+}$Lepr$^{db/J}$) of 6 weeks old were used (Janvier laboratories, Sain Berthevin Cedex, France). All the experiments were conducted following the protocols approved by the Institutional Ethical Committee for Animal Experimentation of the University of the Basque Country (Procedure number: M20_2015_155_ HERNÁNDEZ MARTÍN). Each mouse was housed individually under a 12 h light-dark cycle, and they had *ad libitum* access to standard rodent chow and water.

#### *2.4.2. Wound healing assay*

This assay was performed following the procedure described by Michaels *et al.* [37]. Mice were anesthetised with isoflurane (Isoflo®, Esteve, Spain) and their dorsal hair was removed. In order to avoid healing through wound contraction, and thus enhance reepithelisation, two silicone rings of 1 cm in diameter were sutured on the back of the mice, in each side of the midline using a 3-0 nylon suture (Aragó, Spain). In the middle of each splint, a full thickness wound extending through the *panniculus carnosus* was created using an 8 mm in diameter punch biopsy tool (Acu-Punch, Acuderm, USA). Afterwards, treatments were applied and finally the wounds were covered with petrolatum gauze (Tegaderm®, 3M, Minnesota, USA) and adhesive.

On days 4, 8, and 11, the membranes were removed and new treatments were applied. On day 8, half of the mice were sacrificed through $CO_2$ inhalation, and the remaining mice were sacrificed on day 15.

Mice were divided in 3 groups of 8 animal each (n=8). Each group received a different treatment: (i) untreated control, (ii) a dressing of 1.5x1.5 cm of PLGA-AV membrane previously hydrated in PBS, and (iii) a dressing of 1.5x1.5 cm of PLGA-AV-NLC membrane previously hydrated in PBS.

#### *2.4.3 Evaluation of wound healing*

The effectiveness of the treatments was evaluated assessing the wound closure percentage in each wound. On days 1, 4, 8, 11 and 15 photographs of the wounds were taken using a digital camera (Lumix FS16, Panasonic®, Japan) and the area of each wound ($px^2$) was measured using an image analysis programme (ImageJ®, Biophotonics Facility, University of McMaster, Canada). The wound closure percentage was calculated using the following equation (Eq. 4):

$$\text{Wound closure (\%)} = \frac{\text{Final area}}{\text{Initial area}} \times 100 \quad (4)$$

*2.4.4 Hystological analysis of healing*

After mice sacrifice, the wound and surrounding tissue (about 1x1 cm) were excised and fixed in 3.7% paraformaldehyde. Tissue was allowed to fix during 24 h and then, the biopsies were bisected, embedded in paraffin and sectioned in layers of a thickness of 5 µm. Those slices were processed by hematoxylin-eosin (H&E) staining to evaluate their progress through wound healing.

The reepithelisation process was evaluated in accordance with the scale established by Sinha *et al.* [38]. Each wound was semi-quantitatively rated with a value within a range from 0 to 4: 0, reephitelisated area was confined to wound margins; 1, the new epithelium covers less than half of the wound area; 2, the new epithelium covers more than half of the wound area; 3, the entire wound is reepithelised with irregular thickness; and 4, the entire wound is reepithelised and the new epithelium has normal thickness.

The resolution of the inflammatory process and wound maturity was assessed following the scale established by Cotran *et al.* [39]. Wounds were scored according to the following criteria: 0, absence of inflammation; 1, acute inflammation, in this phase the fibrin clot and the pyogenic membrane are formed and the leucocytes and polynuclear neutrophils migrate to the wound; 2, diffuse acute inflammation, this phase comprises the formation of the granulation tissue, and the disappearance of the pyogenic membrane; 3, chronic inflammation, this phase consists on fibroblast proliferation and 4; resolution and healing: this phase consist on the disappearance of chronic inflammation, although occasionally round cells can be observed.

*2.4.5 Immunohistochemical analysis*

In order to perform immunohistochemical studies, tissue slices were deparaffinised and automatically processes according to the U Ultra View DAB detection kit (Roche, Switzerland). First, tissue biopsies were incubated with the primary antibodies at 37 °C. The incubation period varied depending on the antibody, 12 min for the anti-CD68 (clone KP-1, Roche, Switzerland), 32 min for the anti-CD4 (SP-35, Roche, Switzerland) and 44 min for the anti-CD8 (SP-57, Roche, Switzerland). Subsequently, biopsies were stained with DAB and hematoxylin as counterstain. Finally, positive cells were counted using the QuPath analysis software (Centre for Cancer Research & Cell Biology at Queen's University, UK). Immunohistochemical analyses were performed on biopsies of day 8, because on day 15 complete healing was achieved in some groups, and therefore no differences were expected.

*2.5 Statistical analysis*

Results were expressed as the mean ± standard deviation. Results were analysed through student T-test to compare two groups or through one-way ANOVA test for multiple comparisons. Based on the Levene test for the homogeneity of variances, Bonferroni of Tamhane post-hoc were applied. All the statistical tests were performed using SPSS 22.0.01 (SPSS®, INC., Chicago, IL, USA).

## 3. Results

*3.1 Nanofiber characterisation*

The mean size of the NLCs incorporated into the nanofibrous membranes was 139.92 ± 5.02 nm with a PDI of 0.185 ± 0.0025, which indicate a stable polydisperse system. The zeta potential revealed that the surface charge of the NLCs was -20.79 ± 0.87 mV.

The morphology of the nanofibrous membranes is displayed in Fig. 1, SEM images showed that both membranes were composed of uniform nanofibers, with a diameter of 0.96 ± 0.34 µm and 1.10 ± 0.42 µm for the PLGA-AV-NLC and PLGA-AV nanofibrous membranes, respectively (Table 1). Both membranes presented a similar porosity, being 81.55 ± 1.16% for PLGA-AV membranes and 84.23 ± 0.85 % for PLGA-AV-NLC membranes. The PLGA-AV-NLC membrane was slightly thicker than the PLGA-AV membrane, with a value of 178.04 ± 42.05 µm and 158.03 ± 17.41 µm, respectively.

The integrity and elasticity of the membranes was evaluated calculating the mechanical properties of each membrane. The ultimate tensile strength was significantly higher in the PLGA-AV-NLC membranes than in the PLGA-AV membranes, as shown on table 1, the values were 2.61 ± 0.46 MPa and 1.69 ± 0.35 MPa, respectively (*** p>0.001).

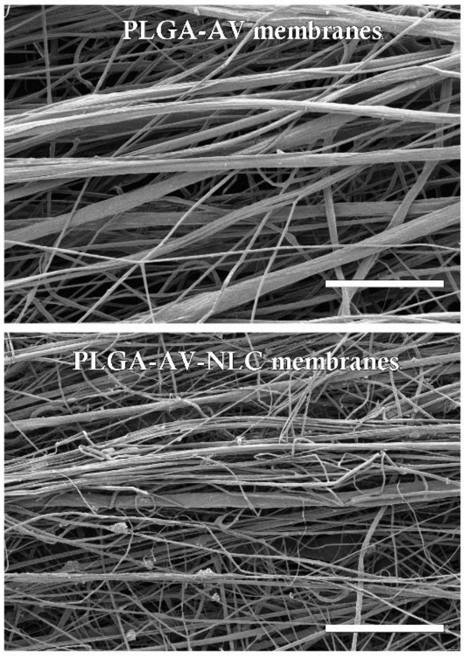


**Fig 1.** SEM images of the PLGA-AV and PLGA-AV-NLC membranes. The scale bar of each image indicates 100 µm.

**Table 1.** Dressing characterisation: nanofibers diameter (nm), membrane porosity (%), membrane thickness (µm), tensile strength (MPa), water uptake (%) and WVTR (g/m$^2$day). Data are expressed as the mean ± SD.

| Nanofiber composition | Nanofiber diameter (µm) | Porosity (%) | Thickness (µm) | Tensile strength (MPa) | Water uptake (%) | WVTR (g/m$^2$day) |
|---|---|---|---|---|---|---|
| PLGA-AV membrane | 1.10 ± 0.42 | 81.55 ±1.16 | 158.03 ±17.41 | 1.69 ±0.35 | 369.06 ±28.09 | 1128.06 ±93.23 |
| PLGA-AV-NLC membrane | 0.96 ± 0.34 | 84.23 ±0.85 | 178.04 ±42.05 | 2.61 ±0.46 | 384.32 ±35.65 | 1097.6 ±102.83 |

The water uptake of the membranes was quantified to determine their hydrophilicity. The results showed that both membranes presented a similar water uptake in 72 hours, being 369.06 ± 28.09 % in PLGA-AV nanofibrous membranes and 384.32 ± 35.65 % in PLGA-AV-NLC membranes.

The ability of the dressings to regulate wound moisture was assessed measuring their WVTR. As observed in table 1, both membranes presented similar values, although it was slightly lower for PLGA-AV-NLC nanofibers, with a value of 1128.06 ± 93.23, g/m$^2$day while it was 1097.6 ± 102.83 g/m$^2$day in the case of PLGA-AV-NLC nanofibers.

Regarding to the thermal behaviour, the thermograms of the raw materials, presented the following aspect: PLGA's glass transition temperature ($T_g$) was 156.95 ± 1.30 °C; AV did not show any marked peak, it was a curve; and NLCs presented an endothermic peak at 54.81 ± 0.30 °C, as depicted in Table 2. The physical blends of the components and the nanofibrous membranes had the same peaks than the raw materials, including the curve observed in the thermogram of AV. Nevertheless, a minor decrease on the $T_g$ of PLGA was observed on the nanofibers, and the peak of the NLCs was slightly increased on the physical blend and on the nanofibers.

**Table 2.** DSC peaks. The endothermic DSC peaks of the nanofibers, their components blends and their components itself. Data are expressed as mean ± SD.

| | Endothermic DSC peak (°C) |
|---|---|
| PLGA | 156.95 ± 1.30 |
| NLC | 54.81 ± 0.30 |
| PLGA + AV blend | 156.38 ± 2,88 |
| PLGA+AV+NLC blend | 56.26 ± 2.94<br>157.73 ±0.78 |
| PLGA-AV membrane | 153.27 ± 042 |
| PLGA-AV-NLC membrane | 59.98 ± 0.17<br>152.86 ± 0.08 |

### *3.2* In vitro *cell viability studies*

In order to assess the cytocompatibility of the membranes, they were incubated with culture medium for 24 h, and then the medium was incubated with keratinocytes and fibroblasts. After 48 h, cell viability was measured through a CCK-8 assay. Fig. 4 illustrates the results obtained in the CCK-8 assay. None of the membranes were cytotoxic showing percentages of cell viability greater than 70% in in both cell lines tested. When the extracted medium was cultured with fibroblasts, both membranes achieved a significantly higher cell viability in comparison to the control. Among them, the highest cell proliferation was observed with PLGA-AV membranes, and the difference between them was statistically significant. Nevertheless, when the extracted medium of any of the membranes was cultured with keratinocytes, cell viability was lower than in the control group.

*3.3 Cell adhesion studies*

To assess whether the cells were able to adhere to the nanofibrous membranes or not, they were seeded on top of the membranes and SEM images were taken or adhered cell number counted. Although the counting process showed that some cells were able to adhere to the membranes, they could not be observed in SEM images, as illustrated in Fig. 3A.  As dep-

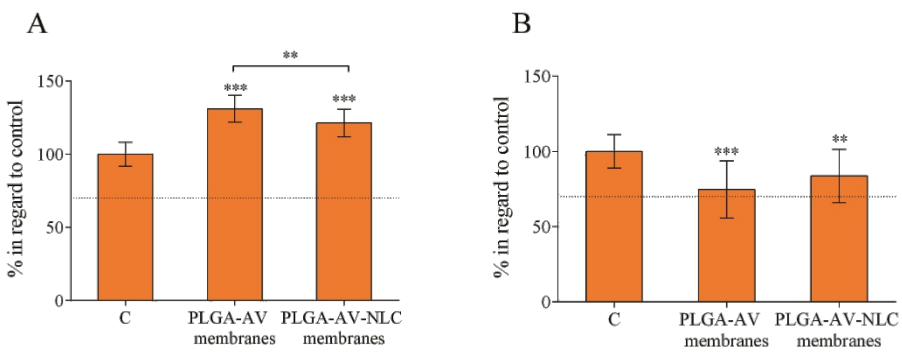


**Fig 2.** Cell viability study. (A) CCK-8 results after culturing the membranes´ extracted medium with fibroblast. *** p<0.001 comparing PLGA-AV-NLC and PLGA-AV membranes with the control; and ** p<0.01 comparing PLGA-AV membranes with PLGA-AV-NLC membranes. (B) CCK-8 results after culturing the membranes´ extracted medium with keratinocytes. *** p<0.001 comparing PLGA-AV nmemebranes with the control; and ** p<0.01 comparing PLGA-AV-NLC membranes with the control. Results are given as the mean % of living cells regarding to the control ± SD.

icted in Fig. 3B and 3C, in comparison to the bottom of the wells, both cell lines had a significantly impaired adhesion to the membranes. It is noteworthy to mention, that in HaCaT cells, the adhesion was significantly lower when the cells were seeded on top of PLGA-AV-NLC membranes than on top of PLGA-AV membranes, since the percentage of adhered cells were 25.45 ± 11.89 % and 56.23 ± 23.59%, respectively.

### *3.4* In vivo *wound healing assay*

The efficacy of the membranes was assessed in full thickness wounds inflicted to *db/db* mice. One of the parameters measured was the wound closure, expressed

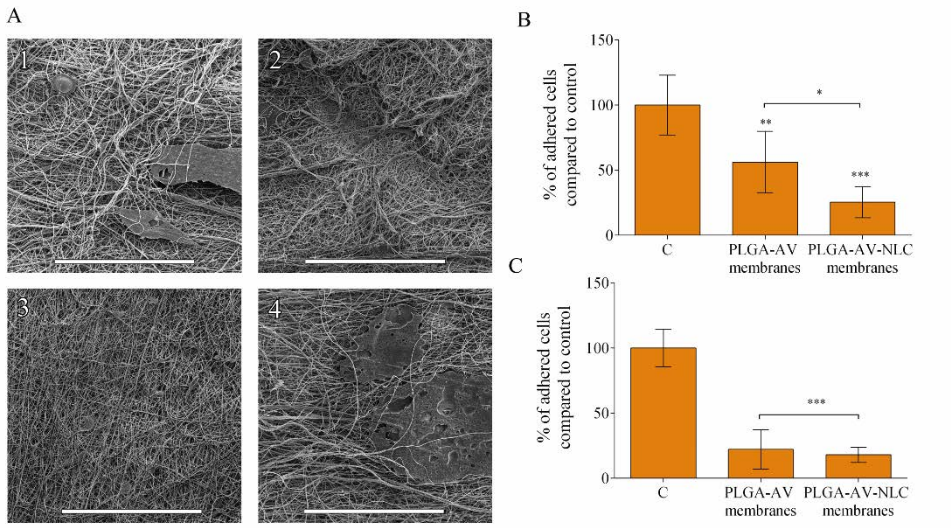


**Fig. 3.** In vitro adhesion assay. (A) SEM images of membranes with cells seeded on top: 1, PLGA-AV-NLC nanofibers incubated with keratinocytes; 2, PLGA-AV-NLC membranes incubated with fibroblasts; 3, PLGA-AV membranes incubated with keratinocytes; and 4, PLGA-AV membranes incubated with fibroblasts. The scale bar in each image indicates 500 µm. (B) Keratinocytes adhesion percentage. *** $p<0.001$ comparing PLGA-AV-NLC membranes with control group; ** $p<0.01$ comparing PLGA-AV membranes with control group; * $p<0.05$ comparing both membranes. (C) Fibroblasts adhesion percentage. *** $p<0.001$ comparing PLGA-AV-NLC and PLGA-AV membranes with control group.

as the percentage of wound area reduction compared to the initial wound area. On that regard, photographs of the wounds were taken on days 1, 4, 8, 11 and 15 and their area measured as $px^2$.

As illustrated by the gross images of the wounds, mice treated with any type of nanofibrous membranes showed a higher rate of wound closure (Fig. 4A). That observation was in concordance with the wound closure depicted in Fig. 4B, since the groups treated with PLGA-AV or PLGA-AV-NLC membranes presented a statistically significant faster wound area reduction in comparison to the untreated group. However, there was no difference between both treatments. It is noteworthy that on day 15, wounds treated with the dressings were almost closed (wound closure was 95.53 ± 4.96 % and 91.95 ±6.08 % on the groups treated with PLGA-AV and PLGA-AV-NLC membranes, respectively) while the untreated wounds presented a closure of 62.19 ± 11.84 %.

In addition, histological analyses were performed to assess the effectiveness of the treatments. Slides were stained with H&E and analysed following the criteria established by Sinha *et al.* and Cotran *et al.* to evaluate the reepithelisation grade and the resolution of the inflammatory process, respectively [38,39].

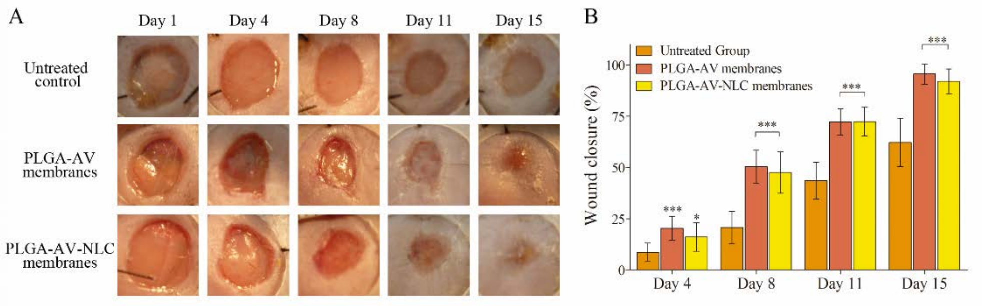


**Fig. 4.** *In vivo* wound closure. (A) Wounds photographs of each group on days 1, 4, 8, 11 and 15. (B) Wound closure represented as the percentage of reduction of the initial area on days 4, 8, 11 and 15 postinjury. * p<0.05 comparing PLGA-AV-NLC membranes groups with the untreated groups, *** p>0.001 comparing with the untreated group.

Regarding the reepithelisation grade, on day 8 there were no significant differences among groups, although a small increase in the reepithelisation was observed in the groups treated with the dressings in comparison with the untreated control, as illustrated in Fig. 5A. The groups treated with the developed formulations achieved a value around 2 in the scale described by Sinha *et al.* (2 ± 0.82 and 1.75 ± 1.04 for PLGA-AV-NLC membranes and for PLGA-AV membranes, respectively), which indicates that the new epithelium covered more than half of the wound. The untreated group, instead, obtained a value around 1, 1.36 ± 1.06 exactly, which means that less than half of the wound was covered by new epithelium. On day 15, the same tendency was maintained, since a higher reepithelisation grade was observed with the treated groups. In this case, the difference between the treated groups and the untreated control was statistically significant. A complete reepithelisation was observed in the treated groups (4 on the scale described by Sinha *et al.*); while the untreated wounds were not completely covered by new epithelium, since a value around 2 was obtained (1.875 ± 0.64).

The evaluation of the resolution of the inflammatory process showed that mice treated with the dressings achieved a faster wound maturation than the untreated group as depicted in Fig. 5B. On day 8, no statistically significant differences were observed among groups. PLGA-AV-NLC and PLGA-AV membranes reached a value higher than 2 in the in the scale described by Cotran *et al.*, which means that wound were in the diffuse acute inflammation phase, the values were 2.5 ± 1.10 and 2.25 ± 0.46, respectively. Untreated mice, on the contrary, were on the acute inflammation phase, since they did not achieve a value of 2 (1.88 ± 0.99). On day 15, mice treated with the dressings reached a value around 3, which means that the main process occurring on the wounds was fibroblast proliferation. In untreated mice, on the contrary, the wounds were still on the diffuse acute inflammation phase. The difference between the PLGA-AV membranes group and the untreated control was statistically significant.

Furthermore, immunohistological analyses were conducted to evaluate the number of immune cells on the wound on day

8. In that regard, tissue biopsies were stained with antibodies anti-CD4, CD8 and CD68, markers for helper T lymphocytes, cytotoxic T lymphocytes and macrophages, respectively. The analysis of the lymphocytes was done analysing the total number of positive cells and the ratio between the CD4+ and CD8+ lymphocytes. The results did not show any statistically significant differences among groups, although the group treated with PLGA-AV membranes showed the highest number of T lymphocytes, both helper and cytotoxic (Fig. 6A). The highest ratio between CD4+ and CD8+ cells was obtained with the PLGA-AV-NLC membranes treated group. Regarding the macrophages, the groups treated with the dressings showed a lower number in comparison to the untreated group. Furthermore, that difference was statistically significant, and the level of significance was higher with the group treated with PLGA-AV-NLC membranes, since the number of macrophages observed on that group was the lowest among the groups treated with nanofibers, as depicted in Fig. 6C.

## 5. Discussion

Nanofibrous membranes produced by electrospinning present several characteristics that make them a promising alternative for wound dressing applications. The-

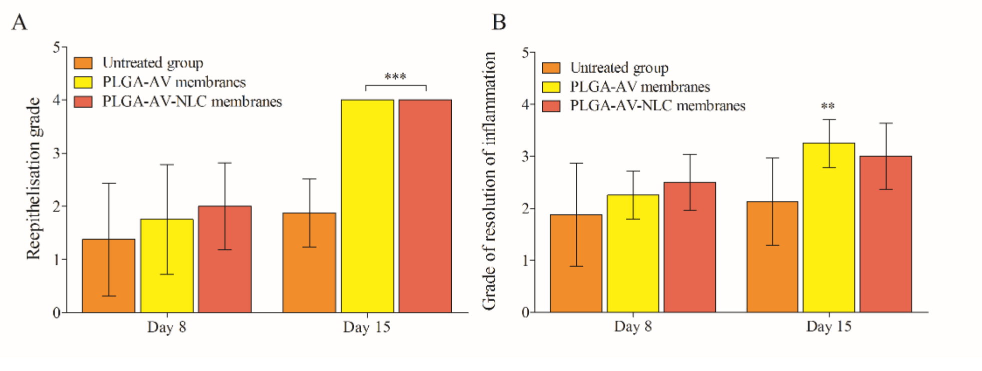


**Fig. 5.** Histological evaluation of the wounds. (A) Reepithelisation grade on days 8 and 15. *** p<0.001 comparing groups treated with the dressings and untreated group. (B) Grade of resolution of the inflammatory process. ** p0.01 comparing the group treated with PLGA-AV membranes and the untreated group.

refore, in a previous study, our research group developed a composite membrane of PLGA RG508 and the largest possible amount of *Aloe vera* extract, within which EGF was uniformly distributed [14]. In the present study, EGF was not added since we aimed to develop a medical device; instead lipid nanoparticles were included to improve the removal of the membrane during the dressing change. In addition, another polymer was used, PLGA 824 LG, which has a higher molecular weight, because it allowed a better incorporation of the nanoparticles. The average diameter of the nanofibers was increased with increasing the polymer molecular weight, from about 500 nm in the previous study to about 1 µm in the current study. The rise of the diameter was probably due to the greater viscosity of the polymer solution prepared with the high molecular weight PLGA. In this regard, previous studies have shown that solution viscosity is critical to control the nanofibers morphology, including their diameter [40]. The high porosity is one of the characteristics that makes electrospun membranes a suitable approach for wound dressing, since it allows gas permeation, and thus cell respiration. Although that high porosity, nanofibers present a very small pore size, which creates a physical barrier that can prevent bacterial growth [3]. The characterisation of the nanofibers showed that the addition of the NLCs into the formulation improved their mechanical properties, and therefore, the handling of the membranes. The PLGA-AV-NLC membranes pre-

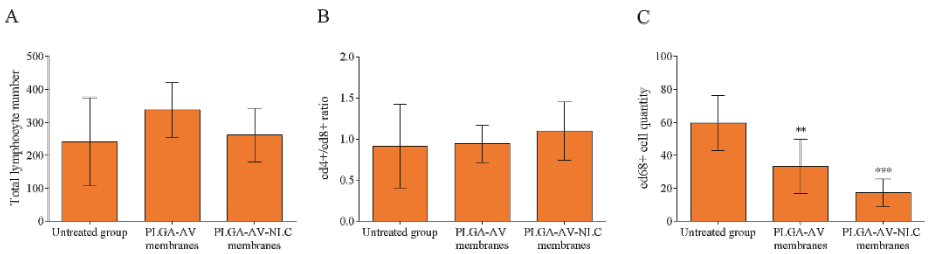


**Fig 6.** Immunohistological analysis. (A) Number of lymphocytes (CD4+ and CD8+ cells) on day 8. (B) Ratio between CD8+ and CD4+ cells on day 8. (C) Number of CD68+ cells on day 8. ** $p<0.01$ comparing the group treated with PLGA-AV membranes with the untreated group. *** $p<0.001$ comparing the group treated with PLGA-AV-NLC membranes with the untreated group.

sented an increased thickness and tensile strength, which makes more difficult to break or bend the dressing during the application, and therefore makes easier to apply it. The increased thickness of the membrane was probably due to the higher solids percentage of the solution containing the NLCs. The increment of the tensile strength may be due to the uniform distribution of the nanoparticles in the polymer matrix, as observed by Thomas et al. Therefore, the stress might be uniformly distributed into the nanofibers, minimizing the stress concentration centres, and increasing the interfacial area to transfer that stress from the polymer matrix to the NLCs, which result in improved mechanical properties [41]. The tensile strength of both formulations was below the tensile strength of human skin, which ranged from 5.7 MPa to 12.6 MPa [42]. However, this does not weaken their potential as wound dressings, because wounds are immobilized during healing and thus dressings are rarely under a high tensile strength [43]. Moreover, nanofibrous dressings with a low tensile strength ranging from 1-3 MPa have been previously developed for wound healing [44-46].

As described previously the water uptake (%) increased with rising concentration of the hydrophilic compound [14,47]. Therefore, since *Aloe vera* concentration was very similar in both formulations, it was expected that they would have a similar water uptake. Their swelling ability was very high, about 380 %, which helps to drain the exudates while retaining moisture to help wound healing. In addition to water uptake, moisture was also controlled by the water vapour transmision of the dressing [3,48]. The WVTR of the developed formulations was within the range of commercial wound dressings (426-2047 g/m$^2$day), thus they presented an adequate ability to allow most of the exudate to evaporate, while maintaining some moisture into the wound [49]. The PLGA-AV-NLC membranes showed a slightly lower WVTR value which can be translated into a slightly higher occlusivity.

The analysis of the thermal behaviour showed a decrease of the PLGA $T_g$, in both nanofibers in comparison to the raw PLGA and the physical blend of the components. That decrease can be due to a higher degree of alignment and orientation of the polymer chains into the electrospun membrane [14,50]. Every formulation containing NLCs presented a peak around 55°C that presumably corresponds to Precirol [51]. The NLCs thermogram showed a slight lower melting point of the Precirol in comparison to the physical blend or PLGA-AV-NLC membranes, which could indicate an interaction between the NLCs and the AV. It is noteworthy to mention that the peaks corresponding to PLGA and NLCs and the curve pattern of AV were found in both PLGA-AV-NLC nanofibers and physical blend, which reveals that the components of the nanofibers presented an immiscible blend morphology.

Regarding the biocompatibility of the dressings, none of them showed indirect cytotoxicity after the incubation of their extracted medium along with keratinocytes or fibroblasts, since their viability was maintained above the 70%, which indicated a good biocompatibility. The results obtained with fibroblasts, showed an increased viability after the incubation with the extracted medium of the nanofibers, probably due to the proliferative effect of the Aloe vera into fibroblasts [14,21,23]. The higher fibroblasts viability observed with the PLGA-AV nanofibers might be due to a faster release of the AV from the nanofibers, since the interaction between the AV and NLCs exposed in the DSC analysis could have aminorate the rate of AV release.

The main reasons to include NLCs into the nanofibers were the hypothesis that they could improve their handling and to ease the removal of the dressing from the wound, avoiding pain and damage of the newly formed tissue during dressing change. The characterisation of the membranes showed that NLCs were able to improve the handling and mechanical strength of the nanofibers. Therefore, cell adhesion was analysed and it revealed a lower keratinocyte adhesion to the formulation containing NLCs. Nevertheless, no differences were found in fibroblast attachment, since both membranes with or without NLCs presented a very low adhesion. Considering those results, more studies should be performed to assess dressing attachment into wounded tissue, analysing the dressing removal *in vivo* or using a texture analyzer to evaluate the adhesion strength to the wounded tissue.

Finally, the efficacy of the membranes was evaluated *in vivo* in a full thickness splinted wound model carried out in db/db mice. *db/db* mice were chosen because they present an impaired wound healing secondary to diabetes, and thus, they resemble better a chronic wound model. In addition, they mimic better human wound healing than other rodent models, since they have impaired wound contraction due to their obesity, and therefore their healing occurs mainly via reepithelisation, as human healing [52,53]. In order to impair even more contraction and enhance reephitelisation, silicone splints were sutured around the wounds [37].

Overall, both membranes achieved similar improvement in wound healing. Comparable results were obtained in wound closure and reepithelisation, as both were able to accelerate healing in comparison to untreated control. Regarding the resolution of the inflammatory process, on day 15 only PLGA-AV membranes presented an improved outcome in comparison to the control group. On day 8, no differences were observed in the histological analysis, although the developed formulations, and especially the PLGA-AV-NLC membranes, were able to reduce the macrophage infiltration in the wound bed that usually is augmented in rodent wound models with diabetes or impaired healing. [54,55]. In addition, the macrophages found on those wounds present an impaired ability to phagocyte apoptotic cells, increasing the level of proinflammatoy cytokines, and thus, perpetuating a continuous inflammatory state [56]. Accordingly, both formulations showed an enhancement of wound maturation, the PLGA-AV-NLC membranes on macrophage infiltration on the early stage of healing and the PLGA-AV membranes on the general inflammatory state of the later stage.

The effect of the nanofibrous dressings on wound healing can be partially explained by the incorporation of *Aloe vera*, since it has shown to improve wound healing, mainly by affecting fibroblast growth factor, and thus, improving their activity and proliferation [23]. In addition, the characteristics of the nanofibrous structure also contribute to the improvement of wound healing. In fact, the high surface to volume area and the nanoporosity create an adequate environment for cell migration and proliferation to the wound bed. Moreover, that proliferating environment is involved in the improvement of the granulation tissue formation and reepithelisation by enhancing the release of healing mediators, such as growth factors, angiogenic factors or collagen [3,40]. Finally, the chosen polymer is also involved in the enhancement of reepithelisation, since one of its degradation products, lactate, has shown to be able to induce a faster wound healing [18].

Regarding to the inclusion of NLCs into the membranes, their effect on the removal of the dressing could not be observed in vivo, since both dressings were humected with PBS prior to their elimination, in order to avoid any possible damage on the newly formed tissue. Nevertheless, an improvement on the handling of the membranes containing NLCs was observed along the characterisation of the formulations. Hence, the nanofibrous dressing with NLCs showed a benefit concerning handling, although more studies are needed to assess their effect in dressing removal.

**4. Conclusion**

In the current study two composite electrospun dressings were developed, the first one was composed of an emulsion of PLGA and *Aloe vera* (1:1), and in the second one lipid nanoparticles (NLCs) were added to the aforementioned emulsion. Both dressings showed a similar characterisation, although an enhanced handling was observed in the PLGA-AV-NLC formulation regarding to elasticity and thickness. Finally, their effectivity in wound healing was assessed in a full thickness wound healing assay performed in *db/db* mice, achieving similar results with both formulations. Accordingly, the PLGA-AV-NLC nanofibrous membrane might be a promising strategy for the treatment of chronic wound, since it improved handling in comparison to the formulation without NLCs.

**6. Acknowledgments**

I. García-Orue thanks the Basque Government for the fellowship grant. The authors thank for technical and human support provided by SGIker of UPV/EHU and European funding (ERDF and ESF). This project has been funded by the Basque Government (ELKARTEK 2015, Nanoplatform, KK-2015/0000036 and Consolidated Groups, IT-428-10 and IT-528-10).

## 7. References

[1] M. Liu, X. Duan, Y. Li, D. Yang, Y. Long, Electrospun nanofibers for wound healing, Mater. Sci. Eng. C Mater. Biol. Appl. 76 (2017) 1413-1423. doi: 10.1016/j.msec.2017.03.034.

[2] H.P. Felgueiras, M.T.P. Amorim, Functionalization of electrospun polymeric wound dressings with antimicrobial peptides, Colloids Surf. B Biointerfaces 156 (2017) 133-148. doi: //doi.org/10.1016/j.colsurfb.2017.05.001.

[3] M. Abrigo, S.L. McArthur, P. Kingshott, Electrospun nanofibers as dressings for chronic wound care: advances, challenges, and future prospects, Macromol. Biosci. 14 (2014) 772-792. doi: 10.1002/mabi.201300561.

[4] I. Garcia-Orue, J.L. Pedraz, R.M. Hernandez, M. Igartua, Nanotechnology-based delivery systems to release growth factors and other endogenous molecules for chronic wound healing, J. Drug Deliv. Sci. Technol. 42 (2017) 2-17. doi: 10.1016/j.jddst.2017.03.002.

[5] Matthew S. Brown, Brandon Ashley, Ahyeon Koh, Wearable Technology for Chronic Wound Monitoring: Current Dressings, Advancements, and Future Prospects, Frontiers in Bioengineering and Biotechnology 6 (2018). doi: 10.3389/fbioe.2018.00047.

[6] L. Pachuau, Recent developments in novel drug delivery systems for wound healing, Expert. Opin. Drug Deliv. 12 (2015) 1895-1909. doi: 10.1517/17425247.2015.1070143.

[7] K. Järbrink, G. Ni, H. Sönnergren, A. Schmidtchen, C. Pang, R. Bajpai, J. Car, The humanistic and economic burden of chronic wounds: a protocol for a systematic review, Syst. Rev. 6 (2017). doi: 10.1186/s13643-016-0400-8.

[8] C.K. Sen, G.M. Gordillo, S. Roy, R. Kirsner, L. Lambert, T.K. Hunt, F. Gottrup, G.C. Gurtner, M.T. Longaker, Human skin wounds: a major and snowballing threat to public health and the economy, Wound Repair Regen. 17 (2009) 763-771. doi: 10.1111/j.1524-475X.2009.00543.x.

[9] G. Han, R. Ceilley, Chronic Wound Healing: A Review of Current Management and Treatments, Adv. Ther. 34 (2017) 599-610. doi: 10.1007/s12325-017-0478-y.

[10] R.F. Diegelmann, M.C. Evans, Wound healing: an overview of acute, fibrotic and delayed healing, Front. Biosci. 9 (2004) 283-289. doi: //dx.doi.org/10.2741/.

[11] T. Velnar, T. Bailey, V. Smrkolj, The wound healing process: an overview of the cellular and molecular mechanisms, J. Int. Med. Res. 37 (2009) 1528-1542. doi: 10.1177/147323000903700531.

[12] S. Schreml, R. Szeimies, L. Prantl, M. Landthaler, P. Babilas, Wound healing in the 21st century, J. Am. Acad. Dermatol. 63 (2010)

866-881. doi: //dx.doi.org/10.1016/j. jaad.2009 .10.048.

[13] P.S. Briquez, J.A. Hubbell, M.M. Martino, Extracellular matrix-inspired growth factor delivery systems for skin wound healing, Adv. Wound Care (New Rochelle) 4 (2015) 479-489. doi: 10.1089/wound.2014.0603.

[14] I. Garcia-Orue, G. Gainza, F.B. Gutierrez, J.J. Aguirre, C. Evora, J.L. Pedraz, R.M. Hernandez, A. Delgado, M. Igartua, Novel nanofibrous dressings containing rhEGF and Aloe vera for wound healing applications, Int. J. Pharm. 53 (2016) 556-566. doi: //dx.doi.org/ 10.1016/j.ijpharm.2016.11.006.

[15] K.K. Chereddy, G. Vandermeulen, V. Préat, PLGA based drug delivery systems: Promising carriers for wound healing activity, Wound Repair Regen. 24 (2016) 223-236. doi: 10.1111/wrr.12404.

[16] T. Garg, G. Rath, A.K. Goyal, Comprehensive review on additives of topical dosage forms for drug delivery, Drug Deliv. 22 (2015) 969-987. doi: 10.3109/10717544. 2013.879355.

[17] T. Garg, G. Rath, A.K. Goyal, Biomaterials-based nanofiber scaffold: targeted and controlled carrier for cell and drug delivery, J. Drug Target. 23 (2015) 202-221. doi: 10.3109/1061186X.2014.992899.

[18] P. Porporato, V. Payen, C. De Saedeleer, V. Préat, J. Thissen, O. Feron, P. Sonveaux, Lactate stimulates angiogenesis and accelerates the healing of superficial and ischemic wounds in mice, Angiogenesis 15 (2012) 581-592. doi: 10.1007/s10456-012-9282-0.

[19] A.D. Dat, F. Poon, K.B. Pham, J. Doust, Aloe vera for treating acute and chronic wounds, Cochrane Database Syst. Rev. (2012). doi: 10.1002/14651858.CD008762.pub2.

[20] S. Choi, M. Chung, A review on the relationship between aloe vera components and their biologic effects, Semin. Integr. Med. 1 (2003) 53-62. doi: //dx.doi.org/10.1016/S1543 -1150(03)00005-X.

[21] S.A. Hashemi, S.A. Madani, S. Abediankenari, The Review on Properties of Aloe Vera in Healing of Cutaneous Wounds, Biomed. Res. Int. 2015 (2015) 714216. doi: 10.1155 /2015/714216.

[22] A. Surjushe, R. Vasani, D.G. Saple, Aloe vera: a short review, Indian J. Dermatol. 53 (2008) 163-166. doi: 10.4103/0019-5154.4478

[23] M.D. Boudreau, F.A. Beland, An evaluation of the biological and toxicological properties of Aloe barbadensis (miller), Aloe vera., J. Environ. Sci. Health C Environ. Carcinog. Ecotoxicol. Rev. 24 (2006) 103-154. doi: 10.1080/10590500600614303.

[24] S. Suganya, J. Venugopal, S. Ramakrishna, B.S. Lakshmi, V.R.G. Dev, Naturally derived biofunctional nanofibrous scaffold for skin tissue regeneration, Int. J. Biol. Macromol. 68 (2014) 135-143. doi: //dx.doi.org/10. 1016/j.ijbiomac.2014.04.031.

[25] V. Bhaarathy, J. Venugopal, C. Gandhimathi, N. Ponpandian, D. Mangalaraj, S. Ramakrishna, Biologically improved nanofibrous scaffolds for cardiac tissue engineering, Mater. Sci Eng C Mater. Biol. Appl. 44(2014)268-277 doi: //dx.doi.org/10.1016/j.msec.2014.08. 018

[26] P. Karuppuswamy, J.R. Venugopal, B. Navaneethan, A.L. Laiva, S. Sridhar, S. Ramakrishna, Functionalized hybrid nanofibers to mimic native ECM for tissue engineering applications, Appl. Surf. Sci. 322 (2014) 162-168. doi: //dx.doi.org/10.1016/j.apsusc.2014.10.074.

[27] S.A. Kheradvar, J. Nourmohammadi, H. Tabesh, B. Bagheri, Starch nanoparticle as a vitamin E-TPGS carrier loaded in silk fibroin-poly(vinyl alcohol)-Aloe vera nanofibrous dressing, Colloids Surf. B Biointerfaces 166 (2018) 9-16. doi: //doi.org/10.1016/j.colsurfb.2018.03.004.

[28] A. Jouybar, E. Seyedjafari, A. Ardeshirylajimi, A. Zandi-Karimi, N. Feizi, M. Khani, I. Pousti, Enhanced Skin Regeneration by Herbal Extract-Coated Poly-L-Lactic Acid Nanofibrous Scaffold, Artif. Organs 41 (2017) E307. doi: 10.1111/aor.12926.

[29] F. David, J. Wurtz, N. Breton, O. Bisch, P. Gazeu, J. Kerihuel, O. Guibon, A randomised, controlled, non-inferiority trial comparing the performance of a soft silicone-coated wound contact layer (Mepitel One) with a lipidocolloid wound contact layer (UrgoTul) in the treatment of acute wounds, Int. Wound J. 15 (2018) 159-169. doi: 10.1111/iwj.12853.

[30] M. Benbow, Urgotul™: alternative to conventional non-adherence dressings, Br. J. Nurs.   11 (2002) 135-138. doi: 10.12968/bjon.2002.11.2.9315.

[31] M. Benbow, G. Iosson, A clinical evaluation of Urgotul to treat acute and chronic wounds, Br. J. Nurs.   13 (2004) 105-109. doi: 10.12968/bjon.2004.13.2.12042.

[32] P.W.W. Tan, W.C. Ho, C. Song, The use of Urgotul in the treatment of partial thickness burns and split-thickness skin graft donor sites: a prospective control study, Int. Wound J. 6 (2009) 295-300. doi: 10.1111/j.1742-481X.2009.00611.x.

[33] G. Gainza, M. Pastor, J.J. Aguirre, S. Villullas, J.L. Pedraz, R.M. Hernandez, M. Igartua, A novel strategy for the treatment of chronic wounds based on the topical administration of rhEGF-loaded lipid nanoparticles: In vitro bioactivity and in vivo effectiveness in healing-impaired db/db mice, J. Control Release 185 (2014) 51-61. doi: //dx.doi.org/10.1016/j.jconrel.2014.04.032.

[34] G. Gainza, D.C. Bonafonte, B. Moreno, J.J. Aguirre, F.B. Gutierrez, S. Villullas, J.L. Pedraz, M. Igartua, R.M. Hernandez, The topical administration of rhEGF-loaded nanostructured lipid carriers (rhEGF-NLC) improves healing in a porcine full-thickness excisional wound model, J. Control Release 197 (2015) 41-47. doi: //dx.doi.org/10.1016/j.jconrel..10.033.

[35] I. Garcia-Orue, G. Gainza, C. Girbau, R. Alonso, J.J. Aguirre, J.L. Pedraz, M. Igartua, R.M. Hernandez, LL37 loaded nanostructured lipid carriers (NLC): A new strategy for the topical treatment of chronic wounds, Eur. J. Pharm. Biopharm. (2016). doi: //dx.doi.org/10.1016/j.ejpb.2016.04.006.

[36] C. Li, R. Fu, C. Yu, Z. Li, H. Guan, D. Hu, D. Zhao, L. Lu, Silver nanoparticle/chitosan oligosaccharide/poly(vinyl alcohol) nanofibers as wound dressings: a preclinical study, Int. J. Nanomedicine 8 (2013) 4131-4145. doi: 10.2147/IJN.S51679 [doi].

[37] J. Michaels, S.S. Churgin, K.M. Blechman, M.R. Greives, S. Aarabi, R.D. Galiano, G.C. Gurtner, db/db mice exhibit severe wound-healing impairments compared with other murine diabetic strains in a silicone-splinted excisional wound model, Wound Repair Regen. 15 (2007) 665-670. doi: 10.1111/j.1524-475X.2007.00273.x.

[38] U.K. Sinha, L.A. Gallagher, Effects of Steel Scalpel, Ultrasonic Scalpel, CO2 Laser, and Monopolar and Bipolar Electrosurgery on Wound Healing in Guinea Pig Oral Mucosa, Laryngoscope 113 (2003) 228-236. doi: 10.1097/00005537-200302000-00007.

[39] R. Cotran, G.K. Kumar, T. Collins, Reparación de los tejidos: proliferacion celular, fibrosis y curaicón de las heridas (2000) 95-120.

[40] S. Shahverdi, M. Hajimiri, M.A. Esfandiari, B. Larijani, F. Atyabi, A. Rajabiani, A.R. Dehpour, A.A. Gharehaghaji, R. Dinarvand, Fabrication and structure analysis of poly(lactide-co-glycolic acid)/silk fibroin hybrid scaffold for wound dressing applications, Int. J. Pharm. 473 (2014) 345-355. doi: //dx.doi.org/10.1016/j.ijpharm.2014.07.021.

[41] R. Thomas, K. Soumya, J. Mathew, E. Radhakrishnan, Electrospun Polycaprolactone Membrane Incorporated with Biosynthesized Silver Nanoparticles as Effective Wound Dressing Material, Appl. Biochem. Biotechnol. 176 (2015) 2213-2224. doi: 10.1007/s12010-015-1709-9.

[42] C. Jacquemoud, K. Bruyere-Garnier, M. Coret, Methodology to determine failure characteristics of planar soft tissues using a dynamic tensile test, J. Biomech. 40 (2007) 468-475. doi: //dx.doi.org/10.1016/j.jbiomech.2005.12.010.

[43] G. Jin, M.P. Prabhakaran, D. Kai, S.K. Annamalai, K.D. Arunachalam, S. Ramakrishna, Tissue engineered plant extracts as nanofibrous wound dressing, Biomaterials 34 (2013) 724-734. doi: //doi.org/10.1016/j.biomaterials.2012.10.026.

[44] A.M. Loordhuswamy, V.R. Krishnaswamy, P.S. Korrapati, S. Thinakaran, G.D.V. Rengaswami, Fabrication of highly aligned fibrous scaffolds for tissue regeneration by centrifugal spinning technology, Materials Science and Engineering: C 42 (2014) 799-807. doi: //doi.org/10.1016/j.msec.2014. 06.011.

[45] U. Dashdorj, M.K. Reyes, A.R. Unnithan, A.P. Tiwari, B. Tumurbaatar, C.H. Park, C.S. Kim, Fabrication and characterization of electrospun zein/Ag nanocomposite mats for wound dressing applications, Int. J. Biol. Macromol. 80 (2015) 1-7. doi: //dx.doi.org/10.1016/j.ijbiomac.2015.06.026.

[46] S. Tort, F. Acartürk, A. Beşikci, Evaluation of three-layered doxycycline-collagen loaded nanofiber wound dressing, International Journal of Pharmaceutics 529 (2017) 642-653. doi: //doi.org/10.1016/j.ijpharm.2017.07.027.

[47] S. Son, R. Franco, S. Bae, Y. Min, B. Lee, Electrospun PLGA/gelatin fibrous tubes for the application of biodegradable intestinal stent in rat model, J. Biomed. Mater. Res. 101B (2013) 1095-1105. doi: 10.1002/jbm.b.32923.

[48] S. Natarajan, D. Williamson, A.J. Stiltz, K. Harding, Advances in Wound Care and Healing Technology, Am. J. Clin. Dermatol. 1

(2000) 269-275. doi: 10.2165/00128071-200001050-00002.

[49] Y. Tu, M. Zhou, Z. Guo, Y. Li, Y. Hou, D. Wang, L. Zhang, Preparation and characterization of thermosensitive artificial skin with a Sandwich structure, Mater. Lett. 147(2015)4-7 doi: //dx.doi.org/10.1016/j.matlet.2015.01.163

[50] H. Fouad, T. Elsarnagawy, F.N. Almahjdi, K.A. Khalil, Preparation and in vitro thermo-mechanical characterization of electrospun PLGA nanofibers for soft and hard tissue replacement, Int. J. Electrochem. Sci. 8 (2013) 2293-2304.

[51] J. Hamdani, A.J. Moës, K. Amighi, Physical and thermal characterisation of Precirol ® and Compritol ® as lipophilic glycerides used for the preparation of controlled-release matrix pellets, Int. J. Pharm. 260 (2003) 47-57. doi: 10.1016/S0378-5173(03)00229-1.

[52] R.C. Fang, T.A. Mustoe, Animal models of wound healing: uility in transgenic mice, J. Biomater. Sci. Polym. Ed. 19 (2008) 989-1005. doi: 10.1163/156856208784909327.

[53] V.I. Tkalcevic, S. Cužic, M.J. Parnham, I. Pašalic, K. Brajša, Differential Evaluation of Excisional Non-occluded Wound Healing in db/db Mice, Toxico. Pathol. 37 (2009) 183-192. doi: 10.1177/0192623308329280.

[54] Tsubame Nishikai-Yan Shen, Shigeyuki Kanazawa, Makiko Kado, Kayoko Okada, Lin Luo, Ayato Hayashi, Hiroshi Mizuno, Rica Tanaka, Interleukin-6 stimulates Akt and p38 MAPK phosphorylation and fibroblast migration in non-diabetic but not diabetic mice, PLoS One 12 (2017) e0178232. doi: 10.1371/journal.pone.0178232.

[55] J. Yeh, L. Yeh, S. Jung, T. Chang, H. Wu, T. Shiu, C. Liu, W.W. Kao, P. Chu, Impaired skin wound healing in lumican-null mice, Br. J. Dermatol. 163 (2010) 1174. doi: 10.1111/j.1365-2133.2010.10008.x.

[56] Savita Khanna, Sabyasachi Biswas, Yingli Shang, Eric Collard, Ali Azad, Courtney Kauh, Vineet Bhasker, Gayle M Gordillo, Chandan K Sen, Sashwati Roy, Macrophage Dysfunction Impairs Resolution of Inflammation in the Wounds of Diabetic Mice, PLoS One 5 (2010) e9539. doi: 10.1371/journal.pone.0009539.

[43] G. Jin, M.P. Prabhakaran, D. Kai, S.K. Annamalai, K.D. Arunachalam, S. Ramakrishna, Tissue engineered plant extracts as nanofibrous wound dressing, Biomaterials 34 (2013) 724-734. doi: //doi.org/10.1016/j.biomaterials.2012.10.026.

[44] A.M. Loordhuswamy, V.R. Krishnaswamy, P.S. Korrapati, S. Thinakaran, G.D.V. Rengaswami, Fabrication of highly aligned fibrous scaffolds for tissue regeneration by centrifugal spinning technology, Materials Science and Engineering: C 42 (2014) 799-807. doi: //doi.org/10.1016/j.msec.2014.06.011.

[45] U. Dashdorj, M.K. Reyes, A.R. Unnithan, A.P. Tiwari, B. Tumurbaatar, C.H. Park, C.S. Kim, Fabrication and characterization of electrospun zein/Ag nanocomposite mats for wound dressing applications, Int. J. Biol. Macromol. 80 (2015) 1-7. doi: //dx.doi.org/10.1016/j.ijbiomac.2015.06.026.

[46] S. Tort, F. Acartürk, A. Beşikci, Evaluation of three-layered doxycycline-collagen

loaded nanofiber wound dressing, International Journal of Pharmaceutics 529 (2017) 642-653. doi: //doi.org/10.1016/j.ijpharm.2017.07.027.

[47] S. Son, R. Franco, S. Bae, Y. Min, B. Lee, Electrospun PLGA/gelatin fibrous tubes for the application of biodegradable intestinal stent in rat model, J. Biomed. Mater. Res. 101B (2013) 1095-1105. doi: 10.1002/jbm.b.32923.

[48] S. Natarajan, D. Williamson, A.J. Stiltz, K. Harding, Advances in Wound Care and Healing Technology, Am. J. Clin. Dermatol. 1 (2000) 269-275. doi: 10.2165/00128071-200001050-00002.

[49] Y. Tu, M. Zhou, Z. Guo, Y. Li, Y. Hou, D. Wang, L. Zhang, Preparation and characterization of thermosensitive artificial skin with a Sandwich structure, Mater. Lett. 147 (2015) 4-7. doi: //dx.doi.org/10.1016/j.matlet.2015.01.163.

[50] H. Fouad, T. Elsarnagawy, F.N. Almahjdi, K.A. Khalil, Preparation and in vitro thermo-mechanical characterization of electrospun PLGA nanofibers for soft and hard tissue replacement, Int. J. Electrochem. Sci. 8 (2013) 2293-2304.

[51] J. Hamdani, A.J. Moës, K. Amighi, Physical and thermal characterisation of Precirol ® and Compritol ® as lipophilic glycerides used for the preparation of controlled-release matrix pellets, Int. J. Pharm. 260 (2003) 47-57. doi: 10.1016/S0378-5173(03)00229-1.

[52] R.C. Fang, T.A. Mustoe, Animal models of wound healing: uility in transgenic mice, J. Biomater. Sci. Polym. Ed. 19 (2008) 989-1005. doi: 10.1163/156856208784909327.

[53] V.I. Tkalcevic, S. Cužic, M.J. Parnham, I. Pašalic, K. Brajša, Differential Evaluation of Excisional Non-occluded Wound Healing in db/db Mice, Toxico. Pathol. 37 (2009) 183-192. doi: 10.1177/0192623308329280.

[54] Tsubame Nishikai-Yan Shen, Shigeyuki Kanazawa, Makiko Kado, Kayoko Okada, Lin Luo, Ayato Hayashi, Hiroshi Mizuno, Rica Tanaka, Interleukin-6 stimulates Akt and p38 MAPK phosphorylation and fibroblast migration in non-diabetic but not diabetic mice, PLoS One 12 (2017) e0178232. doi: 10.1371/journal.pone.0178232.

[55] J. Yeh, L. Yeh, S. Jung, T. Chang, H. Wu, T. Shiu, C. Liu, W.W. Kao, P. Chu, Impaired skin wound healing in lumican-null mice, Br. J. Dermatol. 163 (2010) 1174. doi: 10.1111/.1365-2133.2010.10008.x.

[56] Savita Khanna, Sabyasachi Biswas, Yingli Shang, Eric Collard, Ali Azad, Courtney Kauh, Vineet Bhasker, Gayle M Gordillo, Chandan K Sen, Sashwati Roy, Macrophage Dysfunction Impairs Resolution of Inflammation in the Wounds of Diabetic Mice, PLoS One 5 (2010) e9539. doi: 10.1371/journal.pone.0009539.

# CHAPTER 4

## Development of a gelatin/chitosan bilayer hydrofilm for wound healing

I. Garcia-Orue[a,b]+; E. Santos-Vizcaino[a,b]+; A. Etxabide[c]; J. Uranga[c]; A. Bayat[d]*; P. Guerrero[c]; M. Igartua[a,b]; K. de la Caba[c]; R.M. Hernandez[a,b]*

[a] NanoBioCel Group, Laboratory of Pharmaceutics, School of Pharmacy, University of the Basque Country (UPV/EHU), Paseo de la Universidad 7, 01006 Vitoria-Gasteiz, Spain

[b] Biomedical Research Networking Centre in Bioengineering, Biomaterials and Nanomedicine (CIBER-BBN), Vitoria-Gasteiz, Spain

[c] BIOMAT Research Group, Chemical and Environmental Engineering Department, Engineering College of Gipuzkoa, University of the Basque Country (UPV/EHU), Plaza de Europa 1, 20018 Donostia-San Sebastián, Spain

[d] Plastic & Reconstructive Surgery Research, Division of Musculoskeletal & Dermatological Sciences, School of Biological Sciences, University of Manchester, Manchester, UK.

+ These two authors contributed equally to this work.

* Corresponding author: Dr. A. Bayat and Dr. R.M. Hernandez

## ABSTRACT

In the current study, we developed a novel gelatin-based bilayer wound dressing. We used different crosslinking agents to confer unique properties to each layer, obtaining a multifunctional hydrofilm able to fulfil the requirements for wound healing applications. First, we produced a resistant and non-degradable upper layer by lactose-mediated crosslinking of gelatin, which provided mechanical support and protection to overall design. For the lower layer, gelatin was crosslinked with citric acid, resulting in a porous matrix with a great swelling ability. In addition, we incorporated chitosan into the lower layer to harness its wound healing ability. The influence of the crosslinker was demonstrated by FTIR and SEM analysis, lactose addition changed the secondary structure of gelatin leading to a more compact and smoother structure. Results showed that the hydrofilm was able to swell 407.3 ± 108.6 % of its dry weight while maintaining mechanical integrity. Besides, its water vapour transmission rate was 1381.5 ± 108.6 g/m$^2$day. *In vitro*, it showed a good biocompatibility. Finally, its efficacy was tested through an *ex vivo* wound healing assay in human skin. The hydrofilm achieved similar results to the control. Altogether, the developed bilayer hydrofilm showed suitable characteristics to be used as a wound dressing.

**Sent to:** European Journal of Pharmaceutics and Biopharmaceutics

## 1. Introduction

Bilayer dressings are a promising approach for wound healing, since they are able to provide a structure that mimics the bilayer structure of skin, with an upper protective layer resembling the epidermis, and a thicker flexible lower layer like the dermis. Taking that into account, the dense upper layer is designed to cover the wound, giving mechanical strength to the dressing. In addition, it needs to control moisture transmission to prevent fluid loss and dehydration, while allowing exudate removal. Furthermore, the upper layer prevents bacterial penetration and thus wound infection. On the other hand, the lower layer is a porous or sponge like structure that is able to absorb wound exudate and smoothly adhere to the wet wound bed to accommodate newly formed tissue [1-3].

Usually, both layers are composed of different polymers; however, gelatin is able to exhibit the characteristics needed to constitute both layers, depending on its crosslinking degree and nature. Gelatin is a natural polymer derived from collagen, and in comparison to it, gelatin is more inexpensive and less antigenic, since it is partially denatured [4,5]. Moreover, it has been extensively used in medical and pharmaceutical applications due to its biocompatibility and biodegradability, and it has been recognized as GRAS (Generally Recognized As Safe) by the FDA [6]. In addition, it has multiple characteristics that make it a suitable option to develop wound dressings, such as an excellent ability to form films and hydrogels. Secondly, the gelatin chains contain arginine-glycine-aspartic (RGD) motifs, an important sequence in the promotion of cell adhesion, which gives gelatin an improved biological behaviour in comparison to other polymers [7]. Lastly, the flexible amino acidic structure of gelatin presents diverse free functional groups that allow chemical conjugation and thus the modification of the gelatin structure.

Gelatin presents an excellent ability to absorb large volumes of water and thereby create hydrogels. They show a variety of advantages for their use as wound dressings, such as fluid absorption or wound hydration, since they can absorb or donate water depending on their environment; cooling of the wound surface; pain control; permeability to water vapour and oxygen without water leaks; and suitability for unusual wound shapes due to their jelly-like nature [8].

In order to increase gelatin mechanical properties and reduce its solubility and degradation rate in aqueous environment, crosslinking is essential when it comes to developing a gelatin wound dressing. It is noteworthy to mention that depending on the crosslinking degree and nature (e.g. sensitivity of the bound to hydrolytic degradation), gelatin can adopt physical forms ranging from amorphous gels to semi-stiff sheets. Therefore, a correct choice of crosslinking agents and protocols may enable gelatin to constitute both layers of a bilayer dressing [8]. Crosslinking methods include physical, biological and chemical methods [9]. Among chemical methods, aldehydes such as glutaraldehyde are the most commonly used reagents, although unreacted toxic products can get trapped into the hydrogel [10]. In this sense, genipin, a natural crosslinking compound has gained importance due to its lower citotoxycity and higher biocompatibility [11].

On the other hand, in order to accelerate wound healing, natural polymers such as chitosan can be added to the dressings. Chitosan is a biocompatible and biodegradable polymer derived from chitin, a compound of the exoskeleton of insects and crustaceans [12]. It has shown to accelerate wound healing through diverse mechanisms. It presents antibacterial and haemostatic activity, acting in the early phases of healing [13]. In addition, it promotes the migration of polymorphonuclear neutrophils and the activity of macrophages. Lastly, it enhances the formation of the granulation tissue by inducing the proliferation of dermal fibroblasts [14].

The efficacy of wound dressings, is usually tested in wound healing assays conducted in animals. However, animal models do not accurately mimic the structure of human skin or the process of wound healing [15]. Moreover, ethical concerns discourage their use [16]. An alternative to reduce the use of animal experimentation are *in vitro* and *ex vivo* models. Among *in vitro* models single cell culture, co-culture and organotypic culture can be distinguished. Single monolayer cell cultures of ke-ratinocytes, fibroblasts or endothelial cells are used to analyse basic physiological processes through scratch, chemotaxis or tube formation assays [17]. Co-cultures of keratinocytes and fibroblast using transwell systems are used to analyse the interaction between those cell types [18]. Finally, organotypic culture consists on seeding keratinocytes on top of a collagen gel containing fibroblast. Those systems have been used to investigate scar pathology [19]. Nevertheless, the use of all those models is limited due to the lack of extracellular matrix (ECM) components and the skin native structure. To overcome those limitations, whole skin biopsies in culture can be used. Those *ex vivo* models mimic more closely normal skin, and they enable an evaluation of wound healing process both in implicated cells and in the surrounding ECM components. These models have already been established as a useful tool to evaluate wound healing. For that purpose, partial or full-thickness wounds are made in the centre of the biopsies, and wound healing assessed after an incubation period [20,21].

Accordingly, the aim of this study was to develop a bilayer wound dressing based on gelatin. In order to regulate the crosslinking degree and nature of each layer, and thereby their properties, different crosslinking agents were used. The upper layer was crosslinked with lactose, to obtain a rigid layer able to provide mechanical strength and protection to the dressing. The lower layer was crosslinked with citric acid, and the obtained hydrogel was able to absorb a larger volume of water and degrade. In addition, chitosan was added to the lower layer to enhance wound healing. Firstly, both layers and the resulting bilayer hydrofilm were characterised in terms of protein structure, morphology, crosslinking degree, structure, swelling ability and oclussivity. Additionally, cytotoxicity studies were performed to evaluate the safety of the developed formulation. Finally, the efficacy of the dressing was evaluated using an *ex vivo* model of a full thickness wound.

## 2. Materials and methods

### 2.1 Hydrofilm production

Type A fish gelatin, with a 240 bloom value and average molar mass of 125-250 kDa (Healan Ingredients, UK), was used as the main component of film forming formulations. Lactose and anhydrous citric acid (Panreac, Spain) were used as cross-linkers and glycerol with a purity of 99.01% (Panreac, Spain) was used as plasticizer. Chitosan, with a deacetylation degree higher than 75% and molecular weight of 375 kDa (Sigma Aldrich, Spain), was used as a bioactive compound.

On the one hand, gelatin films with lactose (Lac) were prepared. Hence, 5 g gelatin and 20 wt % lactose (on gelatin dry basis) were dissolved in 100 ml distilled water for 30 min at 80 °C under continuous stirring to obtain a good blend. After that, 20 wt % glycerol (on gelatin dry basis) was added to the solution, pH was adjusted to 10 with NaOH (0.1 M), and solution was maintained at 80 °C for other 30 min under stirring. Finally, 17 ml of film forming solution were poured into each Petri dish and left drying 48 h at room temperature to obtain films. The films peeled from the Petri dishes were heated at 105 °C for 24 h to obtain lactose-crosslinked films.

On the other hand, gelatin films with citric acid (CA) and chitosan (Chit) were prepared. Firstly, 10 wt % (on gelatin basis) citric acid solutions were prepared. Then, 9 wt % chitosan (on gelatin basis) was dissolved in 100 ml of citric acid solution and it was maintained under continuous stirring for 30 min. After that, 5 g gelatin were added and the resultant solution was heated at 80 °C for 30 min and stirred at 200 rpm. Finally, 20 wt % glycerol (on gelatin basis) was added, pH was adjusted to 4.5 using NaOH (0.1 M), and the solution was stirred for other 30 min at 80 °C and 200 rpm. Finally, 17 ml of film forming solution were poured into each Petri dish and left drying 48 h at room temperature to obtain chitosan-incorporated films crosslinked with citric acid. Films without chitosan were also prepared.

Additionally, films without glycerol were produced. Furthermore, bilayer films were prepared with lactose-crosslinked

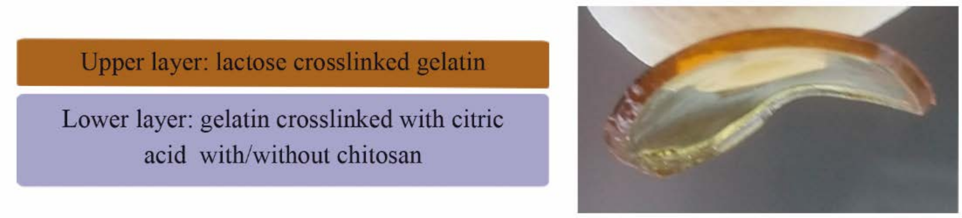


**Fig. 1.** Scheme and photograph of gelatin bilayer films.

films as the upper layer and citric acid-crosslinked films as the lower layer, as shown in Fig. 1. Both layers were glued together spraying ethanol on them and letting them air dry.

All films were conditioned in an ACS Sunrise 700 V bio-chamber (Alava Ingenieros, Madrid, Spain) at 25 °C and 50% relative humidity before testing. The developed formulations are summarised in table 1.

*2.2 Fourier transform infrared (FTIR) spectroscopy*

Fourier transform infrared (FTIR) spectra were recorded on a Nicolet 380 FTIR spectrometer equipped with horizontal attenuated total reflectance (ATR) crystal (ZnSe). The spectra were collected in absorbance mode on sample films. The measurements were recorded between 4000 and 800 $cm^{-1}$. A total of 32 scans were made for each sample, at 4 $cm^{-1}$ resolution. All spectra were smoothed using the Savitzky–Golay function. Second-derivative spectra of the amide region were used at peak position guides for the curve fitting procedure, using OriginPro 9.1 software.

*2.3 Scanning electron microscopy (SEM)*

The morphology of the cross-section of the films was visualized using a Hitachi S-4800 scanning electron microscopy (Hitachi, Japan). The cross-section was prepared using mechanical means like conventional cutter. Then, samples were mounted on a metal stub with double-side adhesive tape and coated under vacuum with gold, using a JEOL fine-coat ion sputter JFC-1100 (Izasa, Spain) in an argon atmosphere prior to observation. All samples were examined using an accelerating voltage of 15 kV.

*2.4 Swelling*

A swelling curve was created weighing the water uptake of the different hydrofilms at different time points. Firstly, dry samples of each formulation were cut in discs of 12 mm in diameter. Then, discs were weighed and soaked in 1 ml of PBS at 4 °C (pH 7.4, Gibco® Life technologies, USA). At various time points (30 min, 2 h, 24 h, 48 h and 72 h) hydrofilms were re moved from the PBS, the excess of liquid dried with a filter paper, and the wet weight determined. Subsequently, discs were immersed again in PBS until they reached a state of equilibrium. The percentage of water uptake or swelling (S) was calculated through the following equation (Eq. 1):

$$S(\%)=\frac{W\text{-}W_0}{W_0}\times 100 \qquad \text{(Eq. 1)}$$

**Table 1**. Summary of the developed hydrofilms (HF) and bilayer hydrofilms (HFb) based on gelatin and prepared with (+) or without (-) glycerol.

| Name | Upper layer crosslinking agent | Lower layer crosslinking agent | Chitosan addition to the lower layer | Glycerol |
|---|---|---|---|---|
| Lac+ HF | Lactose | - | - | Yes |
| Lac- HF | Lactose | - | - | No |
| CA+ HF | - | Citric acid | No | Yes |
| CA- HF | - | Citric acid | No | No |
| CA Chit+ HF | - | Citric acid | Yes | Yes |
| CA Chit- HF | - | Citric acid | Yes | No |
| LacCA+ HFb | Lactose | Citric acid | No | Yes |
| LacCA- HFb | Lactose | Citric acid | No | No |
| LacCA Chit+ HFb | Lactose | Citric acid | Yes | Yes |
| LacCA Chit- HFb | Lactose | Citric acid | Yes | No |

Where, W is the weight of the wet sample at every time point and $W_0$ is the weight of the dry samples.

*2.5 Hydrolytic degradation*

Discs of 12 mm in diameter were immersed in PBS at 4 °C until they reached the absorption equilibrium determined in 2.4 section. Then, they were washed with MilliQ water and they were left to dry for 7 days. When they were completely dried, discs were weighed and the percentage of the remaining weight was calculated using the following equation (Eq. 2):

$$RM\ (\%) = \frac{\text{Dry weight}}{\text{Initial weight}} \times 100 \qquad \text{(Eq. 2)}$$

2.6 Water vapour transmission rate (WVTR)

In order to analyse the ability of hydrofilms to regulate moisture, WVTR was calculated. The WVTR of the CA HF (with and without chitosan and glycerol) were not measured since wet hydrofilms lose the structural stability to seal the Franz diffusion cell due to their great ability to swell water. The WVTR was quantified following the method described by Etxabide *et al.* [22]. Briefly, the receptor compartment of a Franz diffusion cell was completely filled with MilliQ water and its receptor arm was sealed with parafilm. Then, hydrofilm discs slightly bigger than the aperture between compartments (10 mm) were placed between them, to make the hydrofilm the only way for water vapour to leave the system. The complete assembly was weighed at the beginning of the study and after a 48 h incubation at room temperature. The WVTR was calculated using the following equation (Eq. 3):

$$WVTR = \frac{M_1 - M_0}{A \times T} \qquad \text{(Eq. 3)}$$

Where $M_0$ is the weight of the assembly at the beginning of the assay, $M_1$ is its weight after the incubation time, A is the exposure area (0.79 $cm^2$) and T is the exposure time (2 days).

2.7 Cytotoxicity study

Cytotoxicity studies were performed using the L-929 fibroblasts (ATCC, Manassas, USA), since it is the cell line recommended by the ISO 10993-5:2009 guideline for biological evaluation of medical devices. Cells were cultured on Eagle's Minimum Essential Medium (EMEM; ATCC, Manassas, USA) supplemented with 10 % (v/v) inactivated Horse Serum and 1 % (v/v) penicillin-streptomycin, and incubated at 37 °C in a humidified incubator with a 5 % $CO_2$ atmosphere. Cell passages were performed every 2-3 days depending on cell confluence.

Indirect cytotoxicity was assessed incubating cells with the extracted medium of the hydrofilms. Firstly, the hydrofilms were sterilized by impregnating both sides with 70 % ethanol and exposing them to UV light for 20 min. Subsequently, the hydrofilms were divided into two groups that received a different processing method. Hydrofilms in the first group were dialyzed in 1 l of MilliQ water for 72 h and then they were maintained in culture medium for 24 h to achieve an osmotic equilibrium. The second group was simply hydrated for 15 min in culture medium. Afterwards, 16 mm discs of each hydrofilm were incubated with 0.5 ml of culture medium for 24 h at 37 °C, to obtain the extracted medium.

Meanwhile, cells were seeded on 96 well plates at a density of 5000 cell/well and incubated overnight to allow cell attachment. Then, the medium was replaced by the extracted medium of the hydrofilms, although some wells were replaced by fresh culture medium to be used as controls. After 24 h of incubation, cell viability was assessed using the CCK-8 colorimetric assay (Cell Counting Kit-8, Sigma-Aldrich, Saint Louise, USA). Briefly, 10 µL of the CCK-8 reagent was added to the cells and incubated for 4 h. Then, the absorbance of the wells was read at 450 nm, using 650 nm as reference wavelength (Plate Reader Infinite M200, Tecan, Switzerland). The absorbance value was directly proportional to the number of living cells in each well. Results were given as the percentage of living cells regarding to control.

*2.8* Ex vivo assay

*2.8.1* Ex vivo *assay procedure*

Explants were obtained from three healthy patients undergoing routine elective surgery, demographic data are summarised on table 2. Ethical approval for this study was provided by the north-west of England, research ethics committee (11/NW/0683).

Explants were washed several times in phosphate buffer solution (PBS, Sigma-Aldrich, UK) and soaked in Dulbecco's modified Eagle's medium (DMEM, D6429-500 ml, Sigma-Aldrich, UK) supplemented with 100 UI/ml of penicillin-streptomycin (Sigma-Aldrich, UK), 0.1 % (v/v) insulin (Sigma-Aldrich, UK) and 0.001 % (w/v) hydrocortisone (Sigma-Aldrich, UK).

The ex vivo assay was conducted modifying the method described by Hodgkinson et al. and Mendoza-Garcia et al. [23,24]. Explants were cut in 6 mm in diameter biopsies using a punch biopsy (Kai Europe, GmbH, Germany) and allowed to equilibrate overnight in culture medium at 37 °C in a humidified incubator with a 5 % $CO_2$ atmosphere. Afterwards, full thickness excisional wounds (donut-shaped model) of 3 mm in diameter were made in the centre of the samples. Biopsies were then transferred to transwell inserts (Corning, USA) and cultured in 24 well plates. The dermis was immersed into supplemented DMEM medium and the epidermis was exposed to liquid-air interface. Biopsies were incubated for 8 days at 37 °C in a humidified incubator with a 5 % $CO_2$ atmosphere. Culture medium was changed every day.

**Table 2.** Demographic data and source of explants.

| Patient number | Gender | Age (years) | Anatomical source of skin |
|---|---|---|---|
| 1 | Female | 50 | Abdomen |
| 2 | Male | 60 | Abdomen |
| 3 | Female | 49 | Breast |

Biopsies were divided into three groups: (i) the control group did not receive any treatment; (ii) a disc of 6 mm diameter of LacCA Chit- HFb was applied to the biopsies; and (iii) a disc of 6 mm diameter of Lac- HF was applied to the biopsies. Before their application, the hydrofilms were sprayed with ethanol in both sides, kept under UV light for 30 min and hydrated for 15 min. Treatments were changed on day 4.

*2.8.2 LDH assay*

On days 4 and 8, 50 µl of the medium were collected from the wells to perform a LDH (lactate dehydrogenase) assay (Pierce™ LDH Cytotoxicity Assay Kit, ThermoFisher Scientific Inc., USA), in order to assess the viability of the biopsies. The LDH assay was conducted according to the manufacturer instructions. Briefly, 50 µL of lysis buffer was added to an extra biopsy included to be used as the control of this assay and the mixture was incubated for 45 min. Then, 50 µl of each biopsy (including the one treated with the lysis buffer) were transferred into a 96 well plate and 50 µl of the LDH reagent were added to the wells. The mixture was incubated for less than 30 min at room temperature and protected from light. The reaction was stopped with 50 µl of the stop reagent and the absorbance was read at 492 nm, using 680 nm as reference wavelength. Cell viability was expressed using the equation 4.

$$\text{Cell viability (\%)}=\frac{A_L\text{-}A_S}{A_L}\times 100 \qquad \text{(Eq. 4)}$$

Where, AL is the absorbance of the samples incubated with the lysis buffer and AS is the absorbance of the tested samples.

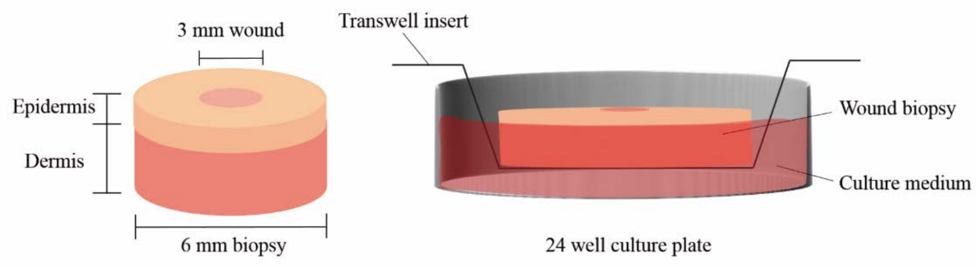


**Fig. 2.** *Ex vivo* assay scheme

*2.8.3 Tissue processing*

On days 1 and 8, samples were processed to assess wound healing. Tissues biopsied were fixed in 3.7 % paraformaldehyde for 24 h and then they were embedded in paraffin and sectioned in layers of 5 µm in thickness.

Regarding histogical analyses, tissue sections were stained with Hematoxylin-Eosin (H&E) and with Herovici staining to evaluate wound closure and collagen deposition, respectively.

In addition, immunohistochemical analyses were conducted using antibodies against α-SMA (1:250 dilution, ab5696, Abcam, UK), proliferating cell nuclear antigen (PCNA) (ab181797, Abcam, UK), cytokeratin 10 (1:5000, ab 76318, Abcam, UK) and cytokeratin 14 (1:250, Abcam, UK). Briefly, sections were deparaffinised, and after the blocking step, they were incubated with the primary antibodies overnight at 4 °C. Thereafter, sections were revealed using the ImmPRESS™ Peroxidase Detection Kit (Vector Laboratories LTD., UK) and ImmPACT DAB substrate (Vector Laboratories LTD., UK) following the manufacturer's instructions. Finally, sections were counterstained with hematoxylin (Vector Laboratories LTD., UK), dehydrated and mounted.

Images were acquired in a 3D-Histech Pannoramic-250 microscope slide-scanner using a 20x objective (Zeiss, Germany). Snapshots of the slide-scans were taken using the Case Viewer software (3D-Histech, Hungary). The stained area in each tissue section or the positive cell numbers were measured using the Tissue Studio analysis software (Definiens AG, Germany).

*2.9 Statistical analysis*

Results were expressed as the mean ± standard deviation (SD), except the results of the histological and immunohistochemical analysis that were expressed as the mean ± standard error of the mean. Results were analysed through one-way ANOVA test for multiple comparisons. Based on the Levene test for the homogeneity of variances, Bonferroni or Tamhane post-hoc were applied. All the statistical tests were performed using SPSS 22.0.01 (SPSS® INC., USA).

## 3. Results

### *3.1 Film structure*

In this work, the structure and thus, the physical performance of gelatin films has been modified by crosslinking. One of the layers was crosslinked by means of a non-enzymatic glycation (Maillard reaction) between gelatin and lactose, as shown in Fig. 3A; the other layer was crosslinked by the amide linkage formed between the amino groups of gelatin and the carboxylic groups of citric acid (Fig. 3B).

These facts were confirmed by analyzing the effect of lactose and citric acid in protein structure by FTIR. The most relevant peaks in FTIR spectra were related to the peptide bonds of the protein: C=O stretching at 1630 cm-1 (amide I), N-H bending at 1530 cm- 1 (amide II), and C-N stretching at 1230 cm- 1 (amide III). The broad band observed in the 3500-3000 cm−1 range is attributable to free and bound -OH and -NH- groups, which are able to form hydrogen bonding with the carbonyl group of the peptide linkage in the protein. As shown in Fig. 4, the most

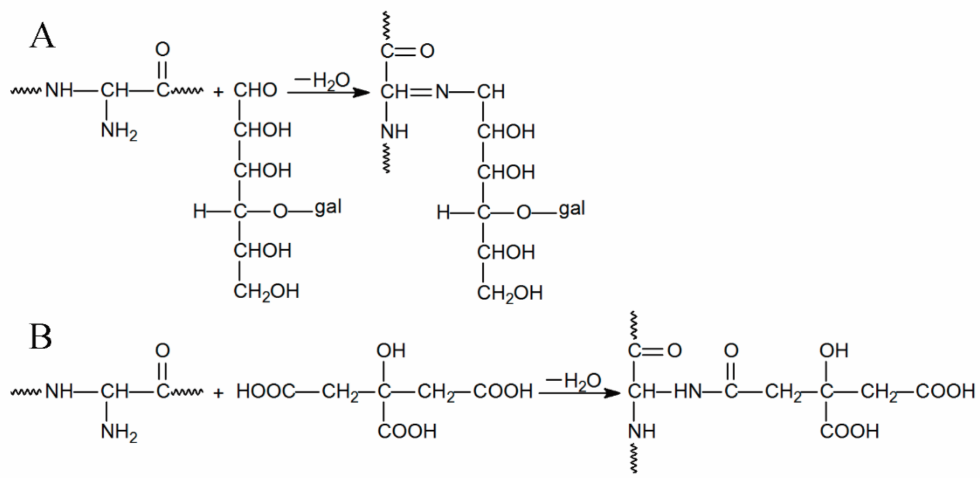


**Fig. 3.** Gelatin crosslinking. (A) The early stage of Maillard reaction between gelatin and lactose (gal=galactose). (B) Chemical reaction between gelatin and citric acid.

notable change can be observed in the relative intensity between amide I and amide II, indicating the change of gelatin structure as a consequence of the crosslinking.

In addition to the qualitative analysis carried out above, the band corresponding to amide I was used for the quantitative analysis of the changes in the secondary structures of protein backbone due to crosslinking, in particular, the changes in the intensity of the bands assigned to α-helix/unordered structures at 1650 $cm^{-1}$ and to β-sheets at 1615-1630 $cm^{-1}$ and 1680-1700 $cm^{-1}$. This quantitative analysis is shown in table 3. The area of the two bands at 1625 and 1689 $cm^{-1}$ is higher for Lac+ HF than for CA+ HF and, in contrast, the area related to α-helix/unordered structures is lower.

This change of structure was also observed by SEM analysis of the film cross-section. As can be observed in Fig. 5, a more homogeneous and smoother stratified structure was found for the hydrofilms crosslinked whit lactose (Fig. 5A).

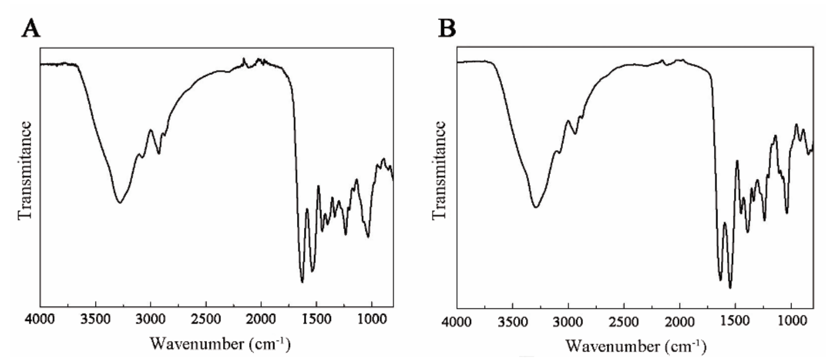


**Fig. 4.** FTIR analysis. (A) FTIR spectra of Lac+ HF. (B) FTIR spectra of CA+ HF.

**Table 3**. Protein conformation in gelatin films crosslinked with lactose or citric acid.

| Hydrofilms | Amide I area (%) | | |
|---|---|---|---|
| | β-sheet (1615-1630 cm-1) | α-helix (1650 cm-1) | β-sheet (1680-1700 cm-1) |
| Lac+ HF | 54 | 37 | 9 |
| CA+ HF | 43 | 53 | 4 |

### *3.2 Swelling*

Water uptake assay showed that after 120 h in PBS all the hydrofilms reached an equilibrium. As depicted in Fig. 6, the swelling curve demonstrated the same tendency in almost every time point tested. The hydrofilms with the greatest swelling ability were CA+ HF and CA+ Chit HF; in equilibrium they showed a swelling ability of 800 %, and 600-650 % in the case of CA- HF and CA- Chit HF. Lac- and Lac+ HF absorbed 4-5-fold less water than the previous ones, with a swelling value about 130-180 %.

Bilayer hydrofilms presented intermediate values, LacCA Chit+ HFb showed a swelling of 504 ± 4 %, LacCA+ HFb showed a value of 401 ± 29 %, LacCA Chit- HFb showed a value of 407 ± 15 % and the LacCA- HFb showed a value of 345 ± 9 %.

In equilibrium and comparing CA HF and LacCA HFb with the same composition, the statistical analysis showed significant differences among CA Chit+ HF and LacCA Chit+ HFb (** $p<0.01$), CA+ HF and LacCA+ HFb (* $p<0.05$) and CA- HF and LacCA- HFb (* $p<0.05$). In addition, the difference between Lac HF (with and without glycerol) and the rest of hydrofilms was significant.

The addition of chitosan did not produce any difference in the ability to absorb water. The addition of glycerol, on the

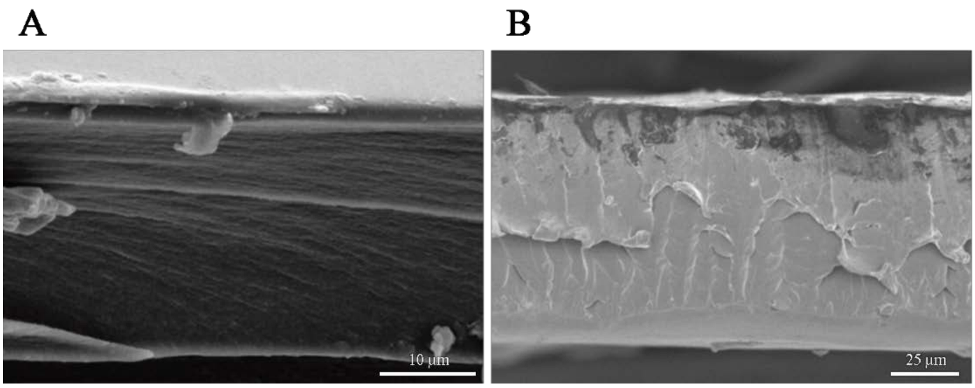


**Fig. 5.** SEM analysis. (A) Lac+ HF cross-section. (B) CA+ HF cross-section.

contrary, increased significantly the ability to absorb water on the CA HF without chitosan (* $p<0.05$) and on the LacCA HFb without chitosan (** $p<0.01$). The same tendency was observed on CA Chit HF and LacCA Chit HFb.

*3.3 Hydrolytic degradation*

In order to assess the degradation of the hydrofilms in an aqueous environment, they were immersed in PBS until they reached the water absorption equilibrium (120 h). The remaining weight of all the formulations was above the 80 % of the initial weight (Fig. 7). Two groups could be observed, the hydrofilms containing glycerol showed a remaining weight of about 88 % and the hydrofilms without glycerol showed a weight of about 96 %, that difference was statistically significant in every hydrofilm type, except in the Lac HF.

*3.3 WVTR*

The occlusivity of the hydrofilms was assessed trough the WVTR. As observed in Fig. 4, the addition of glycerol did not affect the permeability to water vapour of each hydrofilm type. In addition, there was no difference among bilayer hydrofilms (LacCA and LacCA Chit HFb with and without glycerol) as all of them showed similar values. Lac HF, on the contrary, showed a significantly less occlusive character as they achieved higher WVTR values.

*3.5 Cytotoxicity assay*

Cytotoxicity assay was performed to evaluate the effect of the hydrofilms on cells. Two processing methods were used before the assay. The first method was a 72 h dialysis, to remove the glycerol and the rest of compounds (e.g. unreacted crosslinkers) released from the hydrofilms. The second method consisted in hydrating the hydrofilms for 15 min. In addition, hydrofilms with and without glycerol were tested.

Results of the CCK-8 are shown in Fig. 9, and they proved that none of the hydrofilms was cytotoxic, since cell viability was above 70 % after fibroblast incubation with the release medium of each hydrofilm. There were no differences between hydrofilms with different processing methods or with and without glycerol, showing that processing the samples before using them is needless, since glycerol was dissolved in the hydrating step.

### *3.6* Ex vivo *assay*

In order to assess the efficacy of the hydrofilms on wound healing, an *ex vivo* assay in human skin was performed. Full thickness wounds of 3 mm were made on skin explants, and they were cultured for 8 days in transwell culture inserts.

Taking the results obtained in the previous assays into account, LacCA Chit- HFb and Lac- HF were the only ones analysed *ex vivo*. The assay was only conducted on hydrofilms without glycerol, since the characterisation results showed that its use as plasticiser was expendable because it was dissolved during the hydration process. Among bilayer hydrofilms, the only one evaluated was LacCA Chit- HFb, to assess the effect of chitosan in wound healing, since hydrofilms with and without chitosan presented similar characteristics. In addition, among single layer hydrofilms, only Lac- HF was tested, since wet CA HF did not have enough structural stability to be used as dressings on their own.

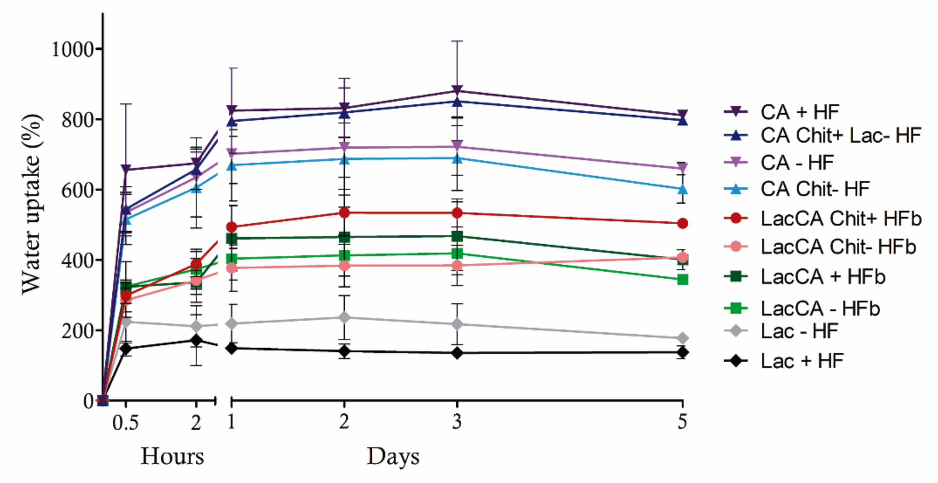


**Fig. 6.** Swelling curve. The percentage of water uptake regarding dry weight of the hydrofilms at different time points. Data are shown as mean ± SD.

On days 4 and 8 of the study, a LDH assay was carried out, to assess the viability of the tissue and thus the reliability of the assay. The viability remained above 70 % in all the time points and tested groups, therefore the treatments proved their bio-compatibility on the *ex vivo* model, as illustrated on Fig. 10.

Although there was no cytotoxicity, significant differences were observed among groups. On day 4, the viability was about 90 % in all the groups, although the difference between the control and the group treated with LacCA Chit- HFb was significant. On day 8, the differences among groups were more pronounced. The viability groups treated with LacCA Chit-HFb and Lac- HF, decreased to values around 70 %, and 80 %, respectively.

Wound closure was evaluated measuring the epithelial gap on H&E stained tissue sections, as observed in Fig. 11A. On day 8, a slight acceleration in wound closure was observed in the group treated with Lac- HF, although it was not statistically significant, as depicted on Fig. 11B.

Collagen deposition was analysed through Herovici staining. Fig. 12A displays images of the biopsy sections proce-

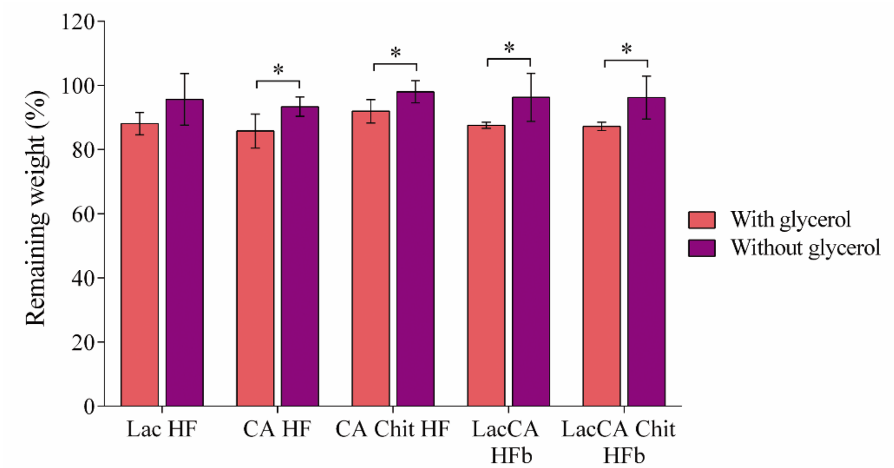


**Fig. 7.** Hydrolytic degradation. Results are shown as the percentage of the remaining weight regarding the initial weight. * $p<0.05$ comparing the hydrofilms with and without glycerol. Results are given as mean ± SD.

ssed with Herovici staining, while Fig. 12B shows the ratio between the stained area of collagen III and collagen I, since collagen III corresponds to the newly produced collagen that forms the new ECM and collagen I corresponds to mature collagen [25]. The results showed that Lac-HF presented a similar collagen III/I ratio as the control group, achieving values higher than baseline. The collagen ratio of the wounds treated with LacCA Chit- HFb, on the contrary, was significantly lower than that of the other two groups.

In addition, immunohistological analyses were performed. Tissue sections were stained against proliferating cell nuclear antigen (PCNA), a marker for cellular proliferation, which gives an insight about the cellular proliferation into the wound [26]. Results were represented as the percentage of positive cells in regards to baseline of each patient, in order to decrease the interindividual variability. Results depicted in Fig. 13A show non-significant differences in cell proliferation.

Wound contraction was analysed using antibodies against α-smooth muscle actin (α-SMA), a marker of myofibroblast differentiation and thus wound contraction [27]. Unfortunately, no differences were found among groups, analysing the percentage of the stained area, although a 2-fold increase regarding baseline was observed (Fig. 13B).

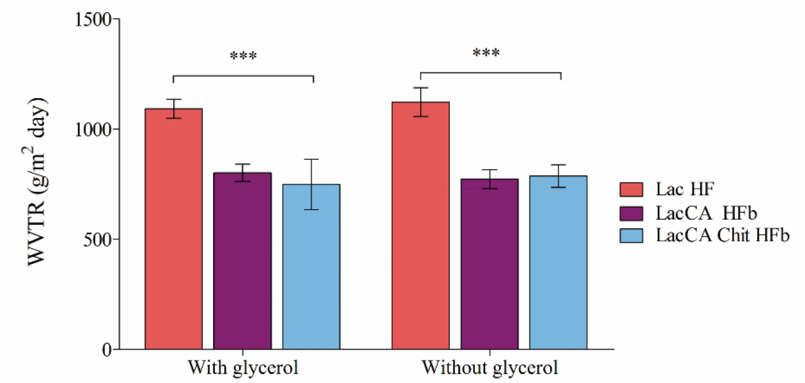


**Fig 8.** WVTR. Graphical representation of the WVTR of the hydrofilms with and without glycerol. *** $p<0.001$ comparing Lac HF (with and without glycerol) with LacCA and LacCA Chit HFb. Results are given as mean ± SD.

The expression of two cytokeratins was also evaluated, cytokeratin 14 and 10, precisely. Cytokeratin 14 is a marker for stratifying keratinocytes into the epithelial tongue. Cytokeratin 10, on the contrary, is a marker found in differentiated keratinocytes, which is not found on epithelial tongue, just in the mature epithelium [24,28,29]. The analysis of the stratifying keratinocytes (cytokeratin 14) showed similar values in all the groups on day 8 (Fig. 13C). Results obtained from the analysis of cytokeratin 10 are illustrated on Fig. 13D, showing a lower stained area on the group treated with the Lac- HF, while the group treated with LacCA Chit- HFb presented a similar value to the control group.

## 4. Discussion

The aim of the current study was to develop a bilayer dressing composed of gelatin. In order to mimic the natural structure of the skin, the characteristics of both layers varied, since different crosslinkers were used. The upper layer was composed of gelatin crosslinked with lactose, to obtain a stiffer and non-hydrolytically labile layer. Lactose and gelatin react in presence of heat leading to a non-enzymatic glycation of the protein chains, known as Maillard reaction [30]. This hydrofilm was previously characterised by our research group [22]. It forms a homogeneous and transparent layer of about 50 µm of thick-

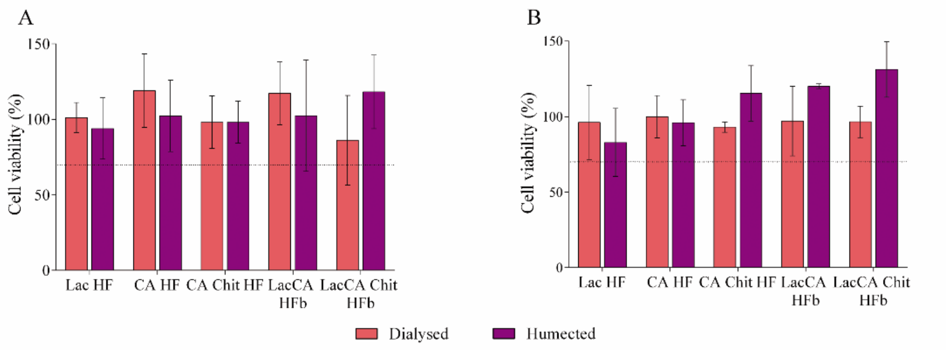


**Fig. 9** Cytotoxicity assay. (A) Cell viability after incubating fibroblasts with the release medium of hydrofilms containing glycerol. (B) Cell viability after incubating fibroblasts with the release medium of hydrofilms without glycerol. Results are shown as mean ± SD.

ness that maintained its initial appearance after being immersed in PBS at 37 °C or incubated with cells for 8 days. The lower layer was composed of gelatin crosslinked with citric acid, due to its reaction with the amine group of the protein chains [31]. These hydrofilms presented a more jelly-like structure, as they were able to absorb a considerable larger volume of water and they lost their integrity after a few hours immersed in PBS at 37 °C (data not shown). The influence of the crosslinker was demonstrated by FTIR results, which showed that a progressive conversion of residual regular structures and unordered segments into intermolecular β-sheets occurred for the films crosslinked by lactose compared to citric acid-crosslinked films. This change in the secondary structure of gelatin led to a more compact and smoother microstructure when crosslinking was promoted by lactose addition, as shown by SEM analysis.

Chitosan was added to the lower layer in order to promote wound healing process, as chitosan has previously demonstrated various beneficial effects in wound

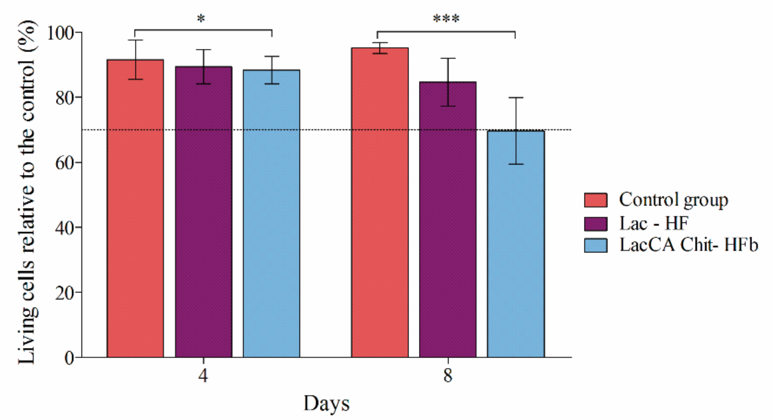


**Fig. 10.** LDH assay of the *ex vivo* assay. The results were represented as the viability of the three groups on different time points. * p<0.05 comparing the control group and the group treated with LAcCA Chit- HFb, on day 4; *** p>0.001 comparing each group with the other two, on day 8; ** p<0.001 comparing the control group with the group treated with Lac- HF on day 11; ●●● p<0.001 comparing the control group and the group treated with LacCA Chit- HFb, on day 11 and 15. Results are shown as mean ± SD.

healing. In fact, it presents antibacterial and hemostatic activity, acting in the early phases of healing [13]; it promotes the activity of macrophages and the migration of polymorphonuclear neutrophils [14]; it is able to induce the proliferation of fibroblasts and keratinocytes both in vitro and in vivo [32,33]; and it regulates in a biphasic manner the expression of TGFβ1, inducing an increment in its expression during the early healing phases, which lead to an increment in collagen production, while downregulating its expression in the later phases, thereby reducing the scar formation [34]. It is noteworthy, that none of the developed layers showed cytotoxicity.

Both layers were glued together spraying ethanol on them and letting them air dry. The swelling ability of the resulting bilayer was evaluated in order to compare the behaviour of the different hydrofilms. As swelling studies were performed only to determine the differences among hydrofilms, they were performed at 4 °C instead of being performed at skin temperature, since CA HF lost their structural stability in a warm aqueous environment.

As expected, hydrofilms with the highest crosslinking degree (Lac HF) had the lowest ability to absorb water, and the ones with the lowest crosslinking degree (CA HF) had the highest water uptake [35]. Bilayer hydrofilms had intermediate values since they were composed of both layers. The addition of chitosan did not produce any change in swelling. The addi-

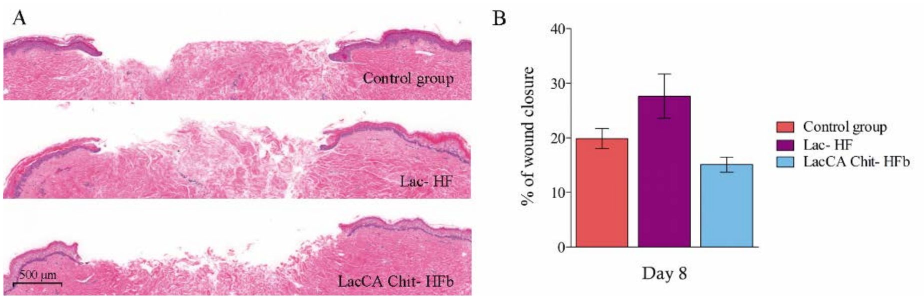


**Fig. 11.** Wound closure. (A) Histological images of tissue sections of each group on day 8, processed with H&E. The scale bar indicates 500 µm. (B) Percentage of wound closure on days 8. Results are shown as the mean ± standard error of the mean.

tion of glycerol increased the water uptake in CA HF and LacCA HFb probably because of an increased hydrophilicity of the hydrofilms [36].

The hydrolitical stability of the hydrofilms was also carried out at 4 °C to allow a longer study time where compare the characteristics of the different formulations. Two groups of hydrofilms could be distinguished, the ones without glycerol and the ones containing glycerol. Hydrofilms in the first group maintained about the 96 % of their dry weight after being immersed in PBS. This weight loss may be due to the dissolution of the unreacted crosslinker, as described previously in gelatin films crosslinked with lactose. On the other hand, the remaining weight in hydrofilms containing glycerol was about 88 %. In this case, besides of releasing the unreacted crosslinker, glycerol was probably also dissolved in the aqueous medium, since it interacts with gelatin through hydrogen bonding [37].

The occlusivity of the hydrofilms was evaluated measuring the WVTR, in order to assess if they were able to maintain an acceptable level of moisture into the wounds. The WVTR of the bilayer hydrofilms was within the range of commercial wound dressings (426-2047 g/m$^2$day). Thus, they presented an adequate control of moisture; allowing exudate to evaporate, while maintaining some moisture into

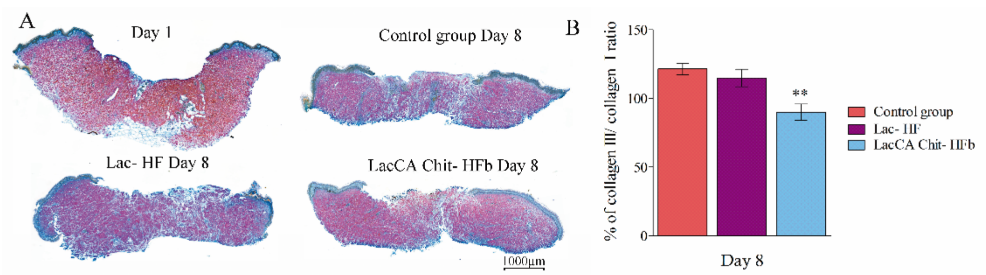


**Fig. 12.** Collagen deposition. (A) Tissue section images processed with Herovici staining. Collagen I or mature fibres are stained with red and collagen III or new fibres are stained with blue. The scale bar indicates 1000 µm. (B) Quantitative analysis of the collagen deposition. ** p<0.01 and comparing the group treated with LacCA Chit- HFb with the other groups. Results are shown as the mean ± standard error of the mean.

the wound to prevent tissue dehydration, help in reepithelisation and angiogenesis, and reduce pain [38-40]. Lac HF, however, showed a higher WVTR value, which can be translated into a lower occlusivity, because it allowed a larger volume of water vapour to be evaporated from the wound. The higher permeability could be explained by the lower thickness of the Lac HF in comparison to bilayer hydrofilms, as previously reported [41].

Prior to evaluating the efficacy of the dressings *ex vivo*, their cytocompatibility was assessed. The results obtained in the indirect cytotoxicity assay with all the hydrofilms tested showed viability values above 70 % with respect to the control group, which suggest an excellent biocompatibility according to the ISO 10992-5:2009 guidelines for biological evaluation of medical devices. The direct cytotoxicity assay was not performed, since CA HF partially dissolve at 37 °C, thereby increasing the viscosity of the medium and impeding the removal of the hydrofilms to perform the CCK-8 assay.

With the viability assay, the effect of glycerol on cell viability and the need of a previous conditioning step were analysed. Regarding the effect of glycerol, the results showed that hydrofilms containing glycerol presented similar biocompatibility than the hydrofilms without it. In addition, the assay demonstrated that there was no need of processing the hydrofilms through dialysis, as the same viability re-

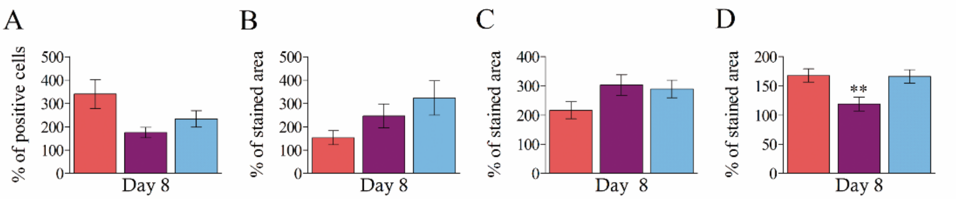


**Fig. 13.** Immunohistochemical analysis. (A) Representation of PCNA positive cells percentage regarding to baseline. (B) Representation of quantitative analysis of α-SMA stained area. (C) Representation of quantitative analysis of cytokeratin 14 stained area. (D) Representation of quantitative analysis of cytokeratin 10 stained area. ** $p>0.001$ comparing the group treated with the Lac- HF and the other two groups on day 8. Results are shown as the mean ± standard error of the mean.

sults were obtained hydrating them for 15 min prior to the assay. The biocompatibility of dry hydrofilms was not tested, since in a previous study carried out in Lac+ HF, incubating cells with the extracted medium of dry hydrofilms lead to a decrease in cell viability due to an increase in medium osmolarity caused by the rapid release of unreacted lactose and glycerol [22]. Thereby, a conditioning step of 15 min hydration was still needed in order to remove the unreacted crosslinker and glycerol.

Dressings efficacy was evaluated using an *ex vivo* assay in order to reduce the use of animals in research and to use human skin instead of animal skin, thus avoiding the differences in wound healing among species [15]. Although it is not standardized, *ex vivo* human full thickness wound models have been already used to evaluate the effect on wound healing of different dressings and formulations such as, a hyaluronic acid/alginate dressing containing platelet lysate and vancomycin [42], a chitosan oleate nanoemulsion containing α-tocopherol [43], an electrospun silk fibroin dressing [23], a cellular (containing fibroblasts and mesenchymal stem cells) or acellular collagen-glycosaminoglican flowable matrix [44] and Integra® dermal template or Integra® supplemented with hyaluronan [45].

In order to evaluate the viability of the biopsies a LDH assay was conducted on days 4 and 8. All groups presented viability values above 70 %. On one hand, those values demonstrated that cells of the biopsies remained alive during the whole study, which highlights the reliability and suitability of the model. On the other hand, this study proved the lack of cytotoxicity of the developed hydrofilms, as previously observed in the cytotoxicity assay carried out on fibroblasts. Moreover, assessing the viability assay into the *ex vivo* model gives an insight of the behaviour of the hydrofilms in a more complex structure than a monolayer single cell culture.

In addition, the wound healing process was assessed to analyse the effect of the hydrofilms. In general, the application of the hydrofilms, did not hinder healing, since no differences were observed among groups in the majority of parameters evaluated, such as wound closure, cellular proliferation, wound contraction and expression of new undifferentiated keratinocytes. Nevertheless, collagen deposition was decreased in the group treated with Lac- HF and the expression of new mature keratinocytes was lower in the group treated with LacCA Chit- HFb. Those negative results could be explained by the great swelling ability of the dressings, which led to the absorption of some of the culture medium, decreasing the quantity of nutrients available for cells. In addition, the great water uptake of the hydrofilms and the incubation in a humidified incubator, presented an overly moist environment for the epidermis, which do not favour healing. Therefore, the hydrofilms and specially the CA HF should be optimised, in order to create a more adequate environment for healing.

Accordingly, the results obtained in the *ex vivo* assay, showed the suitability of the model to assess wound healing, as a screening method prior to conduct an *in vivo* study. In addition, it showed that the developed hydrofilms could be useful as wound dressings. In order to improve the efficacy of the hydrofilms, in future studies active molecules such as growth factors will be encapsulated or immobilised into the lower layer.

## 5. Conclusion

In the current study a bilayer wound dressing has been developed based on gelatin. Firstly both layers and the resulting bilayer hydrofilms were characterised, showing that the upper layer (Lac HF) was more resistant and that the lower layer (CA and CA Chit HF) had a greater ability to absorb water. Overall, the dressing presented good swelling and occlusivity characteristics and it did not show cytotoxicity against fibroblasts. In order to evaluate its efficacy an *ex vivo* wound healing assay was performed, which demonstrated on one hand the suitability of the model to assess wound healing, and on the other hand that the hydrofilms did not hinder healing in the majority of the evaluated parameters.

## 6. Acknowledgments

I. García-Orue and J. Uranga thank the Basque Government for the fellowship grant. This project has been partially supported by the Basque Government (Consolidated Groups, IT-428-10 and IT-528-10). The Bioimaging Facility Slide Scanning Service used in this study was purchased with grants from BBSRC, Wellcome and the University of Manchester Strategic Fund. Special thanks goes to Roger Meadows and Steve Marsden for their help with the microscopy. BIOMAT group thanks the Provincial Council of Gipuzkoa for the financial support.

## 7. References

[1] R.A. Franco, Y. Min, H. Yang, B. Lee, Fabrication and biocompatibility of novel bilayer scaffold for skin tissue engineering applications, J. Biomater. Appl. 27 (2013) 605-615. doi: 10.1177/0885328211416527.

[2] M. Zilberman, D. Egozi, M. Shemesh, A. Keren, E. Mazor, M. Baranes-Zeevi, N. Goldstein, I. Berdicevsky, A. Gilhar, Y. Ullmann, Hybrid wound dressings with controlled release of antibiotics: Structure-release profile effects and in vivo study in a guinea pig burn model, Acta Biomater. 22 (2015) 155-163. doi: 10.1016/j.actbio.2015.04.029.

[3] L. Ding, X. Shan, X. Zhao, H. Zha, X. Chen, J. Wang, X. Wang, C. Cai, G. Li, J. Hao, G. Yu, Spongy bilayer dressing composed of chitosan–Ag nanoparticles and chitosan–Bletilla striata polysaccharide for wound healing applications, Carbohydr. Polym. 157 (2017) 1538-1547. doi: 10.1016/j.carbpol.2016.11.040.

[4] P.B. Malafaya, G.A. Silva, R.L. Reis, Natural–origin polymers as carriers and scaffolds for biomolecules and cell delivery in tissue engineering applications, Adv. Drug Deliv. Rev. 59 (2007) 207-233. doi: 10.1016/j.addr.2007.03.012.

[5] G.D. Mogoşanu, A.M. Grumezescu, Natural and synthetic polymers for wounds and burns dressing, Int. J. Pharm. 463 (2014) 127-136. doi: //dx.doi.org/10.1016/j.ijpharm.2013.12.015.

[6] A.O. Elzoghby, Gelatin-based nanoparticles as drug and gene delivery systems: Reviewing three decades of research, J. Control. Release 172 (2013) 1075-1091. doi: 10.1016/j.jconrel.2013.09.019.

[7] H. Wang, O.C. Boerman, K. Sariibrahimoglu, Y. Li, J.A. Jansen, S.C.G. Leeuwenburgh, Comparison of micro- vs. nanostructured colloidal gelatin gels for sustained delivery of osteogenic proteins: Bone morphogenetic protein-2 and alkaline phosphatase, Biomaterials 33 (2012) 8695-8703. doi: 10.1016/j.biomaterials.2012.08.024.

[8] D. Eisenbud, H. Hunter, L. Kessler, K. Zulkowski, Hydrogel wound dressings: where do we stand in 2003?, Ostomy Wound Manage. 49 (2003) 52.

[9] M. Foox, M. Zilberman, Drug delivery from gelatin-based systems, Expert Opin. Drug Deliv. 12 (2015) 1547-1563. doi: 10.1517/17425247.2015.1037272.

[10] N. Reddy, R. Reddy, Q. Jiang, Crosslinking biopolymers for biomedical applications, Trends Biotechnol. 33 (2015) 362-369. doi: 10.1016/j.tibtech.2015.03.008.

[11] V. Chiono, E. Pulieri, G. Vozzi, G. Ciardelli, A. Ahluwalia, P. Giusti, Genipin-crosslinked chitosan/gelatin blends for biomedical applications, J. Mater. Sci. : Mater. Med. 19 (2008) 889-898. doi: 10.1007/s10856-007-3212-5.

[12] T. Dai, M. Tanaka, Y.Y. Huang, M.R. Hamblin, Chitosan preparations for wounds and burns: antimicrobial and wound-healing effects, Expert Rev. Anti Infect. Ther. 9 (2011) 857-879. doi: 10.1586/eri.11.59.

[13] M.B. Dreifke, A.C. Jayasuriya, A.A. Jayasuriya, Current wound healing procedures and potential care, Mater. Sci. Eng. C Mater. Biol. Appl.   48 (2015) 651-662. doi: 10.1016/j.msec.2014.12.068.

[14] V. Patrulea, V. Ostafe, G. Borchard, O. Jordan, Chitosan as a starting material for wound healing applications, Eur. J. Pharm. Biopharm. 97 (2015) 417-426. doi: 10.1016/j.ejpb.2015.08.004.

[15] S.H. Mathes, H. Ruffner, U. Graf-Hausner, The use of skin models in drug development, Adv. Drug Deliv. Rev. 69-70 (2014) 81-102. doi: 10.1016/j.addr.2013.12.006.

[16] S. Pfuhler, R. Fautz, G. Ouedraogo, A. Latil, J. Kenny, C. Moore, W. Diembeck, N.J. Hewitt, K. Reisinger, J. Barroso, The Cosmetics Europe strategy for animal-free genotoxicity testing: Project status up-date, Toxicol. in Vitro 28 (2014) 18-23. doi: 10.1016/j.tiv. 2013.06.004.

[17] Nicola J Hewitt, Robert J Edwards, Ellen Fritsche, Carsten Goebel, Pierre Aeby, Julia Scheel, Kerstin Reisinger, Gladys Ouédraogo, Daniel Duche, Joan Eilstein, Alain Latil, Julia Kenny, Claire Moore, Jochen Kuehnl, Joao Barroso, Rolf Fautz, Stefan Pfuhler, Use of human in vitro skin models for accurate and ethical risk assessment: metabolic considerations, Toxicol. Sci. 133 (2013) 209-217. doi: 10.1093/toxsci/kft080.

[18] P.D. Butler, D.P. Ly, M.T. Longaker, G.P. Yang, Use of organotypic coculture to study keloid biology, Am. J. Surg. 195 (2008) 144-148. doi: 10.1016/j.amjsurg.2007.10.003.

[19] Wei Xu, Seok Jong Hong, Shengxian Jia, Yanan Zhao, Robert D Galiano, Thomas A Mustoe, Application of a partial-thickness human ex vivo skin culture model in cutaneous wound healing study, Lab. Invest. 92 (2012) 584-599. doi: 10.1038/labinvest.2011.184.

[20] K.Q. Zhu, L.H. Engrav, R.N. Tamura, J.A. Cole, P. Muangman, G.J. Carrougher, N.S. Gibran, Further similarities between cutaneous scarring in the female, red Duroc pig and human hypertrophic scarring, Burns 30 (2004) 518-530. doi: 10.1016/j.burns.2004.02.005.

[21] S. Ud-Din, A. Bayat, Non-animal models of wound healing in cutaneous repair: In silico, in vitro, ex vivo, and in vivo models of wounds and scars in human skin, Wound Repair Regen. 25 (2017) 164-176. doi: 10.1111/wrr.12513.

[22] A. Etxabide, C. Vairo, E. Santos-Vizcaino, P. Guerrero, J.L. Pedraz, M. Igartua, K. de la Caba, R.M. Hernandez, Ultra thin hydrofilms based on lactose-crosslinked fish gelatin for wound healing applications, Int. J. Pharm.

530 (2017) 455-467. doi: 10.1016/j.ijpharm. 2017.08.001.

[23] T. Hodgkinson, X. Yuan, A. Bayat, Electrospun silk fibroin fiber diameter influences in vitro dermal fibroblast behavior and promotes healing of ex vivo wound models, J. Tissue Eng. 5 (2014) 2041731414551661. doi: 10.1177/2041731414551661.

[24] J. Mendoza-Garcia, A. Sebastian, T. Alonso-Rasgado, A. Bayat, Optimization of an ex vivo wound healing model in the adult human skin: Functional evaluation using photodynamic therapy, Wound Repair Regen. 23 (2015) 685-702. doi: 10.1111/wrr.12325.

[25] P. Bainbridge, Wound healing and the role of fibroblasts, J. Wound Care 22 (2013) 407-412. doi: 10.12968/jowc.2013.22.8.407.

[26] J. Chen, B. Lin, H. Hu, C. Lin, W. Jin, F. Zhang, Y. Zhu, C. Lu, X. Wei, R. Chen, NGF accelerates cutaneous wound healing by promoting the migration of dermal fibroblasts via the PI3K/Akt-Rac1-JNK and ERK pathways, Biomed Res. Int. 2014 (2014) 547187.

[27] B.M.d. Almeida, M.F.d. Nascimento, R.N. Pereira-Filho, G.C.d. Melo, J.C.d. Santos, C.R.d. Oliveira, M.Z. Gomes, S.O. Lima, Albuquerque-Júnior, Ricardo Luiz Cavalcanti de, Immunohistochemical profile of stromal constituents and lymphoid cells over the course of wound healing in murine model, Acta Cir. Bras. 29 (2014) 596-602. doi: 10.1590/S0102-8650201400150007.

[28] R. Moll, M. Divo, L. Langbein, The human keratins: biology and pathology, Histochem. Cell. Biol. 129 (2008) 705-733. doi: 10.1007/s00418-008-0435-6.

[29] M.L. Usui, J.N. Mansbridge, W.G. Carter, M. Fujita, J.E. Olerud, Keratinocyte Migration, Proliferation, and Differentiation in Chronic Ulcers From Patients With Diabetes and Normal Wounds, J. Histochem. Cytochem. 56 (2008) 687-696. doi: 10.1369/jhc.2008.951194

[30] A. Etxabide, M. Urdanpilleta, P. Guerrero, K. de la Caba, Effects of cross-linking in nanostructure and physicochemical properties of fish gelatins for bio-applications, React. Funct. Polym. 94 (2015) 55-62. doi: 10.1016/j. reactfunctpolym.2015.07.006.

[31] A. Oryan, A. Kamali, A. Moshiri, H. Baharvand, H. Daemi, Chemical crosslinking of biopolymeric scaffolds: Current knowledge and future directions of crosslinked engineered bone scaffolds, Int. J. Biol. Macromol. 107 (2018) 678-688. doi: 10.1016/j.ijbiomac.2017.08.184.

[32] G.I. Howling, P.W. Dettmar, P.A. Goddard, F.C. Hampson, M. Dornish, E.J. Wood, The effect of chitin and chitosan on the proliferation of human skin fibroblasts and keratinocytes in vitro, Biomaterials 22 (2001) 2959-2966. doi: 10.1016/S0142-9612(01) 00042-4.

[33] A.K. Azad, N. Sermsintham, S. Chandrkrachang, W.F. Stevens, Chitosan membrane as a wound-healing dressing: Characterization and clinical application, J. Biomed. Mater. Res. B Appl. Biomater. 69B (2004) 216-222. doi: 10.1002/jbm.b.30000.

[34] R.M. Baxter, T. Dai, J. Kimball, E. Wang, M.R. Hamblin, W.P. Wiesmann, S.J. McCarthy, S.M. Baker, Chitosan dressing promotes healing in third degree burns in mice:

Gene expression analysis shows biphasic effects for rapid tissue regeneration and decreased fibrotic signaling, J. Biomed. Mater. Res. A 101A (2013) 340-348. doi: 10.1002/jbm.a.34328.

[35] A. Saarai, V. Kasparkova, T. Sedlacek, P. Saha, On the development and characterisation of crosslinked sodium alginate/gelatine hydrogels, J. Mech. Behav. Biomed. Mater.   18 (2013) 152-166. doi: 10.1016/j. jmbbm.2012.11.010.

[36] D. Prabu, A.F. Majdalawieh, I.A. Abu-Yousef, K. Inbasekaran, T. Balasubramaniam, N. Nallaperumal, C.J. Gunasekar, Preparation and characterization of gatifloxacin-loaded sodium alginate hydrogel membranes supplemented with hydroxypropyl methylcellulose and hydroxypropyl cellulose polymers for wound dressing, J. Pharm. Investig. 6 (2016) 86. doi: 10.4103/2230-973X.177810.

[37] A. Etxabide, J. Uranga, P. Guerrero, K. de la Caba, Improvement of barrier properties of fish gelatin films promoted by gelatin glycation with lactose at high temperatures, LWT - Food Sci. Technol. 63 (2015) 315-321. doi: 10.1016/j.lwt.2015.03.079.

[38] Y. Tu, M. Zhou, Z. Guo, Y. Li, Y. Hou, D. Wang, L. Zhang, Preparation and characterization of thermosensitive artificial skin with a Sandwich structure, Mater. Lett. 147 (2015) 4-7. doi: //dx.doi.org/10.1016/j.matlet.2015.01.163.

[39] N. Mayet, Y.E. Choonara, P. Kumar, L.K. Tomar, C. Tyagi, L.C. Du Toit, V. Pillay, A Comprehensive Review of Advanced Biopolymeric Wound Healing Systems, J. Pharm. Sci. 103 (2014) 2211-2230. doi: 10.1002/jps.24068

[40] B. Singh, S. Sharma, A. Dhiman, Design of antibiotic containing hydrogel wound dressings: Biomedical properties and histological study of wound healing, Int. J. Pharm. 457 (2013) 82-91. doi: 10.1016/j.ijpharm.2013.09.028.

[41] V. Morillon, F. Debeaufort, G. Blond, M. Capelle, A. Voilley, Factors Affecting the Moisture Permeability of Lipid-Based Edible Films: A Review, Crit. Rev. Food Sci. Nutr. 42 (2002) 67-89. doi: 10.1080/10408690290 825466.

[42] S. Rossi, M. Mori, B. Vigani, M.C. Bonferoni, G. Sandri, F. Riva, C. Caramella, F. Ferrari, A novel dressing for the combined delivery of platelet lysate and vancomycin hydrochloride to chronic skin ulcers: Hyaluronic acid particles in alginate matrices, Eur. J. Pharm. Sci. 118 (2018) 87-95. doi: 10.1016/j.ejps.2018.03.024.

[43] M.C. Bonferoni, F. Riva, A. Invernizzi, E. Dellera, G. Sandri, S. Rossi, G. Marrubini, G. Bruni, B. Vigani, C. Caramella, F. Ferrari, Alpha tocopherol loaded chitosan oleate nanoemulsions for wound healing. Evaluation on cell lines and ex vivo human biopsies, and stabilization in spray dried Trojan microparticles, Eur. J. Pharm. Biopharm. 123 (2018) 31-41. doi: 10.1016/j.ejpb.2017.11.008.

[44] T. Hodgkinson, A. Bayat, Ex vivo evaluation of acellular and cellular collagen-glycosaminoglycan flowable matrices, Biomed. Mater. 10 (2015) 041001.

[45] T. Hodgkinson, A. Bayat, In vitro and ex vivo analysis of hyaluronan supplementation of Integra® dermal template on human dermal fibroblasts and keratinocytes, J. Appl. Biomater. Funct. Mater. 14 (2016) 0. doi: 10.5301/jabfm.5000259..

# Discussion

The treatment of chronic wounds has gained a great importance due to the alarming increase in their incidence. They are becoming a challenging clinical problem, in fact, only in the US, chronic wounds annually affect 5.7 million people (around 2% of the population) and cost $20 billion [1]. In Europe, 6000-10000 € are spent in wound associated expenses, such as nursing time, hospitalisation, dressing changes and wound infections management [2,3].

The growth of chronic wounds incidence is related to the rise of diseases associated with wound chronicity, such as, obesity, venous insufficiency and diabetes [4]. Those wounds fails to progress through the physiological phases of healing (hemostasis, inflammation, proliferation and remodelling), delaying the restoration of skin integrity, and frequently relapsing [5-7]. The main reason of this impaired healing is their continuous inflammatory state, since neutrophils are present during the whole process, releasing an excessive amount of proinflammatory cytokines and proteases, which creates a proteolytic microenvironment that degrades healing mediators and extracellular matrix (ECM) [8,9].

Currently, the therapies for chronic wounds cannot guarantee an effective healing. Therefore, the search of an effective treatment has gained a huge importance, and significant efforts have been made in that search to develop new treatments or improve the current ones. The topical administration of endogenous molecules involved in wound healing is one of those novel treatments. Unfortunately, most of those molecules present a very short stability *in vivo* due to their proteic nature. To overcome this limitation, they can be encapsulated into different systems, such as lipid nanoparticles, and more specifically in nanostructured lipid carriers (NLCs). NLCs, besides protecting the encapsulated peptide, present numerous advantages for wound healing: they allow controlled release, due to their adhesiveness and occlusivity they increase skin hydration, and their small size ensures a close contact with the skin [10].

Another approach to fulfil the requirements for wound care application includes nanofibrous membranes. Those dressings are usually generated by electrospinning, a technique that draws nanometric fibers from a polymeric solution using the electric force [11]. Nanofibers produced using this technique exhibit a unique structure, that consist of a high surface are to volume ratio and a high porosity. Those characteristics enhance wound healing by promoting cell breathing, retaining moisture and allowing the removal of exudates, since they allow gas permeation and they control wound moisture [12]. Furthermore, their structure mimics the native ECM three dimensional structure, which makes them an interesting option for tissue engineering [13,14].

Finally, bilayer dressings have received significant interest for wound healing application, due to their outstanding characteristics. Their structure mimics the bilayer structure of the skin, with an upper protective layer resembling the epidermis, and a thicker flexible lower layer like the dermis. Taking that into account, the dense upper layer is designed to cover the wound, giving mechanical strength to the dressing. In addition, it needs to control moisture transmission to prevent fluid loss and dehydration, while allowing exudate removal. Furthermore, the upper layer prevents bacterial penetration and thus wound infection. On the other hand, the lower layer is a porous or sponge like structure that is able to absorb wound exudate and smoothly adhere to the wet wound bed to accommodate newly formed tissue [15-17].

Bearing these considerations in mind, in the current doctoral thesis we have focused on the development of different approaches to promote wound healing. In a first step, we developed a formulation containing the human peptide LL37, since it has been proven that this antimicrobial molecule modulates wound healing by activating angiogenesis [18,19], enhancing epithelial cell migration and proliferation [20,21] and acting as chemotactic to monocytes, neutrophils and dendritic cells [22]. As the LL37 presents a short stability *in vivo*, it was encapsulated into NLCs in order to protect it. Thereby, the first formulation developed in this thesis were NLCs loaded with LL37 (NLC-LL37).

The NLCs were produced emulsifying a melted lipid phase containing a solid (Precirol ATO5) and a liquid lipid (Mygliol® 812N) with a warm aqueous phase containing surfactants. Both phases were mixed, the LL37 added to the mixture, and then they were emulsified by sonication. The NLCs obtained using this preparation method had a mean size of 273.6 ± 27.64 nm and a zeta potential of about -31 mV. The encapsulation efficiency of the LL37 was 96.4 ± 0.41 %, with a peptide loading of 16.76 ± 0.07 µg LL37/mg NLC.

Prior to the *in vitro* activity assay, the biocompatibility of the NLC-LL37 was determined, assaying the viability of fibroblast that were incubated with NLCs. Once it was demonstrated that the formulation was not cytotoxic, the activity of the formulation was evaluated to determine whether the encapsulation process affects the bioactivity of the peptide. In that regard, the RAW 267.4 macrophage cell line was activated with lipopolysaccharide (LPS) and treated with free LL37, NLC-LL37 and empty NLCs. To quantify if the formulations were able to inhibit the macrophage activation, the release of TNF-α was measured by ELISA. As depicted in Fig. 1, the NLC-LL37 was able to reduce the TNF-α production in the same extent as the free LL37, which suggest that the peptide remained active after the encapsulation process. Moreover, the empty NLCs did not show any effect, which highlights that the effect was due to the LL37 of the NLC-LL37. To achieve that neutralisation, the LL37 needs to bind both the LPS, through electrostatic and hydrophobic interactions, and the CD14 receptor of the macrophages through a selective union [23-25].

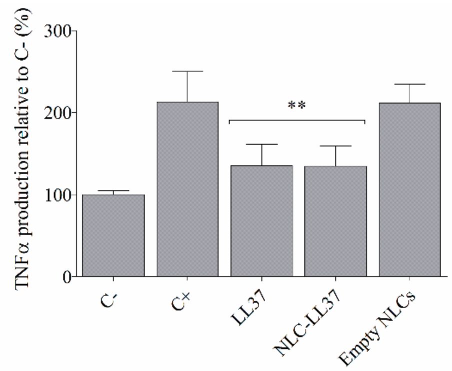


**Fig. 1.** Inhibition of the activation of the macrophages. The results are given as the mean % of TNF-α production relative to the control ± SD. ** significantly greater than empty NLC and C+ ($p<0.01$). Controls are C- (cells without any addition) and C+ (cells after the addition of LPS).

Subsequently, the antimicrobial activity of the NLC-LL37 was tested against *E. coli*, because it is one of the most common bacteria in infected wounds [26]. Briefly, free LL37, NLC-LL37 and empty NLCs were incubated with *E. coli* for 4 h. Then, samples were taken, inoculated in an agar plate, incubated for 24 h and the grown colonies counted. The results showed that the free LL37 killed all the bacteria, whereas the percentage of cells killed by the NLC-LL37 was lower. The most plausible explanation for the lower effect observed in the group treated with NLC-LL37 is that the LL37 was released in a sustained manner from the NLC-LL37, and thus the available dose at the beginning of the study was lower. Thereby, the NLC-LL37 were not able to kill all the bacteria at the beginning, and the subsequent exponential growth of the remaining bacteria hampered the effect of the NLC-LL37. However, *in vivo* the bacteria are proliferating constantly in the wound, which makes more necessary a sustained release of the peptide rather than a high initial dose.

Finally, the efficacy of the formulation was analysed *in vivo* in a full thickness splinted model in *db/db* mice. A rodent model was chosen, since it is easier to work with small animals, although pig dermis is more similar to that of humans [27]. Nevertheless, *db/db* mice present some advantages over other rodent models. Firstly, *db/db* mice present a mutation of the leptin receptor and thus, they possess a type II diabetes phenotype, which leads to an impaired healing, and to a better resemblance of a chronic wound [28,29]. Secondly, contraction is impaired in these mice, because their extreme obesity reduces the looseness of their skin [30,31]. Therefore, reepithelisation is enhanced, making the healing process more similar to human's one. In addition, wound contraction is even more hampered by placing silicone splint around the wounds [32]. The animals received two dosis of NLC-LL37 topically, one group received 6 µg of LL37 encpasulated into NLCs and the other group received 2 µg of LL37 into NLCs.

Wound healing was evaluated measuring the following parameters: (i) wound closure, it was evaluated measuring wound areas from photographs; (ii) reepithelisation grade, it was evaluated semi-quantitatively applying the scale described by Sinha *et al.* to tissue sections processed with H&E [33]; (iii) the resolution of the inflammatory process, as the previous one, it was evaluated from H&E stained tissue sections, but this time according to the scale described by Cotran *et al. [34];* (iv) collagen deposition, it was assessed from tissue sections stained with Masson trichrome following the scale described by Gal *et al. [35];* and (v) angiogenesis, which was evaluated counting the newly formed blood vessels in tissue sections immunohistochemically stained with antiCD31 monoclonal antibody.

The results showed that in both wound closure and reepithelisation, the administration of NLC-LL37 accelerated wound healing in comparison to empty NLCs, free LL37 and untreated group, as observed in Fig. 2. The administration of NLC-LL37 also enhanced the resolution of the inflammatory process, but in this case in the same extent as the administration of free LL37. Nevertheless, collagen deposition and angiogenesis did not show any differences among groups.

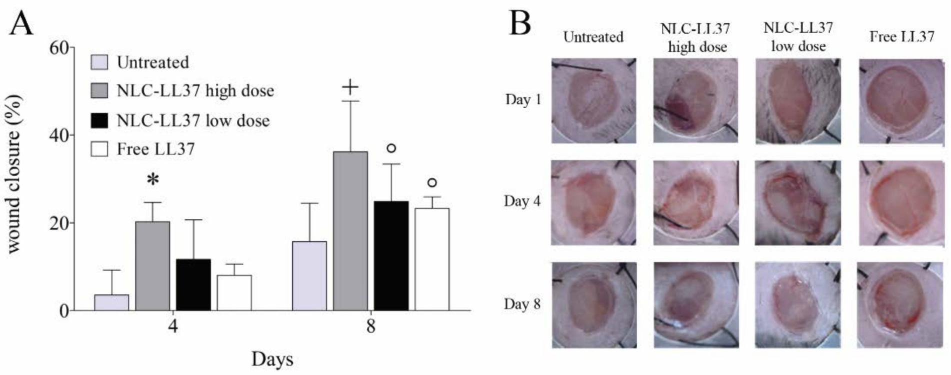


**Fig. 2.** In vivo wound closure. (A) Wound closure represented as the percentage of reduction of the initial area. * Significantly greater than untreated group ($p<0.05$); ○ significantly greater than untreated group ($p>0.05$), + significantly greater than the rest of the groups ($p<0.05$). (B) Wound images.

Overall, the encapsulated peptide presented an enhanced activity that might be due to the protective effect of the NLCs against both, chemical and enzymatic degradation. In addition, the NLCs alloweede a controlled release profile, extending the duration of the effect of the LL37 [36,37]. Moreover, in comparison to other nanoparticles loaded with LL37 previously developed [38], the NLC-LL37 allowed a topical administration, an easy, comfortable and safe route for the patient. Taking into account all these findings, it can be concluded that the topical administration of NLC-LL37 might present an interesting strategy for the treatment of chronic wounds.

In the second step of the thesis, a nanofibrous membrane dressing was developed to encapsulate the Epidermal Growth Factor (EGF). This trophic factor is a key signalling molecule in wound healing due to its effect stimulating keratinocyte and fibroblast proliferation and migration [39]. It has been proven that its exogenous application promotes wound healing, however its short half-life hampers its clinical application [40,41].

Therefore, we hypothesized that the encapsulation of EGF in nanofibrous membranes can protect the peptide from the harmful environment, moreover their structure can enhance wound healing. The nanofibrous dressing was produced by electrospinning an emulsion composed of of PLGA dissolved in hexafluoroisopropanol and an aqueous phase containing *Aloe vera* extract and EGF. The emulsion was loaded into a syringe, which needle was attached to a power supply. The high voltage charged the emulsion, creating an electrostatic repulsion that stretched the droplet of the needle ejecting it to the collector. The final nanofibers were formed during the ejection process in which the solvent was evaporated, allowing the arrival of solid nanofibers to the collector [42,43]. This setup enables the production of nanofibrous membranes composed of PLGA and *Aloe vera* (1:1) loaded with EGF (PLGA-AV-EGF membranes). *Aloe vera* was added to the formulation, since it has been reported to promote wound healing inducing fibroblast growth factor, and thereby, stimulating fibroblast's activity and proliferation and their collagen production [44,45]. To the best of our knowledge, that was the first time were electrospun membranes containing such a large proportion of *Aloe vera* were developed for wound dressing applications. In addition, nanofibrous membranes without EGF (PLGA-AV membrane) and without EGF and *Aloe vera* (PLGA membrane) were produce. The characterisation of the electrospun nanofibers is summarised in table 1 and shown in Fig. 3. The electrospinning process produces membranes composed of nonwoven uniform and randomly oriented fibres. The structure presents a great porosity (above 79%) and a high area to volume ratio, allowing cell respiration and moisture control [11].

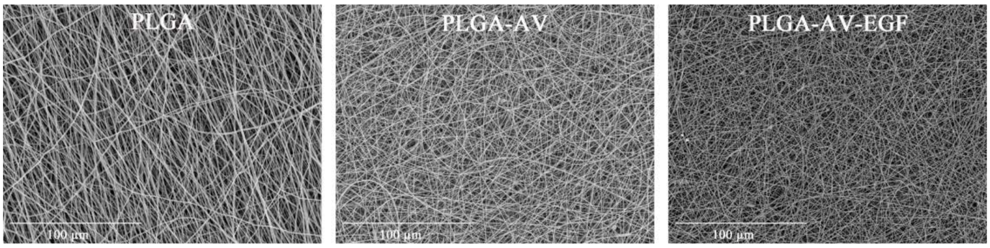


**Fig. 3.** SEM photographs of PLGA, PLGA-AV and PLGA-AV-EGF membranes. The scale bar in each image indicates 100 µm.

**Table 1.** Nanofiber characterisation: membrane porosity (%), membrane thickness (µm), nanofibers diameter (nm), tensile strength (MPa), water uptake (%), WVPR (g/m$^2$day) and peptide loading (µg/cm2). Data are expressed as the mean ± SD.

| Nanofiber composition | Membrane porosity (%) | Membrane thickness (µm) | Nanofiber diameter (nm) | Tensile strength (MPa) | Water uptake (%) | WVPR (g/m$^2$day) | Peptide loading (µg/cm$^2$) |
|---|---|---|---|---|---|---|---|
| PLGA | 79.50 ±7.42 | 59.17 ±1.83 | 561.61 ±124.28 | 3.06 ±0.35 | 218.17 ±45.03 | 1861.28 ±372.89 | - |
| PLGA-AV | 87.92 ±11.96 | 56.76 ±1.27 | 486.99 ±114.73 | 4.66 ±0.90 | 273.92 ±42.19 | 1690.09 ±190.25 | - |
| PLGA-AV-EGF | 87.52 ±6.62 | 45.92 ±0. 78 | 356.03 ±112.05 | 2.21 ±0.49 | 290.58 ±49.92 | 1907,39 ±228.82 | 9.76 ±1.75 |

The biggest differences among fibers were found in their diameter and water uptake. The addition of *Aloe vera* reduces nanofibres diameter from 561.6 ± 124.3 nm to 487 ± 114.7 nm and the addition of EGF to 356 ± 112 nm. Regarding the differences in water uptake it was found that the membranes with *Aloe vera* were able to swallow more water, suggesting that this compound enhances the hydrophilic properties of the membrane [46].

It is noteworthy that the mechanical properties, assessed under displacement control on an Instron 5848 microtester, were very similar to that of human skin, which ranged from 5.7 MPa to 12.6 MPa [47]. In addition, the water vapour permeability rate (WVPR) was within the range of commercial skin dressings (426-2047 g/$m^2$day), which suggest that the developed dressings were able to achieve an adequate moisture control [48]. To assess the WVPR, cups containing silica gel desiccant and sealed with the membranes were placed on a climatic chamber for 24 h, and the WVPR calculated weighing the assembly before and after the exposure time.

The thermal behaviour of the membranes was assessed through a differential scanning calorimetry (DSC). The obtained results showed that the electrospun PLGA presented a high degree of alignment and orientation of polymer chains, since the glass transition temperature ($T_g$) was lower in the PLGA membrane (49.84 ± 0.23 °C) than in the raw PLGA (53.85 ± 0.16 °C), as previously reported [49]. In addition, similar thermal peak were detected in the PLGA-AV and PLGA-AV-EGF electrospun membranes and the physical blend of PLGA and Aloe vera, revealing an immiscible blend morphology of this two components in the nanofibers. The peak of EGF was not observed, probably due to it small proportion into the membranes.

The *in vitro* release of the EGF loaded into the PLGA-AV-EGF membranes was tested on a Franz diffusion cell system. A humidified piece membrane of 1x1 cm was placed on the donor chamber above a nylon filter (0.45 µm pore size) and 5 ml of PBS were added to the receptor chamber. On selected time points, samples from the receptor chamber were taken and the released EGF determined through a commercial ELISA. The results showed a biphasic prolife; with an initial burst release that lasted 8 h where 35% of the drug was released, and a slower release phase were 50% of the total EGF was released on 7 days. The initial burst release was related to the surface-associated protein and was advantageous to obtain a rapid activation of the keratinocytes of the wound edge [50]. It is noteworthy that although only the 50% of EGF was released, the release may be accelerated *in vivo*, since the enzymes of the wound can lead to a faster polymer degradation [51].

Once the dressings were characterised their bioactivity was evaluated. On the one hand, the antimicrobial activity of *Aloe vera* was assessed [52], determining the inhibition zone created after placing discs of PLGA-AV and PLGA membranes on culture plates seeded with *Staphilococcus aureus* and *Staphilococcus epidermidis.* Around PLGA membranes there was not inhibition zone, highlighting that the one observed around PLGA-AV membranes was due to the *Aloe vera* . However, a bigger inhibitory zone was observed around commercial discs ambedded with *Aloe vera* solution, probably due to the immediate availability of the whole *Aloe vera* dose, as observed in the results obtained with the NLC-LL37 formulation. Moreover, nanofibrous dressings prevent microorganism entry, due to their small pore size.

On the other hand, the effect of EGF and *Aloe vera* on fibroblast proliferation was assessed, in order to determine if the electrospinning process affects their activity [53,54]. Proliferation was evaluated incubating fibroblasts with the medium released from the nanofibers for 48 h, and then measuring cell viability through a CCK-8 assay. The highest cell proliferation was achieved with PLGA-AV-EGF membranes. In fact, it was higher than incubating cells with the same concentration of free EGF, revealing the beneficial effect of the combination. In addition, an increased proliferation was observed with PLGA-AV membranes, but not with PLGA membranes. Therefore, these results suggests that the effect was caused exclusively by the EGF and the *Aloe vera*, but not by the PLGA.

Since the membranes were designed to be changed during the treatment, cells adhesion or tissue ingrowth should be prevented in order to avoid damage of the newly formed tissue or pain during the dressing removal [11]. Thereby, we decided to evaluate if cells were able to adhere to the membranes, incubating fibroblasts on their top for 24 h, and then detaching and counting the cells adhered or taking SEM photographs of them as depicted in Fig. 4A. As can be observed in the graph (Fig. 4B), cell adhesion was highly hindered by the membranes in comparison to the bottom of the plates, demonstrating their suitability as temporary wound dressings.

Finally, the efficacy of the membranes was studied using the splinted full thickness wound healing model in *db/db* mice. For that purpose, wound area reduction, reepithelisation grade, the resolution of the inflammatory process and collagen deposition were evaluated, as in the previous study. On day 4, the PLGA-AV-EGF membranes accelerated wound closure in comparison to the rest of the groups, namely, free EGF, PLGA-

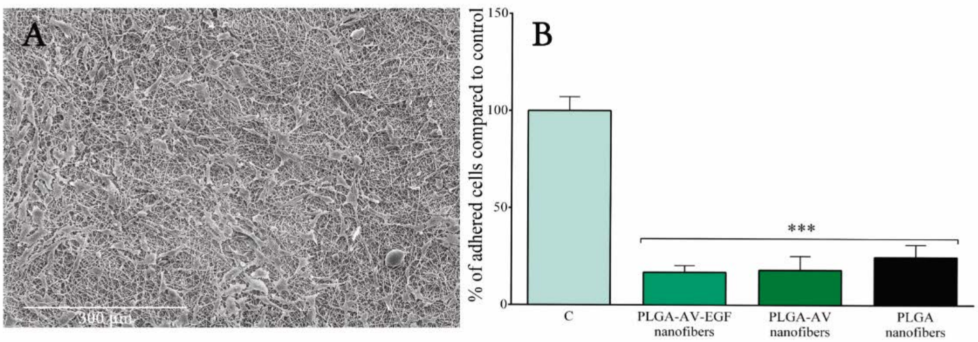


**Fig. 4.** In vitro adhesion assay. (A) SEM image of the nanofibers with cells attached. The scale bar indicates 300 µm. (B) The cell adhesion results are given as the mean ± SD of the % of cells counted in comparison to the control. *** p<0.001 comparing PLGA-AV-EGF, PLGA-AV and PLGA membranes with the control group.

AV membranes, PLGA membranes and untreated control. On day 8, the highest improvement of wound closure was achieved with PLGA-AV-EGF membranes, but PLGA-AV membranes were also able to enhance wound closure. Reepithelisation grade was also improved applying both PLGA-AV-EGF and PLGA-AV membranes, since according to the scale used to measured reepithelisation those group presented the highest value, which correspond to a complete reepithelisation with irregular thickness [33]. No differences were observed in the resolution of the inflammatory process and in collagen deposition. However, a slight tendency in agreement with the rest of the evaluated parameters was detected.

Overall, the results obtained in the *in vivo* study showed that the application of PLGA-AV-EGF membranes was more advantageous than the application of free EGF or PLGA-AV membranes. That can be partially explained by the protective effect of the nanofibrous membranes against proteases present in the wound bed, as previously reported [40,55]. In addition, the sustained release from the nanofibrous membranes extended the duration of the EGF in the wound and thus its effect was improved.

Both, the *Aloe vera* and the nanofibrous membranes themselves, were also involved in the wound healing effect. On the one hand, Aloe vera has proven to enhance wound healing, mainly by inducing fibroblast growth factor, and thus, improving their activity and proliferation [53]. On the other hand, as previously commented, the unique structure of electrospun membranes promote wound closure, allowing gas and water permeability [56]. Accordingly, the improvement of wound closure was due to the combination of the three elements, the EGF, the *Aloe vera* extract and the nanofibrous structure, leading to a dressing that might be a suitable strategy for the treatment of chronic wounds.

Taking into account that the nanofibrous membranes without EGF also promoted wound healing, in the following step, we focused on the development of a nanofibrous dressing based on PLGA and *Aloe vera,* since the lack of EGF brings a new approach to develop a medical device. In order to improve some of the membranes properties NLCs were added during the electrospinning process, assuming that the lipid component could avoid the adhesion to the wound, easing the removal of the dressing. Moreover, we hypothesize that the addition of NLCs could improve some features of the dressing, such as, handling, elasticity and occlusivity.

Nanofibrous membranes with and without NLCs (PLGA-AV-NLC and PLGA-AV) were developed to assess the effect of adding the NLCs. In this case, a PLGA with a higher molecular weight was used, since it allowed an easier incorporation of the NLCs. Therefore, their characterisation results were slightly different, as showed in table 2. Porosity values were similar to the ones obtained in the previous study, around 80%, which allows gas permeation and thus cell breathing. On the other hand, nanofibers diameter increased from about 500 nm obtained in to around 1 µm in the current one. That increment was probably due to the greater viscosity of the polymer solution prepared with the high molecular weight PLGA, since solution viscosity is critical to control the nanofibers morphology [56]. Moreover, water uptake was higher than in the previous study, about 380%, which helps to drain the exudates while retaining moisture [3,46].

**Table 2.** Dressings characterisation: nanofibers diameter (nm), membrane porosity (%), membrane thickness (µm), tensile strength (MPa), water uptake (%) and WVTR ($g/m^2 day$). Data are expressed as the mean ± SD.

| Nanofiber composition | Nanofiber diameter (µm) | Porosity (%) | Thickness (µm) | Tensile strength (MPa) | Water uptake (%) | WVTR ($g/m^2 day$) |
|---|---|---|---|---|---|---|
| PLGA-AV membrane | 1.10±0.42 | 81.55 ±1.16 | 158.03 ±17.41 | 1.69 ±0.35 | 369.06 ±28.09 | 1128.06 ±93.23 |
| PLGA-AV-NLC membrane | 0.96±0.34 | 84.23 ±0.85 | 178.04 ±42.05 | 2.61 ±0.46 | 384.32 ±35.65 | 1097.6 ±102.83 |

The thickness of the fibres was also higher than in the previous study, and moreover, it was higher in the PLGA-AV-NLC membranes than in the PLGA-AV membranes, which suggest that the incorporation of the NLCs was able to improve the handling of the membranes. The occlusivity of the membranes was also improved by the addition of NLCs, since the WVTR was slightly lower in the PLGA-AV-NLC membranes than in the membranes without NLCs. In addition, the WVTR rate value (1097.6 ± 102.83 $g/m^2$day) was within the range of commercial dressings. Finally, the tensile strength was also increased by the addition of NLCs, which makes more difficult to break or bend the dressing during it application. As observed by Thomas *et al*., the increment of tensile strength may be due to the uniform distribution of the nanoparticles, which distributes uniformly the forces, minimizing the stress concentration centres and thus easing the its transfer from the polymer matrix to the NLCs [57].

Thermal analysis of nanofibrous membranes was performed by DSC, and as in the previous study a high degree of alignment and orientation of the PLGA chains was observed, evidenced by the decrease of the $T_g$ [49]. Peaks corresponding to PLGA and NLCs and the curve pattern of AV were found in both PLGA-AV-NLC membranes and the physical blend of the components, although a slight increase in the peak of the NLCs was observed, which could suggest an interaction between the NLCs and the AV.

In the previous study, we proved that the electrospinning process did not affect the activity of the *Aloe vera*, since its antimicrobial activity and its effect on fibroblasts proliferation was maintained on the nanofibers. Therefore, in this study we analyse directly the biocompatibility of the membranes, following the method used in the previous study. We incubated fibroblasts and keratinocytes with the extracted medium of the nanofibers for 48 h, and then a CCK-8 assay was conducted to evaluate the viability. The results illustrated in Fig. 5, showed that the membranes were biocompatible with both cell lines, since the viability was above 70% in comparison to control. The results obtained with fibroblasts showed an increased viability, probably due to the proliferative effect of *Aloe vera* [45,53].

In addition to their effect on the dressing handling, the main reason to include NLCs into the nanofibers was the hypothesis that they could ease the removal of the dressing from the wound. Thereby, a cell adhesion study was performe. Membranes were placed on the bottom of a 24 well plate and fibroblasts or keratinocytes incubated on their top for 24 h. Then, the attachment was analysed by detaching and counting the cells adhered to the membranes. In addition, SEM photographs of the membranes were taken, however, cells were not visible on the images. Cell counting revealed that both membranes hindered cell adhesion in comparison to the bottom of the wells. Fibroblasts attachment was similar in both membranes, while keratinocytes adhesion was significantly lower in the

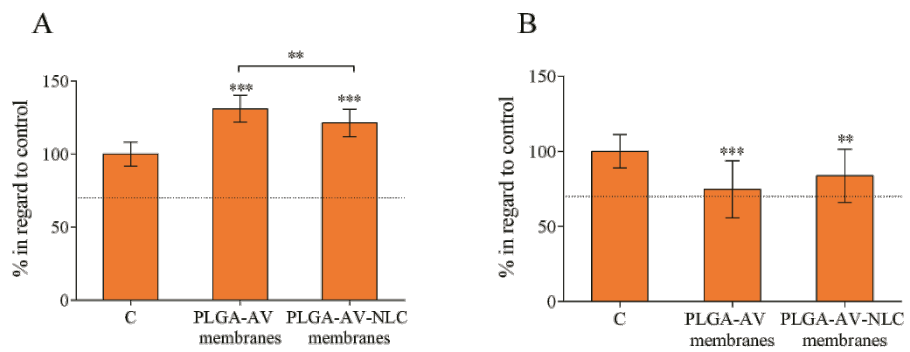


**Fig. 5.** Cell viability study. (A) CCK-8 results after culturing the membranes extracted medium with fibroblasts. *** $p<0.001$ comparing PLGA-AV-NLC and PLGA-AV membranes groups with the control group; and ** $p<0.01$ comparing PLGA-AV membranes with PLGA-AV-NLC membranes. (B) CCK-8 results after culturing the membranes extracted medium with keratinocytes. *** $p<0.001$ comparing PLGA-AV membranes group with the control group; and ** $p<0.01$ comparing PLGA-AV-NLC membranes group with the control group. Results are given as the mean % of living cells regarding to the control group ± SD.

formulation containing NLCs. Nevertheless, more studies should be performed to assess dressing attachment into wounded tissue.

As in the previous studies, the efficacy of the dressings was evaluated on a full thickness wound healing model in *db/db* mice, although some changes were introduced in respect to the other studies: animals were sacrificed at 8 and 15 days postinjury; the collagen deposition was not analysed, since it presented a great variability; and the presence of inflammatory cells was assessed through immunohistochemical studies.

Overall, both membranes achieved similar improvement in wound healing. Comparable results were obtained in wound closure and reepithelisation, as both were able to achieve a complete reepithelisation on day 15. Regarding the resolution of the inflammatory process, on day 15 only PLGA-AV membranes presented an improved outcome in comparison to the control group. On day 8, no differences were observed in the histological analysis, although the developed membranes, and especially the PLGA-AV-NLC membranes, were able to reduce the macrophage infiltration in the wound bed, which usually is augmented in rodent wound models with diabetes or impaired healing. [58,59]. Therefore, both formulations enhanced wound maduration, the PLGA-AV-NLC membranes on the early stage of healing and the PLGA-AV membranes on the later stage.

We could not observe the effect of NLCs on the removal of the dressings, since prior to their removal they were humected with PBS, in order to avoid any possible damage on newly formed tissue.

Accordingly, the PLGA-AV-NLC nanofibrous membrane might be a promising strategy as wound care dressings, since the addition of NLCs improved the handling of the membranes, achieving a similar efficacy on wound healing. Nevertheless, more studies are needed to assess their effect in dressing removal.

For the last step of the thesis we developed a bilayer dressing composed of gelatin and chitosan. Bilayer dressings represent an interesting alternative since they are able to provide a structure similar to that of human skin, with an upper protective layer resembling the epidermis, and a thicker flexible lower layer as the dermis [16]. Depending on its crosslinking degree, gelatin is able to present the characteristics required for both layers. This natural polymer has been extensively used in pharmaceutical applications due to its biocompatibility and biodegradability [60]. Its chains contain arginine-glycine-aspartic (RGD) motifs, an important sequence in the promotion of cell adhesion [61]. In addition, gelatin presents an excellent ability to absorb large volumes of water and thereby create hydrogels, which present multiple advantages to be used as wound dressings. For instance they are able to maintain an adequate moisture on the wound since they can absorb or donate water depending on their environment, they cool the wound surface and they reduce pain [62].

Thereby, two gelatin hydrofilms were developed, one of them to be the upper layer of the dressing and the other to act as the lower layer. Both layers were produced by casting lipid gels into suitable molds. To produce the upper layer, a gelatin solution was mixed with glycerol and lactose. The glycerol acted as a plasticiser and the lactose as the crosslinker, since it glycated the protein chains of gelatin in presence of heat, which is known as the Maillard reaction [63]. The obtained hydrofilm was stiff and resistant to water degradation [64]. It was designed to cover the wound, giving mechanical strength to the dressing. In addition, it needs to control moisture transmission and prevent bacterial penetration [15-17].

The lower layer was produced mixing the gelatin solution with glycerol and citric acid. The citric acid was added since it reacts with the amine groups of the protein chains, crosslinking the gelatin [65]. The resulting hydrofilm was more porous and had a great swelling ability to absorb wound exudates [15-17]. In addition, chitosan was added to the lower layer to promote the healing process, since it has shown to accelerate wound healing through several mechanism: it has antibacterial and hemostatic activity [66], it promotes the proliferation of fibroblasts and keratinocytes [67,68] and it is involved in the regulation of the inflammatory process [69].

Hydrofilms with and without glycerol and chitosan were produced, and both layers were glued together spraying ethanol on them. The effect of the crosslinking in the structure of gelatin was analysed by Fourier transform infrared (FTIR). The most notable changes on the spectra were observed in the relative intensity between the peaks at 1630 $cm^{-1}$ (C=O stretching, amide I) and 1530 $cm^{-1}$ (N-H bending amide II). In addition, measuring the amide I area %, it can be observed that in gelatin crosslinked with lactose a increment of intermolecular β-sheets ocurred, in comparison to gelatin crosslinked with citric acid. This change was also noticed in SEM analysis, since a more compact and smoother microstructure was found when crosslinking was promoted by lactose addition, as illustrated in Fig 6.

The swelling ability of the bilayer dressing and of both layers was assessed in order to compare the behaviour of the different hydrofilms (Fig. 7). The study was performed at 4 °C instead of being performed at skin temperature, because hydrofilms crosslinked

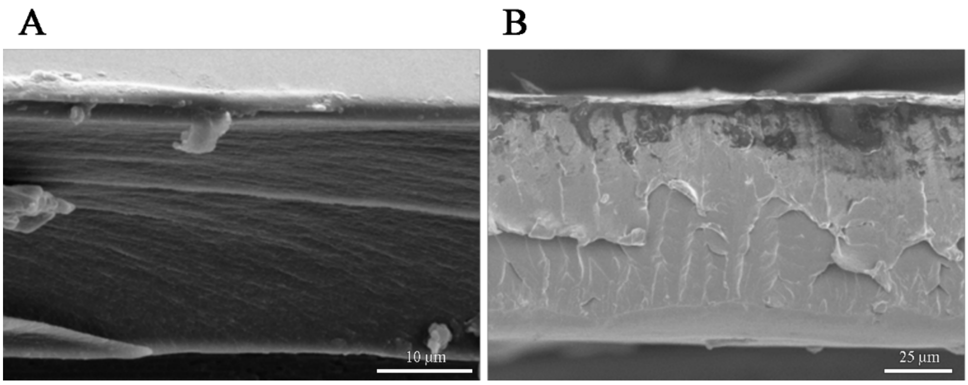


**Fig. 6.** SEM analysis. (A) Lac+ HF cross-section. (B) CA+ HF cross-section.

with citric acid lost their integrity in a warm aqueous environment. Therefore, weighed hydrofilm discs were immersed in cold PBS for determined time points, and then the excess water was dried and the wet discs weighed to measure the water uptake. As expected, water absorption was controlled by the crosslinking degree of the gelatin. Thereby, hydrofilms crosslinked with lactose had the lowest ability to absorb water, the ones crosslinked with citric acid the highest and bilayer hydrofilms presented intermediate values, since they were composed of both layers [70].

The hydrolytical stability of the hydrofilms was assessed immersing discs in cold PBS and letting them dry once they reached an equilibrium. Results showed that hydrofilms with glycerol maintained about 88% of their initial weight, while hydrofilms without glycerol maintained the 96 %. The weight lost can be easily explained by the dissolution of glycerol and the unreacted crosslinker in the aqueous medium.

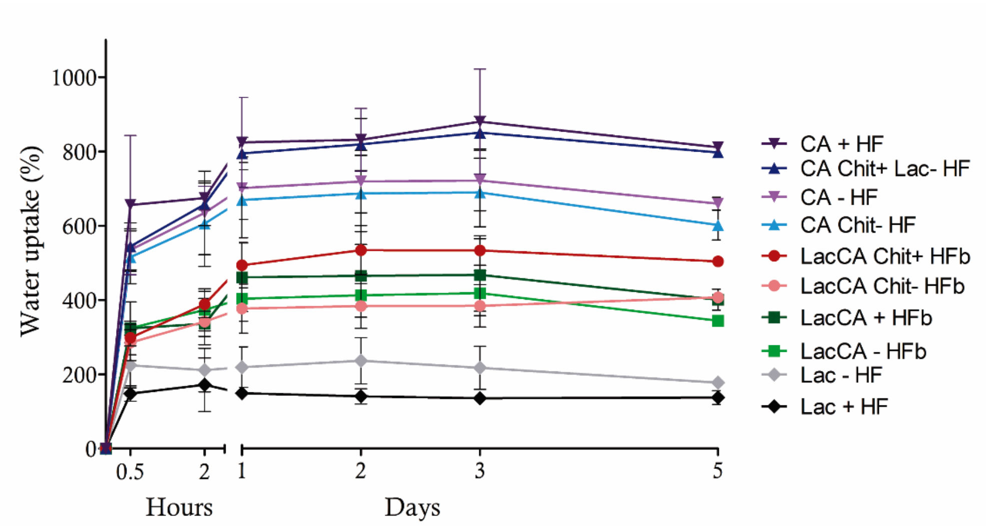


**Fig. 7.** Swelling curve. The percentage of water uptake regarding dry weight of the hydrofilms at different time points. Data are shown as mean ± SD.

Afterwards, the occlusivity of the hydrofilms was evaluated measuring the WVTR, but the method used was slightly different from the method used to analyse the nanofibrous dressings. Franz diffusion cells were filled with water and the receptor arm sealed with parafilm. The hydrofilms were placed between both compartments, this way water vapour could only leave the system through the hydrofilms. The difference in weight of the assembly after 48 hours was recorded to determine the WVTR. The occlusivity of the hydrofilms crosslinked with citric acid was not evaluated, since wet hydrofilms loss the ability to seal the aperture between both compartments. The results of the bilayer hydrofilms showed that they could present an adequate control of moisture into the wounds, since their WVTR value was within the range of commercial dressings aforementioned. The hydrofilms crosslinked with lactose, however, showed a higher WVTR value, which indicated a lower occlusivity. That higher permeability could be explained by the lower thickness of those hydrofilms [71].

As in the previous studies, once the formulations were characterised, their biocompatibility was assessed, following the guidelines of the ISO 10992-5:2009 for biological evaluation of medical devices. That guideline proposes the direct and the indirect cytotoxicity assays, but we could not perform the direct assay, since hydrofilms crosslinked with citric acid were partially dissolved at 37°C, hampering the removal of the hydrofilms to perform the CCK-8 assay. Therefore, we only performed the indirect assay, incubating together the extracted medium of the hydrofilms with fibroblasts for 24 hours and then measuring cell viability by a CCK-8 assay. All the hydrofilms presented a viability above 70 % in the indirect assay, demonstrating that they were biocompatible. In addition, it was demonstrated that there was no need of a previous conditioning step, since similar viability results were obtained dialyzing hydrofilms for 72 h and hydrating them for 15 min prior to conduct the assay.

Finally, the efficacy of the dressings on wound healing was analysed. The assay was only conducted on hydrofilms without glycerol since the characterisation results showed that its use as plasticiser was expendable, since it dissolved in the hydration step. Among bilayer hydrofilms, the only one evaluated was the one containing chitosan in the lower layer, to assess the effect of chitosan in wound healing, since hydrofilms with and without chitosan presented similar characteristics. In addition, monolayer hydrofilms crosslinked with lactose were evaluated, but not the ones crosslinked with citric acid because they did not have enough structural stability to be used as dressings on their own.

In the current study, the efficacy was not evaluated using the *db/db* mice model; instead we used a human skin *ex vivo* model, in order to reduce the use of animals in research. Besides of the ethical concerns, using human skin instead of animal skin, the differences in wound healing among species can be avoided [72]. Briefly, skin explants from routine elective surgery were cut in 6 mm diameter biopsies and full thickness excisional wounds of 3 mm were made on their centre. Afterwards, the biopsies were transferred to transwell inserts and cultured in 24 well plates, leaving the epidermis exposed to the air-liquid interphase as depicted in Fig. 8. Hydrated hydrofilms were applied on days 1 and 4, and the explants cultured for 8 days.

On day 4 and 8, LDH assay was carried out to analyse the viability of the biopsies. The viability was maintained above 70% in all the time points and tested groups, which means that the cells of the biopsies remained alive, demonstrating the reliability of the results obtained in the study. In addition, it corroborates the results obtained in the

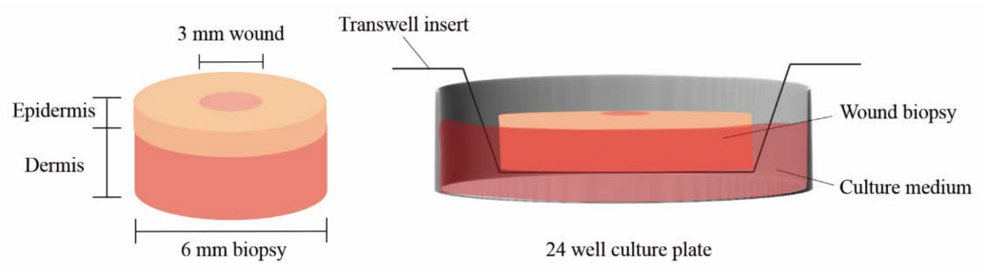


**Fig 8.** *Ex vivo* assay scheme.

cytotoxicity assay carried out in fibroblasts, demonstrating the biocompatibility of the hydrofilms in a more complex structure than a monolayer single cell culture.

In order to assess the efficacy of the hydrofilms, wound healing was evaluated from histological and immunohistochemical analyses performed on biopsies sections. Overall, similar results were obtained in the groups treated with the hydrofilms and in the untreated groups, since no differences were observed in wound closure, cellular proliferation, wound contraction and the expression of new undifferentiated keratinocytes. Nevertheless, collagen deposition was decreased in the group treated with the gelatin hydrofilm crosslinked with lactose and the expression of mature keratinocytes was hindered in the group treated with the bilayer hydrofilm containing chitosan. Those negative results could be explained by the overly moist environment created on the wound, due to the high humidity of the incubator and the ability of the hydrofilms to absorb a portion of the culture medium. Therefore, the hydrofilms, and specially the gelatin hydrofilms crosslinked with citric acid, should be optimised in order to create a more adequate environment for healing.

Accordingly, the results obtained in the *ex vivo* assay, showed the suitability of the model to assess wound healing, as a screening method prior to conduct an *in vivo* study. In addition, it showed that the developed hydrofilms could be useful as wound dressings. In order to improve the efficacy of the hydrofilms, in future studies active molecules such as growth factors will be encapsulated or immobilised into the lower layer.

In summary, considering all the results obtained in this thesis, we can conclude that with this work we have taken a step forward in the development of new strategies for the treatment of chronic wounds. In these years, we have developed different therapeutic approaches to promote healing on chronic wounds, such as NCLs containing the LL37 peptide, PLGA-*Aloe vera* nanofibrous membranes containing EGF or NLCs and bilayer dressings based on gelatin and chitosan.

## REFERENCES

[1] K. Järbrink, G. Ni, H. Sönnergren, A. Schmidtchen, C. Pang, R. Bajpai, J. Car, The humanistic and economic burden of chronic wounds: a protocol for a systematic review, Syst. Rev. 6 (2017). doi: 10.1186/s13643-016-0400-8.

[2] V.W. Wong, G.C. Gurtner, Tissue engineering for the management of chronic wounds: current concepts and future perspectives, Exp. Dermatol. 21 (2012) 729-734. doi: 10.1111/j.1600-0625.2012.01542.x.

[3] J. Posnett, F. Gottrup, H. Lundgren, G. Saal, The resource impact of wounds on health-care providers in Europe, J. Wound Care 18 (2009) 154. doi: 10.12968/jowc.2009.18.4.41607.

[4] G. Han, R. Ceilley, Chronic Wound Healing: A Review of Current Management and Treatments, Adv. Ther. 34 (2017) 599-610. doi: 10.1007/s12325-017-0478-y.

[5] C.K. Sen, G.M. Gordillo, S. Roy, R. Kirsner, L. Lambert, T.K. Hunt, F. Gottrup, G.C. Gurtner, M.T. Longaker, Human skin wounds: a major and snowballing threat to public health and the economy, Wound Repair Regen. 17 (2009) 763-771. doi: 10.1111/j.1524-475X.2009.00543.x.

[6] P.S. Briquez, J.A. Hubbell, M.M. Martino, Extracellular matrix-inspired growth factor delivery systems for skin wound healing, Adv. Wound Care (New Rochelle) 4 (2015) 479-489. doi: 10.1089/wound.2014.0603.

[7] T. Velnar, T. Bailey, V. Smrkolj, The wound healing process: an overview of the cellular and molecular mechanisms, J. Int. Med. Res. 37 (2009) 1528-1542. doi: 10.1177/147323000903700531.

[8] G. Gainza, S. Villullas, J.L. Pedraz, R.M. Hernandez, M. Igartua, Advances in drug delivery systems (DDSs) to release growth factors for wound healing and skin regeneration, Nanomedicine 11 (2015) 1551-1573. doi: //dx.doi.org/10.1016/j.nano.2015.03.002.

[9] N.B. Menke, K.R. Ward, T.M. Witten, D.G. Bonchev, R.F. Diegelmann, Impaired wound healing, Clin. Dermatol. 25 (2007) 19-25. doi: //dx.doi.org/10.1016/j.clindermatol.2006.12.005.

[10] J. Pardeike, K. Schwabe, R.H. Müller, Influence of nanostructured lipid carriers (NLC) on the physical properties of the Cutanova Nanorepair Q10 cream and the in vivo skin hydration effect, Int. J. Pharm. 396 (2010) 166-173. doi: //dx.doi.org/10.1016/j.ijpharm.2010.06.007.

[11] M. Abrigo, S.L. McArthur, P. Kingshott, Electrospun nanofibers as dressings for chronic wound care: advances, challenges, and future prospects, Macromol. Biosci. 14 (2014) 772-792. doi: 10.1002/mabi.201300561.

[12] L. Pachuau, Recent developments in novel drug delivery systems for wound healing, Expert. Opin. Drug Deliv. 12 (2015) 1895-1909. doi: 10.1517/17425247.2015.1070143.

[13] C.P. Barnes, S.A. Sell, E.D. Boland, D.G. Simpson, G.L. Bowlin, Nanofiber technology: Designing the next generation of tissue engineering scaffolds, Adv. Drug Deliv. Rev. 59 (2007) 1413-1433. doi: //dx.doi.org/10.1016/j.addr.2007.04.022.

[14] N. Bhattarai, D. Edmondson, O. Veiseh, F.A. Matsen, M. Zhang, Electrospun chitosan-based nanofibers and their cellular compatibility, Biomaterials 26 (2005) 6176-6184. doi: //dx.doi.org/10.1016/j.biomaterials.2005.03.027.

[15] R.A. Franco, Y. Min, H. Yang, B. Lee, Fabrication and biocompatibility of novel bilayer scaffold for skin tissue engineering applications, J. Biomater. Appl. 27 (2013) 605-615. doi: 10.1177/0885328211416527.

[16] M. Zilberman, D. Egozi, M. Shemesh, A. Keren, E. Mazor, M. Baranes-Zeevi, N. Goldstein, I. Berdicevsky, A. Gilhar, Y. Ullmann, Hybrid wound dressings with controlled release of antibiotics: Structure-release profile effects and in vivo study in a guinea pig burn model, Acta Biomater. 22 (2015) 155-163. doi: 10.1016/j.actbio.2015.04.029.

[17] L. Ding, X. Shan, X. Zhao, H. Zha, X. Chen, J. Wang, X. Wang, C. Cai, G. Li, J. Hao, G. Yu, Spongy bilayer dressing composed of chitosan–Ag nanoparticles and chitosan–Bletilla striata polysaccharide for wound healing applications, Carbohydr. Polym. 157 (2017) 1538-1547. doi: 10.1016/j.carbpol.2016.11.040.

[18] R. Koczulla, G. von Degenfeld, C. Kupatt, F. Krötz, S. Zahler, T. Gloe, K. Issbrücker, P. Unterberger, M. Zaiou, C. Lebherz, A. Karl, P. Raake, A. Pfosser, P. Boekstegers, U. Welsch, P.S. Hiemstra, C. Vogelmeier, R.L. Gallo, M. Clauss, R. Bals, An angiogenic role for the human peptide antibiotic LL-37/hCAP-18., J Clin Invest 111 (2003) 1665-1672.

[19] S.B. Coffelt, S.L. Tomchuck, K.J. Zwezdaryk, E.S. Danka, A.B. Scandurro, Leucine Leucine-37 Uses Formyl Peptide Receptor–Like 1 to Activate Signal Transduction Pathways, Stimulate Oncogenic Gene Expression, and Enhance the Invasiveness of Ovarian Cancer Cells, Molecular Cancer Research 7 (2009) 907-915. doi: 10.1158/1541-7786.MCR-08-0326.

[20] K. Hase, L. Eckmann, J.D. Leopard, N. Varki, M.F. Kagnoff, Cell Differentiation Is a Key Determinant of Cathelicidin LL-37/Human Cationic Antimicrobial Protein 18 Expression by Human Colon Epithelium, Infection and Immunity 70 (2002) 953-063. doi: 10.1128/IAI.70.2.953-963.2002.

[21] R.C. Anderson, M. Rehders, P.L. Yu, Antimicrobial fragments of the pro-region of cathelicidins and other immune peptides, Biotechnol. Lett. 30 (2008) 813-818.

[22] Y. Kai-Larsen, B. Agerberth, The role of the multifunctional peptide LL-37 in host defense, Front. Biosci 13 (2008) 3760-3767.

[23] J. Turner, Y. Cho, N. Dinh, A.J. Waring, R.I. Lehrer, Activities of LL-37, a Cathelin-Associated Antimicrobial Peptide of Human Neutrophils, Antimicrobial Agents and Chemotherapy 42 (1998) 2206-2214.

[24] R. Ramos, J.P. Silva, A.C. Rodrigues, R. Costa, L. Guardão, F. Schmitt, R. Soares, M. Vilanova, L. Domingues, M. Gama, Wound healing activity of the human antimicrobial peptide LL37, Peptides 32 (2011) 1469-1476. doi: //dx.doi.org/10.1016/j.peptides.2011.06.005.

[25] Y. Rosenfeld, N. Papo, Y. Shai, Endotoxin (Lipopolysaccharide) Neutralization by Innate Immunity Host-Defense Peptides: peptide properties ad plausible modes of action, Journal of Biological Chemistry 281 (2006) 1636-1643. doi: 10.1074/jbc.M504327200.

[26] A.R. Siddiqui, J.M. Bernstein, Chronic wound infection: Facts and controversies, Clin. Dermatol. 28 (2010) 519-526. doi: //dx.doi.org/10.1016/j.clindermatol.2010.03.009.

[27] M. Seaton, A. Hocking, N.S. Gibran, Porcine Models of Cutaneous Wound Healing, ILAR Journal 56 (2015) 127-138. doi: 10.1093/ilar/ilv016.

[28] P. Losi, E. Briganti, C. Errico, A. Lisella, E. Sanguinetti, F. Chiellini, G. Soldani, Fibrin-based scaffold incorporating VEGF- and bFGF-loaded nanoparticles stimulates wound healing in diabetic mice, Acta Biomater. 9 (2013) 7814-7821. doi: //dx.doi.org/10.1016/j.actbio.2013.04.019.

[29] Y. Guillemin, D. Le Broc, C. Ségalen, E. Kurkdjian, J.N. Gouze, Efficacy of a collagen-based dressing in an animal model of delayed wound healing, J. Wound Care 25 (2016) 406-413. doi: 10.12968/jowc.2016.25.7.406.

[30] R.C. Fang, Z.B. Kryger, D.W. Buck II, M. De La Garza, R.D. Galiano, T.A. Mustoe, Limitations of the db/db mouse in translational wound healing research: Is the NONcNZO10 polygenic mouse model superior?, Wound Repair Regen. 18 (2010) 605-613. doi: 10.1111/j.1524-475X.2010.00634.x.

[31] V.I. Tkalcevic, S. Cužic, M.J. Parnham, I. Pašalic, K. Brajša, Differential Evaluation of Excisional Non-occluded Wound Healing in db/db Mice, Toxico. Pathol. 37 (2009) 183-192. doi: 10.1177/0192623308329280.

[32] J. Michaels, S.S. Churgin, K.M. Blechman, M.R. Greives, S. Aarabi, R.D. Galiano, G.C. Gurtner, db/db mice exhibit severe wound-healing impairments compared with other murine diabetic strains in a silicone-splinted excisional wound model, Wound Repair Regen. 15 (2007) 665-670. doi: 10.1111/j.1524-475X.2007.00273.x.

[33] U.K. Sinha, L.A. Gallagher, Effects of Steel Scalpel, Ultrasonic Scalpel, CO2 Laser, and Monopolar and Bipolar Electrosurgery on Wound Healing in Guinea Pig Oral Mucosa, Laryngoscope 113 (2003) 228-236. doi: 10.1097/00005537-200302000-00007.

[34] R. Cotran, G.K. Kumar, T. Collins, Reparación de los tejidos: proliferacion celular, fibrosis y curaicón de las heridas (2000) 95-120.

[35] P. Gál, T. Toporcer, B. Vidinský, M. Mokrý, M. Novotný, R. Kilík, K. Smetana, T. Gál, J. Sabo, Early changes in the tensile stregnth and morphology of primary sutured skin wounds in rats, Folia Biol. (Praha) 52 (2006) 109-115.

[36] M. Schäfer-Korting, W. Mehnert, H. Korting, Lipid nanoparticles for improved topical application of drugs for skin diseases, Adv. Drug Deliv. Rev. 59 (2007) 427-443. doi: //dx.doi.org/10.1016/j.addr.2007.04.006.

[37] J. Pardeike, A. Hommoss, R.H. Müller, Lipid nanoparticles (SLN, NLC) in cosmetic and pharmaceutical dermal products, Int. J. Pharm. 366 (2009) 170-184. doi: //dx.doi.org/10.1016/j.ijpharm.2008.10.003.

[38] K.K. Chereddy, C. Her, M. Comune, C. Moia, A. Lopes, P.E. Porporato, J. Vanacker, M.C. Lam, L. Steinstraesser, P. Sonveaux, H. Zhu, L.S. Ferreira, G. Vandermeulen, V. Préat, PLGA nanoparticles loaded with host defense peptide LL37 promote wound healing, J. Control Release 194 (2014) 138-147. doi: //dx.doi.org/10.1016/j.jconrel.2014.08.016.

[39] R.J. Bodnar, Epidermal Growth Factor and Epidermal Growth Factor Receptor: The Yin and Yang in the Treatment of Cutaneous Wounds and Cancer, Adv. Wound Care (New Rochelle) 2 (2013) 24-29. doi: 10.1089/wound.2011.0326.

[40] J.S. Choi, K.W. Leong, H.S. Yoo, *In vivo* wound healing of diabetic ulcers using electrospun nanofibers immobilized with human epidermal growth factor (EGF), Biomaterials 29 (2008) 587-596. doi: //dx.doi.org/10.1016/j.biomaterials.2007.10.012.

[41] G. Gainza, D.C. Bonafonte, B. Moreno, J.J. Aguirre, F.B. Gutierrez, S. Villullas, J.L. Pedraz, M. Igartua, R.M. Hernandez, The topical administration of rhEGF-loaded nanostructured lipid carriers (rhEGF-NLC) improves healing in a porcine full-thickness excisional wound model, J. Control Release 197 (2015) 41-47. doi: //dx.doi.org/10.1016/j.jconrel.2014.10.033.

[42] M. Liu, X. Duan, Y. Li, D. Yang, Y. Long, Electrospun nanofibers for wound healing, Mater. Sci. Eng. C Mater. Biol. Appl. 76 (2017) 1413-1423. doi: 10.1016/j.msec.2017.03.034.

[43] H.P. Felgueiras, M.T.P. Amorim, Functionalization of electrospun polymeric wound dressings with antimicrobial peptides, Colloids Surf. B Biointerfaces 156 (2017) 133-148. doi: //doi.org/10.1016/j.colsurfb.2017.05.001.

[44] S. Choi, M. Chung, A review on the relationship between aloe vera components and their biologic effects, Semin. Integr. Med. 1 (2003) 53-62. doi: //dx.doi.org/10.1016/S1543-1150(03)00005-X.

[45] S.A. Hashemi, S.A. Madani, S. Abediankenari, The Review on Properties of Aloe Vera in Healing of Cutaneous Wounds, Biomed. Res. Int. 2015 (2015) 714216. doi: 10.1155/2015/714216.

[46] S. Son, R. Franco, S. Bae, Y. Min, B. Lee, Electrospun PLGA/gelatin fibrous tubes for the application of biodegradable intestinal stent in rat model, J. Biomed. Mater. Res. 101B (2013) 1095-1105. doi: 10.1002/jbm.b.32923.

[47] C. Jacquemoud, K. Bruyere-Garnier, M. Coret, Methodology to determine failure characteristics of planar soft tissues using a dynamic tensile test, J. Biomech. 40 (2007) 468-475. doi: //dx.doi.org/10.1016/j.jbiomech.2005.12.010.

[48] Y. Tu, M. Zhou, Z. Guo, Y. Li, Y. Hou, D. Wang, L. Zhang, Preparation and characterization of thermosensitive artificial skin with a Sandwich structure, Mater. Lett. 147 (2015) 4-7. doi: //dx.doi.org/10.1016/j.matlet.2015.01.163.

[49] H. Fouad, T. Elsarnagawy, F.N. Almahjdi, K.A. Khalil, Preparation and in vitro thermo-mechanical characterization of electrospun PLGA nanofibers for soft and hard tissue replacement, Int. J. Electrochem. Sci. 8 (2013) 2293-2304.

[50] A. Schneider, X.Y. Wang, D.L. Kaplan, J.A. Garlick, C. Egles, Biofunctionalized electrospun silk mats as a topical bioactive dressing for accelerated wound healing, Acta Biomater. 5 (2009) 2570-2578. doi: //dx.doi.org/10.1016/j.actbio.2008.12.013.

[51] S. Fredenberg, M. Wahlgren, M. Reslow, A. Axelsson, The mechanisms of drug release in poly(lactic-co-glycolic acid)-based drug delivery systems—A review, Int. J. Pharm. 415 (2011) 34-52. doi: //dx.doi.org/10.1016/j.ijpharm.2011.05.049.

[52] S. Ghayempour, M. Montazer, M. Mahmoudi Rad, Encapsulation of Aloe Vera extract into natural Tragacanth Gum as a novel green wound healing product, Int. J. Biol. Macromol. 93, Part A (2016) 344-349. doi: //dx.doi.org/10.1016/j.ijbiomac.2016.08.076.

[53] M.D. Boudreau, F.A. Beland, An evaluation of the biological and toxicological properties of Aloe barbadensis (miller), Aloe vera., J. Environ. Sci. Health C Environ. Carcinog. Ecotoxicol. Rev. 24 (2006) 103-154. doi: 10.1080/10590500600614303.

[54] G. Gainza, W.S. Chu, R.H. Guy, J.L. Pedraz, R.M. Hernandez, B. Delgado-Charro, M. Igartua, Development and in vitro evaluation of lipid nanoparticle-based dressings for topical treatment of chronic wounds, Int. J. Pharm. 490 (2015) 404-411. doi: //dx.doi.org/10.1016/j.ijpharm.2015.05.075.

[55] H. Lai, C. Kuan, H. Wu, J. Tsai, T. Chen, D. Hsieh, T. Wang, Tailored design of electrospun composite nanofibers with staged release of multiple angiogenic growth factors for chronic wound healing, Acta Biomater. 10 (2014) 4156-4166. doi: //dx.doi.org/10.1016/j.actbio.2014.05.001.

[56] S. Shahverdi, M. Hajimiri, M.A. Esfandiari, B. Larijani, F. Atyabi, A. Rajabiani, A.R. Dehpour, A.A. Gharehaghaji, R. Dinarvand, Fabrication and structure analysis of poly(lactide-co-glycolic acid)/silk fibroin hybrid scaffold for wound dressing applications, Int. J. Pharm. 473 (2014) 345-355. doi: //dx.doi.org/10.1016/j.ijpharm.2014.07.021.

[57] R. Thomas, K. Soumya, J. Mathew, E. Radhakrishnan, Electrospun Polycaprolactone Membrane Incorporated with Biosynthesized Silver Nanoparticles as Effective Wound Dressing Material, Appl. Biochem. Biotechnol. 176 (2015) 2213-2224. doi: 10.1007/s12010-015-1709-9.

[58] Tsubame Nishikai-Yan Shen, Shigeyuki Kanazawa, Makiko Kado, Kayoko Okada, Lin Luo, Ayato Hayashi, Hiroshi Mizuno, Rica Tanaka, Interleukin-6 stimulates Akt and p38 MAPK phosphorylation and fibroblast migration in non-diabetic but not diabetic mice, PLoS One 12 (2017) e0178232. doi: 10.1371/journal.pone.0178232.

[59] J. Yeh, L. Yeh, S. Jung, T. Chang, H. Wu, T. Shiu, C. Liu, W.W. Kao, P. Chu, Impaired skin wound healing in lumican-null mice, Br. J. Dermatol. 163 (2010) 1174. doi: 10.1111/j.1365-2133.2010.10008.x.

[60] A.O. Elzoghby, Gelatin-based nanoparticles as drug and gene delivery systems: Reviewing three decades of research, J. Control. Release 172 (2013) 1075-1091. doi: 10.1016/j.jconrel.2013.09.019.

[61] H. Wang, O.C. Boerman, K. Sariibrahimoglu, Y. Li, J.A. Jansen, S.C.G. Leeuwenburgh, Comparison of micro- vs. nanostructured colloidal gelatin gels for sustained delivery of osteogenic proteins: Bone morphogenetic protein-2 and alkaline phosphatase, Biomaterials 33 (2012) 8695-8703. doi: 10.1016/j.biomaterials.2012.08.024.

[62] D. Eisenbud, H. Hunter, L. Kessler, K. Zulkowski, Hydrogel wound dressings: where do we stand in 2003?, Ostomy Wound Manage. 49 (2003) 52.

[63] A. Etxabide, M. Urdanpilleta, P. Guerrero, K. de la Caba, Effects of cross-linking in nanostructure and physicochemical properties of fish gelatins for bio-applications, React. Funct. Polym. 94 (2015) 55-62. doi: 10.1016/j.reactfunctpolym.2015.07.006.

[64] A. Etxabide, C. Vairo, E. Santos-Vizcaino, P. Guerrero, J.L. Pedraz, M. Igartua, K. de la Caba, R.M. Hernandez, Ultra thin hydro-films based on lactose-crosslinked fish gelatin for wound healing applications, Int. J. Pharm. 530 (2017) 455-467. doi: 10.1016/j.ijpharm.2017.08.001.

[65] A. Oryan, A. Kamali, A. Moshiri, H. Baharvand, H. Daemi, Chemical crosslinking of biopolymeric scaffolds: Current knowledge and future directions of crosslinked engineered bone scaffolds, Int. J. Biol. Macromol. 107 (2018) 678-688. doi: 10.1016/j.ijbiomac.2017.08.184.

[66] M.B. Dreifke, A.C. Jayasuriya, A.A. Jayasuriya, Current wound healing procedures and potential care, Mater. Sci. Eng. C Mater. Biol. Appl.   48 (2015) 651-662. doi: 10.1016/j.msec.2014.12.068.

[67] G.I. Howling, P.W. Dettmar, P.A. Goddard, F.C. Hampson, M. Dornish, E.J. Wood, The effect of chitin and chitosan on the proliferation of human skin fibroblasts and keratinocytes in vitro, Biomaterials 22 (2001) 2959-2966. doi: 10.1016/S0142-9612(01)00042-4.

[68] A.K. Azad, N. Sermsintham, S. Chandrkrachang, W.F. Stevens, Chitosan membrane as a wound-healing dressing: Characterization and clinical application, J. Biomed. Mater. Res. B Appl. Biomater. 69B (2004) 216-222. doi: 10.1002/jbm.b.30000.

[69] R.M. Baxter, T. Dai, J. Kimball, E. Wang, M.R. Hamblin, W.P. Wiesmann, S.J. McCarthy, S.M. Baker, Chitosan dressing promotes healing in third degree burns in mice: Gene expression analysis shows biphasic effects for rapid tissue regeneration and decreased fibrotic signaling, J. Biomed. Mater. Res. A 101A (2013) 340-348. doi: 10.1002/jbm.a.34328.

[70] A. Saarai, V. Kasparkova, T. Sedlacek, P. Saha, On the development and characterisation of crosslinked sodium alginate/gelatine hydrogels, J. Mech. Behav. Biomed. Mater.   18 (2013) 152-166. doi: 10.1016/j.jmbbm.2012.11.010.

[71] V. Morillon, F. Debeaufort, G. Blond, M. Capelle, A. Voilley, Factors Affecting the Moisture Permeability of Lipid-Based Edible Films: A Review, Crit. Rev. Food Sci. Nutr. 42 (2002) 67-89. doi: 10.1080/10408690290825466.

[72] S.H. Mathes, H. Ruffner, U. Graf-Hausner, The use of skin models in drug development, Adv. Drug Deliv. Rev. 69-70 (2014) 81-102. doi: 10.1016/j.addr.2013.12.006.

# Conclusions

On the basis of the results obtained in the experimental studies of this Doctoral Thesis, the following conclusions were derived:

1. LL37 was successfully encapsulated into NLCs, achieving suitable characteristics for wound healing applications and maintaining the activity of the peptide after the encapsulation process.

2. The topical administration of NLC-LL37 significantly improved wound healing in a full thickness wound model in *db/db* mice in comparison to the same concentration of LL37 in solution; in terms of wound closure, reepithelisation grade and restoration of the inflammatory process.

3. The developed nanofibrous membranes composed of PLGA and *Aloe vera* containing EGF showed adequate characteristics to be used as wound dressings. In addition, the EGF and the *Aloe vera* remained active after the electrospinning process and they accelerated significantly wound closure and reepithelisation in a full thickness wound model carried out in *db/db* mice.

4. The incorporation of NLCs to the PLGA and *Aloe vera* nanofibrous dressings improved their handling. Those membranes were also able to improve wound healing but in a lesser extent.

5. Bilayer gelatin and chitosan dressings were developed using lactose or citric acid as crosslinkers to prepare a resistant upper layer and a porous lower layer, respectively. The developed dressings presented suitable characteristics to be used as a wound dressings, and their biocompatibility was proven *ex vivo*.

# EUSKARAZKO BERTSIOA

# Sarrera

## Orbaintzean erabiltzeko nanoteknologian oinarritutako askatze sistemak, zeintzuk hazkuntza faktoreak edo bestelako molekula endogenoak kapsularatuta dituzten


**SARRERA**

Hazkuntza Faktoreen (*Growth Factor* edo GF) eta bestelako molekula endogenoen (intsulina, intsulinaren antzeko GF-1, zelula estromaletatik eratorritako faktorea, LL37, hesteko peptide basoaktiboa, heparina, melatonina, lipokalina, serpin-A1 eta β-estradiola) administrazio topikoak zauri kronikoen orbaintzea hobetzen dutela frogatuta dago. Dena den, haien *in vivo* egonkortasun txikia dela eta, administrazio topikoa hobetu beharra dago dosiari, askatze sistemari eta segurtasunari dagokionez. Horren harira, Farmakoak Askatzeko Sistema (*Drug Delivery System* edo DDS) berriak erabili izan dira, izan ere, DDSak farmakoak era lokalizatu eta kontrolatuan askatzeko gai dira, zaurian dauden proteasetaz babestuz. Haien artean, nanoteknologian oinarritutako DDSak aipagarriak dira, besteak beste, mikro edo nanopartikula polimerikoak, nanopartikula lipidikoak eta nanozuntzezko mintzak. Berrikuspen honen helburua DDS hauei buruzko ikuspegi orokor bat eskaintzea da. Horretaz gain, berrikuspenak GFek zaurietan duten eginkizunari eta DDSetan erabilitako biomaterial ohikoenei buruzko ideia bat ematen du ere. Formulazio horiek abantaila ugari dituzte, hala nola, farmakoaren babesa, biokonpatibilitate ona, kontrolatutako edo luzatutako askapena, farmako karga handia eta ezaugarri mekaniko onak. Orokorrean, GFen kapsularatzea nanoteknologian oinarritutako DDSen barne potentzial handia erakutsi du zauri kronikoen orbaintzerako.

Zauri kronikoak erronka bat bilakatzen ari dira praktika klinikoan, nahiz eta patologia oso arrunta diren. Izatez, 2012. urtean AEBan gutxi gorabehera 6.5 milioi pertsonek zauri kronikoak pairatu zituzten, eta 25 bilioi dolar gastatu ziren zaurien orbaintzearekin harremandutako arazoetan. Europan, zaurien zainketak batezbesteko 6.000-10.000 € balio du pertsona eta urteko, eta gastu horiek honakoei lotuta daude: erizaintza denborari, ospitalizazioei, zauri apposituen aldaketei eta zaurien infekzioei [1,2]. Gainera, uste da biztanleriaren %1-2-ak zauri kronikoak jasango dituela bizitzan zehar. Izan ere, zauri hauen intzidentzia handitzen ari da, arrisku handiko populazioaren igoeraren ondorioz, hauen artean, pertsona diabetiko, zahar, erretzaile eta obesoak daudelarik [3-5].

Gaur egungo terapiek ezin dute orbaintze efektibo bat bermatu, eta ondorioz, sendaketa denbora asko luzatzen da eta berragerpenak ohikoak dira. Hori dela eta, zauriak era eraginkorrean eta denbora laburrean sendatuko dituen tratamendu bat garatzea beharrezkoa bilakatu da. Zentzu horretan, tratamendu berrien bilaketan eta egungo tratamenduen hobekuntzan ahalegin esanguratsuak egin dira, horien artean, hazkuntza faktoreen (*Growth Factor* edo GF) eta bestelako konposatu endogenoen administrazioa dagoelarik. GFen tratamendua hobetzeko estrategia itxaropentsu bat farmakoak askatzeko sistema (*drug delivery system* edo DDS) berrien garapena da, GFak modu kontrolatu eta lokalean lagatzeko [6].

Berrikuspen honen helburua bi baldintza hauek betetzen dituzten DDSei buruzko ikuspegi orokor bat eskaintzea da: modu kontrolatuan orbaintzerako GFak edo bestelako konposatu endogenoak askatzea eta nanoteknologian oinarrituta egotea. Horien artean, mikro- eta nanopartikula (MP/NP) polimerikoei, nanopartikula lipidikoei eta nanozuntzezko egiturei buruz arituko da zehazki. Horretaz gain, berrikuspenean DDSetan erabilitako biomaterial ohikoenak aipatzen dira.

## 1. Hazkuntza faktoreen eta bestelako molekula endogenoen eginkizuna zaurien orbaintzean

Fisiologikoki, zauriak era antolatu eta eraginkor batean orbaintzen dira, zeinean 4 fase bereizi baina gainjarri dauden: hemostasia, hantura, proliferazioa eta birmoldatzea, 1. irudian ikus daitekeen bezala [7]. Prozesu hau oso estuki araututa egon behar du, orbaintzea ahalbidetzen duen ingurune molekular orekatu bat lortzeko. Erregulazioa GF eta zitokina ugariren menpe dago, zeinek seinale sare konplexu bat osatzen duten itu zelulen hazkuntza, desberdintzea eta metabolismoa aldatzeko [8,9]. GFak haien ekintza betetzeko hartzaile espezifikoetara lotzen dira, zenbait ur-jauzi molekularren aktibazioa eraginez [10,11].

Hala eta guztiz ere, zenbait kasutan zauriak ez dira gai izaten orbaintze prozesu normalaren faseetan zehar igarotzeko, orbaintze denbora luzatuz eta maiz zauriaren berragerpena eraginez. Horren adibide dira, ultzera diabetikoak, baskularrak edo presio-ultzerak [3,12,13]. Zauri kroniko horien fisiopatologiak zenbait desberdintasun ditu zauri akutuenekin alderatuz. Haien arteko desberdintasun nagusia zauri kronikoen etengabeko hantura egoera da, kontrolik gabeko hantura seinaleen atzeraelikadura (*feedback*) positiboaren ondorioz gertatzen dena. Hori dela eta, orbaintze prozesu osoan zehar neutrofiloak zaurian egoten dira, matrizearen proteinasa metaliko (*matrix metallo proteinase* edo MMPak) ugari jariatuz, zauriaren matrizea degradatzen dutenak. Gainera, lortutako mikroingurune proteolitikoak GFen degradazioa eragiten du, haien funtzioa inhibituz eta beraz, orbaintze prozesuaren erregulazioa aldatuz. Horretaz gain, fibroblastoen jokaera ere asaldatuta agertzen da, orbaintzea are gehiago atzeratuz; fibroblastoek alde batetik, migratzeko ahalmena kaltetuta izaten dute eta bestetik, GFen estimuluei erantzuteko gaitasuna murriztuta. Azkenik, zauri kronikoak infekzioetara sentikorragoak dira, orbaintze denboraldi luzeen ondorioz [5,6].

Ingurune proteolitikoaren ondorioz, zauri hauetan GFen maila txikituta dagoenez haien tratamendurako erabili den estrategia erakargarri bat GFen administrazio exogenoa da [8]. Izatez, zenbait GF

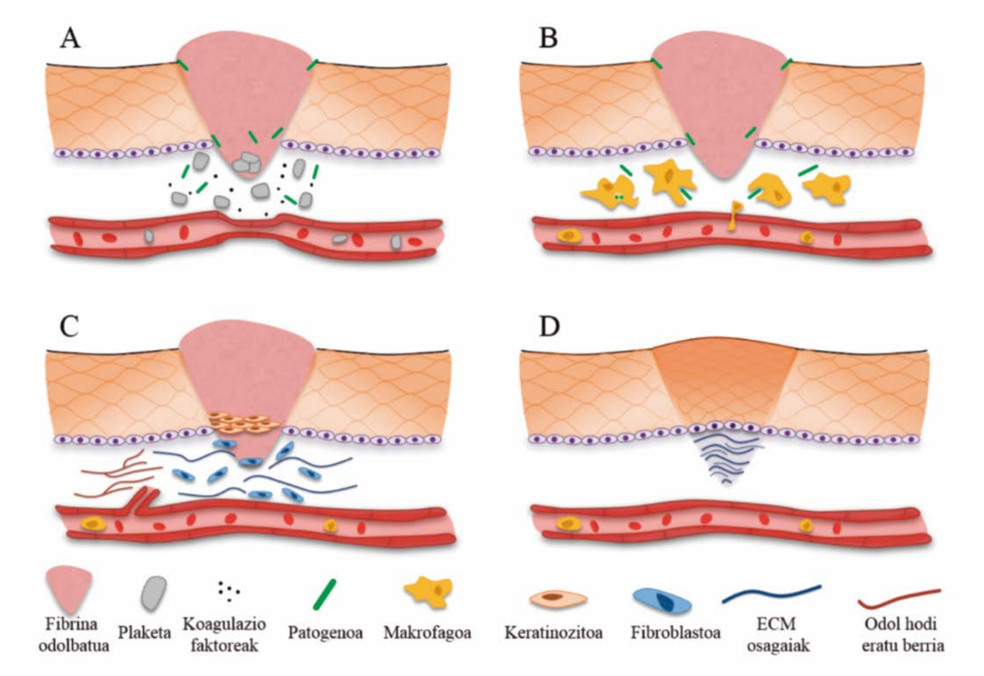


**1. Irudia**. Zauriaren orbaintze prozesua. (A) Hemostasia. Azalaren lesioaren ostean, basouzkurtze labur bat gertatzen da odol jarioa saihesteko, eta ondoren plaketak aktibatzen dira koagulazioa eragiteko eta fibrina odolbatua sortzekoa. (B) Hanturazko fasea. Fase honetan neutrofiloak, makrofagoak eta linfozitoak zaurira infiltratzen dira, infekzioak galarazteko eta kaltetutako ehuna ezabatzeko. (C) Fase proliferatiboa. Aurreko faseetan askatutako seinale kimiotaktikoei erantzunez, fibroblastoak eta keratinozitoak zaurira migratzen dute, non proliferatzen duten. Horretaz gain, fibrobastoek ECM berria eratzeko proteinak askatzen dituzte, eta ECM berri horrek fibrina odolbatua ordezkatzen du. Azkenik angiogenesia gertatzen da zauriari behar dituen oxigeno eta nutrienteak helarazteko. (D) Erremodelazio fasea. Fase honetan epitelio berria eta orbain ehunaren garapena gertatzen da. Horretarako, aurreko fasean eratu den behin behineko ECMaren osaketa eta antolaketa aldatzen da ehun normalarena lortzeko.

.

merkaturatu dira zauri kronikoen tratamendurako, besteak beste, PDGFa (Regranex®), EGFa (Heberprot-P®, Regen-D™ eta Easyef®) eta bFGFa (Fiblast®) [6]. Horretaz gain, GFen eta kimiozinen konbinazio fisiologikoa imitatzeko asmoz, plaketetan aberatsa den plasma (*platelets rich plasma* edo PRP) aztertu da zaurien orbaintzerako. PRPa giza plaketa kontzentrazio handia duen plasma autologoaren bolumen txiki bat da, zeinean zaurien orbaintzerako garrantzizkoak diren GF eta bestelako proteina aktibo ugari dauden [14].

Zoritxarrez, GFak proteinak direnez oso egonkortasun eskasa daukate *in vivo*, maiztasun handiko administrazioak behar dituztelarik. Muga hori gainditzeko, GFak DDStan barneratu dira, haietan kapsularatuta daudenean, zauriko proteasetaz babestuta baitaude. Orbaintzea erregulatzen duten bestelako molekula endogeno batzuk ere DDSen barne formulatu dira. 1. taulan DDSetan kapsularatu diren GFen eta bestelako molekulen zerrenda dago, haien jatorria eta funtzio nagusiak laburbilduz.

## 2. Orbaintzerako nanoteknologian oinarritutako DDSak garatzeko biomaterialak

DDS berriak garatzeko askotariko biomaterialak erabili izan dira, baina denek honako ezaugarriak betetzea komenigarria da, egonkortasun ona, biobateragarritasun eta biodegradazio onak, farmako karga handia, ezaugarri mekaniko onak, farmakoaren lagapen luzatu edo kontrolatua eta farmakoaren babesa [6,35].

Polimeroak, natural zein sintetikoak, oso erabiliak dira nanozuntz, MP eta NPen garapenean. 2. taulan aplikazio honetarako gehien erabiltzen diren polimeroak zerrendatuta daude, haien abantaila eta mugekin. Naturalen artean hurrengoak daude: alginatoa, gelatina, fibrina, kitosanoa, kolagenoa, azido hialuronikoa… Polimero horiek oso erabiliak izan dira, giza gorputzak ezagutzen dituen makromolekulen antzekoak direnez biobateragarritasun handia dutelako. Gainera, haietako zenbait kaltetutako ehunen konponketan parte hartzen dute eta zelulentzako lotura gune eta seinale biomolekularrak dituzte, horrek balio erantsia

**1. Taula.** GF eta orbaintzean parte hartzen duten hainbat molekula endogenoen ekintza eta jatorriaren laburpena.

| GF | Jatorria | Ekintza | Erref. |
|---|---|---|---|
| FGF-1 (fibroblastoen GF-1) | Zelula endotelial eta makrofagoak | Kolagenasa eta plasminogenoaren aktibatzailearen askapena eragin<br>Fibroblastoen proliferazioa eta diferentziazioa estimulatu<br>Zelula endotelialen eta keratinozitoen migrazioa eta proliferazioa sustatu<br>Zitokinen ekoizpena induzituz, makrofagoen migrazioa sustatu | [15-17] |
| b-FGF (fibroblasto basikoaren GF) | Kondroizito, fibroblasto, zelula endotelial, keratinozito, makrofago, mastozito eta muskulu leuneko zelulak | ECM-ko zenbait konposatuen sintesi eta metaketa erregulatu<br>Fibroblasto eta zelula endotelialen migrazioa eta proliferazioa sustatu<br>Errepitelizazioan zehar keratinozitoen migrazioa handitu | [10,15,16] |
| EGF (GF epidermikoa) | Fibroblasto, makrofago eta plaketak | Keratinozito eta fibroblastoen migrazioa eta proliferazioa sustatu<br>Fibronektinaren moduko proteinen ekoizpena estimulatu<br>seinaleztapen bide proliferatiboan parte hartzen duten K6 eta K16 keratinen espresioa handitu | [6,10,14,18] |
| VEGF (GF baskular endoteliala) | Zelula endotelial, fibroblasto, keratinozito, makrofago, neutrofilo, plaketa eta muskulu leuneko zelulak | Zelula endotelialen migrazioa, proliferazioa eta desberdintzapena sustatu (faktore angiogeniko potentea)<br>Iragazkortasun baskularra induzitu<br>Linfaangiogenesia eragin | [6,10,16,19] |
| PDGF (Plaketetatik eratorritako GF) | Zelula endotelial, fibroblasto, keratinozito, makrofago eta plaketak | Neutrofilo, makrofago, fibroblasto eta muskulu leuneko zelulentzat kimiotaktikoa<br>GFak ekoiztu eta askatu ditzaten makrofagoak estimulatu<br>Perizitoak kapilareetara erakartzen parte hartu, haien egituraren osotasuna handituz<br>Fibroblastoen proliferazioa handitu eta miofibroblasto fenotipoa eragin<br>ECM-ko proteinak ekoizteko eta kolageno matrizea uzkurtzeko fibroblastoak estimulatu | [8,10,11] |

| GF | Jatorria | Ekintza | Erref. |
|---|---|---|---|
| IGF-I (intsulinaren antzeko GF-I) | Fibroblasto, hepatozito, makrofago, neutrofilo eta gihar eskeletikoko zelulak | Keratinozitoen migrazioa eta proliferazioa handitu<br>Fibroblastoen proliferazioa estimulatu | [8] |
| Intsulina | Pankreako β-zelulak | Keratinozitoen migrazioa, proliferazioa eta desberdintzapena estimulatu<br>Fibroblastoen proliferazioa eta ECM-ko proteinen ekoizpena sustatu<br>Zitokina inflamatorioen askapena modulatu | [21] |
| SDF-1α (estromako zeluletatik eratorritako faktorea -1α) | Fibroblasto dermal eta zelula endotelialak | Zelula endotelial mikrobaskularren apoptosia inhibitu<br>Proliferazio endoteliala eta hodien formazioa sustatu<br>Hezur muineko ama zelulen aktibazioa, mugikortasuna eta lesio gunean geratzea estimulatu | [11,22,23] |
| LL37 | Zelula dendritiko, keratinozito, linfozito, makrofago, mastozito, neutrofilo eta NK zelulak | Patogenoen aurrean lehenengo defentsa da, aktibitate antibakteriano, antibiofilm, antibiriko eta antifungikoa duelarik<br>Monozito, neutrofilo, zelula dentritiko, makrofago, fibroblasto eta keratinozitoentzako kimiotaktikoa da<br>Zitokina pro- eta anti-inflamatorioen ekoizpena orekatu<br>Keratinozitoen eta zelula endotelialen aurrekarien migrazioa eta | [24] |
| VIP (hesteko peptido basoaktiboa) | SNZ-ko neurona eta birikietako eta heste meheko zelulak | TGF-α-ren sintesia estimulatu<br>Angiogenesia sustatu<br>Fibroblasto eta keratinozitoen proliferazioa sustatu | [20,25-27] |
| Heparina desulfatatua | Basofilo eta mastozitoak | Hanturazko fase erregulatzen du agente pro- eta anti-inflamatorioei lotuz<br>Fibroblasto, gihar ehun leuneko zelulen eta keratinozitoen proliferazioa sustatu<br>GF ugarirekin elkarrekintzak ditu, haien efektua sustatuz | [9] |

| GF | Jatorria | Ekintza | Erref. |
|---|---|---|---|
| Melatonina | Guruin pineala | Bitartekari inflamatorioak askatu<br>Angiogenesian eta zelulen proliferazio eta migrazioan parte hartu<br>Lesio gunean kolagenoaren eta glikosaminoglikanoen (GAG) pilaketa sustatu | [28] |
| Lipokalina-2 | Zelula glialak | Keratinozitoen migrazioa sustatu | [29,30] |
| Serpin-A1 | Batez ere gibela, baina baita hesteko zelula epitelial, makrofago, monozito eta neutrofiloak ere | Elastasaren aktibitatea inhibitu<br>Aktibitate anti-inflamatorio handia dauka | [31,32] |
| β-estradiola | Obulutegia | Zaurian granulozitoen eta makrofagoen pilaketa mugatu<br>Errepitelizazioa sustatu<br>Fibroblastoen TGF-β1-aren jariaketa estimulatzen du<br>Kolageno metaketa handitu | [33,34] |

ematen dielarik [36]. Hala eta guztiz ere, zenbait muga dituzte, besteak beste, lote arteko aldakortasuna, gurutzatutako kutsadurari sentikortasuna, immunogenizitatea, atal immunogeno edo patogenoen agerpena eta garestiak izatea. Horretaz gain, haien ezaugarri mekaniko ezegokiek elektroirute prozesua eta nanozuntzen erabilera zailtzen dute [35].

Nanozuntzezko mintzen garapenari dagokionez, polimero sintetikoek ezaugarri mekaniko hobeak dituzte, elektroirute prozesua erraztuz. Horretaz gain, polimero naturalekin alderatuz honako abantailak dituzte: lote arteko errepikakortasuna, ezaugarri fisiko-kimiko kontrolagarriak, prezio baxuagoa eta ondo zehaztutako egitura zein degradazio zinetika [37]. Dena den, badituzte zenbait muga, hala nola, ez dute zelulentzako lotura-gune aproposik eta zelulekiko afinitate eskasa daukate. Polimero sintetiko erabilienak azido polilaktikoa (PLA), poli(ε-kaprolaktona) (PCL), azido poliglikolikoa (PGA) eta haien arteko konbinazioak (PLGA eta PLLCL) dira [35,38].

Jatorri sintetiko eta naturaleko polimeroak elkarrekin erabili daitezke DDSak garatzeko, bien abantailez baliatzeko asmoz. Era horretan lortutako formulazioek osagai guztien indarguneak izango dituzte, esaterako, polimero naturalen bioaktibitatea eta sintetikoen degradazio abiadura [39].

NP lipidikoetan erabiltzen diren lipidoek polimeroen antzeko ezaugarriak izan behar dituzte, hots, biobateragarritasun eta biodegradazio egokiak, askapen kontrolatua, bideratutako farmako lagapena, farmako karga handia eta farmakoaren babesa. Horretaz gain, azaleko lipidoak neurri batean fluidotzen dituzte eta farmakoen banaketa handitzen dute, horrela, farmakoaren garraioa erraztuz [40].

DDS motaren arabera lipido desberdinak erabiltzen dira. Alde batetik, liposomak normalean fosfolipidoez, kolesterolez eta inguru urtsu batez osatuta daude. Fosfolipidoak liposomen osagai nagusia dira eta azalaren tenperaturan likidoak dira. Haien artean erabilienak fosfatidilkolina naturalak dira, profil toxikologikoagatik eta prezioagatik. Kolesterola bikapa lipidikoari zurruntasuna emateko erabiltzen da, baina farmako hidrofilikoen kapsuralatze eraginkortasuna txikitu dezake eta azalean zeharreko barneraketa zailagotu [40,41]. Beste aldetik, nanopartikula solido lipidikoak (*solid lipid nanoparticle* edo SLN) lipido solidoak erabiliz ekoizten dira, besteak beste, mono-, di- eta triglizeridoak, gantz azidoak, argizariak eta esteroideak. Gainera, surfaktanteak gehitzen zaizkie egonkortasun esterikoa lortzeko, haien artean fosfolipidoak, poloxameroak eta polisorbatoak daudelarik [42]. Azkenik, garraiatzaile lipidiko nanoegituratuak (*nanostructured lipid carried* edo NLC) ekoizteko, lipido solidoaz gain, giro tenperaturan likidoa den lipido bat erabiltzen da, eduki osoaren %30-a izaten dena [43].

## 3. Nanoteknologian oinarritutako askatze sistemak zaurien orbaintzerako

### *3.1 MP eta NP polimerikoak*

Proteinen administrazioak dituen zenbait arazo gainditzeko erabili izan den metodo bat, proteinak sistema polimeriko koloidalen barnean kapsularatzea izan da. Esaterako, erdibizitza *in vivo* asko hobetzen da kapsularazioaren ondoren, MP eta NPek zaurian ageri diren proteasen aurrean duten efektu babesgarriari esker. Gainera, partikulek kapsularatutako osagaiaren askapen kontrolatua lortzen dute, maiztasun handiko administrazioak saihestuz, eta zenbait kasutan dosia txikitzea ahalbidetuz. Dosifikazioaren hobekuntza horrek eta administrazio lokalak, tratamenduaren eraginkortasuna hobetzen dute, izan ere, dosi altuek edo esposizio sistemikoek eragindako bigarren mailako efektuak saihesten dira horrela [6,51,52]. Atal honen amaieran dagoen 3. taulan orbaintzerako garatu diren MP eta NP polimerikoen laburpena dago.

bFGFa sarritan kapsularatu da MPen barnean. Adibidez, Liu *et. al.*-ek alginato mikroesferetan bFGFa kapsularatu zuten eta ondoren hidrogel batean barneratu, zeina karboximetil kitosano eta alkohol polibiniliko (*polyvinyl alcohol* edo PVA) konposite batez osatuta zegoen. Garatutako formulazio horrek, hidrogel soila eta bFGF askea zuen hidrogelarekin konparatuz gero, orbaintze tasa azkartu zuen, errepitelizazioa eta dermisaren leheneratzea bizkortuz [53]. Horretaz gain, Place *et. al.*-ek bFGFz kargatutako formulazio bat garatu zuten polielektrolito konplexuetan

**2. Taula.** Orbaintzerako eta nanoteknologian oinarritutako DDSak garatzeko gehien erabiltzen diren polimeroen abantaila eta mugak

| Polimero naturalak | | | | | | |
|---|---|---|---|---|---|---|
| Polimeroa | Degra-dazioa | Ezaug. meka-nikoak | Ezaugarri fisiko-kimikoak | Abantailak | Mugak | Erref. |
| Kolagenoa | Entzi-matikoa | Ahula | Hidrofiloa | Integrinentzako lotze lekua<br>Antigenizitate baxua<br>Orbaintzea sustatzen du | Koste altua<br>Prozesamendu zaila<br>Kontaminatzeko erraztasuna<br>3. mailako erreduretan eta gaixo sensible/alergikoetan kontraindikatua | [35,39] |
| Gelatina | Entzi-matikoa | Ahula | Hidrofiloa | Koste baxua<br>Integrinentzako lotze lekua<br>Antigenizitaterik ez<br>Aldaketa kimikoak onartzen ditu | Fixatu behar da tenperaturarekin disolbatzea edo izoztea ekiditeko | [35,44,45] |
| Fibrina | Entzi-matikoa | Ahula | Hidrofiloa | Behinbehineko matrize bezala jokatzen du zaurietan<br>Koagulazioan parte hartzen du | Egonkortasun baxua<br>Sendotasun mekaniko ahula<br>Prozesamendu zaila | [35,44] |
| Kitosanoa | Entzi-matikoa | Ahula | Hidrofiloa | Antigenizitaterik ez<br>Biologikoki berriztagarria<br>Koagulazio eta granulazio ehunaren sorreran parte hartzen du<br>Efektu antimikrobianoa | Hornikuntza mugatua<br>Prozesamendu denbora luzea | [35,39,46,47] |
| Alginatoa | Entzi-matikoa | Ahula | Hidrofiloa | Azidoekiko erresistentzia<br>Ur kantitate handiak xurga ditzake | Koste altua<br>Farmako galera lixibiazioagatik | [35,39,47] |
| Zeta fibroina | Entzi-matikoa | Sendoa | Hidrofiloa | Agregazioa txikitzen du<br>Itsasgarria<br>Exudatuak xurgatzen ditu<br>Immunogenizitate baxua<br>Degradazio tasa kontrolagarria | Koste altua<br>Gehiegizko hidratazioa | [35,39,47,48] |
| Azido hialuronikoa | Entzi-matikoa | Ahula | Hidrofiloa | Funtzionalizatzeko erraza<br>Kontrolatzeko erraza | Koste altua | [35] |

| Polimero sintetikoak | | | | | | |
|---|---|---|---|---|---|---|
| Polimeroa | Degradazioa | Ezaug. Mekanikoak | Ezaugarri fisiko-kimikoak | Abantailak | Mugak | Erref. |
| PGA | Hidrolitikoa | Sendoa | Hidrofiloa | Bioxurgatze aurreikusgarria | Degradazio azkarra (2-4 aste)<br>Lekuko pHaren igoera zorrotza | [35,39,44,49] |
| PLA | Hidrolitikoa (Tasa geldoak) | Sendoa | Hidrofoboa | Biobirxurgatze ona<br>Degradazio produktuei esker orbaintzean parte hartzen du | Hezegarritasun baxua<br>Degradazio produktu azidoengatik erreakzio lokal edo sistemikoak<br>Zurruntasun baxua | [35,44] |
| PLGA | Hidrolitikoa | Sendoa | Aldakorra | Endo-lisosometatik ihes azkarra<br>Indar mekaniko altua<br>Degradazio produktuei esker orbaintzean parte hartzen du<br>Beste polimeroekin bateragarria | Degradazio produktu azidoengatik erreakzio lokal edo sistemikoak<br>Zelulek ezagutu ditzaketen motibo eza | [35,39,50] |
| PCL | Hidrolitikoa (Tasa geldoak) | Oso elastikoa | Hidrofoboa | Erlatiboki koste baxua<br>Epe luzerako askapena | Erreakzio lokal edo sistemikoak<br>Zelulek ezagutu ditzaketen motibo eza | [35,39,44,50] |
| PLLCL | Hidrolitikoa | Sendoa | Hidrofoboa | Disolbatzaileekiko flexibilitate altua<br>PLA-ren indar mekanikoa mantentzen du | Degradazio produktu azidoengatik erreakzio lokal edo sistemikoak<br>Zelulek ezagutu ditzaketen motibo eza | [35,39,44,50] |
| PU | Hidrolitikoa | Ahula | Aldakorra | Farmakoa kargatzeko ahalmen altua | Degradazio geldoa | [35] |

oinarrituta, zehazki polisakarido kationiko (kitosano eta N,N,n-trimetil kitosano) eta glikosaminoglikano anionikoez (heparina eta kondroitin sulfatoa) osatutako NPak garatu zituzten. NP horiek agrekanoa imitatzeko diseinatuta zeuden, proteoglikano horrek GFentzako gordailu moduan jokatzen baitu. Hori dela eta, GFa proteasen aurrean egonkortzeaz gain, formulazio honek bFGFa testuinguru biomimetiko batean aurkezten du, inguruko ehunekin duen elkarrekintza erraztuz. Formulazioaren eraginkortasuna *in vitro* entseguen bidez erakutsi zen, izan ere formulazio honek muineko zelula estromalen proliferazioa eta jarduera metabolikoa handitu zituen bFGF askearekin eta agrekanoari lotutako bFGFarekin konparatuz [54].

Li eta bere kideek bFGFa gelatina MPetan kapsularatu zuten, haien arteko elkarrekintza elektrostatikoak MPen efektu babesgarria areagotu dezakelako. Partikulak kolageno/zelulosa nanokristalez osatutako egitura porotsu batean barneratu ziren. Lortutako formulazioa angiogenesia handitzeko gai izan zen, *in vitro* zein *in vivo* [55]. Park et. al.-ek bFGF-z kargatutako gelatina MPak garatu zituzten ere, eta kasu honetan kitosano bio-aldamio porotsu batean sartu zituzten. Apposituaren eraginkortasuna *in vivo* aztertu zen, sagu zaharrei egindako presio ultzeretan, non zaurien itxiera tasa handitu zuen. Horretaz gain kitosanoari esker, animaliek proteasa maila baxuagoak zituzten, eta horren ondorioz bFGF endogeno zein exogeno maila handiagoak [56]. Beste ikerketa batean, Kawai eta kideek bFGFdun MPak merkaturatutako dermis artifizial (Pelnak™) batean barneratu zituzten. Pelnak™ bi geruza dituen dermis artifizial bat da, barrualdean kolageno esponja bat eta kanpoaldean silikona geruza bat. Formulazio honen eraginkortasuna bi animalia eredutan ikertu zuten, akurietan egindako lodiera osoko zauri eszisionaletan eta sagu diabetikoetan egindako *decubito* presio-ultzeretan. Bi kasuetan formulazioak fibroblastoen proliferazioa eta kapilareen sorrera azkartu zituen. Gainera, sagu diabetikoen kasuan infekzioen aurrean erresistentzia handitua behatu zen [57,58].

Huang eta kolaboratzaileek beste bigeruzadun apositu bat garatu zuten, zeinaren barne bFGFdun MPak sartu zituzten. Bioaldamioaren barne geruza gelatinazko esponja bat zen, bere egitura porotsuari esker proliferatzen dauden zelulentzako ostalari modura jokatzen duena; eta kanpo geruza poliuretano (PU) elastomerikoz osatuta zegoen, zeinak bio-aldamioaren ezaugarri mekanikoak hobetzen dituen. Apositua york txerrietan egindako lodiera osoko zaurietan ezarri zen, eta emaitzek erakutsi zutenez, zaurien itxiera bizkortu zuen eta azalaren birmoldaketa hobetu zuen [59]. Uluybaram *et. al*.-ek, bigeruzadun apositu horren barnean EGFaz kargatutako MPak sartu zituzten eta *in vivo* zuten eraginkortasuna aztertu zuten untxietan egindako zauri eszisionaletan. Ikertutako dosi altuenarekin, apositua izan zuten animalietan EGF disoluzioa izan zutenetan baino askoz gehiago txikitu zen zauriaren azalera. Gainera, azterketa histologikoek erakutsi zutenez, ehun berriak azal osasuntsuaren egitura ia berdina eskuratu zuen [60]. Ondoren, bio-aldamioaren barne geruza (gelatinazko esponja EGFdun gelatina MPekin) zauri eszisionaletan aplikatu zuten, arratoi normal zein estreptozotozinak eragindako arratoi diabetikoetan. Arratoi ez-diabetikoetan zaurien itxiera bereziki handitu zen, nahiz eta diabetikoetan hobekuntza txiki bat ere somatu zen. Analisi histologikoei dagokienez, aposituaren efektua esanguratsuki desberdina izan zen arratoi normal eta diabetikoetan, baina orokorrean granulazio ehunaren sorrera eta errepitelizazioa hobetu zituen [61].

Horretaz gain, Zhou eta kideek EGFa beste polimero natural batean kapsularatu zuten, kitosanoan, zehazki. EGFa zuten kitosano NPak fibrina gel batera gehitu zituzten, eta horrela faktorearen askapen luzatua lortu zuten, 7 egunez mantenduz fibroblastoen proliferazioa estimulatzeko gaitasuna [62]. EGFa polimero sintetikoez osatutako MPetan ere kapsularatua izan da, adibidez PLGA MPtan, zeinekin fibroblastoen hazkuntza tasa hobetu zen *in vitro* [63]. Beste ikerketa batean, EGFdun PLGA NPek lesioaren itxiera bizkortu zuten arratoi diabetikoetan egindako lodiera osoko zaurietan, izan ere, NPek askatutako EGFak fibroblastoen proliferazioa sustatu zuen [64]. Gure ikerketa taldeak burututako ikerketa batean EGFa PLGA-alginato MPtan barneratu zen. Alginatoa kapsularazio efizientzia hobetzeko erabili zen, izan ere, MPen barneko fase urtsuaren likatasuna handituz, GFen barreiadura mugatu daiteke. MPetan kapsularatu ostean

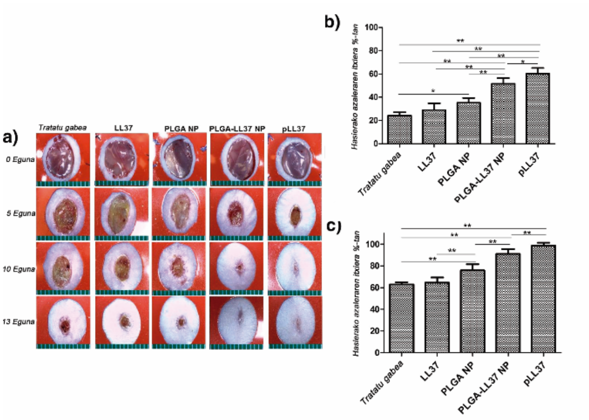


**2. Irudia.** PLGA-LL37 NPek orbaintzea bizkortzen dute. (A) Aztertutako bost taldeen zaurien irudi adierazgarriak: tratatu gabea, LL37, PLGA NP, PLGA-LL37 NP eta LL37 (kontrol positiboa). (B) Zauriaren azalera 5. egunean (n=13) eta (C) 10. Egunean (n=10) (batazbestekoa± desbideratze estandarra (SD). Chereddy *et al*.-etik [67] baimenarekin kopiatu eta moldatua (© 2014).

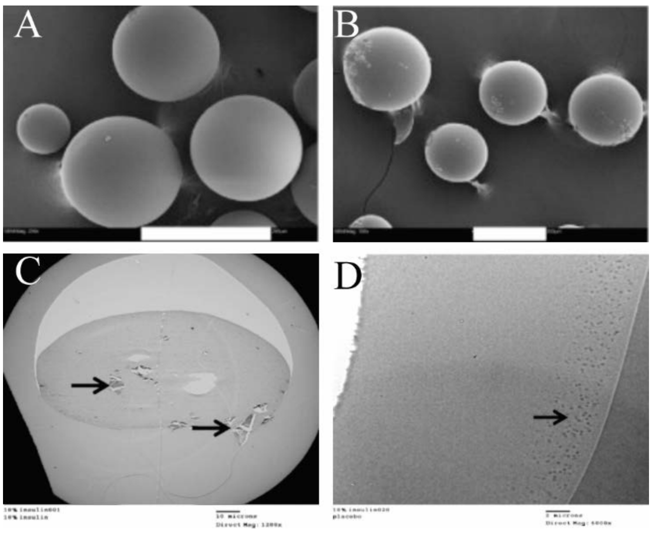


**3. Irudia**. Intsulina kristalak dituzten PLGA MPak. MPen itxura eta gainazal morfologia (A) intsulina gabe eta (B) %10-eko intsulina kargarekin. Tamaina barra txuriek 200 µm adierazten dute. (C) %10 (p/p) intsulina kristalak dauzkaten PLGA MPen zeharkako irudiak. Gezi beltzek MPen barnean eta gainazalean dauden intsulina kristalak seinalatzen dituzte. Tamaina barrak 10 µm adierazten du. (D) Gezi beltzak PLGA MPen kanpo eremu porotsua seinalatzen du. Tamainu barrak 2 µm adierazten du. Hrynyk *et al.*-etik [68] baimenarekin kopiatu eta moldatua (© 2010).

EGFaren aktibitatea mantentzen zela frogatu zen *in vitro*. Ondoren, *in vivo* injekzio intralesional bakarraren ostean, orbaintze azkarragoa eta eraginkorragoa eragin zuten, zauriaren itxierari, errepitelizazioari eta hantura prozesuaren ebazpenari dagokionez. *In vivo* entsegua estreptozotozinari dela eta diabetiko ziren arratoietan egindako lodiera osoko zaurietan burutu zen [65].

PLGA beste konposatu aktibo batzuk kapsularatzeko erabilia izan da ere bai, hala nola, FGF-1, LL37 eta intsulina. Alde batetik, FGF-1ez kargatutako MPak fibrina gel batean sartu ziren, eta formulazioak fibroblastoen proliferazioa hobetu zuen [66]. Beste aldetik, LL37a zuten NPak lodiera osoko zaurietan ezarri ziren, non ondorengoak hobetu zituzten: granulazio ehunaren sorrera, errepitelizazioa, kolagenoaren metaketa eta neoangiogenesia, 2. irudian ikus daitekeen modura [67]. Intsulinaren kapsularatzeari dagokionez (3. irudia), intsulina zuten PLGA MPek zauriaren itxiera hobetu zuten keratinozitoen migrazio entsegu batean, *in vitro* [68]. Ondoren MP horiek alginato edo alginato-polietilenglikol (PEG) esponjetan sartu ziren, prozesu horren ostean intsulinaren bioaktibitatzea mantendu zelarik [69]. Jarraian, apposituaren eraginkortasuna arratoiei eragindako erredura eredu batean frogatu zen. Apposituarekin tratatutako lesioek orbaintze azkarragoa eta erregeneratiboagoa lortu zuten, honakoei esker: hildako ehunaren desagertze tasaren handitzea, estres oxidatiboaren txikitzea, kolageno metaketaren estimulazioa sustatzea eta angiogenesiaren areagotzea [70].

VEGFa NPen barne sartzeak angiogenesia hobetzen duela *in vitro* zein *in vivo* frogatu da. Alde batetik, VEGFa zuten fibrinazko NPak kitosano-azido hialuroniko esponja batean barneratu ziren. Apositua medioarekin inkubatu zen eta zelula endotelialei *in vitro* gehitu ostean, angiogenesia areagotu zen [71]. Beste aldetik, VEGFa zuten alginato kaltzikozko MPak *in vivo* larruazalpean ezarri ziren, non angiogenesia handitu zuten [72]. Angiogenesia aztertzeaz gain, kapsularatutako VEGFak orbaintzean duen eragina ere aztertu da. Horretarako VEGFa zuten PLGA NPak sagu ez-diabetiko eta diabetikoetan egindako lodiera osoko zaurietan aplikatu ziren, non kolageno metaketa, granulazio ehunaren sorrera, angiogenesia eta errepitelizazioa hobetu zuten, efektu onuragarria VEGFari eta PLGAren degradaziotik sortutako laktatoari esker lortu zelarik [73].

Losi *et. al.* urrats bat haratago joan ziren eta bi GF batera kapsularatu zituzten PLGA NPtan, bFGFa eta VEGFa zehazki, izan ere biek eginkizun gakoa betetzen dute orbaintzean. NPak bigeruzadun bioaldamio batean sartu ziren, barnealdeko fibrina geruzak farmakoa askatzeko sistema modura jokatzen zuelarik, eta kanpoaldeko polieter-uretano-polidimetilsiloxano (PEtU /PDM) geruzak sendotasun mekanikoa ematen ziolarik. Garatutako apositua *in vivo* sagu diabetikoetan egindako zaurietan ezarri zen. GF askeekin edo bio-aldamio hutsarekin konparatuz, formulazioak zauriaren itxiera hobetu zuen, dena den, ez zen desberdintasunik behatu formulazioaren eta GFak zuzenean bio-aldamioaren barnean administratzearen artean [74]. Beste ikerketa batean, VEGFa EGFarekin batera kapsularatua izan zen. Kasu honetan, GFak kitosano MPtan barneratu ziren eta ondoren MPak dextranoan oinarritutako hidrogel batera gehitu ziren, 4. irudian ikus daitekeen bezala. Garatutako formulazioa GF askeen administrazio maizago batekin konparatu zen. Emaitzek erakutsi zutenez, formulazioak orbaintzea bizkortu zuen erredura zaurietan, MPen erabilgarritasuna GFen administrazioan agerian utziz [75].

Horretaz gain, GF eta zitokina ugari batera kapsularatu daitezke MP eta NPtan plaketen lisatua edo PRPa erabiliz. Fontana

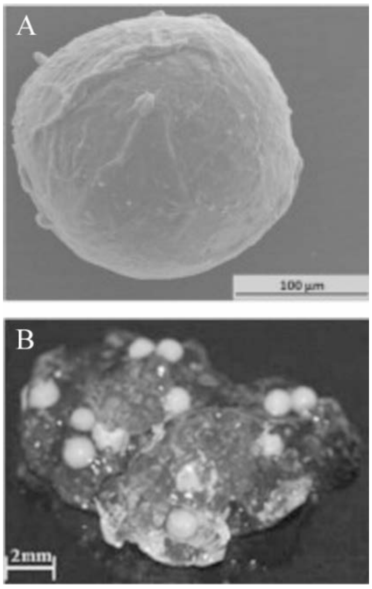


**4. Irudia**. EGFa eta VEGFa duten kitosano MPak dextranoan oinarritutako hidrogel batean sartuak. (A) Kitosano MPen SEM irudia 400x. (B) MPak barneratuta dituen dextrano gelaren irudia. Ribeiro *et al.*-etik [75] baimenarekin kopiatua eta moldatua (© 2013).

*et. al.*-ek plaketen lisatua silikona porotsuzko MPtan sartu zuten, emaitza desiragarriak lortuz *ex vivo* zauri eredu batean. Formulazioak kontrol positiboak (plaketen lisatua partikula modura) baino efektu proliferatibo handiago lortu zuen eta kolageno fibren azidofilia labur baina efektiboa ere bai, erregenerazioa abian dagoelaren seinale dena [76]. PRP edo plaketa lisatuetatik GFen askapen luzatuagoa lortzeko estrategia bat heparina daramaten NPen ekoizpena da, izan ere, heparinak GFak lotzen ditu, haien gordailu modura jokatuz. Horren harira, PRPa daramaten fragmina-protamina MP/NPak garatu ziren, haien oinarria protamina fragminarekin (pisu molekular baxuko heparina) lotzean sortzen diren konplexu solugaitzak direlarik. Partikula horiek arratoiei egindako zaurietan administratu ziren, erabilitako ereduarekin azal-mentuak lortzeko emaileei egindako lodiera partzialeko zauriak islatzen dira. Partikulek zaurien itxiera bizkorragoa eta angiogenesi handitua eragin zuten [77]. Emaitza horiek La eta kideek lortutakoekin bat datoz, haiek ere berdina behatu baitzuten, garatu zuten formulazioa timorik gabeko saguei egindako zauri handietan ezarri ostean. Garatu zuten formulazioa heparinarekin konjugatutako PLGA NPez osatuta zegoen, zeintzuk PRPa kapsularatuta zuten eta fibrina gel batean barneratuta zeuden [78].

Heparinak GFak egonkortzeaz gain, eragin antiinflamatorioa ere badu, erredu-retan erabilgarria dena. Helburu horrekin Lakshmi *et. al.*-ek heparina desulfatatua kitosanozko NPtan kapsularatu zuten, eta ondoren NPak kolageno matrize batean sartu zituzten. Garatutako formulazioa arratoietan egindako erredura zaurietan hantura erregulatzeko gai izan zen, ondorioz zauriaren itxiera eta granulazio ehunaren sorrera bizkorragoak lortuz [79].

Lezitina moduko lipido negatiboek kitosanoarekin duten elkarrekintza elektrostatikoei esker NPak ekoiztu daitezke, Blazevik eta kideek egin zutena, hain zuzen. NP horiek melatoninarekin kargatu zituzten, eta *in vitro* entseguetan orbaintzea sustatu zezaketela frogatu zuten [80].

Zenbait kasutan, DDSak garatzeko ez-ohiko polimeroak erabili izan dira, haien ezaugarri bereziez baliatzeko asmoz.

Horren harira, Petersen eta kolaboratzaileek ondorengo polianhidrido anfifilikoez osatutako MPak garatu zituzten: 1,6-bis(p-karboxifenoxi)hexanoa (CPH) eta 1,6-bis(p-karboxifenoxi)-3,6-dioxaoktanoa (CPTEG). Polimero hauek beste polimero sintetiko batzuek ez bezala, egitura osoko zein gainazaleko higadura aurkeztu dezakete eta haien degradazio produktuek azidotasun gutxiago dute. Hori dela eta, hezetasunak eragindako agregazioaren arriskua txikitzen dute eta proteinentzako ingurune egokiago bat sortzen dute. Polimero hauekin ekoiztutako MPetan lipokalin-2 proteina barneratu zen. Ondoren, proteina kapsularatuaren eta askearen *in vitro* aktibitateak konparatu zituzten, eta MPen barnean zegoen lipokalin-2-ak zelulen migrazio tasa handitzen zuela nabarmendu zen, ziurrenik MPek eragindako askapen luzatuari esker [29].

Horretaz gain, zenbait polimero erabiltzearen arrazoia kapsularatutako farmakoa itu ehun edo zeluletara bideratzeko duten gaitasuna da. Horren adibide poli-(1,4-fenileneazetona dimetilene tioketala) (PPADT) da, izan ere, polimero hau oxigeno espezie erreaktiboekiko (*reactive oxygen species* edo ROS) sentikorra da eta zaurian dauden ROS maila altuak direla eta bertan depolimerizatzen da batez ere. Hori dela eta, PPADT NPak garatu ziren SDF-1α askatzeko. Markatutako NPak erabiliz, PPADTa zaurietan bereziki depolimerizatzen zela frogatu zen, bertan SDF-1α askatuz. Gainera, formulazio honekin tratatutako saguen zauriek itxiera azkarragoa eta handitutako baskularizazioa izan zuten [81].

Beste aldetik, polimeroen erabilgarritasuna handitzeko asmoz funtzionalizatu daitezke, Wang eta kideek egin zuten bezala, VIP askatzeko *in situ* sortutako MPak ekoiztuz. Horretarako, lehenbizi PCL nanozuntzak dopaminarekin funtzionalizatu zituzten. Ondoren, VIPa nanozuntzetan absorbatu zuten, dopaminaren ezaugarri itsaskorrei esker. Azkenik, nanozuntzak azetonan denbora labur batez murgildu zituzten, partzialki disolbatutako PCLaren hauspeatzea eraginez, eta horrela *in situ* MPak lortuz. *In vivo* zauri eredu batean administratu ostean, garatutako formulazioak orbaintzea era esanguratsuan sustatu zuen, granulazio ehunaren sorrera eta angiogenesia hobetuz [25].

**3. Taula.** GF eta beste konposatu aktiboak askatzeko garatutako MP eta NP polimerikoen laburpena eta haiekin lortutako emaitza nagusiak

| DDS | GF | Emaitzak | Erref. |
|---|---|---|---|
| Alginato MPak karboximetil kitosano-PVA hidrogelean | bFGF | Arratoiei engindako lodiera osoko erredura zaurietan aztertu ziren. Formulazioak zauriaren berreskuratze tasa azkarragoa lortu zuen, errepitelizazio eta dermisaren erregenerazio azkarragoarekin. | [53] |
| Agrekanoa imitatzen duten polielektrolito konplexuen NPak | bFGF | Formulazioak bGFGaren akitibititea mantendu zuen *in vitro*, aktibitate metaboliko eta proliferazioaren entsegu banatan. | [54] |
| Gelatina MPak kolageno/zelulosa porotsuzko nanokristalen bio-aldamioetan | bFGF | Formulazio honekin zelula endotelialen proliferazioa handitu zen. Eta arratoietan larruazalpean ezarri ostean angiogenesia sustatu zen *in vivo*. | [55] |
| Gelatina MPak kitosano porotsuzko bio-aldamioetan | bFGF | Formulazioa sagu zaharrei egindako presio ultzeratan aztertu zen. 7. egunera arte, bio-aldamio hutsak zein bFGFdun bio-aldamioak zauriaren itxiera bizkortu zuten. Horretaz gain, bFGFdun bio-aldamioak proteasen maila txikitu zuen 10. egunera arte. | [56] |
| Gelatina MPak dermis artifizial (Pelnac®)batean | bFGF | Formulazioa akurietan egindako lodiera osoko zauri eszisionaletan eta *db/db* saguetan egindako *decubito* presio ultzeratan aztertu zen. MPekin bFGFaren *in vivo* erretentzioa luzatu zen. Horretaz gain, bi ereduetan formulazioak fibroblastoen proliferazioa eta kapilareen sorrera handitu zuen, dosiaren menpeko eran. | [57,58] |
| Gelatina MPak bigeruzadun bio-aldamio batean (gelatina esponja eta poliuretano mintza) | bFGF | York txerrietan egindako lodiera osoko zaurietan aztertu zen. Bio-aldamioaren aplikazioak zauriaren itxiera azkartu zuen eta erremodelazioa hobetu. | [59] |
| Gelatina MPak bigeruzadun Bio-aldamio batean (gelatina esponja eta poliuretano mintza) | EGF | Formulazioa untxietan egindako lodiera osoko zauri eszionaletan aztertu zen. Erabilitako dosi altuenak zauriaren azaleraren murrizketa handiena eragin zuen. Azterketa histologikoek erakutsi zutenez, ehun berriaren egitura azal normalarenaren ia berdina zen. | [60] |
| Gelatina MPak gelatina esponjetan | EGF | Formulazioa lodiera osoko zauri ereduetan aztertu zen arratoi diabetiko eta ez-diabetikoetan. Formulazioak zauriaren itxiera sustatu zuen, bereziki arratoi ez-diabetikoetan. Gainera, bi animalia ereduetan kalifikazio histologikoak hobetu zituen (errepitelizazioa, granulazio ehunaren sorrera eta neobaskularizazioa). | [61] |

| DDS | GF | Emaitzak | Erref. |
|---|---|---|---|
| Kitosano NPak fibrina gel batean | EGF | Formulazioak ezaugarri bio-itsasgarriak erakutsi zituen, eta NPak edo gela bakarrik erabilita baino askapen luzatuagoa lortu zuen. Horretaz gain, kapsularazio prozesuaren ostean EGFaren bioaktibitatea mantendu zen, fibroblastoen proliferazioa sustatzeko gai izan baitzen. | [62] |
| PLGA MPak | EGF | Formulazioek fibroblastoen hazkuntza tasa hobetu zuten *in vitro.* | [63] |
| PLGA NPak | EGF | Arratoi diabetikoen zauri eredu batean, NPek zauriaren itxiera bizkortu zuten EGF askearekin konparatuz. | [64] |
| PLGA-Alginato MPak | EGF | Formulazioa arratoi diabetikoetan egindako lodiera osoko zauri eredu batean aztertu zen. Formulazioak orbaintze azkarrago eta eraginkorragoa eragin zuen, errepitelizazio eta hantura prozesuaren ebazpenari dagokioenez. | [65] |
| PLGA MPak fibrina bio-aldamio batean | FGF-1 | Bio-aldamioak fibroblastoen proliferazioa sustatu zuen *in vitro.* | [66] |
| PLGA NPak | LL37 | NPek zaurien itxiera hobetu zuten NMRI arratoietan, errepitelizazio, kolageno metaketa, granulazio ehunaren sorrera eta neoangiogenesiari dagokionez. | [67] |
| PLGA MPak | Intsulina | Formulazioa keratinozitoetan egindako urradura entsegu batean aztertu zen, non zauriaren itxiera azkartu zuen. | [68] |
| PLGA MPak alginato edo alginato-PEG esponjetan | Intsulina | Apositua arratoietan egindako erredura lesioetan aplikatu zen. Orbaintze azkarrago eta erregeneratiboagoa lortu zuen honakoengatik: itxiera bizkortua, hildako ehunaren desintegrazio tasa altuagoa, estres oxidatibo txikitua, eta kolagenoaren metaketa eta heltze hobetuak. | [69,70] |
| Fibrina NPak kitosano-azido hialuroniko esponjetan | VEGF | Formulazioak *in vitro* kapilare-gisako tubuluen formazioa (angiogenesia) handitu zuen. | [71] |
| Kaltzio alginatozko MPak | VEGF | MPak larruazalpean ezarri ziren, eta angiogenesia sustatu zuten inguruko ehunaren 0,6-0,8 mm-ko luzeran. | [72] |
| PLGA NPak | VEGF | NPek, in vitro keratinozitoen proliferazioa eta migrazioa hobetu zuten eta VEGFR-2-aren espresioa gain-erregulatu zuten. Ondoren, sagu diabetiko eta ez diabetikoetan egindako zauri ereduetan aztertu ziren, non granulazio ehunaren sorrera, kolageno edukia, errepiteliazioa eta angiogenesia hobetu zituzten. | [73] |

| DDS | GF | Emaitzak | Erref. |
|---|---|---|---|
| PLGA NPak PEtU/PDM edo fibrinan oinarritutako Bio-aldamioetan | VEGF eta bFGF | Formulazioak sagu diabetikoetan egindako lodiera osoko zauri eredu batean aztertu ziren. Formulazioek GF askeekin konparatuta orbaintzea hobetu zuten, baina ez zen aldaketarik sumatu GFak zuzenean bio-aldamioetan barneratutako apposituekin konparatuz gero. | [74] |
| Kitosano MPak dextranoan oinarritutako hidrogeletan | EGF eta VEGF | Hidrogelak arratoietan egindako erredura zaurietan aplikatu ziren. GF askeen administrazio maizago batekin konparatuta, hidrogelek orbaintzea azkartu zuten. | [75] |
| Silikona porotsuzko MPak | Plaketen lisatua | Formulazioak *in vitro* egindako zaurien itxiera hobetu zuen. *Ex vivo* egindako zaurietan erregenerazioa sustatu zuen, gertatutako efektu proliferatiboak eta azidofiliak frogatu zutenez. | [76] |
| Fragmina-protamina MP/NPak | PRP | Formulazioa arratoietan egindako lodiera partzialeko zaurietan administratu zen, non errepitelizazioa eta angiogenesia sustatu zuen. | [77] |
| Heparinarekin konjugatutako PLGA NPak fibrina gel batean. | PRP | Formulazioarekin tratatutako zauriek itxiera azkarragoa eta sustatutako angiogenesia erakutsi zuten, sagu atimikoetan. | [78] |
| Kitosano MPak kolageno matrize batean | Heparina desulfatatua | Formulazioa erredura zaurietan aplikatu ostean, orbaintzea azkartu zuen. Izan ere hantura lehenago murriztu zen eta granulazio ehuna bizkorrago sortu zen. | [79] |
| Lezitina/kitosano NPak | Melatonina | *In vitro* urradura entsegu batean, HaCaT zelulen migrazioa hobetu zuten. | [80] |
| CPH eta CPTEGean oinarritutako, polianhidrido anfifilikozko MPak | Lipokalina-2 | Proteina askea administratzearekin konparatuta, formulazioak zelulen migrazioa handitu zuen, luzatutako askapena dela eta. | [29] |
| PPADT NPak (ROSari sentikorra den nanomateriala) | SDF-1α | NPek farmakoaren bideratze eta askatze eraginkorra egin zuten zaurira, bertan dagoen ROS eduki altuagatik. Gainera, NPekin tratatutako zauriek itxiera azkarragoa eta handitutako baskularizazioa erakutsi zuten sagu eredu batean. | [81] |
| In situ sortutako PCL MPak PCL nanoxaflatan | VIP | Saguetan egindako zauri eszisional batean, formulazioak orbaintzea era esanguratsuan hobetu zuen, granulazio ehunaren sorrera eta angiogenesia sustatuz. | [25] |

*3.2 Nanopartikula lipidikoak*

4. taulan laburtuta ageri denez, NP lipidikoak GF eta beste molekula endogenoak askatzeko DDS egokiak dira. Haien artean, liposomak sakonki ikertuak izan dira, 1960-ko hamarkadan aurkitu zirenetik [82]. Liposomak bigeruza lipidikozko mintz batez osatutako xixku esferikoak dira [83]. Lipidoek ematen dizkieten ezaugarrietaz gain (biobateragarritasuna eta biodegradazioa), zenbait abantaila dituzte haien egitura dela eta: (i) konposatu hidrofilo zein lipofiloak kapsularatzeko gaitasuna, hidrofiloak konpartimentu urtsuan eta lipofiloak bigeruza lipidikoan; (ii) luzatutako askapena lortzeko gaitasuna; eta (iii) epidermiseko konposaketa imitatzen dutenez, azalean farmako pilaketa handitzeko gaitasuna. Dena den, liposomek muga ugari dauzkate, besteak beste, farmakoen kontrolik gabeko askapena eragin dezakeen egonkortasun baxua, kapsularatze efizientzia baxua eta biltegiratzean zehar sedimentazio, agregazio edo fusioa pairatzeko aukera [84, 85].

1988an, Brown eta kideek zaurien orbaintzerako GF bat liposoma batean barneratu zuten lehendabiziz, aukeratutakoa EGFa izan zelarik. EGFa lezitina liposoma geruzanitzetan kapsularatu zuten eta liposoma horiek arratoiei egindako 5 cm-ko ebakiduretan aplikatu zituzten. Liposomek EGFaren esposizio denbora luzatu zuten, eta EGF askearen administrazioarekin konparatuz honako hobekuntzak lortu zituzten: %200-ean handitutako trakzio indarra, kolageno sorreraren sustapena eta fibroblastoen proliferazioaren igoera [86]. Ondoren, beste ikerketa talde batek EGFa zuten beste liposoma geruzanitz batzuk garatu zituzten. Formulazio berri honen eraginkortasuna *in vivo* aztertu zuten bigarren mailako erreduretan, EGF askearekin eta liposoma hutsekin konparatuz. Formulazioak orbaintze bizkorrena lortu zuen hurrengoei dagokienez: kolageno formazioa, zauriaren uzkurdura, fibroblastoen proliferazioa eta epitelioaren berreskuratzea [87]. Liposomen administrazioa errazteko asmoz, kitosano gel batean sartu ziren, zeinak zauria heze mantentzen zuen. Formulazio berri hau bigaren mailako erreduretan aztertu zen ere, liposomekin izandako antzeko emaitzak lortuz. Horrek liposomak kitosano gel batean barneatzearen onura erakusten duelarik [88].

Pierre *et al.*-en arabera, IGF-Iez kargatutako liposomak topikoki administratuz gero, orbaintzea IGF eta hazkuntza hormonaren dosi altuagoak sistemikoki administratuta bezain sustatuta egongo litzateke. Arratoietan egindako orbaintze entsegu bati esker haien hipotesia frogatu zuten, errepitelizazioa neurtuz, hain zuzen ere [89].

Xiang eta kideek liposomek farmakoak barneratzeko duten ahalmena ikertu zuten. Zentzu horretan, bFGFa liposometan kapsularatzeko 4 metodoen egokitasuna aztertu zuten. Metodo denek antzeko abantailak eskaintzen zituzten, prestaketa erraza eta ekoizpen-baldintza arinak, esaterako. Baina, zenbait desberdintasun zituzten, besteak beste, kapsularatze tasa, bioaktibitatea eta egonkortasun fisikoa. Aztertutako metodoen artean, pH gradientearen metodoa egokiena zela erabaki zuten. Horregatik jarraian egindako *in vivo* entsegurako, metodo honen bidez ekoitzi ziren liposomak. *In vivo* entsegua arratoiei egindako bigarren mailako erreduretan burutu zen, eta bertan, formulazioak orbaintzea sustatzeko, proliferazio dermala bizkortzeko eta kolagenoa sortzeko gaitasuna erakutsi zuen [90]. Azkenik, SDF-1α zuen liposoma formulazio bat garatu zen, eta merkaturatutako dermis azelular baten (Alloderm®) barne dispertsatu zen. SDF-1αa bi eratan barneratu zen dermis artifizialean, liposometan kapsularatua edo aske. Liposometan sartuta dispertsatzea estrategia hobea dela frogatu zen, izan ere, sagu diabetikoetan egindako lodiera osoko zaurietan, liposometako SDF-1αak zelulen proliferazio iraunkorragoa, granulazio ehun lodiagoa eta zauriaren itxiera hobetua lortu zituen [91].

Liposomek dituzten mugak gainditzeko asmoz, NP lipidikoen belaunaldi berri bat garatu zen, nanopartikula solido lipidikoak (*solid lipid nanoparticle* edo SLN). SLNak giro tenperaturan solido diren lipidoez eta egitura egonkortzen duten surfaktanteez osatutako NPk dira [92]. Liposomekin alderatuz gero, askapena erregulatzeko malgutasun handiagoa dute eta barneratutako farmakoen babes hobea eskaintzen dute, haien egoera solidoak inguruko fase urtsuarekin farmako hidrofiloen trukea txikitzen baitu [93,94]. Hala eta guztiz ere, SLNek egonkortasun mugatua dute, izan ere, biltegiratzean zehar sare kristalinoaren akatsak murrizten dira, farmakoen kanporaketa eraginez [40]. Arazo hau gainditzeko, garraiatzaile lipidiko nanoegituratuak (*nanostructured lipid carrier* edo NLC) garatu ziren, hauek matrize amorfoa duten NP lipidikoak dira eta lipido solido eta likidoen nahasketez osatuta daude [95,96]. Horretaz gain, NLCek SLNek baino farmako gehiago kargatzeko ahalmena dute eta amaierako dispertsioan ur eduki txikiagoa dute. SLNen mugen arren, bi NP mota hauek abantaila ugari dituzte orbaintzean erabiliak izateko, hauetako zenbait liposomekin partekatzen dituztelarik: (i) kontrolatutako askapena ahalbidetzen dute; (ii) azalaren hidratazio efektua handitzen dute, haien itsaskortasun eta oklusibitateari esker; (iii) haien tamaina txikiak azalarekin kontaktu estua ahalbidetzen du; eta (iv) administrazio topikoa baimentzen dute, esposizio sistemikoa ekidinez [95].

Esandakoa kontuan izanda, gure ikerketa taldeak EGFa SLN eta NLCtan kapsularatu zuen. Garatutako formulazioek EGFaren bioaktibitatea mantendu zuten ekoizte prozesuaren zein gamma esterilizazio prozesuaren ondoren. Orduan, haien eraginkortasuna sagu diabetikoetan (*db/db* saguak) egindako loditaera osoko zauri eszisional eredu batean frogatu zen. Formulazio biek orbaintzea antzeko neurrian sustatu zuten, EGFaren dosi altuago batekin konparatuz gero. Formulazioek orbaintzearen ondorengo atalak hobetu zituzten: zauriaren itxiera, errepitelizazioa eta hantura prozesuaren ebazpena. Dena den, NLCak egokiagoak zirela erabaki zen haien abantailengatik, hots, kapsularatze efikazia altuagoa eta disolbatzaile organikoen erabilera eza ekoizpen prozesuan zehar [97]. Hori dela eta, txerrietan egindako *in vivo* entseguan EGFdun NLCak erabili ziren soilik (5. irudia). Marruskariekin konparatuz, txerriak maneiatzeko zailago dira, haien tamaina handia dela eta. Baina, beste aldetik, haien orbaintze prozesua gizakiarenaren antzekoagoa da, eta zauri handiagoak egitea baimentzen dute, kasu honetan zauriek 30 $cm^2$-ko azalera zuten. Entsegu honetan lortutako emaitzak aurrekoekin bat datoz, izan ere, NLCek zauriaren itxiera bizkortu zuten eta orbaintzearen kalitatea hobetu zuten EGF askearen dosi altuago batekin konparatuz [98]. Azkenik, haien administrazio topikoa errazteko asmoz, EGFz kargatutako SLN eta

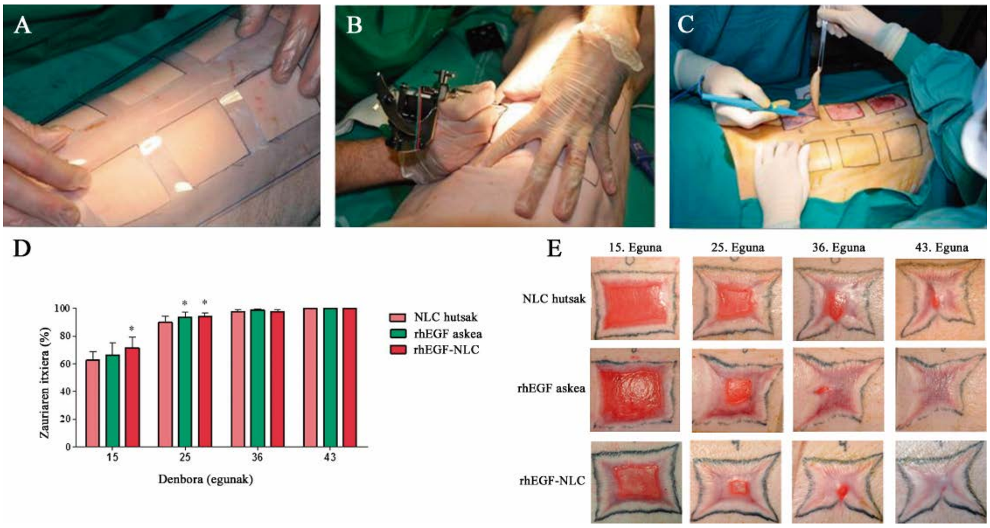


**5. Irudia.** *In vivo* zauri eredua txerrietan EGFa duten NLCak administratzeko. (A-C) Zauria egiteko prozesu-kirurgikoa: (A) Zauriaren azalera estandarizatzeko plastikozko markoa. (B) Zauriaren perimetroaren tatuajea. (C) Diatermia monopolarra erabiliz lodiera osoko zauriak egiteko prozedura kirurgikoa. (D) Zauriaren itxieraren irudikapen grafikoa bigarren astetik entseguaren amaieraraino. Datuak batazbesteko ± SD moduan daude. Esangura estatistikoa $*p<0,05$ NLC hutsekin konparatuta. (E) Talde experimental bakoitzaren zaurien irudiak. Gainza *et al.*-etik [99] baimenarekin kopiatua eta moldatua (© 2014).

NLCak hidrogel erdisolidoetan (Noveon AA-1 eta Pluronic F-27an oinarrituta) edo fibrinan oinarritutako bio-aldamioetan barneratu ziren. Formulazio denek EGFaren askapen luzatua erakutsi zuten gutxienez 48 orduz. Horretaz gain, barneraketa minimoa erakutsi zuten azal osoko *stratum corneumean* zehar eta antzeko xurgapena kaltetutako azalean zehar *in vitro* entseguek erakutsi zuten moduan. Haien artean, fibrinan oinarritutako formulazioak abantailatsuenak zirela erabaki zen, honakoei esker: biobateragarritasun ona, egonkortasun hobea, fibrinaren gaitasuna bitartekari hemostatikoa izateko eta ehun berria sortzen den bitartean matrize moduan aritzeko duen gaitasuna [99].

EGFa NLCtan kapsularatuz lortutako emaitza onen ondorioz, ikerketa berri batean LL37 peptido antimikrobianoa NLtan barneratzea erabaki genuen. kapsularatze prozesuak ez zuen farmakoaren bioaktibitatea aldatu, izan ere, bere ekintza antimikrobianoa mantendu zuen *E. coli*ren aurka eta baita bere ekintza antiinflamatorioa ere, lipopolisakarikoak (LPS) eragindako makrofagoen aktibazioa ekidinez. Formulazioaren eraginkortasuna aztertzeko *db/db* sagu diabetikoetan egindako lodiera osoko zauri eszisional eredu bat erabili zen. Emaitzek erakutsi zutenez, garatutako formulazioa orbaintzea hobetzeko gai izan zen zauriaren itxiera, errepitelizatioa eta hantura prozesuaren ebazpenari dagokienez [100]. Fumakia *et al.*-ek LL37a SLNtan barneratu zuten, serpin-A1arekin batera. Garatutako formulazioak *E. coli* eta *S. aureus*en aurrean aktibitate antibakterianoa erakutsi zuen, *in vitro* fibroblasto eta keratinozitoetan egindako zaurien itxiera sustatu zuen eta *in vitro* LPSaren aurkako makrofagoen ekintza inflamatorioa ekidin zuen [31].

*3.3 Nanozuntzezko egiturak*

Nanozuntz sareak, haien egitura bereizgarria dela eta, apositu moduan erabiliak izateko oso aproposak dira, 5. taulan laburtzen den bezala. Orokorrean, elektroirutearen bitartez ekoizten dira. Teknika honek indar elektrostatikoa erabiltzen du tanta batetik nanozuntzak sortzeko [101]. Horrela sortutako nanozuntz polimerikoak biodegradagarriak eta ehundu gabeak dira, eta haien diametroa nanometro gutxi batzuetatik mikrometrotara bitartekoa da [35,102]. Orbaintzean erabiltzeko zenbait ezaugarri onuragarri dituzte, haien artean, bolumenaren araberako azalera handia eta porositate altua. Bi ezaugarri horiek gasen sarrera eta exudatuen garbiketa ahalbidetzen dute, horrela zelulen arnasketa baimenduz eta zaurian hezetazuna mantenduz deshidratatu ez dadin [103]. Horretaz gain, nanozuntzezko mintzak oso erakargarriak dira ehun ingeniaritzarako, izan ere, matrize extrazelularrarekin (*extracellular matrix* edo ECM) duten antzekotasuna dela eta, zelulen migrazio eta proliferazioa sustatzen dute eta ehunaren sorrerarako euskarri moduan jokatzen dute [44,104].

Farmakoen garraioari dagokionez, apositu hauek farmakoak kargatzeko ahalmen altua daukate, eta gainera, inguruneko

**4. Taula.** GF eta beste konposatu aktiboak askatzeko garatutako NP lipidikoen laburpena eta haiekin lortutako emaitza nagusiak.

| DDS | GF | Emaitzak | Erref. |
|---|---|---|---|
| Lezitinazko liposoma geruzanitzak | EGF | EGF askearekin konparatuz, formulazioak EGFaren iraupen lokala luzatu zuen arratoiei egindako 5 cm-ko ebakietan. Horregatik, formulazioak zauriaren trakzio indarra, kolageno eraketa eta fibroblastoen proliferazioa handitu zituen. | [86] |
| Kolesterol eta DPPC-ko liposoma geruzanitzak | EGF | Formulazioaren eraginkortasuna arratoietan egindako bigarren mailako erreduretan aztertu zen, non gainontzeko taldeekin alderatuz orbaintze azkarrena lortu zuen, kolageno eraketa, zauriaren uzkurdura, zelulen proliferazioa eta epitelioaren birsortzeari dagokionez. | [87] |
| Kolesterol eta DPPC-ko liposoma geruzanitzak kitosano gel batean | EGF | Arratoiei egindako bigarren mailako erreduretan administratu ostean, formulazioak ondorengoek baino errepitelizazio bizkorragoa lortu zuen: EGFa zuzenean kitosano gelean sartuta eta EGFdun liposomen administrazio zuzena. Beste aldetik, garatutako formulazioarekin eta aipatutako bi kontrolekin fibroblastoen proliferazioa antzekoa izan zen. | [88] |
| Liposomak | IGF- I | Arratoietan eragindako erredura eredu batean ondorengoak aplikatu ziren: garatutako formulazioa, hazkuntza hormona eta IGF zein IGF-Iez kargatutako liposomen dosi sistemiko altuagoak. Hiru formulazioek antzeko neurrian sustatu zuten orbainzea. | [89] |
| Soiaren lezitinaz eta kolesterolez osatutako liposomak | bFGF | Formulazioa arratoietan egindako bigarren mailako erreduretan administratu zen. Aplikatutako dosi ertainak orbaintze osoagoa lortu zuen ondorengoei dagokionez: behaketa morfologikoa, zelula dermalen proliferazioa eta TGF-β1en espresioa. Beste aldetik, orbaintze denbora eta kolageno metaketaren sustapena antzekoak izan ziren aplikatutako dosi ertain eta altuarekin. | [90] |

| DDS | GF | Emaitzak | Erref. |
|---|---|---|---|
| DSPC, DSPA eta kolesterolezko liposomak dermis azelular batean (Alloderm) | SDF-1 | Liposomek SDF-1aren aktibitatea mantendu zuten i*n vitro*. *In vivo* zauri eszisional eredu murino diabetiko batean administratu ziren, non SDF-1 askearen administrazioarekin konparatuz honakoak hobetu zituzten: dermisean epe luzerako zelulen proliferazioa sustatu zuten, granulazio ehuna loditu zuten eta zauriaren itxiera apur bat azkartu zuten. | [91] |
| SLNak (precirol) eta NLCak (precirol eta mygliol) | EGF | Sagu diabetikoen zaurietan administratu ostean, bi formulazioek orbaintzea hobetu zuten EGF askearekin konparatuz, zauriaren itxiera, errepitelizazioa eta hantura prozesuaren ebazpenari dagokionez. | [97,98] |
| SLN eta NLCak hidrogel erdisolidoetan (Noveon AA-1 eta Pluronic F-27) edo fibrinan oinarritutako bio-aldamioetan | EGF | Kapsularatze eraginkortasuna altuagoa izan zutelako eta ekoizpen prozesuan ez direlako disolbatzaile organikorik behar, NLCak erabili ziren ondoren egindako *in vivo* entseguan txerri eredu batean. Bertan, NLCek zauriaren itxiera eta kalitatea hobetu zuten EGF-aren dosi altuago batekin konparatuz. | [99] |
| NLCak (precirol eta mygliol) | LL37 | Formulazio denak antzekoak izan ziren ondorengoetan: EGF askapena, EGF sarrera kaltetutako azalean eta sarrera minimoa azal osasuntsuan.<br>NLCak in vitro eragin antimikrobiano eta anti-inflamatorioa izan zuten. In vivo sagu diabetikoetan egindako lodiera osoko zauri eszisionaletan administratu ostean, zauriaren itxiera, errepitelizazioa eta hantura prozesuaren ebazpena hobetzeko gai izan ziren. | [100] |
| SLNak (glizeril monoesteraratoa eta α-fosfatidilkolina | LL37 eta Serpin-A1 | Formulazioak E. coli eta S. aureusen aurrean eragin antimikrobianoa aurkeztu zuen. In vitro egindako urradura entsegu batean zauriaren itxiera sustatu zuen. LPS-ren aurrean, hazkuntzaren geruzabakarraren osotasuna babestu zuen eta eragin anti-inflamatorioa erakutsi zuen. | [31] |

kalteen aurrean babes bikaina ematen diete. Horretaz gain, formulazio hauek apar-teko askapen kontrolatua eskaintzen dute, farmakoen aktibitate terapeutikoa luzatuz [35]. Elektroirute teknika erabiliz, farmakoak 3 eratan sar daitezke nanozuntz mintzetan: (i) koposatu aktiboa zuzenean nahastuz edo emultsionatuz elektroirute disoluzioan; (ii) elektroirute ardazkidea erabiliz, teknika honetan bi osagai nahasezin aldi berean elektroiruten dira elikadura kapilar desberdinen bidez, muin-azal moduko egiturak lortuz; eta (iii) farmakoak nanozuntzen gainazalean immobilizatuz, elkarrekintza ahul (hidrogeno lotura, edo elkarrekintza elektrostatiko, hidrofobiko zein van der Waalsena) zein lotura kobalenteen bidez haien gainazalean aldaketa kimikoak eraginez [105].

Aurreko paragrafoan aipatutako 3 metodoak erabiliak izan dira, orbaintzerako nanozuntzen barne GFak eta bestelako molekula aktiboak sartzeko. Karga zuzenaren artean, gure ikerketa taldeak EGFa eta *Aloe vera* estraktua PLGArekin emultsionatu zituen, bi konposatu aktiboen efektu onuragarriak gehitzeko. *In vitro*, nanozuntzek fibroblastoen proliferazioa sustatu zuten, eta eragin antimikrobianoa erakutsi zuten *S. aureus* eta *S. epidermidisen* aurrean. *In vivo*, zauriaren itxiera eta errepitelizazioa era esanguratsuan bizkortu zituzten sagu diabetikoei egindako lodiera osoko zaurietan [106]. Emultsioen elektroirute teknika, EGFa PC eta hialuronan nanozuntzetan eta bFGFa poli(etilenglikol)-poli(D-L-laktiko) (PELA) nanozuntzetan barneratzeko erabili izan da ere bai. Teknika hau erabiltzearen helburua kapsularatze eraginkortasuna handitzea eta askapenaren eztanda edo *burst* efektua arintzea izan zen. Estrategia honen bitartez garatutako bi formulazioek zaurien orbaintzea hobetzeko gai izan ziren *in vivo* [107,108].

Konposatu hidro- zein lipofiloak dagozkien elektroirute disoluzio hidro- zein lipofiloetan zuzenean disolbatuz, apositu moduan erabiltzeko formulazioak garatu izan dira. Nanozuntz hidrofiloen artean, Bertoncelj *et al.*-ek PRPa kitosano/PEO mintz batean barneratu zuten. Mintz horrek, *in vitro* zelulen proliferazioa estimulatu zuen, zelulen morfologia aldatu zuen eta haien mugikortasuna mugatu zuen [109]. Beste ikerketa batean, β-estradiol konposatu lipofiloa poliuretano/dextrano nanozuntzetan barneratu zen, menopausia ostean erabiltzeko apositu bat garatzeko asmoz. *In vivo* egindako zauri partzialetan ezarri ostean itxiera bizkortzeko gaitasuna erakutsi zuen [34].

Askapen kontrolatuago bat lortzeko asmoz, GFak zuzenean nanozuntzetan barneratu beharrean, NPetan kapsularatuta barneratu daitezke nanozuntzetan. Zentzu horretan, Lai eta kideek sare dual bat garatu zuten, kolageno eta azido hialuronikozko zuntzez osatua, EGF, bFGF, VEGF eta PDGFaren askapen fisiologikoa imitatzeko helburuarekin. Hori dela eta, EGFa eta bFGFa zuzenean barneratu ziren zuntzetan, haien askapen azkarra lortzeko; eta VEGFa eta PDFGa gelatina NPtan kapsularatuta barneratu ziren nanozuntzetan, askapen geldoago bat lortzeko. Behin itxarondako askapen profila lortzen zela *in vitro* egiaztatu ondoren, apposituaren eraginkortasuna *in vivo* aztertu zen. Estreptozotozinak eragindako diabetesa zuten arratoiei egindako lodiera osoko zaurietan aplikatu ziren eta 6. irudian ikus daitekeen bezala, emaitza bikainak lortu ziren [110]. Estrategia berdina erabiliz, Xie *et al*.-ek kitosano/PEO nanozuntzak garatu zituzten. VEGFaren askapen azkarra eta PDGF-BBaren askapen geldoa lortzeko asmoz, VEGFa zuzenean barneratu zuten nanozuntzetan eta PDGF-BBa PLGA NPtan kapsularatu ondoren sartu zuten nanozuntzetan. *In vitro* askapen entseguek bilatutako profila lortu zela baieztatu ostean, formulazioaren eraginkortasuna arratoietan *in vivo* ikertu zen merkaturatutako apositu baten aurrean (Hydrofera Blue®). Emaitzek erakutsi zutenez, garatutako apposituak orbaintzea azkartzeko gai izan ziren etapa goiztiar zein berantiarretan; goiztiarrean angiogenesia sustatuz, errepitelizazioa handituz eta granulazio ehunaren sorrera kontrolatuz; eta berantiarrean kolageno metaketa azkartuz eta erremodelazioa aurreratuz [111].

Scheneider eta kideek EGFa zuzenean barneratu zuten zeta fibroinezko nanozuntz mintz batean. Formulazioak hasieran eztanda edo *burst* moduko askapen bat erakutsi zuen, keratinozitoen aktibazio azkarrarentzat komenigarria dena, *in vitro* gizaki azal baliokide batean egindako zaurietan frogatu zen bezala. Entsegu horretan, apposituak zauriaren itxiera bizkortu

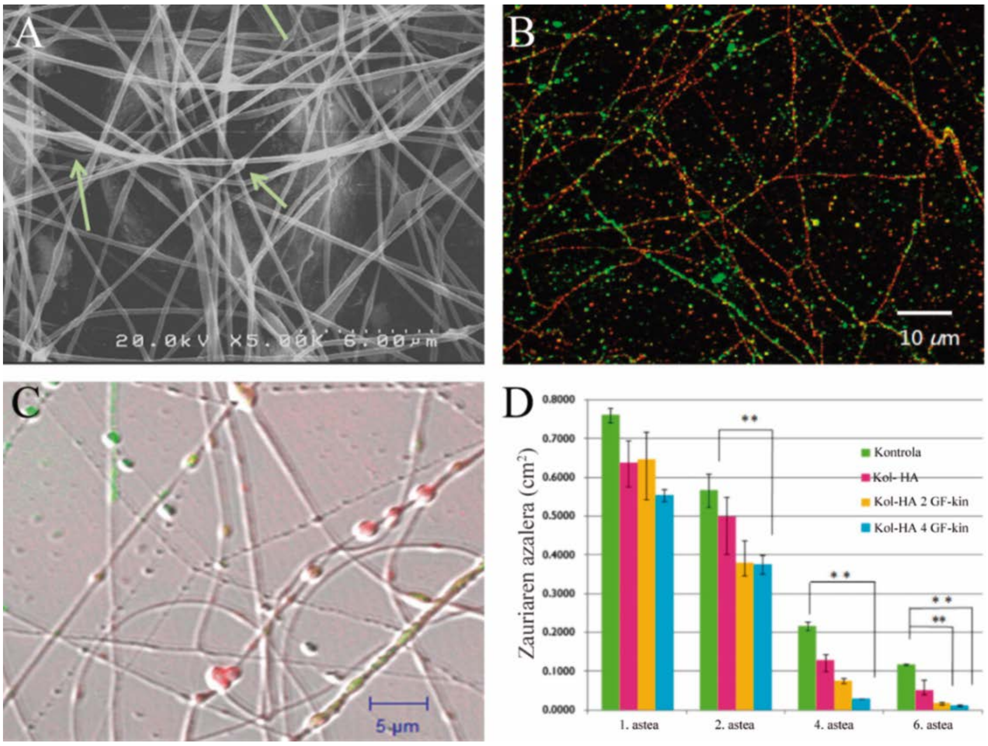


**6. Irudia**. Kolageno eta azido hialuroniko nanozuntzen konpositea, barnean GF askeak (bFGF eta EGF) eta gelatina NPetan kapsularatutako GFak (VEGF eta PDGF) dituena. (A) Nanozuntzen morfologiaren SEM irudiak (Geziek gelatina NPak adierazten dituzte, eskala barra 6 μm). (B) Nanozuntzen irudi fluoreszentea mikroskopia konfokalarekin aterata. Kolagenoa gorriz tindatua eta azido hialuronikoa berdez. (C) Mikroskopia konfokalaz lortutako irudi fluoreszentea, zeinean kolageno nanozuntzetan fluoreszeinaz (gorri) kargatutako gelatina NPak dauden eta azido hialuroniko nanozuntzetan rodamina B-z (berdea) kargatutako gelatina NPak dauden. (D) Zauriaren azalera denbora desberdinetan ondorengo taldeetan: tratatu gabeak, kolageno/azido hialuroniko nanozuntzak, kolageno/azido hialuroniko nanozuntzak bFGF eta EGF-rekin eta kolageno/azido hialuroniko nanozuntzak bFGF, EGF ,VEGF eta PDGFrekin (**p<0,01 eta *p<0,05). Lai *et al.*-etik [111] baimenarekin kopiatua eta moldatua (© 2014).

eta errepitelizazioa sustatu zituen [48]. Dena den,ondoren egindako *in vivo* orbaintze entsegu batean, farmakoaren barneraketa zuzenaren eta konjugazio kimikoaren arteko alderaketa egin zen. EGFa gainazalean konjugatuta zuen formulazioarekin emaitza arinki hobeak lortu ziren, zauriaren itxiera tasa eta epidermiseko desberdintzapenari dagokienez [112]. Beste ikerketa batean, EGFaren barneraketa zuzena elektroirute ardazkidearekin alderatu zen PLCLLC eta gelatina nanozuntzetan. Elektroirute ardazkidearekin emaitza hobeak lortu ziren, izan ere, formulazio horrek farmakoaren askapen luzatuagoa baimentzen zuen eta horren eraginez, gantzetik eratorritako zelula amen (*adipocyte derived stem cells* edo ADSC) proliferazioa eta desberdintzapena gehiago sustatu zituen [113].

Beste aukera interesgarri bat poli(3hexiltifenea) (P3HT) erabiltzea da. Polimero honek argi estimulazioaren energia optikoa energia elektrikoan bilakatzen du. Prozesu hori fotokorronte izenaz ezagutzen da eta azalaren erregenerazioan emaitza onuragarriak erakutsi ditu. P3HTaren biobateragarritasuna hobetzeko asmoz, elektroirute ardazkidea erabili zuten EGFa eta P3HTa gelatina/PLLCL nanozuntzen muinean kapsularatzeko. Formulazioak fibroblastoen proliferazioa eta zaurien itxiera hobetu zituen *in vitro* eta argiaren estimulazioaren ostean ADSCak keratinozitoetan desberdintzatzea eragin zuen [114].

Efektu terapeutiko luzeagoak lortzeko asmoz, EGFa nanozuntzen gainazalean immobilizatu daiteke lotura kobalenteen bidez, nanozuntzen gainazalean agerian dauden amina taldeekin lotuz, adibidez. Horren harira, Tigli eta kideek PCL eta PCL/gelatina bio-aldamioetan EGFa immobilizatu zuten. *In vitro* formulazioaren gainean ereindako fibroblastoen hedatze goiztiarragoa eta proliferazio azkarragoa lortu zen [115]. Beste ikerketa batean, EGFa PCL/kolageno nanozuntzen gainazalean kobalenteki lotu ostean antzeko emaitzak lortu ziren, izan ere, keratinozitoen poliferazio eta hedatzea bizkortu zen. Horretaz gain, mintzaren gainean ereindako keratinozitoek desberdintzatzeko ahalmen handitua erakutsi zuten, lorikrinaren espresioaren igoerak erakutsi zuen bezala [116].

Choi *et al.*-ek EGFa kobalenteki lotuta zuen beste formulazio bat garatu zuten. Kasu honetan, EGFa PEG/PCL kopolimero blokeez osautako nanozuntzetan immobilizatu zuten. Formulazio honen eraginkortasuna nanozuntzen gain EGF disoluzioa zuen formulazioarekin konparatu zen. EGFa kobalenteki lotuta zuen formulazioak aktibitate terapeutiko hobea erakutsi zuen *in vitro* zein *in vivo* orbaintze entseguetan, immobilizazioak EGFari eskaintzen dion babes handiagoa dela eta. *In vitro*, keratinozitoen gene espezifikoen espresioaren igoera behatu zen, eta *in vivo* zauriaren itxiera azkartua eta EGFRaren espresio handitua ikusi ziren [117]. Ikerketa horietan lortutako emaitza onuragarriak kontuan hartuta, ondorengo lan batean PEG/PC kopolimero blokeez osatutako nanozuntzen gainazalean EGFa immobilizatzeaz gain, bFGFa muinean kapsularatu zuten elektroirute ardazkidea erabiliz. Fomulazio honetan bFGFak hasierako eztanda moduko askapena erakutsi zuen, EGFaren askapenik, ordea, ez zen behatu. GF bakarra zuten formulazioekin konparatuta, bi GFak zituen formulazioak erredura zaurien itxiera bizkortu zuen, zauri helduagoak lortuz zazpigarren egunerako, estreptozotozinak eragindako diabetesa zuten saguetan [117].

Song eta kideek erakutsi zutenez, nanozuntzen gainazalean konposatu aktiboak kobalenteki lotzeko era gehiago daude. Zentzu horretan, Cys-KR12 (LL37 peptido antimikrobianotik eratorritako motiboa) zeta fibroinazko nanozuntzekin konjugatu zuten, EDC/NSH eta tiol-maleimida *klick* kimikaren bitartez. Konjugazio prozesuak ez zuen Cys-KR12aren bioaktibitatea kaltetu, izan ere, *in vitro* eragin antimikrobianoa eta proliferatiboa mantentzen zituen, baita LPSak eragindako hantura deuzesteko gaitasuna ere [119].

Patel *et al.*-ek burututako ikerketa batean, bFGFa eta laminina PLLaren gainazalean immobilizatuak izan ziren, heparinak molekula endogenoekin lotzeko duen gaitasunean oinarrituta. Horrretarako, PLLa heparinarekin funtzionalizatu zen eta ondoren bFGFa eta laminina lotu zitzaizkion. Ondoriozko formulazioak orbaintzea hobetzeko gai izan zen *in vitro* urradura saio batean, batez ere, nanozuntzak zauriraen elkarzut kokatuta zeudenean [120].

**5. Taula**. GF eta beste konposatu aktiboak askatzeko garatutako nanozuntz mintzen laburpena eta haiekin lortutako emaitza nagusiak

| DDS | GF | Karga metodoa | Emaitzak | Erref. |
|---|---|---|---|---|
| PLGA eta Aloe vera nanozuntzak | EGF | Karga zuzena, emultsifikazioz | *In vitro* fibroblastoen proliferazioa hobetu zuten eta eragin antimikrobianoa izan zuten. Sagu diabetikoetan egindako zauri eredu batean zauriaren itxiera eta errepitelizazioa azkartu zituzten. | [106] |
| PCL eta hialuronan nanozuntzak | EGF | Karga zuzena, emultsifikazioz | Formulazioak keratinozitoen eta fibroblastoen proliferazioa eta infiltrazioa sustatu zituen *in vitro*. Eta *in vivo*, azal funtzional baten birsortzea bultzatu zuen. | [107] |
| PELA nanozuntzak | bFGF | Karga zuzena, emultsifikazioz | Formulazioak fibroblastoen adhesioa, proliferazioa eta ECMko proteinen jariaketa sustatu zituen. Arratoi diabetikoei egindako zaurietan ezartzean orbaintzea hobetu zuten, 2 asteetan errepitelizazio osoa eta azaleko apendizeen birsortzea lortuz. | [108] |
| Kitosano/PEO nanozuntzak | PRP | Karga zuzena, nahastuz | Formulazioak zelulen proliferazioa estimulatu zuen, haien morfologia aldatu zuen eta haien mugikortasuna mugatu. | [109] |
| PU eta dextrano nanozuntzak | β-estradiola | Karga zuzena, nahastuz | Formulazioa arratoiei egindako lodiera partzialeko zaurietan aztertu zen, non zauriaren itxiera bizkortu zuen. | [34] |
| Kolageno eta azido hialuroniko nanozuntz dualak | VEGF, bFGF, PDGF eta EGF | Karga zuzena. bFGF eta EGF zuzenean eta VEGF eta PDGF gelatina NPen barne | Formulazioak zelula endotelialen hazkuntza tasa handitu zuen, eta haien arteko saretzea hobetu zuen. Arratoi diabetikoei egindako zaurietan, formulazioak zauriaren itxiera bizkortu zuen, kolageno metaketa handitu zuen eta hodien heltzea sustatu zuen. | [110] |
| Kitosano eta PEO nanozuntzak | VEGF eta PDGF-BB | Karga zuzena. VEGF zuzenean eta PDGF-BB PLGA NPen barne | Hydrofera Blue® komertzialarekin konparatuz, formulazioak zaurien itxiera bizkortu zuen arratoietan, fase goiztiar (angiogenesia sustatuz, errepitelizazioa handituz eta granulazio ehunaren sorrera kontrolatuz), zein berantiarretan (kolageno metaketa azkartuz eta erremodelazioa aurreratuz). | [111] |

| DDS | GF | Karga metodoa | Emaitzak | Erref. |
|---|---|---|---|---|
| Zeta nanozuntzak | EGF | Karga zuzena, nahastuz | Nanozuntzek zauriaren itxiera eta errepitelizazioa sustatu zuten, *in vitro* giza azal baliokidean egindako zaurietan | [48] |
| Zeta nanozuntzak | EGF eta zilar sulfadiazina | Karga zuzena eta gainazaleko konjugazioa | Farmakoa konjugatua zuen formulazioarekin tratatutako saguek zauriaren itxiera arinki azkarragoa izan zuten eta epidermisaren desberdintzea ile folikulu eta gantz guruinetara handitua. | [112] |
| PLLCL eta gelatina nanozuntzak | EGF, intsulina, hidrokortisona eta azido erretinoikoa | Karga zuzena eta elektroirute ardazkidea | Askapen luzeagoa eragin zuenez, elektroirute ardazkidez ekoiztutako formulazioak zelulen proliferazio eta desberdintzapen handiagoa eragin zuen. | [113] |
| Gelatina/ PLLCL eta P3HT nanozuntzak | EGF | Elektroirute ardazkidea, muina EGF eta P3HT-z osatua | Formulazioak fibroblastoen proliferazio eta zauriaren itxiera hobetu zituen *in vitro*. Argi izpiez estimulatu ostean, formulazioak ADSCak keratinozitoetara desberdintzeko gai izan zen, P3HTak energia optikoa elektriko bihurtzeko duen gaitasunari esker. | [114] |
| PCL eta PCL/gelatina nanozuntzak | EGF | Gainazalean konjugatua | EGFaren immobilizazioari esker, nanozuntzen gainean ereindako fibroblastoen hedatzea eta proliferazioa azkartu zen. | [115] |
| PCL eta PCL/kolageno nanozuntzak | EGF | Gainazalean konjugatua | Formulazioak keratinozitoen hedapena, proliferazioa eta desberdintzeko ahalmena handitu zituen. | [116] |
| PEG eta PCL nanozuntzak | EGF | Gainazalean konjugatua | Formulazioa sagu diabetikoetan egindako erredura zaurietan administratu zenean, zauriaren itxiera hobea eta EGFRaren espresioaren igoera behatu ziren. Horretaz gain, *in vitro* keratinozitoen gene espezifikoen espresioa sustatu zuen. | [117] |
| PCL/PEG nanozuntzak | bFGF eta EGF | EGFa gainazalean konjugatua eta bFGFa elektroirute ardazkideaz sartuta | Formulazioak askatze profil bimodala erakutsi zuen, hasierako bFGFaren eztanda askapenarekin eta EGFren askapenik gabe. Sagu diabetikoetan egindako erredura zaurietan formulazioa zauriaren itxiera azkartzeko eta heltzea sustatzeko gai izan zen. | [118] |

| DDS | GF | Karga metodoa | Emaitzak | Erref. |
|---|---|---|---|---|
| Zeta fibroina nanozuntzak | Cys-KR12 | Gainazalean konjugatua | Kapsularatutako farmakoak bere ekintza antimikrobiano eta proliferatiboak mantendu zituen nanozuntzetan, baita keratinozitoen desberdintzea sustatzeko eta LPSak eragindako hantura inhibitzeko ahalmena ere. | [119] |
| PLLA nanozuntzak heparinarekin | Laminina eta bFGF | Gainazalean konjugatua | Formulazioa orbaintzea sustatzeko gai izan zen *in vitro* urradura entsegu batean, batez ere, nanozuntzak urradurarekiko elkarzut kokatzean. | [120] |

## 4. Ondorioak eta etorkizuneko ikuspegia

Azken urteotan, zauri kronikoen intzidentzia era kezkagarrian handitu da, arriskuan dagoen populazioa hazi den heinean. Horretaz gain, tratamendu eraginkorren gabezia dela eta, zauri kronikoak zama ekonomiko zein kliniko handia bilakatzen ari dira. Prozesu fisiologikoarekin konparatuz, zauri kronikoen orbaintzean hainbat asaldura gertatzen dira, hala nola, GFen eta prozesuaren erregulazioan parte hartzen duten beste molekula batzuen mailaren jaitsiera. Hori dela eta, konposatu horien administrazio exogenoa estrategia itxaropentsua da orbaintzerako, baina haien erabilera klinikoa murriztuta dago, *in vivo* daukaten egonkortasun baxua dela eta. Arazo hau gainditzeko bide bat, konposatu bioaktibo horiek DDS berrietan kapsularatzea da, zeinen artean, MP/NP polimerikoak, NP lipidikoak, nanozuntzezko egiturak eta haien arteko konbinazioak daudelarik. DDS horiek, kapsularatutako farmakoa babesteaz gain, honako abantailak dituzte: biobateragarritasun ona, askapen kontrolatu edota luzatua, farmako karga handia eta ezaugarri mekaniko onak. Horretaz gain, erabilitako DDS mota eta polimeroaren arabera ezaugarri zehatzak lor daitezke, hala nola, zuzendutako garraioa edo ECMa imitatzen duen ingurunea.

Laburbilduz, nanoteknologian oinarritutako DDSetan GFen eta bestelako molekula endogeno aktiboen barneraketak potentzial handia erakutsi du zauri kronikoen tratamenduan eta azalaren leheneratzean. Dena den, momentura arte, GFak askatzen dituzten DDSen ikerketak fase preklinikoan jarraitzen du, eta ikerketa gehiago behar dira fase klinikora heltzeko. Egiteke dauden ikerketa preklinikoen artean hurrengoak daude: animalia ereduetan tolerantzia eta toxizitate saioak eta txerrien moduko animalia eredu handiagoetan eraginkortasun saioak.

Aipatutako DDS gehienak sistema topikoak direnez, haien onarpenaren aurretik gai kritiko bat ikertu behar da, kapsularatutako farmakoaren xurgapen sistemikoa, alegia. Horretaz gain, polimeroen egokitasuna aztertu behar den beste gai gako bat da, izan ere, deskribatutako zenbait DDS garatzeko erabili diren polimeroak ez daude onartuta klinikan erabiliak izateko.

Nahiz eta entsegu klinikorik edo merkaturatutako produkturik ez dagoen GFak dituzten DDS hauekin, badaude nanoteknologian oinarritutako bi produktu orbaintzerako merkaturatuak. Horietatik lehena Altrazeal® da, hauts txuri kristalino bat, liofilizatutako poli-2-hidroxietilmetakrilatozko (pHEMA) eta poli-2hidroxipropilmetakrilatozko (pHPMA) NPtaz osatuta dagoena. Nanoflex teknologiari esker, zauriaren exudatuarekin kontaktuan sartzean NPak hidratatu eta agregatzen dira mintz heze eta malgu bat bilakatuz [121]. Bigarren produktua Talymed® da, poli-N-azetil glukosaminaz (pGIcNAc) osatutako nanozuntz laburtuez osatutako matrize aurreratu bat [122]. Horietaz gain, gaur egun partehartzaileak aukeratzeko fasean dagoen entsegu kliniko bat dago, zeinean, SPINNERaren jokaera eta segurtasuna aztertuko diren. SPINNERa eskuko elektroirute tresna bat da, *in situ* nanozuntzezko apposituak ekoizteko balio duena [123].

## 5. Eskerrak

I. Garcia-Oruek Eusko Jaurlaritzari doktoratu aurreko laguntza eskertzen dio. Projektu hau neurri batean Espainiako Ekonomia eta Lehiakortasun Ministerioak finantziatu du (INNPACTO, IPT-2012-0602-300000, 2012). Horretaz gain, partzialki Eusko Jaurlaritzak finantziatu du (ELKARTEK 2015, Nanoplatform, KK-2015/0000036).

**Erreferentzien zerrenda 43-53 orrialdeetan aurkitzen da.**

# Helburuak

Sarreran zehaztu denez, zauri kronikoak osasun arazo bat bilakatzen ari dira, izan ere egungo terapiek ezin dute orbaintze eraginkor bat ziurtatu. Gainera, haien intzidentzia hazten ari da, arrisku-handiko populazioa, pertsona diabetiko, obeso, erretzaile edota zaharrez osatua dagoena, era kezkagarrian hazten ari delako. Hori dela eta, atzeratutako orbaintzea tratatzeko terapia berrien garapenak garrantzia irabazi du azken urteotan. Beste batzuen artean, orbaintze prozesuan parte hartzen duten molekula endogenoen administrazioa terapia horietako bat da. Dena den, *in vivo* egonkortasun laburra dute, eta ondorioz zaurian dauden proteasetaz babestuko dituen eramaile baten barne kapsularatu behar dira, hala nola nanopartikula lipidikoetan. Orbaintzerako beste alternatiba interesgarri bat nanozuntzezko mintzen erabilera da, haien egitura bereizgarriak orbaintzea sustatzen baitu, dituen porositate eta bolumenarekiko gainazal azalera altuak direla eta. Azkenik, beste aukera prometigarri bat bigeruzadun apposituen garapena da, geruza bakoitzaren ezaugarri eta funtzioak bateratzen baititu, hain zuzen ere, gaineko geruza trinkoak funtzio babesgarria du eta azpiko geruza porotsua zauriaren exudatua xurgatzeko diseinatua dago.

Azaldutakoa kontuan hartuz, tesi honen helburua zauri kronikoen tratamendurako baliabide terapeutiko berrien garapena eta karakterizazioa izan zen. Zehazki, ikerketa honen helburuak honakoak dira:

1. LL37 giza peptidoa kapsularatua duten nanoegituratutako eramaile lipidikoen (NLCs) garapena, karakterizazioa eta haien eraginkortasunaren *in vivo* ebaluazioa.

2. EGFa kapsularatuta duten PLGA eta *Aloe verako* elektroirundako nanozuntz apposituen garapena, karakterizazioa eta haien eraginkortasunaren *in vivo* ebaluazioa.

3. PLGA/*Aloe vera* appositetan NLCen barneratzea, haien ezaugarrietako batzuk hobetzeko asmoz, hala nola, zauritik kentzea, elastizitatea, oklusibitatea eta maneiua.

4. Gelatinaz eta kitosanoz osatutako bigeruzadun hidrofilm baten garapena, karakterizazioa eta bere eraginkortasunaren *ex vivo* ebaluazioa.

# Lan experimentala

## 1. KAPITULUA

## LL37a duten nanoegituratutako eramaile lipidikoak (NLC): zauri kronikoen tratamendu topikorako estrategia berri bat.


**LABURPENA**

LL37a giza peptido antimikrobiano bat da, zeinak espektro antimikrobiano zabala izateaz gain, orbaintzea modulatzen duen, angiogenesian, zelula epitelialen migrazio eta proliferazioan eta erantzun immunean parte hartuz. Ikerketa honetan, LL37a nanoegituratutako eramaile lipidikoetan (NLC) barneratu zen, bere eraginkortasuna hobetzeko asmoz. NLCak urtze-emulsifikazio metodoaren bidez ekoiztu ziren, eta haien karakterizazioak erakutsi zuenez, 270 nm-ko batazbesteko tamaina, -26 mV-ko zeta potentziala eta %96,4-ko kapsularatze eraginkortasuna zuten. Giza prepuzioko fibroblastoetan egindako zitotoxikotasun entseguak frogatu zuen formulazioak ez zuela zelulen bideragarritasunean eraginik. Horretaz gain, peptidoa kapsularatze prozesuaren ostean aktibo mantentzen zela *in vitro* egindako bioaktibitate entseguaren bidez frogatu zen. Izan ere, kapsularatutako LL37ak soluzioan zegoen LL37aren hein berean inhibitu zuen LPSak eragindako makrofagoen aktibazioa. *In vitro* egindako entsegu antimikrobianoan NLC-LL37ek *E. coliren* aurkako eraginkortasuna erakutsi zuten. Nanopartikulen eraginkortasuna *db/db* sagu ereduan egindako lodiera osoko zauri eszisionaletan aztertu zen. NLC-LL37ak esanguratsuki hobetu zuen orbaintzea kontzentrazio berdina zuen LL37 disoluzioarekin konparatuz, zauriaren itxierari, errepitelizazio graduari eta hantura prozesuaren ebazpenari dagokionez. Orokorrean, aurkikuntza hauek garatutako formulazioa zauri kronikoen orbaintzean potentzial handia duela iradokitzen dute.

## 1. Sarrera

Orbaintzen ez diren zauri kronikoen intzidentzia esponentzialki handitu da. Horren arrazoi nagusiak populazioaren zahartzea eta horrek dakartzan komorbilitateak dira, hots, diabetesa, bena-gutxiegitasuna eta haiei lotutako gaixotasun kronikoak. Estimatu denez, herrialde garatuen populazioaren %1-2-ak zauri kronikoak pairatuko ditu, Nazio Batuen arabera Europako osasun aurrekontuaren %2-a dena [1,2].

Azaleko zaurien orbaintzea prozesu ordenatua da, bere helburua azalaren hesi funtzioa eta homeostasia berreskuratzea delarik. Denboran eta espazioan gainjartzen diren honako prozesuen bidez gauzatzen da: hasierako hantura erantzuna, fase proliferatiboa eta amaierako erremodelazio fasea [3,4]. Zauri kronikoek ezin dute fase hauetan zehar igaro, hantura fase iraunkor batean harrapatuta geratuz, zeinean zauria ezin den orbaindu. Hantura honek etengabeko makrofago eta neutrofiloen infiltrazioa eragiten du, zelula horiek gehiegizko kolagenasa, proteasa eta oxigenoarekiko espezie erreaktiboak ekoizten dituztelarik. Entzima horiek orbaintzearen bitartekariak degradatzen dituzte eta matrize extrazelular zein epitelio berriaren sorkuntza oztopatzen dute. Horretaz gain, zauri hauek maiz infektatzen dira eta ixteko denbora luzea behar dute, zenbaitetan gaixoaren bizitza arriskuan jarriz [1,5].

Gaur egun, orbaintzeari buruzko ikerketen arreta tratamendu berrien bilaketan jarrita dago, adibidez, orbaintzearen bitartekarien administrazioan. Horren harira, LL37 giza peptido antimikrobianoaren administrazioa garrantzia irabazi duen aukera bat da. Izan ere, LL37aren azpi erregulazioa ultzera kronikoak pairatzeko arrisku handituarekin erlazionatu da [6].

LL37aren preforma inaktiboa (hCAP-18) zelula immune eta dermal-epitelialetan aurkitu da. Azal lesio baten ostean, zelulen degranulazioa dela eta hCAP18a inguru extrazelularrera jariatzen da, aktibatuz eta LL37 peptidoa emanez [4,7]. Molekula honek orbaintzea modulatzen duela ikusi da angiogenesia aktibatuz [8,9] eta zelula epitelialen migrazioa eta proliferazioa sustatuz [10,11]. Are gehiago, espektro antimikrobiano, antibiral eta antifungiko zabala dituela frogatu da [12-15].

Horretaz gain, LL37ak eragin immunomodulatzailea dauka, izan ere, monozito, neutrofilo eta zelula dendritikoentzat kimiotaktikoa da [13]. Gainera, makrofagoek lipopolisakaridora (LPS) lotzean duten erantzun proinflamatorioa neutralizatzeko gai da ere [13,16].

Gaur egun arte burutu diren *in vivo* orbaintze entseguek LL37 askearen dosi eta administrazio maiztasun handiak [15,17] edo terapia genikoa [18] behar izan dituzte orbaintzea hobetzeko, peptidoaren degradazioa azkarra dela eta. Muga horiek gainditzeko asmoz, Chereddy eta kolaboratzaileek LL37a PLGA nanopartikulen barnean kapsularatu zuten, orbaintzearen hobekuntza esanguratsua lortuz formulazioaren dermisbarneko administrazioaren ondoren [19]. Saiakuntza horren harira, LL37a nanoegituratutako eramaile lipidikoetan (*nanostructured lipid carriers* edo NLC) kapsularatzea aukera itxaropentsu bat izan daiteke bere administrazioa hobetzeko, dosiari, administrazio maiztasunari eta segurtasunari dagokionez. NLCak, peptidoa proteasen degradaziotik babesteaz gain, bide topikotik administratu daitezke, horrela peptidoaren bioerabilgarritasun sistemikoa, eta beraz, efektu sistemikoak txikituz. Horretaz gain, NLCak farmakoaren askapen luzatua ahalbidetzen dute eragite lekuan eta biobateragarritasun ezin hobea daukate, ondorioz zauri kronikoen tratamendurako aukera egokia direlarik [20-22].

Hori dela eta, ikerketa honen helburua zauri kronikoen tratamendurako LL37dun NLCen (NLC-LL37) formulazio topiko bat garatzea da. *In vitro* entseguak formulazioaren biobateragarritasuna eta kapsularatutako LL37aren bioaktibitatea frogatzeko egin ziren. Horretaz gain, *E. coliren* aurka saio antimikrobianoak burutu ziren, NLC-LL37en eraginkortasuna bakterioen aurrean aztertzeko. Azkenik, NLC-LL37-aren eragina orbaintzean *in vivo* ebaluatu zen *db/db* saguetan egindako lodiera osoko zauri eredu batean.

## 2. Material eta metodoak

### *2.1 NLC-LL37en ekoizpena*

NLC-LL37ak urtze-emulsifikazio metodoaren bidez prestatu ziren, gure ikerketa taldeak aurretik deskribatutako prozedura erabiliz [23,24]. Laburki, 3 ml ur, 20 mg Poloxamer 188 (Panreac, Espainia) eta 40 mg Tween® 80 (Panreac, Espainia) zituen fase urtsu epel bat (40°C-tara berotua minutu batez), urtutako fase lipidiko batera gehitu zen, fase lipidikoak 200 mg Precirol® ATO 5 (Gattefossé Spain, Espainia) eta 20 mg Miglyol 812N (Sasol Germany, GmbH) zituelarik. Orduan, LL37 disoluzio baten 50 µL (80 mg/ml; 95,0 % purutasuna, Caslo ApS, Danimarka) gehitu ziren eta jarraian nahastea 15 segunduz emulsifikatu zen 50 W-etara (Branson® 250 sonifier, CT, AEB). Lortutako emultsioa 4°C-tara biltegiratu zen lipidoaren ber-kristalizazioa eta NLCen eraketa ahalbidetzeko. Hurrengo egunean, partikulak 100 kDa-eko pisu molekularreko atalasea zuten zentrifuga filtro unitatetan (Amicon, Ultracell 100k, Millipore, Espainia) zentrifugatuz berreskuratu ziren. Hiru zentrifugazio egin zire 2500 rpm-tara 10 minutuz, haien artean partikulak MilliQ urarekin garbituz. Azkenik, NLC esekidura liofilizatu zen kriobabesle modura trehalosa (Sigma-Aldrich, Espainia) erabiliz, pisatutako lipidoaren %15-eko (p/p) amaierako kontzentrazioan. LL37aren karga teorikoa NLC-LL37etan %2-koa (p/p) zen.

*2.2 Nanopartikulen karakterizazioa*

Partikulen batezbesteko tamaina eta polidispertsio indizea (PDI) argi dispertsio dinamikoaren (*Dynamic Light Scattering* edo DLS) bidez neurtu ziren eta zeta potentziala Laser Doppler mikroelektroforesiaren bidez (Malvern® Zetasizer Nano ZS, Zen 3600 modeloa, Malvern instruments Ltd. EB). Zeta potentziala neurtzeko ingurunea ura izan zen (pH 5,6) eta neurtutako mugikortasun elektroforetikoa zeta potentzialean bihurtu zen Smoluchowski hurbilketaren bitartez. Saio bakoitza hirutan burutu zen nanopartikulen liofilizazioaren ostean. Haien morfologia transmisioko mikroskopia elektronikoaren bidez aztertu zen (TEM, Philips EM208S).

NLC-LL37en kapsularatze eraginkortasuna (EE) zeharka neurtu zen, 2.1 atalean azaldutako iragazpen/zentrifugazio prozesuan lortutako gainjalkinaren LL37 askea neurtuz. LL37 askearen kopurua merkaturatutako LL37arentzako ELISA kit baten bidez kuantifikatu zen (human LL37 ELISA kit, Hycult® biotech, Holanda). EEa (%) hurrengo ekuazioaren bidez kalkulatu zen (1):

$$EE=\frac{\text{kantitate teorikoa-LL37 askea}}{\text{LL37 kantitatea teorikoa}}\times 100 \quad (1)$$

*2.3* In vitro *kultibo zelularreko entseguak*

*2.3.1 Kultibo zelularra*

Giza prepuzioko fibroblastoak (*Human Foreskin Fibroblast* edo HFF; ATCC, Manassas, AEB) DMEM ingurunean (Dulbeccos's Modified Eagle's medium; ATCC, Manassas, AEB) kultibatu ziren, honako gehigarriekin: % 15-eko (b/b) behi fetuen seruma (*fetal bovine serum* edo FBS), % 1-eko (b/b) L-glutamina eta % 1-eko (b/b) penizilina-estreptomizina.

RAW 264.7 lerro zelularra (karraskarien makrofagoak; ATCC, Manassas, AEB) berariazko kultibo ingurune batean kultibatu zen DMEM/F-12, GlutaMAX™ Supplement-ean zehazki (Gibco®, Life Technologies, Espainia). Ingurune honi ere zenbait gehigarri erantsi zitzaizkion, % 10-eko (b/b) FBSa eta % 1-eko (b/b) penizilina-estreptomizina, hain zuzen ere.

Lerro zelularrak 37°C-tan mantendu ziren, % 5-eko $CO_2$ atmosferadun hezetutako inkubagailu batean. Zelula paseak 2-3 egunetik behin egin ziren, lerro zelularraren arabera.

*2.3.2 Zelulen bideragarritasun entsegua*

NLC-LL37en eragina zelulen bideragarritasunean HFF zeluletan aztertu zen. 96 putzuko kultibo plaketan 1000 zelula putzuko erein ziren eta 24 orduz inkubatu ziren zelulen eranstea ahalbidetzeko. Orduan, ingurunea aldatu egin zen, %1 FBSdun DMEM ingurunean egindako NLC-LL37ren disoluzio seriatuengatik (LL37-ren 5000-50 ng/ml-ren baliokideak) eta NLC hutsen disoluzio berdinengatik ordezkatuz. 48 ordu ostean, zelulen bideragarritasuna neurtu zen, putzuetara CCK-8 erreaktiboaren 10 µL gehituz (Sigma-Aldrich, Saint Louise, AEB). Nahastea 4 orduz inkubatu zen eta bere absorbantzia 450 nm-tan neurtu zen, 650nm erreferentziazko uhin luzera modura erabiliz. Lortutako absorbantzia kultiboan bizirik zeuden zelulei zuzenki proportzionala zen.

### *2.3.3 LPSak eragindako makrofagoen aktibazioaren inhibizioa*

Entsegu hau RAW 264.7 lerro zelularrean burutu zen. $10^5$ zelula putzuko erein ziren 96 putzuko kultibo plaka batean eta 24 orduz inkubatu ziren zelulen eranstea ahalbidetzeko. Orduan, ingurunea ondorengo laginengatik ordezkatu zen (denak LPSaren 20 ng/ml zituen 1% FBSdun DMEM/F-12 ingurunean esekita zeuden): (i) 5000 ng/ml LL37 askea, (ii) 5000 ng/ml LL37ren baliokidea den NLC-LL37 kontzentrazioa, (iii) NLC hutsen kontzentrazio berdina. Kontrol negatibo bezala LPSrik gabeko % 1 FBSdun DMEM/F-12 ingurunea erabili zen eta kontrol positibo bezala LPSaren 20 ng/ml zituen 1% FBSdun DMEM/F-12 ingurunea.

6 orduko inkubazioaren ostean, putzuen gainjalkia batu zen makrofagoek askatutako TNF-α kantitatea ELISA kit baten bidez neurtzeko (*Murine TNF-α ELISA development Kit*, PeproTech, EB). Emaitzak kontrol negatiboarekiko konparatuz, talde bakoitzak lortutako absorbantziaren ehuneko modura irudikatu ziren.

### *2.4 Entsegu antimikrobianoa*

Formulazioen eragin antimikrobianoa aztertzeko, *Escherichia coliren* ATCC 25922 anduia gauean zehar hazi zen 37°C-tara Mueller Hinton ingurunean (Conda, Pronadisa, Espainia). Orduan, esekidura bakterianoa $10^5$ CFU (kolonia formatzaile unitate edo *colony forming unit*)/ml –tara diluitu zen. Esekidura honen 1 ml-rekin honako laginak inkubatu ziren 37°C-tara: LL37 askea (20 µg/ml), NLC-LL37 (LL37ren 20 µg/ml-ren baliokidea) eta NLC hutsak (aurreko taldearen kontzentrazio berdina). Horretaz gain, esekidura bakterianoaren 1 ml ere inkubatu zen, kontrol moduan erabiltzeko.

Inkubazioaren 4. orduan, esekidura bakoitzetik laginak hartu ziren, PBSan diluitu eta haien 100 µl inokulatu ziren Mueller Hinton agar plaketan (Conda/Pronadisa, Espainia). Plakak 24 orduz inkubatu ziren 37° C-tara eta ondoren CFUak neurtu ziren, plaka bakoitzean hazitako kolonia kopurua zenbatuz. Hiru entsegu independente burutu ziren eta eragin antibakterianoa, kontrolarekin konparatuz, plaka bakoitzean hildako zelulen ehuneko modura adierazi zen.

### *2.5 Zauriaren orbaintze* in vivo *entsegua*

#### *2.5.1 Animaliak*

*In vivo* entsegurako 16 asteko adina zuten 8 *db/db* (BKS.Cg-$m^{+/+}Lepr^{db/J}$) sagu ar erabili ziren (Janvier laborategiak, Frantzia). Saio guztiak Euskal Herriko Unibertsitateko Animaliekin egiten den Esperimentaziorako Etika Batzordeak onartutako protokoloak jarraituz burutu ziren (Prozedura zenbakia: CEBA/243/2012/HERNANDEZ MARTIN). Animaliak kaioletan banaka ostatatu ziren, 12 orduko argi-ilun zikloan mantendu ziren eta karraskari pentsua zein ura *ad libitum* eman zitzaien.

#### *2.5.2 Orbaintze entsegua*

Entsegu hau Michaels *et al.* [25] deskribatutako prozedura moldatuz burutu zen. Gizakien orbaintze mekanismo nagusiak granulazio ehunaren sorrera eta errepitelizazioa dira, saguena, aldiz, zaurien uzkurdura da. Azken prozesu hori ekiditeko eta, beraz, gizakien orbaintze prozesua hobeto islatzeko, saguak anestesiatu eta bizkarreko ilea kendu ostean, bizkarraren bi aldeetan silikona eraztun bana josi zitzaien, 3-0 nylon hari bat erabiliz (Aragó, Espainia). Orduan, eraztunen erdian, 8 mm-ko diametroko lodiera osoko zauri bana egin zitzaien *panniculus carnosusera* helduz biopsietarako puntzoi (Acu-Punch, Acuderm, AEB) baten bidez. Tratamenduen administrazioaren ostean, zauriak baselinadun gazarekin (Tegaderm® 3M) eta itsasgarriaren bi geruzekin estali ziren.

Saguak lau taldetan banatu ziren (n=4): (i) tratatu gabeko kontrola, (ii) LL37 askearen 6 µg jaso zuen taldea, (iii) NLC-LL37etan kapsularatutako LL37aren 6 µg-rekin tratatutako taldea, eta (iv) NLC-LL37etan kapsularatutako LL37aren 2 µg-rekin tratatutako taldea. Tratamenduak zaurien indukzioaren osteko lehenengo eta laugarren egunean administratu ziren. Horretarako, MilliQ uraren 10 µL-tan eseki ziren eta topikoki administratu ziren, zaurian zehar barreiatzea ahalbidetuz. Zortzigarren egunean saguak $CO_2$ inhalazioaren bidez sakrifikatu ziren.

### *2.5.3 Orbaintzearen ebaluazioa*

Tratamenduen eraginkortasuna, kirurgiaren osteko 1., 4. eta 8. egunetan, zaurien azalera ($px^2$) neurtuz ebaluatu zen. Egun horietan zaurien argazkiak kamera digital batekin atera ziren (Lumix FS16, Panasonic®, Espainia) eta zaurien azalera irudi analisi programa batekin neurtu ziren (ImageJ®, Biophotonics Facility, University of McMaster, Canada). Zaurien itxiera hasierako azaleraren ehuneko modura adierazi zen.

### *2.5.4 Orbaintzearen analisi histologikoa*

Saguen sakrifizioaren ostean, zauria eta inguruko ehuna (~1 cm) erauzi zen eta % 3,7 formaldehidoan fixatu zen 24 orduz. Orduan, ehuna parafinean murgildu zen eta 5 µm lodierako xaflatan ebaki zen. Laginak H&E tindaketaren bidez prozesatu ziren orbaintzea ebaluatzeko eta Masson trikromiko tindaketaren bidez kolagenoaren metaketa ebaluatzeko.

Errepitelizazio prozesua neurtzeko Sinha et al.-ek [26] ezarritako eskala erabili zen. Zauri bakoitzari 0-4 bitarteko puntuazio erdi-kuantitatiboa egotzi zitzaion: 0, errepitelizazioa zauriaren ertzetan; 1, errepitelizazioa zauri erdia baino gutxiago estaliz; 2, errepitelizazioa zauri erdia baino gehiago estaliz; 3, lodiera irregularreko epitelio berria zauri osoa estaliz; eta 4, zauri osoa lodiera arrunteko epitelio berriaz estalia.

Hantura prozesuaren ebazpena eta zauriaren heldutasuna Cotran et al.-ek deskribatutako eskala erabiliz neurtu zen [27]: 1, hantura akutua, fibrinaren odolbatuaren eraketa eta leukozito zein neutrofilo polinuklearren migrazioa gertatzen dira fase honetan; 2, hedatutako hantura akutua, granulazio ehunaren eraketa eta angiogenesia gertatzen dira fase honetan, mintz piogenikoa desagertzen doalarik; 3, hantura kronikoa, granulazio ehuna eta fibroblastoen proliferazioa dira fase honetan nagusi; eta 4, ebazpena eta sendaketa, hantura kronikoa desagertzen da fase honetan, nahiz eta zenbaitetan zelula biribilak aurkitu daitezkeen.

Kolagenoaren metaketa Gal et al.-ek deskribatutako eskalaren arabera zehaztu zen [28]: 0, kolageno eza; 1, kolageno eduki eskasa; 2, kolageno eduki ertaina; eta, 3, kolageno eduki handia.

*2.5.5 Immunohistokimika*

Zaurietan gertatutako neoangiogenesia aztertzeko, ikerketa immunohistokimikoak egin ziren anti-CD31 antigorputz monoklonal zehatza erabiliz (JC70 klona, 760-4378, Ventana-Roche). 5 µm lodierako ehun xaflak antigorputz primarioarekin inkubatu ziren 36 minutuz 37°C-tara. Ondoren, xaflei Ultraview Universal DAB detection kit-a (760-500, Ventana-Roche) gehitu zitzaien antigenoa errebelatzeko. Azkenik, odol hodien kopurua zenbatu zen.

*2.6 Analisi estatistikoa*

Datu guztiak batezbesteko ± desbiderameta estandar (SD) modura adierazi ziren. Normaltasun testaren eta bariantzen berdintasunaren probaren (Levene test) emaitzetan oinarrituz, batezbestekoak bide-bakarreko ANOVA probaren edo Mann-Whitney U testaren bidez konparatu ziren. ANOVA probaren jarraian Student-Newman-Keuls *post-hoc*-a aplikatu zen. Kalkulu estatistiko guztiak SPSS 22.0.01 programa erabi-liz burutu ziren (SPSS® INC., Chicago, AEB).

## 3. Emaitzak eta eztabaida

*3.1 Nanopartikulen karakterizazioa*

1. taulan ageri den bezala, NLC-LL37ek eta NLC hutsek antzeko batezbesteko neurria zuten, nahiz eta NLC-LL37ena apur bat handiagoa zen: 273,6 ± 27,64 nm eta 220,6 ± 5,48 nm, hurrenez hurren. Polidispertsio indizea (PDI) 0,4-ren azpitik zegoen bi formulazioetan, sis-

**1. Taula.** NLCen karakterizazioa: tamaina, PDI, zeta potentziala, EE eta peptido karga. Datuak bastezbesteko ± desbideraketa estandar bezala adierazten dira.

| | Tamaina (nm) | PDI | Zeta Potentziala (mV) | EE % | Peptido karga (µg LL37/mg NLC) |
|---|---|---|---|---|---|
| NLC-LL37 | 273,6 ± 27,64 | 0,31 ± 0,06 | -31,63 ± 1,94 | 96,40 ± 0,41 | 16,76 ± 0,07 |
| NLC hutsak | 220,6 ± 5,48 | 0,27 ± 0,03 | -26,10 ± 0,53 | | |

tema polidispertso egonkorrak direla adieraziz. Zeta potentzialaren analisiak bi formulazioak antzeko azaleko karga zutela erakutsi zuen, NLC-LL37en kasuan -31 mV ingurukoa eta NLC hutsen kasuan -26 mV ingurukoa. Horretaz gain, NLC-LL37ek kapsularatze eraginkortasun altua izan zuten (96,40 ± 0,41 %) eta peptidoaren karga 16,76 ± 0,07 µg LL37/mg nanopartikula izan zen.

Nanopartikulen morfologiaren analisiari dagokionez, TEMean ateratako argazkietan ikusten zen, nanopartikulen tamaina DLSaren bidez lortutakoaren antzekoa zela (1. irudia).

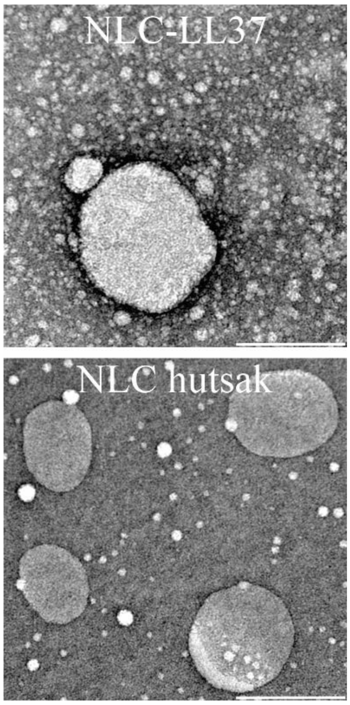


**1. Irudia.** NLC-LL37 eta NLC hutsen TEM argazkiak. Eskala barrak 200 nm adierazten du.

*3.2* In vitro *kultibo zelularreko entseguak*

*3.2.1 Zelulen bideragarritasuna*

NLCen zitotoxikotasuna ebaluatzeko, HFF zelulak 48 orduz inkubatu ziren partikulen presentzian, eta ondoren haien bideragarritasuna CCK-8 saioaren bidez neurtu zen. 2. irudian ikusten den moduan, formulazioek ez zuten zelulen bideragarritasunean eraginik izan, haien toxikotasun falta frogatuz.

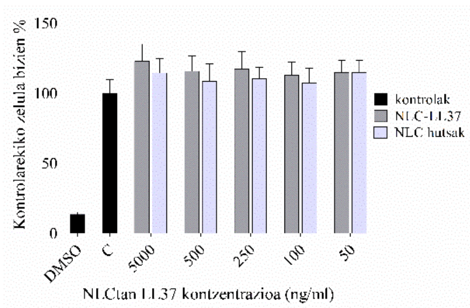


**2. Irudia.** Zelulen bideragarritasuna NLCak gehitu ostean. Emaitzak kontrolarekiko bizirik dauden zelulen % batezbestekoa ± SD bezala adierazita daude. Kontrolak C (zelulak inolako gehigarririk gabe) eta DMSO (zelulak DMSO-ren gehiketaren ostean) dira.

*3.2.2 LPSak eragindako makrofagoen aktibazioaren inhibizioa*

Kapsularatze prozesuak peptidoaren bioaktibitatearengan eragina duen zehazteko, kapsularatutako LL37ak LPSarekin lotzeko zuen gaitasuna ebaluatu zen. Gaitasun hori kuantifikatzeko RAW 267.4 makrofagoek askatutako TNF-α neurtu zen. Izan ere, LL37a LPSarekin lotzean makrofagoen aktibazioa ekiditen du, TNF-α moduko zitokinen askapena etenez.

3. irudian ikusten denez, kapsularatze prozesuaren ostean peptidoa aktibo mantentzen zen. Izan ere, LL37 askearekin zein NLC-LL37ekin tratatu ostean, LPSak aktibatutako makrofagoen TNF-α askapena antzeko neurrian murriztu zen. NLC hutsekin ostera, ez zen murrizketarik ikusi, beraz, makrofagoen inhibizioa LL37ak LPSaren gain duen eraginagatik izan zela ondoriozta dezakegu, aldez aurreko ikerketetan frogatu den modura [14,15].

Dena den, Rosenfeld *et al.*-ek erakutsi zuten modura, LL37aren eta LPSaren arteko lotura ez da nahikoa makrofagoen aktibazioa ekiditeko. Neutralizazioa lortzeko,

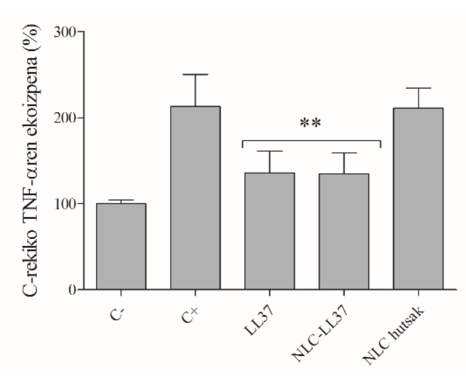


**3. Irudia.** Makrofagoen aktibazioaren inhibizioa. Emaitzak kontrolarekiko TNF-α ekoizpenaren % batezbesteko ± SD bezala adierazita daude. ** NLC eta C+ baino esanguratsuki handiagoa (p<0,01). Kontrolak C- (zelulak inolako gehigarririk gabe) eta C+ (zelulak LPSaren gehiketaren ostean) dira.

LL37ak alde batetik LPS agregatuak apurtu behar ditu, eta bestetik, makrofagoen CD14 hartzaileengatik lehiatu. Hori dela eta, kapsularatze prozesuak ez zuela LL37aren bioaktibitatean eraginik esan daiteke, izan ere, LPSarekin elkarrekintza elektrostatiko eta hidrofobikoak izateaz gain, CD14arekin lotura selektibo baten bitartez lotzeko gai zen ere [16].

*3.3 Entsegu antimikrobianoa*

LL37aren eragin antimikrobianoa E. coliren aurka aztertu zen, zauri infektatuetan bakterio ohikoenetakoa baita [29]. Laburki, LL37 askea, NLC-LL37ak eta NLC hutsak *E. colirekin* inkubatu ziren eta laginak denbora jakinean batu ziren. Lagin horiek, agar plaka batean erein ziren, 24 orduz inkubatu ziren eta hazitako koloniak zenbatu ziren. Emaitzek erakutsi zutenez, LL37 askeak bakterioen % 100-a hil zituen lehenengo 4 ordutan, eta NLC-LL37ek ehuneko baxuagoa hil zuten, % 72,63 ± 13,37 hain zuzen. Hala eta guztiz ere, NLC-LL37ek NLC hutsek baino eragin antimikrobiano handiagoa erakutsi zuten, 4. irudian ikus daitekeenez.

LL37 askea erabiliz dosi osoa eskuragarri zegoen saioaren hasieratik, baina NLC-LL37-ak erabiliz, ordea, hasieran ez zegoen dosi osoa eskuragarri formulazioaren askapen kontrolatua dela eta. Farmakoaren eskuragarritasunean desberdintasun hori izan liteke LL37 askearen eragin antimikrobiano handituaren arrazoia. Horren eraginez ere, NLC-LL37ak ez ziren *E. coli* guztia hasieran hiltzeko gai izan, eta haien hazkuntza esponentziala dela eta, ondoren ere ezin izan zituzten geratzen ziren bakteroa guztiak hil. Hala eta guztiz ere, egindako saioa *in vitro* entsegu bat denez, ez du praktika klinikoa guztiz islatzen, non bakterioak zaurian etengabe proliferatzen dauden. Hori dela eta, peptidoaren askapen kontrolatua, hasieran dosi altu bat eskuragarri izatea baino komenigarriagoa da.

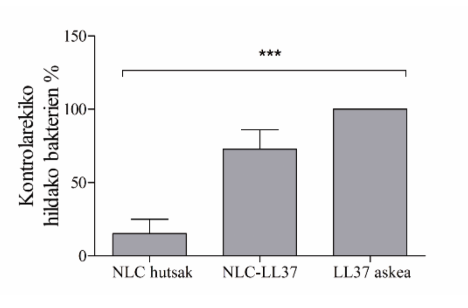


**4. Irudia.** Entsegu antimikrobianoa. Emaitzak kontrolarekiko hildako bakterien ehunekoaren batezbesteko ± SD bezala adierazten dira. *** hiru taldeen artean (p<0.001).

### *3.4* In vivo *orbaintze entsegua*

Tratamenduaren eraginkortasuna ebaluatzeko zaurien itxiera neurtu zen. Horretarako, 1., 4., eta 8. egunetan ateratako argazkien zaurien azalera ($px^2$) neurtu zen, eta zaurien itxiera hasierako azalerei amaierakoa kenduz lortu zen.

Taldeen arteko desberdintasunak zortzigarren egunean nabarmenagoak izan ziren, naiz eta 4. egunean desberdintasun esanguratsuak egon ziren ere. 5A. irudian ikusten denez, azalera murrizketa nagusiena NLC-LL37aren dosi altuenarekin tratatutako saguetan gertatu zen. Zortzigarren egunean, talde horren azaleraren murrizketa gainontzeko taldeena baino esanguratsuki handiagoa izan zen. Laugarren egunean, aldiz, kontrol taldearekin alderatuta bakarrik izan zen esanguratsua desberdintasun hori. Emaitza horiek 5.B irudiko zaurien irudi makroskopikoetan behatzen den azaleraren murrizketa kualitatiboarekin bat datoz, izan ere, txikiagotze handiena NLC-LL37aren dosi altuarekin ikusten zen.

NLC-LL37aren dosi baxuarekin eta LL37 askearekin tratatutako taldeei dagokienez, antzeko zauri itxiera izan zuten, nahiz eta lehenengoak azalera murrizketa apur bat handiagoa izan zuen. Horretaz gain, kontrol taldearekin alderatuz itxieran hobekuntza lortu zuten, nahiz eta 8. egunean bakarrik izan zen esanguratsua.

Zaurien itxieraz gain, tratamenduen eraginkortasuna analisi histologikoen bidez ebaluatu zen. Horretarako, laginak 8. egunean batu ziren eta H&Erekin tindatu ziren errepitelizazio gradua eta hanturaren ebazpena aztertzeko asmoz.

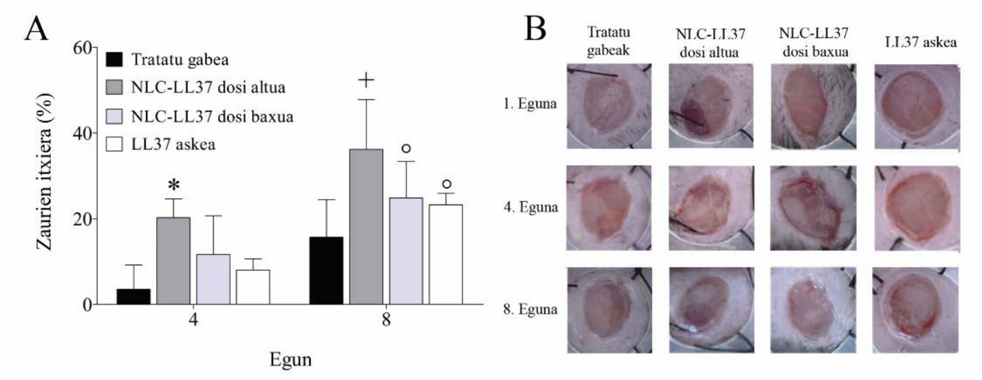


**5. Irudia.** *In vivo* zauriaren itxiera. (A) Zaurien itxiera hasierako gaianazal azalerarekiko murrizketa ehuneko bezala adierazita. * Tratatu gabeko taldearekiko esanguratsua. ($p<0.05$); ○ Tratatu gabeko taldearekiko esanguratsua. ($p<0.05$); + gainontzeko taldeekiko esanguratsua ($p<0.05$). (B) Zaurien irudiak.

Errepitelizazioa gizakien orbaintze prozesu nagusia da, karraskarietan aldiz, prozesu nagusia zaurien uzkurtzea da. Hala eta guztiz ere, hautatutako animalia ereduan errepitelizazioak paper garrantzitsua dauka, *db/db* saguek uzkurtze prozesua kaltetuta daukatelako, haien gizentasunak azalaren malgutasuna txikitzen duelako Fang et al.-en arabera [30,31]. Gainera, zaurien inguruan silikonazko eraztun bana josi zirenez, zaurien uzkurdura are gehiago oztopatu zen [25]. Guzti horren ondorioz, errepitelizazioa prozesu garrantzitsua da animalia eredu honetan.

Errepitelizazioaren analisitik lortutako emaitzek (6A. irudia) erakutsi zutenez, NLC-LL37en dosi altuarekin tratatutako zaurietan errepitelizazio gradua altuagoa lortu zen. Sinha et al.-ek deskribatutako eskalan, 2 inguruko balioa lortu zen batazbesteko, hau da, zauri gehienetan epitelio berriak azaleraren erdia baino gehiago estaltzen zuen [26]. LL37 askearekin tratatutako saguetan eta kontrol taldeko saguetan errepitelizazioak zaurien azaleraren erdia baino gutxiago estaltzen zuen (1 balioa), eta NLC-LL37aren dosi baxuarekin tratatutako saguetan errepitelizazioa zaurien ertzetan baino ez zen behatzen (~0). Emaitza hauek zaurien itxieran lortutakoekin bat datoz, izan ere bi kasuetan NLC-LL37aren dosi altuak orbaintzea sustatu zuen, NLC-LL37aren dosi baxuago batekin edo LL37 askearekin alderatuz gero.

Hanturaren ebazpenaren analisia Cotran *et al.*-ek ezarri zuten irizpidearen arabera burutu zen [27]. 6B. irudian ikusten denez, NLC-LL37aren dosi altuarekin eta LL37 askearekin tratatutako zaurietan hanturaren ebazpena bizkortuta ageri zen, haietan granulazio ehunaren sorrera eta angiogenesia nagusi baitziren, ia ez zeudelarik mintz piogeniko ezta neutroliforik ere (2 gradua). Beste bi taldeetan (NLC-LL37en dosi baxua eta kontrol taldea), ordea, zauriak beste fase batean zeuden, zeinean fibrina odolbatua sortzen ari zen eta leukozitoak zein neutrofilo polimorfonuklearrak zaurira migratzen zeuden (1 gradua). Azkeneko talde hauetan behatzen den neutrofiloen infiltrazio iraunkorra zauri kronikoen ezaugarri bereizgarria da, eta orbaintzea atzeratzea eragiten du, izan ere, neutrofilo horiek gehiegizko proteasa kopurua jariatzen dute, matrize extrazelularra degradatzen dutenak [32].

Aipagarria da, NLC-LL37aren dosi altuarekin zein LL37 askearekin tratatutako saguek hedatutako hantura akutuaren fasean (2 gradua) egon arren, nanopartikulen taldean lortutako balioa arinki altuagoa zen, ondorioz, zauriaren heldutasunean hobekuntza arina lortuz.

Orbaintzearen hasieran, granulazio ehuneko fibroblastoek III. motako kolagenoa sintetizatzen dute, zeina apurka I. motako kolagenoaz ordezkatua izaten den azal osasuntsuaren fenotipoa berreskuratzeko. Kolagenoa, eta batez ere I. motakoa, azal osasuntsuaren pisu lehorraren % 80-a da,

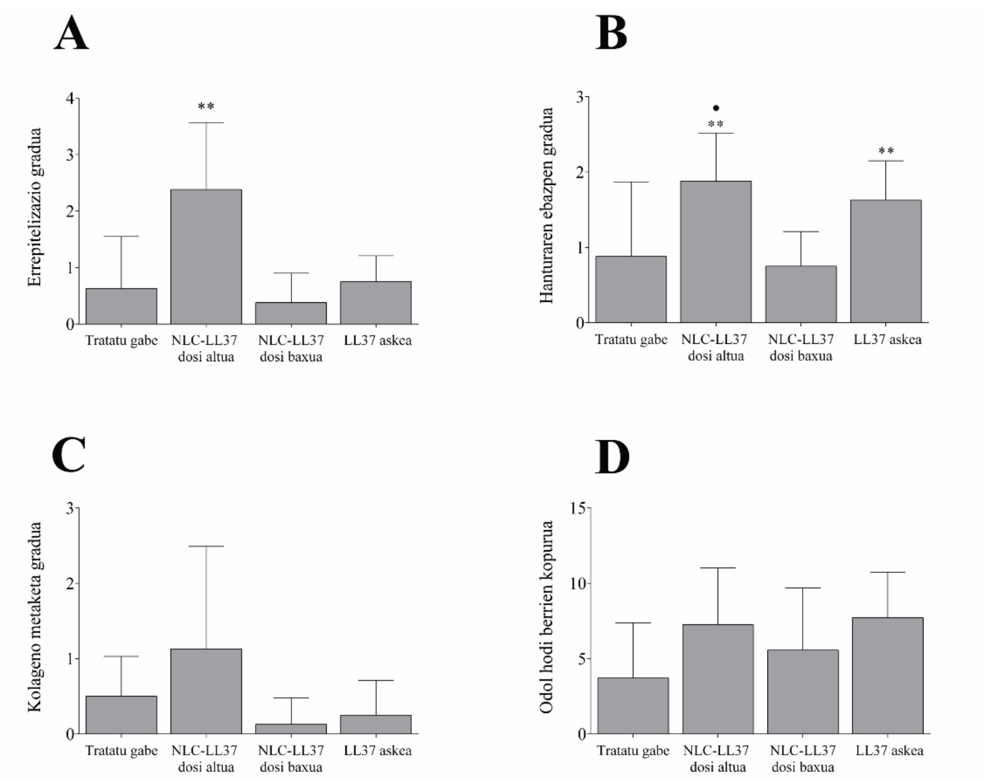


**6. irudia.** Analisi histologikoa. (A) Errepitelizazio gradua. ** Gainontzeko taldeekiko esanguratsuki handiagoa (p>0.01). (B) Hanturaren ebazpenaren gradua. **NLC-LL37aren dosi baxua baino esanguratsuki handiagoa (p<0.01); ● tratatu gabeko taldea baino esanguratsuki handiagoa (p<0.05). (C) Kolageno metaketa. (D) Odol hodixka berrien zenbakia tindatutako ehun xafletan. Emaitza denak batezbesteko ±SD bezala adierazita daude.

beraz, zaurietan dagoen kolageno metaketa, haien heldutasunaren seinale da [33].

Hori kontuan hartuz, Masson trikromikoaren tindaketak agerian utzi zuen, NLC-LL37aren dosi altuak zauriaren heldutasuna arinki bizkortu zuela, izan ere, gainontzeko tratamenduekin konparatuz kolagenoaren metaketa suspertu zuen, 6C. irudian ikus daitekeen modura. Gainontzeko hiru taldeetan (kontrol tratatugabea, LL37 askea eta NLC-LL37aren dosi baxua) batezbesteko zauriek ez zuten kolageno metaketarik erakutsi (Gal *et al.*-en kriterioaren arabera 0 gradua [28]), izan ere zauri gehienek ez zuten kolagenorik (0 gradua) eta gutxi batzuk bakarrik zeukaten kolageno apur bat (1 gradua). NLC-LL37aren dosi altuarekin tratatutako saguek, ordea, kolageno metaketa eskasa erakutsi zuten batezbesteko (1 gradua), nahiz eta zauri batek kolageno eduki handia izan zuen (3 gradua) eta beste batek kolageno metaketa ertaina (2 gradua). Hala eta guztiz ere, kolageno metaketan zeuden desberdintasunek ez zuten esangura estatistikorik lortu, ziurrenik taldeen barne egondako aldakortasun handiagatik. Aldakortasun zabal hori aldez aurretik Trousdale et al.-ek deskribatu zuten *db/db* saguen orbaintzea aztertzean [34].

Prozesu angiogenikoa aztertzeko anti-CD31 antigorputz monoklonalarekin tindatutako odol hodi eratu berriak zenbatu ziren. Emaitzek esangura estatistikoa lortu ez zuten arren, LL37 askearekin eta NLC-LL37aren dosi altuarekin tratatutako zauriek, tratatu gabeko zauriekin konparatuz gero, odol hodi gehiago izan zituzten. Izatez, talde horietako bakoitzean zauri bik 10 odol hodi berri baino gehiago izan zituzten, tratatu gabeko taldean ordea, zauri batek ere ez zuen 8 odol hodi baino gehiago izan. Are gehiago, NLC-LL37aren dosi baxuak, kontrol taldearekin konparatuz, dentsitate mikrobaskularra arinki handitu zuen (zauri bat 10 odol hodi baino gehiagorekin), 6D. irudian ikus daitekeenez.

Orokorrean emaitza horiek honakoa adierazten dute: topikoki administratutako NLC-LL37ak, peptido askearen administrazioarekin konparatuz, orbaintzea sustatu dezaketela lodiera osoko zaurien alderdi hauetan: zauriaren itxiera, errepitelizazioa eta hantura prozesuaren ebazpena. Kapsularatutako peptidoaren eragin handitua NLCen efektu babesgarriari atxiki dakioke, NLCek LL37a degradazio kimikoaren eta zaurian dauden proteasen aurrean babesten baitute. Horretaz gain, NLCek askapen profil kontrolatua daukate, horrela LL37aren eragina luzatuz [20,21]. Hori dela eta, NLC-LL37ak erabiliz, peptido askea administratzean beharrezkoa den dosi maiztasun handia murriztu daiteke.

Aldez aurretik egindako ikerketek LL37a kapsularatzearen erabilgarritasuna frogatu dute [19], dena den, oraingo ikerketa honetan LL37a duten nanopartikulak bide topikotik administratuta dira lehen aldiz, zeinak abantaila ugari dauzkan. Lehenik, NLCen izaera lipidikoak geruza oklusibo bat eratzen du, azalaren hidratazioa handituz eta kapsularatutako LL37aren barneratzea lagunduz [21,35]. Gainera, administrazio topikoa gaixoarentzat bide erraza, erosoa eta segurua da.

## 4. Ondorioak

Ikerketa honetan %2 LL37 zuten NLCak garatu ziren. Haien batezbesteko neurria 270 nm-koa zen eta ez zuten zitotoxizkotasunik erakutsi. Kapsularatutako peptidoak bere bioaktibitatea mantentzen zuen kapsularatze prozesuaren ostean, in vitro egindako saio immunomodulatzailean eta antimikrobianoan ikusi zenez.

*Db/db* saguetan egindako lodiera osoko orbaintze *in vivo* entseguan frogatu zen, orbaintzean eragin handiagoa zuela LL37aren 6 µg NLCen barne topikoki administratzeak, aske administrazeak baino. Aurkikuntza guztiak kontuan hartuz, NLC-LL37en administrazio topikoa zauri kronikoen tratamendurako estrategia interesgarria izan daitekeela ondoriozta daiteke.

## 5. Eskerrak

I. Garcia-Oruek Eusko Jaurlaritzari doktoratu aurreko laguntza eskertzen dio. Egileek UPV/EHU-ko SGIkerren laguntza teknikoa, giza babesa eta Europako finantziazioa (FEDER eta FSE) eskertzen dituzte. Proiektu hau neurri batean Espainiako Ekonomia eta Lehiakortasun Ministerioak finantziatu du (INNPACTO, IPT-2012-0602-300000, 2012) eta baita, Eusko Jaurlaritzak (Talde finkatuak, IT-407-07 eta IT-528-10) eta Euskal Herriko Unibertsitateak ere (UFI11/32).

**Erreferentzien zerrenda 79-81 orrialdeetan aurkitzen da.**

# 2. KAPITULUA

## rhEGF eta *Aloe vera* dituzten nanozuntzezko apositu berriak zaurien orbaintzean erabiltzeko.


**LABURPENA**

Elektroirutearen bidez ekoiztutako nanozuntzezko mintzek bolumenaren araberako gainazal azalera handia dute, zeinak matrize extrazelularraren (*extracellular matrix* edo ECM) hiru-dimentsioetako egitura imitatzen duen. Hori dela eta, nanozuntzezko aposituak zauri kronikoen orbaintzerako aukera itxaropentsua dira, izan ere, ECM naturala ordezkatu dezakete zauria sendatzen den bitartean. Ondorioz, ikerketa honetan PLGAz eginiko nanozuntzezko mintz bat garatu dugu, zeinak giza hazkuntza faktore epidermal errekonbinantea (*recombinant human Epidermal Growth Factor* edo rhEGF) eta *Aloe veraren* (AV*)* erauzkina dituen. Bi konposatuek orbaintzea sustatzen dute, alde batetik, EGFa orbaintzearen bitartekaria delako, eta bestetik, AVa fibroblastoen proliferazioa eta aktibitatea estimulatzen dituelako. Lortutako mintzak ausaz orientatutako zuntz uniformez osatuta zeuden, haien batazbesteko diametroa 356,03 ± 112,05 nm-ko zen, porositatea %87,92 ± 11,96-koa zen eta rhEGF edukia 9,76 ± 1,75 µg/mg-koa zen. *In vitro* bideragarritasun entseguak erakutsi zuenez, rhEGFa eta AVa zuten mintzak fibroblastoen proliferazioa hobetzeko gai ziren, haien elkarketa onuragarria dela frogatuz. Are gehiago, mintz hauek zaurien itxiera eta errepitelizazioa era esanguratsuan bizkortu zuten, *db/db* saguetan egindako lodiera osoko zauri eszisionaletan. Orokorrean, aurkikuntza hauek rhEGFa eta AVa kapsularatuta dituzten PLGA nanozuntzen erabilgarritasuna erakusten dute zauri kronikoen orbaintzean erabiltzeko.

## 1. Sarrera

Orbaintzea prozesu dinamiko eta konplexua da, zeinaren helburua azalaren egitura anatomiko eta funtzionaltasun normalak berreskuratzea den (Diegelmann eta Evans 2004). Helburu hori lortzeko asmoz, zenbait sistema biologikok eta immunologikok era koordinatuan parte hartzen dute orbaintzea osatzen duten 3 fase bereizi baina gainjarrietan. Fase horiek hanturazko erantzuna (non hemostasia eta hantura bereiz daitezkeen), fase proliferatiboa (zeinean proteinen sintesia eta zauriaren uzkurdura gertatzen diren) eta erremodelazio fasea dira (Monaco eta Lawrence 2003; Morton eta Phillips 2016; Schreml, et al. 2010). Hala eta guztiz ere, zenbait zaurik huts egiten diote denboran zein espazioan zehar antolatutako prozesu horretan zehar igarotzeari. Orbaintzearen asaldura zenbait faktorek eragin dezakete, hala nola, infekzioek, nekrosiak, ehunen hipoxiak, exudatuak eta gehiegizko hanturazko zitokinak. Horren ondorioz, zauriak hanturazko fase iraunkor batean harrapatuta geratzen dira. Fase horretan ezohiko zitokinen maila altua egoten da, zeinak matrize extrazelularraren (*extracellular matrix* edo ECM) hondaketa eragiten duen, sendaketa are gehiago kaltetuz (Briquez, et al. 2015; Velnar, et al, 2009).

Gure gizartean, zauri kronikoen tratamenduak garrantzia handia lortu du, azken urteotan gertatu den prebalentziaren igoera kezkagarria dela eta. Gainera, prebalentziak igotzen jarraituko duela uste da, arrisku handiko biztanleria hazten ari delako, haien artean, adindunak, diabetikoak eta obesoak daudelarik (Whittam, et al. 2016). Izatez, garatutako herrialdeetan biztanleriaren % 1-2-ak zauri kronikoak pairatuko dituela zenbatetsi da, Nazio Batuen arabera, haiei elkartutako kostuak Europako osasun aurrekontuaren %2-a direlarik (Sen, et al. 2009). Arazo kliniko hori gainditzeko egiten ari diren ikerketak, orbaintzea sustatzeko gai diren apposituen garapenera bideratuta daude. Apositu horien artean, ehundu gabeko nanozuntzezko mintzak daude, zeintzuengan arreta berezia jarrita dagoen, haien egiturak ECMaren hiru dimentsioetako egitura imitatzen dutelako (Choi, et al. 2015).

Nanozuntzak orokorrean elektroiruteearen bitartez ekoizten dira, teknika sinple, kostu-efektibo eta erabilera anitzekoa dena. Teknika honekin disoluzio polimeriko batetatik zuntz nanometrikoak ardazkatzen dira indar elektrostatikoen bidez (Abrigo, et al. 2014; Gainza, et al. 2015b). Horrela lortutako nanozuntzak bolumenaren araberako gainazal azalera eta porositate handia dute, horrek orbaintzea mekanismo desberdinen bidez sustatzen duelarik. Adibidez, gasen sarrera ahalbidetzen dute, zelulen arnasketa ahalbidetuz; eta hezetasuna mantentzeko gai dira, exudatuen irteera erraztuz (Pachuau 2015). Apposituek zelulen migrazioa eta proliferazioa sustatu beharko lukete, baina aldi berean, ehuna nanozuntzezko mintzaren gain haztea ekidin, apositu hauek zauria orbaintzean kentzeko diseinatuta baitaude (Abrigo, et a. 2014). Horretaz gain, nanozuntzak konposatu aktiboak barneratzeko gai dira orbaintzea bizkortzeko asmoz. Estrategia hori hainbat ikerketetan erabilia izan da, besteak beste honako farmakoak kapsularatuz: hazkuntza faktoreak, Aloe vera extraktua, kurkumina, metformina, ziprofloxazinoa eta kolagenoa (Choi, et al. 2008; Kataria, et al. 2014; Lai, et al. 2014; Lee, et al. 2014; Merrell, et al. 2009; Uslu and Aytimur 2012). Gainera, nanozuntzetan kapsularatzeak farmakoen administrazio topikoa ahalbidetzen du, abantaila ugari daukana. Lehenik eta bien, gaixoek hobeto onartzen dituzte tratamendu topikoak, nork bere buruari administra diezaizkiokelako; bigarrenez, tratamenduaren ahalmen terapeutikoa hobetzen dute, farmakoaren bioerabilgarritasuna eta zaurian mantentzea handitzen baitituzte; eta azkenik farmakoaren toxikotasun sistemikoa txikitzen dute (Pachuau 2015; Whittam, et al. 2016).

Elektroirutearen bitartez lortutako nanozuntzezko mintzak zeluletan oinarritutako terapietan erabiliak izan dira ere. Mintzen eta ECMaren arteko antzekotasunak zelulen sarrera, desberdintzatzea eta atxikipena ahalbidetzen ditu, ordezko azalak edo zelula amen terapiak garatzeko aproposak egiten dituena. Ordezko azalak azal osasuntsuaren egitura antzekoa duten zeluladun bio-aldamioak dira (Dickinson adn Gerecht 2016). Zelula-matrize elkarrekintzak hobetzeko asmoz, bio-aldamioak kolagenoz edo bestez ECMko proteinez ekoizten dira (Hodgkinson and Bayat 2011). Horren harira, Powell et al.-ek elektroirundako kolageno bio-aldamio bat garatu zuten, zeinean gizakien fibroblasto dermalak eta keratinozito epitelialak erein zituzten ( Powell, et al. 2008). Beste ikerketa batean, Han et al.-ek PHVB polimero naturalean oinarritutako bio-aldamio bat garatu zuten, zeinean ileko zelula folikularrak erein zituzten, haien immunogenizitate baxuak alo-transplanteetarako abantailatsu egiten baititu (Han, et al 2007). Beste aldetik, elektroirundako mintzetan zenbait zelula ama mota finkatu dira apositauk garatzeko, zelula horien artean hurrengoak daudelarik: gantzetik eratorritako zelula amak (Gu, et al. 2014; Machula, et al. 2014), zelula ama mesenkimalak (Bhowmick, et al. 2016; Steffens, et al. 2014), murriztu gabeko zelula ama somatikoak (Bahrami, et al. 2016, Keshel, et al. 2014) eta gernutik eratorritako zelula amak (Fu, et al. 2014). Zelula ama horiek orbaintzea hobetzeko gai direla frogatu dute, zelula endotelialetara desberdintzatzeko duten gaitasunagatik eta baita ECMko proteinak zein orbaintzearen bitartekariak expresatzeko duten gaitasunagatik ere.

*Aloe vera* extraktua (AV) apositutzat erabiltzeko nanozuntzetan kapsularatu daitekeen konposatu bat da. *Aloe vera* hosto zukutzuak dituen Liliaceae familiako landare bat da. Bere aktibitate farmakologikoaren barne, eragin anti-inflamatorioak, antiartritikoak, antibakterianoak, antifungikoak eta hipogluzemikoak daude, baina horietaz gain, orbaintzea sustatu dezakela ikusi da ere (Choi and Chung, 2003, Hashemi, et al. 2015). Orbaintzean duen ekintza, glukomanano deritzon konposatuaren bidez gauzatzen du batez ere, honek fibroblastoen hazkuntza faktorean eragina baitu, flibroblastoen aktibitatea eta proliferazioa sustatuz eta zelula hauen kolageno ekoizte eta jariapena handituz (Hashemi, et al. 2015).

Hazkuntza faktoreak nanozuntzezko apositutetan kapsularatzea interesgarria da, izan ere, orbaintzearen ezinbesteko bitartekariak dira (Choi, et al. 2012). Horien artean, hazkuntza faktore epidermikoa (*epidermal growth factor* edo EGF) dago, zeina seinalizazio molekula gakoa den eta fibroblasto eta keratinozitoen proliferazio eta migrazioa estimulatzen dituen, orbaintzea sustatuz (Bodnar 2013). Horretaz gain, zauri kronikoetan administratu ostean orbaintzea bultzatzen duela ikusi da

(Choi, et al. 2008, Gainza, et al. 2015a). Hala ere, EGFaren erabilera klinikoak arazo ugari ditu, bere erdibizitza laburra dela eta, zauriko entzima hidrolitikoek degradatzen baitute. Nanozuntzezko mintzetan kapsularatuz muga horiek gainditu daitezke, formulazio hauen barnean EGFa ingurunetik babestuta egongo litzatekeelako, bere egonkortasuna hobetuz (Pachuau, 2015).

Nanozuntzezko mintzak polimero natural zein sintetikoak erabiliz ekoiztu daitezke. Elektroirutean erabilitako polimero naturalak ECMko osagaiak izaten dira askotan, hala nola, kolagenoa, laminina, fibrina edo elastina, baina beste polimero batzuk izan daitezke ere, besteak beste, kitosanoa, agarosa, gelatina, pektina, zeta, etab. Polimero horiek orbaintzean erabiltzeko egokiak dira honako ezaugarriak direla eta: biobateragarritasuna, toxikotasun eza, ezaugarri fisikokimiko aproposak eta matrize-zelula elkarrekintzak (Garg, et al. 2015). Hala eta guztiz ere, haien ezaugarri mekaniko ahulak eta elektroiruteko dituzten zailtasunak direla eta, askotan polimero sintetikoen bidez sendotu egiten dira (Hodgkinson and Bayat, 2011). Elektroirutean erabilitako polimero sintetikoen artean, zelulosa azetatoa, azido polilaktiko-ko-glikolikoa (PLGA), alkohol polibinilikoa, azido polilaktikoa, poliestirenoa, poliglizerola, azido poliglikolikoa, poliuretanoa, etab. daude. Material hauek sendoagoak eta merkeagoak dira, ondo zehaztutako egitura daukate eta errazago elektroiruten dira (Garg, et al. 2015).

Esandako guztia kontuan hartuz, lan honetan PLGA elektroirun zen rhEGFaz eta AVaz kargatutako nanozuntzezko apositu bat garatzeko. Mintzak karakterizatu ziren orbaintzean erabiltzeko zuten egokitasuna aztertzeko, eta ondoren, *in vitro* saioak burutu ziren kapsularatutako konposatuen bioaktibitatea ebaluatzeko.

Horretaz gain, apposituen eraginkortasuna *in vivo* aztertu zen. Laborategiko animalien artean, ziurrenik txerrien azala da gizakien azalaren antzekoena, baina animalia handiekin lan egiteko zailtasunengatik karraskarien ereduak askoz erabiliagoak dira (Seaton, et al. 2015). Baina, esan bezala, karraskarien orbaintzeak ez du horren ondo imitatzen du gizakiena, haien azal soltea dela eta, duten sendatze mekanismo nagusia zauriaren uzkurtzea baita. Desberdintasun hori ekiditeko asmoz, zauriak leku anatomiko zehatzetan egiten dira, hala nola buruan, belarrietan edo buztanean, non azala tinkoago dagoen. Arazo hau gainditzeko beste aukera bat zaurien inguruan silikonazko eraztunak jostea da, horrela uzkurdura saihesteko. Azken eredu honek gizakien zaurien antzekotasun gehien duen karraskarien eredua da (Fang and Mustoe, 2008).

Zauri kronikoetan gertatzen den sendaketaren atzerapena imitatzeko asmoz, orbaintzea kaltetuta duten karraskarien ereduak erabili daitezke, hala nola, eredu iskemikoak (Elgharably, et al. 2014; Magin, et al. 2016) edo diabetikoak. Eredu diabetikoen artean erabilienak kimikoki eragindako diabetea dutenak edo animalia genetikoki diabetikoak dira. Kimikoki diabetea estreptozotozina injekzioen bidez eragiten da, konposatu horrek areko β-zelulak hondatzen baititu, I. motako diabetesaren antzeko fenotipo bat lortuz (Inpanya, et al. 2012; Moura, et al. 2014). Genetikoki diabetikoak diren animaliak *db/db* saguak dira (BKS.Cg-m +/+ Leprdbj/J), zeintzuek leptinaren hartzailean mutazio bat duten, eta horren ondorioz II. motako diabetearen antzeko fenotipoa duten (Guillemin, et al. 2016; Losi, et al. 2013). Michaels et al.-ek burutako ikerketa batean, orbaintzea *db/db* saguetan estreptozotozina ereduan baino kaltetuagoa zegoela ikusi zen (Michaels, et al. 2007).

Hori dela eta, ikerketa honetan garatutako formulazioen eraginkortasuna aztertzeko, *db/db* sagu ereduan zauri eszisionalak egin ziren eta haien inguruan silikonazko eraztunak josi ziren. Orbaintzea ebaluatzeko, zaurien itxiera, errepitelizazio gradua, hanturaren ebazpena eta kolageno metaketa aztertu ziren.

## 2. Material eta metodoak

### *2.1 Nanozuntzen prestaketa*

rhEGF, AV eta PLGA zituen o/w emultsio bat elektroirun zen PLGA-AV-EGF nanozuntzezko mintza eratzeko. Emultsioaren fase organikoa 140 mg PLGA 50:50 (Resomer RG504, Evonik, Alemania) zituen hexafluoroisopropanolaren 650 µLtan (HFIP, Fluka, Suitza). Fase urtsua, aldiz, 140 mg Aloe vera hauts (Agora Valencia SL., Espainia) eta 5 mg rhEGF (Centre for Genetic Engineering and Biotechnology, Cuba) zituen % 0,5-eko (p/b) alkohol polibiniliko disoluzio baten barne. Bi faseak 3 minutuz nahastu ziren potentzia maximoan emultsioa eratzeko (Vortex-Genie 2, Scientific Industries Inc., AEB).

Lortutako emultsioa Luer-lock xiringa (Norm-Ject) batean kargatu zen, zeinak 18 G-ko orratz bat zeukan. Xiringa ponpa batera atxiki zen, 1ml/h-ko emaria eragiten zuenak, horrela elektroirutea abiaraziz. Emultsioa horizontalki elektroirun zen 12 kV-ko korrontearen bidez eta orratzaren 12 cm-tara zegoen kolektore birakari batean jaso zen (200 r/min).

PLGA-AV eta PLGA nanozuntzen prestaketa, azaldutakoaren oso antzekoa izan zen, desberdintasun bakarra fase urtsuaren osagaietan zegoelarik. PLGA-AV nanozuntzek ez zuten rhEGFrik eta PLGA nanozuntzek ez zuten rhEGF ezta AVrik ere. Antzeko lodierako mintzak lortzeko injektatutako bolumenak normalizatu egin ziren.

Mintzak ekoizteko erabilitako lehengaiak gamma erradiazioaren bidez esterilizatu ziren erabili aurretik. Beste aldetik, elektroirutean erabilitako xiringa, kolektorea eta orratza autoklabatu egin ziren, eta are gehiago, elektroirute prozesua baldintza aseptikoetan burutu zen. Azkenik, *in vitro* eta *in vivo* ikerketen aurretik mintzak esterilizatu egin ziren, 30 minutuz UV argitan mantenduz.

*2.2 Nanozuntzen karakterizazioa*

Nanozuntzezko mintzen morfologia, hau da, mintzen kalitatea eta zuntzen diametroa, ekorketazko mikroskopio elektronikoko irudien bidez aztertu zen (SEM, Jeol JSM-6300). Haien porositatea (P) hurrengo ekuazioaren bidez kalkulatu zen (Ek. 1), non $\rho_{real}$ and $\rho_{app}$ dentsitate erreala eta itxurazkoa diren, hurrenez hurren:

$$P\ (\%)=\left(1-\frac{\rho_{app}}{\rho_{real}}\right)\ x\ 100 \qquad (1)$$

Dentsitate erreala helio piknometro baten bidez neurtu zen (Micromeritics, AccuPyc 1330, AEB), itxurazko dentsitatea, berriz, pisatutako masa eta kalkulatutako bolumena (Luzera × zabalera × altuera) zatituz kalkulatu zen. Mintzaren lodiera estereo mikroskopio (Leica M205 C. Leica LAS, Alemania) baten bitartez lortutako argazkietatik neurtu zen.

Mintzen ezaugarri mekanikoen probak desplazamendu kontrolaren arabera egin ziren 5 N-eko eskala osoko karga zelula bat erabiliz Instron 5848 Microtester ekipoan (Instron®, EB). Laginak 0,01 mm/s-ko desplazamendu abiaduraz luzatu ziren apurtu arte. Ondoren, karga-desplazamendu kurbak tentsio-deformazio kurbetan bihurtu ziren, eta hortik erresistentzia maximoa atera zen, nanozuntz desberdinen ezaugarri mekanikoak alderatzeko. Nanozuntz bakoitzeko gutxienez 5 lagin aztertu ziren eta emaitzak batezbesteko ± desbideraketa estandar bezala aurkeztu ziren.

Nanozuntzek inguru urtsu batean ura xurgatzeko zuten ahalmena *in vitro* aztertu zen, 3 mintzen jokaera alderatzeko asmoz. Nanozuntzen 1x1 cm-ko laginak pisatu ondoren, PBS 1 ml-tan murgildu ziren eta 32°C-tara inkubatu ziren ordu batez. Ondoren, PBStik atera ziren, gehiegizko ura lehortu zen eta berriro pisatu ziren. Hurrengo ekuazioa erabiliz mintzek xurgatutako ura kalkulatu zen (Ek. 2):

$$\text{Ur xurgapena (\%)} = \frac{M - M_0}{M_0} \times 100 \qquad (2)$$

Non, M nanozuntzen amaierako pisua den eta $M_0$ nanozuntzen hasierako pisua den.

Nanozuntzen ur-lurrunaren iragazkortasun abiadura (Water Vapour Permeability Rate edo WVPR) Li *et al.*-ek deskribatutako metodoa moldatuz burutu zen (Li, et al. 2013). Silika gel lehorgarria zuen ontzi baten ahoa (1 cm diametro) aztergai zegoen mintzarekin erabat estali zen, ur-lurruna mintzean zehar bakarrik sar zitekeelarik ontzi barnera. Ontzia 30°C eta % 75-eko hezetasun erlatibo konstantea zuen ganbera batean 24 orduz mantendu zen. Muntaiaren hasierako eta amaierako pisuak eta honako ekuazioa erabiliz WVPRa kalkulatu zen (Ek. 3):

$$\text{WVPR} = \frac{M_1 - M_0}{A \times T} \qquad (3)$$

Non, $M_0$ saioaren hasieran muntaiak zuen pisua den, $M_1$ saioaren amaieran zuen pisua, A mintzaren esposizio azalera den eta T esposizio denbora.

Nanozuntzen, haien osagaien nahaste fisikoen eta lehengaien jokabide termikoa ekorketazko kalorimetria diferentzialaren (*differential scanning calorimetry* edo DSC) bidez aztertu zen (DSC-50, Shimadzu, Japonia). Lagin bakoitza aluminikozko platertxo batean hermetikoki itxi zen eta 25°C-tatik 350°C-tara berotu zen, 10°C/minutuko abiaduraz.

PLGA-AV-EGF nanozuntzen barnean kargatutako rhEGF kantitatea neurtzeko hurrengo prozedura erabili zen. Lehenik mintzaren 1x1 cm-ko zati bat dimetil sulfoxidoaren (DMSO, Scharlau, Espainia) 200 µL-tan disolbatu zen, disoluzio gardena lortu arte irabiatuz eta ondoren PBSaren (Life thecnologies, California, AEB) 800 µL-rekin diluituz. Lortutako disoluzio horretan zegoen rhEGF kantitatea giza EGFarentzako ELISA kit komertzial bat erabiliz neurtu zen, ekoizlearen jarraibideak jarraituz (human EGF ELISA development kit, Peprotech, AEB).

*2.3 rhEGFaren* in vitro *askapena*

Askapen entsegua Franz difusio gelaxketan burutu zen. 1x1 cm-ko PGA-AV-EGF nanountz mintz zati bat (9,76 µg rhEGF zituena) 30 µL PBSrekin hezetu zen eta ganbera emailean kokatu zen, 0,45 µm-ko poro tamaina zuen nylonezko iragazki baten gainean (Tecnokroma®, Espainia). Ganbera hartzailean 5 ml PBS jarri ziren. Sistema irabiatzen mantendu zen eta aukeratutako denbora tarteetan ganbera hartzailearen 1 ml hartu zen eta PBS berriarekin ordezkatu. Ingurunera askatutako rhEGF kopurua 2.2 atalean azaldutako ELISA protokoloa erabiliz neurtu zen. Saioa hiru aldiz burutu zen eta emaitzak denboran zehar metatutako rhEGF ehuneko modura adierazi ziren.

*2.4* In vitro *entsegu antibakterianoa*

PLGA-AV mintzaren eragin antimikrobianoa *Staphilococcus aureus* eta *Staphilococcus epidermidisen* aurrean aztertu zen. Laburki, bakterio bakoitzaren $10^5$ CFU (unitate kolonia eratzaile edo *colony forming unit)*/mL zituen disoluzio banaren 100 µL Mueller Hinton agar plaketan hedatu ziren. PLGA eta PGA-AV nanozuntzak 6 mm-ko disko biribiletan moztu ziren. 6 mm-ko disko txurietan 10 µL AV-aren estraktu urtsua kargatu zen (30 mg/mL) kontrol bezala erabiltzeko. Laginak eta kontrolak plaketan ezarri ziren eta 37°C-tara inkubatu ziren 36 orduz. Azkenik, laginen inguruan inhibizio halorik zegoen behatu zen.

### *2.3* In vitro *kultibo zelularreko entseguak*

#### *2.3.1 Kultibo zelularra*

BalbC/3T3 A31 fibroblastoak (ATCC, Manassas, AEB) DMEM ingurunean (*dulbeccos's modified Eagle's medium;* ATCC, Manassas, AEB) kultibatu ziren, eta inguruneari honako gehigarriak jarri zitzaizkion: % 10-eko (b/b) zekor seruma eta % 1-eko (b/b) penizilina-estreptomizina. Zelulak 37°C-tan mantendu ziren, % 5-eko $CO_2$ atmosferadun hezetutako inkubagailu batean. Zelula paseak 2-3 egunetik behin egin ziren.

#### *2.3.2. Bioaktibitate entsegua*

PLGA-AV-EGF, PLGA-AV eta PLGA nanozuntzen erauzkinek zelulen bideragarritasunean duten eragina fibroblastoetan aztertu zen. Zelulak 96 putzuko plaka batean erein ziren, 6000 zelula/putzu dentsitatearekin eta gauean zehar inkubatu ziren zelulen atxikimendua ahalbidetzeko.

Orduan, honako laginak gehitu ziren putzuetara: (i) kultibo ingurunea kontrol negatibo bezala, (ii) 20 ng/ml rhEGF askea, (iii) 20 ng/ml rhEGFren baliokidea den PLGA-AV-EGF nanozuntzen erauzkina, (iv) PLGA-AV nanozuntzen erauzkina eta (v) PLGA nanozuntzen erauzkina. 48 orduko inkubazioaren ostean zelulen bideragarritasuna CCK-8 kita erabiliz neurtu zen (cell counting kit-8, sigma-Aldrich, AEB). Laburki, CCK-8 erreaktiboaren 10 µL zeluletara gehitu ziren eta nahastea 4 orduz inkubatu zen. Orduan, absorbantzia 450 nm-tara irakurri zen, 650 nm erreferentziazko uhin luzera modura erabiliz (Plate Reader Infinite M200, Tecan, Suitza). Lortutako absorbantzia bizirik zeuden zelulei zuzenki proportzionala zen.

#### *2.5.3 Atxikipen entsegua*

Zelulen atxikipena nanozuntzezko mintzetara aztertzeko asmoz, BalbC/3T3 A31 fibroblastoak mintzen gainean erein ziren eta lotutako zelulak zenbatu ziren.

Laburki, PLGA, PLGA-AV eta PLGA-AV-EGF mintzen 1x1 cm zatiak 96 putzuko plaka batean finkatu ziren, itsasgarri bezala fibrinaren 10 µL erabiliz. Odolbatua eratzea ahalbidetzeko nanozuntzak 30 minutuz inkubatu ziren 37°C-tara, eta ondoren 15000 zelula erein ziren putzu bakoitzean. Kontrol putzuetan ere 15000 zelula erein ziren kultibo ingurune osoan.

Zelulak gauean zehar inkubatu ziren 37°C-tara zelulen atxikipena ahalbidetzeko. Ondoren, mintzak PBSarekin garbitu ziren eta atxikitako zelulak 10 minutuz tripsina-EDTaren (Lonza, Suitza) 50 µL-rekin inkubatuz askatu ziren. Azkenik, tripsina batu zen eta zelulak kontagailu automatiko bat erabiliz zenbatu ziren (Automated Cell Counter TC20™, Bio-Rad, California, AEB). Atxikipena adierazteko kontrolarekin alderatuz mintz bakoitzaren gainean zenbatutako zelulen ehunekoa erabili zen. 3 saio independente burutu ziren.

Horretaz gain, SEM argazkiak atera ziren zelulen atxikipena ikusteko. Kasu honetan, gauean zeharreko inkubazioaren ostean zelulak %2,5-eko glutaraldehido disoluzio batekin fixatu ziren eta etanol serie graduatuak erabiliz deshidratatu zen. Azkenik, irudiak SEM mikroskopio bat erabiliz atera ziren (Hitachi S4800, Tokio, Japonia).

### *2.6 Zauriaren orbaintze* in vivo *entsegua*

#### *2.5.1 Animaliak*

*In vivo* entsegurako 20 *db/db* (BKS.Cg-m+/+Lepr$^{db}$/J) sagu ar (8 asteko adinekoak) erabili ziren (Janvier laborategiak, Frantzia). Saio guztiak Euskal Herriko Unibertsitateko Animaliekin egiten den Esperimentaziorako Etika Batzordeak onartutako protokoloak jarraituz burutu ziren (Prozedura zenbakia: CEBA/243/2012/HERNANDEZ MARTIN). Animaliak banaka ostatatu ziren kaioletan, 12 orduko argi-ilun zikloan. Saguek karraskari pentsua zein ura nahierara izan zuten.

#### *2.5.2 Orbaintze entsegua*

Orbaintze entsegua Michaels *et al.*-ek (Michaels, et al. 2007) deskribatutako prozedura jarraituz burutu zen. Saguak isofluranoarekin (Isoflo, Esteve, Espainia) anestesiatu eta bizkarreko ilea kendu ostean, bizkarraren bi aldeetan 1 cm-ko diametroko silikona eraztun bana josi zitzaien 3-0 nylon hari bat erabiliz (Aragó, Espainia). Eraztunen helburua zaurien uzkurdura ekiditea zen, saguen orbaintze mekanismo nagusia baita. Horrela gizakien orbaintze mekanismo nagusiek, granulazio ehunaren sorrera eta errepitelizazioa, alegia, garrantzia har zezaten. Ondoren, eraztunen erdian, lodiera osoko zauri bana egin zitzaien *panniculus carnosumera* helduz 8 mm-ko diametroko biopsia puntzoi (Acu-Punch, Acuderm, AEB) baten bidez. Tratamenduak zaurien gain ezarri ziren eta azkenik zauriak baselinadun gaza batekin (Tegaderm® 3M) eta itsasgarriaren bi geruzekin estali ziren.

Saguak lau animaliako 5 taldetan banatu ziren jaso zuten tratamenduaren arabera (n=4): (i) tratatu gabeko kontrola; (ii) 10 µg rhEGF askea, 10 µL-tan disolbatuta; (iii) 1x1 cm-ko PLGA-AV-EGF nanozuntzen zati bat; (iv) 1x1 cm-ko PLGA-AV nanozuntzen zati bat eta (v) 1x1 cm-ko PLGA nanozuntzen zati bat.

Mintzak zaurian ezarri aurretik, PBSarekin hidratatu ziren. rhEGF askea, aldiz, PBSren 10 µL-tan disolbatu zen eta topikoki admininistratu zen, zaurian zehar barreiatzea ahalbidetuz. Zortzigarren egunean saguak $CO_2$ inhalazioaren bidez sakrifikatu ziren.

### *2.5.3 Orbaintzearen ebaluazioa*

Tratamenduen eraginkortasuna neurtzeko asmoz, kirurgiaren osteko 1., 4. eta 8. egunetan zaurien azalera ($px^2$) neurtu zen.

Egun horietan zaurien argazkiak atera ziren kamera digital bat erabiliz (Lumix FS16, Panasonic®, Espainia) eta haien azalera irudien analisi programa batekin neurtu zen (ImageJ®, Biophotonics Facility, University of McMaster, Canada). Zaurien itxiera hasierako azaleraren ehuneko modura adierazi zen.

### *2.5.4 Orbaintzearen analisi histologikoa*

Saguen sakrifizioaren ostean, zauriak eta inguruko ehunak (1x1 cm inguru) erauzi ziren eta % 3,7 formaldehidoan fixatu ziren. 24 ordu ondoren, biopsiak parafinan murgildu ziren eta 5 µm lodierako xaflatan ebaki ziren. Laginak H&E tindaketaren eta Masson trikromiko tindaketaren bidez prozesatu ziren, orbaintzea eta kolagenoaren metaketa ebaluatzeko, hurrenez hurren.

Errepitelizazio prozesua Sinha *et al.*-ek (Sinha eta Gallager 2003) ezarritako eskala erabiliz ebaluatu zen. Zauri bakoitzak 0-4 bitarteko puntuazio erdi-kuantitatiboa lortu zuen: 0, zauri ertzak bakarrik daude errepitelizatuta; 1, zauri erdia baino gutxiago dago errepitelizatuta; 2, zauri erdia baino gehiago dago errepitelizatuta; 3, zauri osoa dago errepitelizatuta, baina epitelio berriak lodiera irregularra du; eta 4, zauri osoa dago errepitelizatuta lodiera arrunteko epitelio berriarekin.

Hantura prozesuaren ebazpena eta zauriaren heldutasuna Cotran *et al.*-ek deskribatutako eskalaren arabera aztertu zen (Cotran, et al. 2000). Zauriei balio erdi-kuantitatiboak eman zitzaizkien, honako irizpidea jarraituz: 1, hantura akutua, fase honetan fibrina odolbatua eta mintz piogenikoa eratzen dira eta leukozito zein neutrofilo polinuklearren migrazioa gertatzen da; 2, hedatutako hantura akutua, granulazio ehunaren eraketa eta angiogenesia dira fase honetan nagusi, horretaz gain, mintz piogenikoa desagertzen hasten da; 3, hantura kronikoa, fibroblastoen proliferazioa gertatzen da fase honetan; eta 4, ebazpena eta sendaketa, hantura kronikoaren desagerpena gertatzen da fase honetan, nahiz eta zenbait zelula biribilak aurkitu daitezkeen.

Kolagenoaren metaketa ebaluatzeko Gal *et al.*-ek deskribatu zuten eskala erabili zen (Gál, et al. 2006): 0, kolageno eza; 1, kolageno eduki eskasa; 2, kolageno eduki ertaina; eta, 3, kolageno eduki handia.

*2.6 Analisi estatistikoa*

Datuak batezbesteko ± desbideraketa estandar modura adierazi ziren. Normaltasun testan oinarrituz, batezbestekoak bidebakarreko ANOVA probaren edo Mann-Whitney U testaren bidez konparatu ziren. ANOVAren ostean, Bonferroni edo Tamhane *post-hocak* aplikatu ziren bariantzen berdintasunaren probaren (Levene test) emaitzaren arabera. Kalkulu estatistikoak SPSS 22.0.01 programa erabiliz burutu ziren (SPSS® INC., Chicago, IL, AEB).

## 3. Emaitzak

### *2.1 Nanozuntzen karakterizazioa*

1. irudian agertzen diren SEM argazkiek erakusten dutenez, mintzak ausaz orientatutako nanozuntz uniformez osatuta zeuden. 1. taulan ikus daitekeenez, mintzek % 79 baino porositate altuagoa zuten. Espero zen bezala, mintz ezberdinek antzeko lodiera izan zuten, haien balioak 45,92 ± 0,78 µm; 56,76 ± 1,23 µm eta 59,17 ± 1,83 µm izan ziren, PLGA-AV-EGF, PLGA-AV eta PLGA mintzentzako, hurrenez hurren. Hala eta guztiz ere, nano zuntzen diametroa desberdina izan zen mintzaren arabera, 356,03 ± 112,05 nm PLGA-AV-EGF nanozuntzetan, 486,99 ± 114,73 nm PLGA-AV nanozuntzetan eta 561,61 ± 124,28 nm PLGA nanozuntzetan.

**1. Taula.** Nanozuntzen karakterizazioa: mintzen porositatea (%), mintzen lodiera (µm), nanozuntzen diametroa (nm), tentsio indarra (MPa), ur xurgapena (%), WVPR (g/m$^2$egun) eta peptido karga (µg/cm$^2$). Datuak batazbesteko ± SD modura adierazita daude.

| Nanozuntzen konposaketa | Mintzen porositatea (%) | mintzen lodiera (µm) | Nanozuntzen diametroa (nm) | Tentsio indarra (MPa) | Ur xurgapena (%) | WVPR (g/m$^2$egun) | Peptido karga (µg/cm$^2$) |
|---|---|---|---|---|---|---|---|
| PLGA | 79,50 ±7,42 | 59,17 ±1,83 | 561,61 ±124,28 | 3,06 ±0,35 | 218,17 ±45,03 | 1861,28 ±372,89 | - |
| PLGA-AV | 87,92 ±11,96 | 56,76 ±1,27 | 486,99 ±114,73 | 4,66 ±0,90 | 273,92 ±42,19 | 1690,09 ±190,25 | - |
| PLGA-AV-EGF | 87,52 ±6,62 | 45,92 ±0, 78 | 356,03 ±112,05 | 2,21 ±0,49 | 290,58 ±49,92 | 1907,39 ±228,82 | 9,76 ±1,75 |

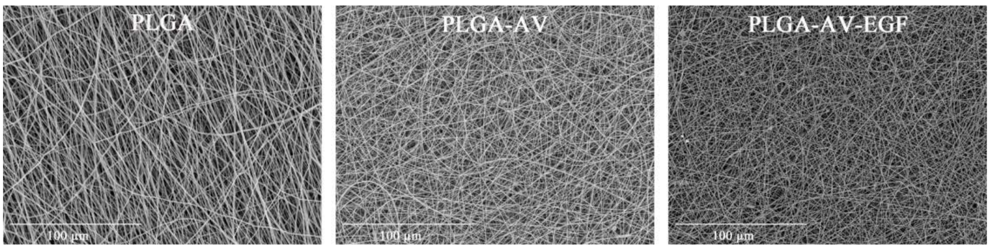


**1. Irudia.** PLGA, PLGA-AV and PLGA-AV-EGF nanozuntzen SEM argazkiak. Irudi bakoitzeko eskalak 100 µm adierazten ditu.

Mintzen osotasuna baieztatzeko asmoz, haien ezaugarri mekanikoak aztertu ziren. PLGA, PLGA-AV eta PLGA-AV-EGF nanozutzen erresistentzia maximoak hurrenez hurren, honakoak izan ziren: 3,06 ± 0,35 MPa, 4,66 ± 0,90 MPa and 2,21 ± 0,49 MPa (1. taula).

Mintzen hidrofilotasuna haien urxurgapena neurtuz ebaluatu zen. Emaitzek erakutsi zuten mintzek antzeko urxurgapena zutela, kasu denetan % 200 baino altuagoa zelarik: % 218,17 ± 45,03 PLGA nanozuntzetan; % 273,9 2 ± 42,19 PLGA-AV nanozuntzetan eta % 290,58 ± 49,92 PLGA-AV-EGF nanozuntzetan, 1. taulan ageri den modura. WVPRa ere, oso antzekoa izan zen mintz guztietan, 1861,28 ± 372,89 g/m$^2$egun, 1690,09 ± 190,25 g/m$^2$egun eta 1907,39 ± 228,82 g/m$^2$egun PLGA, PLGA-AV eta PLGA-AV-EGF nanozuntzentzako, hurrenez hurren.

Jokabide termikoari dagokionez, PLGA nanozuntzen beira-trantsiziozko tenperatura ($T_g$) PLGA lehengaiarena baino baxuagoa izan zen, haien balioak 49,84 ± 0,23°C eta 53,85 ± 0,16°C izan zirelarik, hurrenez hurren (2. taula). Horretaz gain, PLGAren $T_g$-an jaitsiera txiki bat behatu zen ere nanozuntzen osagaien nahasketan, ziurrenik AVaren presentzia dela eta. Aipagarria da, PLGA-AV eta PLGA-AV-EGF nanozuntzen termogrametan ageri ziren tontorrak PLGA eta AVaren nahasketa fisikoaren termograman ageri ziren berdinak zirela. rhEGFaren tontorra, aldiz, ez zen nanozuntzetan ezta osagaien nahaste fisikoetan ageri, ziurrenik proportzio oso txikian erabili zelako (2. taula).

**2. Taula.** DSC emaitzak. Nanozuntzen, osagaien nahastearen eta lehengaien DSC tontorrak. Datuak batazbesteko ± SD modura adierazita daude.

| | DSCaren tontor endotermikoak (°C) | |
|---|---|---|
| PLGA | 53.85±0.16 | |
| Aloe vera | 67.94±0.33 | 155.82±0.37 |
| rhEGF | 63.68±4.11 | 199.10±0.19 |
| PLGA eta Aloe vera nahastea | 52.04±0.83 | 68.89±0.56 |
| PLGA, Aloe vera eta rhEGF nahastea | 52.28±0.5 | 69.01±1.42 |
| PLGA nanozuntzak | 49.84±0.23 | |
| PLGA-AV nanozuntzak | 51.46±1.04 | 70.30±3.76 |
| PLGA-AV-EGF nanozuntzak | 52.04±0.08 | 71.73±1.48 |

PLGA-AV-EGF nanozuntzetan kargatutako rhEGF kantitatea 9,76 ± 1,75 μg/cm$^2$ zen. *In vitro* rhEGFaren askapen profila 2. irudian ageri da. Hasierako batbateko askapena edo *burst* efektua izan zuten nanozuntzek, izan ere, lehen 8 orduetan rhEGF totalaren %35a askatu zen. Ondoren, askapen fase geldoago bat egon zen 7 egunez, farmakoaren % 50a askatu zelarik entsegu honen amaierarako.

### *3.2* In vitro *entsegu antibakterianoa*

PLGA-AV nanozuntzetan zegoen AVaren eragin antibakterianoa aztertzeko inhibizio eremuaren testa erabili zen *S. aureus* eta *S. epidermidisaren* aurka. 3. irudian ikus daitekeen modura, erabilitako bi mikroorganismoetan, AV kontrolen eta PLGA-AV nanozuntzen inguruan hazkuntzaren inhibizio guneak agertu ziren. Hala eta guztiz ere, kualitatiboki begiratuta kontrolen inguruan ageri zen inhibizio gunearen diametroa handiagoa zen. PLGA mintzetan, aldiz, ez zen inolako hazkuntzaren inhibiziorik ikusi.

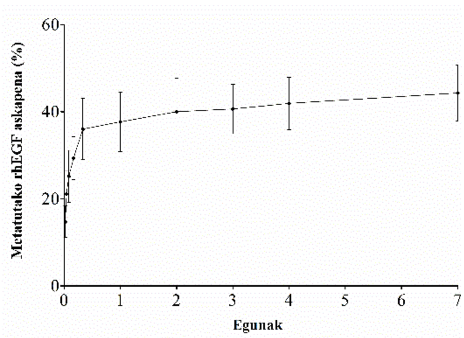


**2. Irudia.** rhEGFaren askapen profila. PLGA-AV-NLC nanozuntzetatik rhEGFaren metatze askapen profila *in vitro*. Emaitzak denboran zehar rhEGFaren metatze ehunekoaren batazbesteko ±SD moduan adierazita daude.

### *3.3* In vitro *bioaktibitate entsegua*

Elektroirute prozesuak osagaien bioaktibitatean eragina zuen aztertzeko fibroblastoak mintzen erauzkinarekin inkubatu ziren. 48 ordu ostean, zelulen proliferazioa CCk-8 entsegu bat eginez neurtu zen.

4. Irudian ageri den bezala, proliferazio zelular handiena PLGA-AV-EGF nanozuntzen erauzkinarekin lortu zen, kontrol taldearekin konparatuz hazkuntza hirukoiztu baitzen. Horretaz gain, PLGA-AV nanozuntzen erauzkinarekin tratatutako zeluletan ere proliferazioa handitu zen kontrolarekin alderatuz, dena den, mintz honekin lortutako igoera PLGA-AV-EGF mintzarekin lortutakoa baino txikiagoa

izan zen. PLGA nanozuntzen erauzkinak, ordea, ez zuen zelulen hazkuntza sustatu.

### *3.4 Atxikipen entsegua*

Zelulek nanozuntzetara itsasteko duten gaitasuna aztertzeko fibroblastoak mintzen gainean erein ziren. SEM irudietan nanozuntzen gainazalean zelulak atxikita zeudela ikus zitekeen (5A. irudia). Dena den, 5B. irudiak erakusten duenez, zelulak ezin ziren erraz atxiki mintzetara, izan ere kontrolarekin konparatuz % 16,85 ± 3,48; %17,99 ± 7,19 eta % 24,73 ± 6,40 bakarrik itsatsi ziren mintzetara, PLGA-AV-EGF, PLGA-AV eta PLGA nanozuntzetan, hurrenez hurren.

### *3.5* In vivo *orbaintze entsegua*

Mintzen eraginkortasuna *db/db* saguetan egindako lodiera osoko zaurien orbaintze entsegu baten bidez aztertu zen. Horretarako, 1., 4. eta 8. egunetan aterako argazkietako zaurien azalera ($px^2$) neurtu zen eta hasierako azalerarekin alderatuz zaurien itxieraren ehunekoa kalkulatu zen.

6A. irudian ikus daitekeen modura, PLGA-AV-EGF nanozuntzekin tratatutako animalietan zaurien azalera gehiago txikitu zen, gainontzeko taldeekin desberdintasuna estatistikoki esanguratsua izan zelarik bi egunetan, nahiz eta 8. egunean

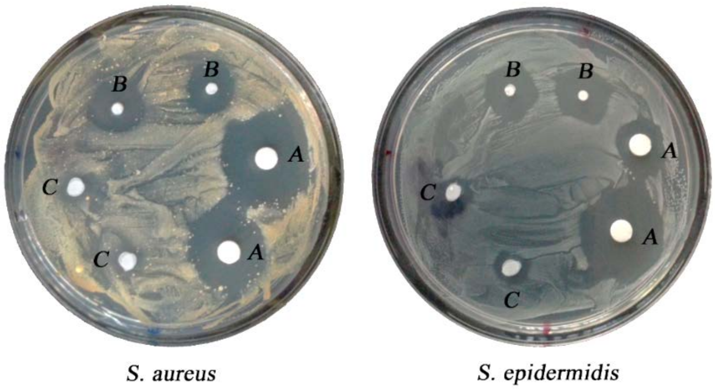


**3. Irudia.** *In vitro* entsegu antimikrobianoa. *S. aureus* eta *S. epidermidisekin* ereindako hazkuntza plaken irudiak. Laginek eragindako inhibizio guneak ikusi daitezke: (A) AV askea kontrol bezala. (B) PLGA-AV nanozuntzak eta (C) PLGA nanozuntzak.

desberdintasuna nabarmenagoa izan zen. Emaitza horiek zaurien behaketa kualitatiboarekin bat datoz (6B. irudia), izan ere PLGA-AV-EGF nanozuntzekin tratatutako zaurietan azalera txikiago ikusten baita. Horretaz gain, rhEGF askearen dosi berdina jaso zuten saguetan ez zen zauriaren itxieraren hobekuntzarik ikusi kontrolarekin alderatuz. Laugarren egunean, ez ziren desberdintasunik behatu gainontzeko taldeen artean. Zortzigarren egunean, aldiz, beste taldeekin konparatuz, PLGA-AV nanozuntzekin tratatuko saguetan zaurien itxiera esanguratsuki handiagoa izan zen.

Garatutako formulazioen eraginkortasuna aztertzeko analisi histologikoak burutu ziren ere bai. Horretarako, zaurien biopsiak H&E edo Masson trikromiko tindaketekin prozesatu ziren, errepitelizazioa, hanturaren ebazpena edo kolagenoaren metaketa aztertzeko, hurrenez hurren. 7A. irudian 8. eguneko ebaketa histologikoen (H&E tindaketa) argazkiak ikus daitezke.

Errepitelizazioren ebaluaketa Sinha *et al.*-ek (Sinha eta Gallagher 2003) ezarritako irizpidearen arabera burutu zen. 7B.

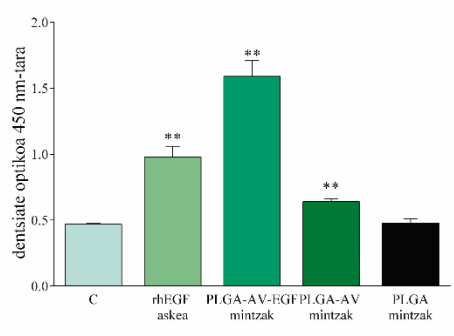


**4. Irudia.** Mintzen bioaktibitate entsegua. Zelulen bideragarritasunaren emaitzak CCK-8 saioan neurtutako dentsitate optikoen batazbesteko ± SD bezala adierazita daude. ** p<0,01 rhEGF askea, PLGA-AV-EGF eta PLGA-AV mintzak elkarrekin eta gainontzeko taldeak alderatuz.

irudian ikus daitekeen moduan, PLGA-AV-EGF eta PLGA-AV nanozuntzekin tratatutako animalien errepitelizazio gradua esanguratsuki handiagoa izan zen. Bi kasuetan, errepitelizazioaren batezbesteko balioa 3 ingurukoa izan zen, aipatutako eskalaren arabera, lodiera irregularreko epitelio berriaz guztiz estalirik dauden zauriei dagokiena. Hala eta guztiz ere, PLGA-AV nanozuntzekin tratatutako zauriek aldakortasun handia izan zuten (2,875 ± 0,991), zenbait zaurietan errepitelizazioak ez baitzuen zauri erdia estaltzen (1 gradua) eta beste batzuetan zauri osoa estaltzen zuelako lodiera arruntarekin (4 gradua).

PLGA-AV-EGF nanozuntzekin tratatutako animalietan, aldiz, aldakortasuna askoz txikiagoa izan zen (2,875 ± 0,354), zortzi zaurietatik zazpitan epitelio berriak zauri osoa estaltzen baitzuen lodiera irregularrez (3).

Kontrol animaliekin alderatuz, PLGA nanozuntzekin tratatutako animaliek ere, errepitelizazioaren hobekuntza esanguratsua izan zuten (0,875 ± 0,641 eta, 1,857 ± 0,9 hurrenez hurren), nahiz eta haien arteko desberdintasuna beste bi mintzek kontrolarekin izan zutena baino txikiagoa izan zen.

Hanturaren ebazpena ebaluatzeko Cotran *et al.*-ek deskribatutako eskala erabili zen (Cotran, et la. 2000). Taldeen artean ez zen desberdintasun esanguratsurik egon, 7C. irudian behatu daitekeenez. PLGA-AV-EGF eta PLGA-AV nanozuntzekin hanturaren ebazpena azkarragoa izateko joera ikusi zen. Talde horietan lortutako batezbesteko balioak 3 ingurukoak izan ziren (3 ± 0,926 eta 2,875 ± 0,835, hurrenez hurren), beste taldeetan 2 ingurukoak izan zirelarik (rhEGF askea 2,25 ± 0,07; PLGA nanozuntzak 2,143 ± 0,9 eta tratatu gabeko taldea 1,75 ± 1,165). Beraz, hasieran aipatutako bi taldeen zauriek heltze azkarragoa izan zutela ondorioztā daiteke, granulazio ehunaren sorrera fasea igaro eta fibroblastoen proliferazio fasera heldu baitziren.

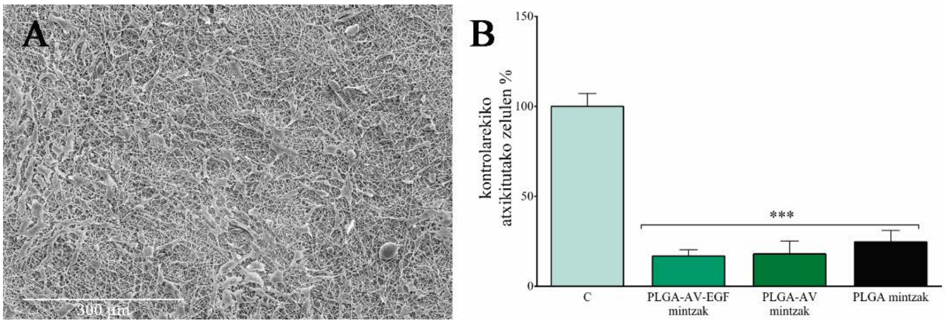


**5. Irudia.** *In vitro* atxikipen saioa. (A) Zelulak atxikituta dituzten nanozuntzen SEM irudiak. Eskala barrak 300 µm adierazten du. (B) Zelulen atxikipen emaitzak kontrolarekin alderatuz zenbatutako zelulen % batazbesteko ± SD moduan adierazita daude. *** p<0,001 PLGA-AV-EGF, PLGA-AV eta PLGA mintzak kontrolarekin alderatuz.

Horretaz gain, osagai aktiboak zituzten nanozuntzekin tratatutako zenbait zaurietan soilik desagertu zen hantura kronikoa (4 gradua), zehazki PLGA-AV-EGF nanozuntzekin tratatutako zaurietatik hiruk izan zuten guztizko sendatzea eta PLGA-AV nanozuntzekin tratatutako zauritetatik bik. Gainera, beste taldeen zenbait zaurik hantura akutuaren fasean (1 gradua) harrapatuta geratu ziren. Fase horretan gertatzen den etengabeko leukozito eta neutrofiloen migrazioa zauri kronikoen berezko ezaugarri da, zelula horiek jariatzen duten gehiegizko proteasa kantitateak ECMa degradatzen duelako, zaurien orbaintzea atzeratuz (Menke, et al. 2007).

Kolageno metaketari dagokionez (7D. irudia) taldeen artean ez zen desberdintasunik behatu. Kolageno metaketa handiena PLGA-AV-EGF eta PLGA nanozuntzekin tratatutako animalietan gertatu zen, zauri gehienek kolageno metaketa eskasa izan baitzuten (1 gradua, Gál et al.-ek ezarritako irizpidearen arabera (Gál, et al. 2006)), eta gutxi batzuk ez zuten kolagenorik edo eduki ertaina izan zuten, 0 edo 2 gradua hurrenez hurren. PLGA-AV nanozuntzekin edo rhEGF askearekin tratatutako zauri gehienek kolageno eduki eskasa izan zuten (1 gradua) eta gainontzekoek ez zuten kolagenorik eduki (0 gradua). Azkenik, aipagarria da kontrol taldean aldakor

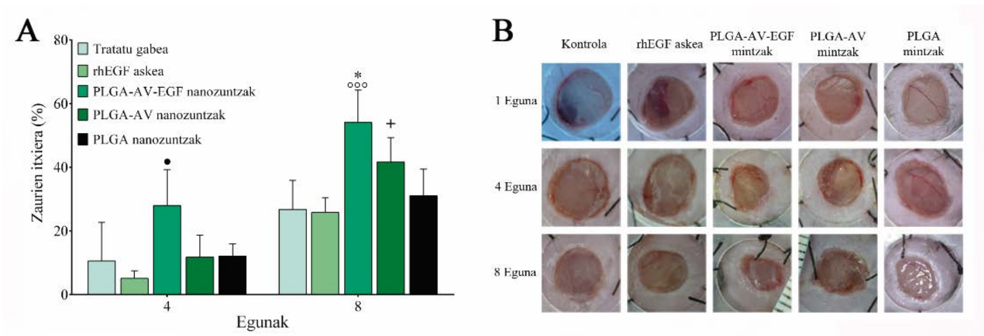


**6. Irudia.** *In vivo* zauriaren itxiera. (A) Zauriaren itxiera hasierako azalerarekiko murrizketa ehuneko bezala adierazita, zauria eragin ondorengo 4. eta 8. egunetan. ●$p<0,05$ PLGA-AV-EGF mintzak gainontzeko taldeekin alderatuz. ○○○ $p<0,001$ PLGA-AV-EGF mintzak rhEGF askearekin, PLGA mintzekin eta tratatu gabeko kontrolarekin konparatuz. * $p<0,05$ PLGA-AV-EGF mintzak PLGA-AV mintzekin alderatuz. + $p<0,05$ PLGA-AV mintzak PLGA mintzekin, rhEGF askearekin eta tratatu gabeko kontrolarekin konparatuz. (B) Zaurien irudiak, 1., 4. eta 8. egunetan.

tasun handia egon zela, izan ere zauri gehienek kolageno edukirik izan ez zuten arren (0 gradua), gutxi batzuk kolageno eduki handia izan zutelako (3 gradua).

## 4. Eztabaida

Elektroirutearen bidez ekoiztutako nanozuntzezko mintzak zaurientzako apositutak garatzeko aukera egokia dira, haien ezaugarri arkitektural bereizgarriak direla eta. Horregatik, ikerketa honen helburua PLGAz eta ahal izan zen AV kantitate handienaz osatutako nanozuntzezko apositu bat garatzea izan zen, zeinean rhEGFa kapsularatu zen.

Ekoiztutako mintzak ausaz orientatutako nanozuntz uniformez osatuta zeuden eta porositate altua zuten. Abrigo *et al.*-en arabera, ezaugarri horiek zelulen arnasketa eta gasen sarrera ahalbidetzen dute eta baita zaurien deshidratazioa ekidin ere (Abrigo, et al. 2014).

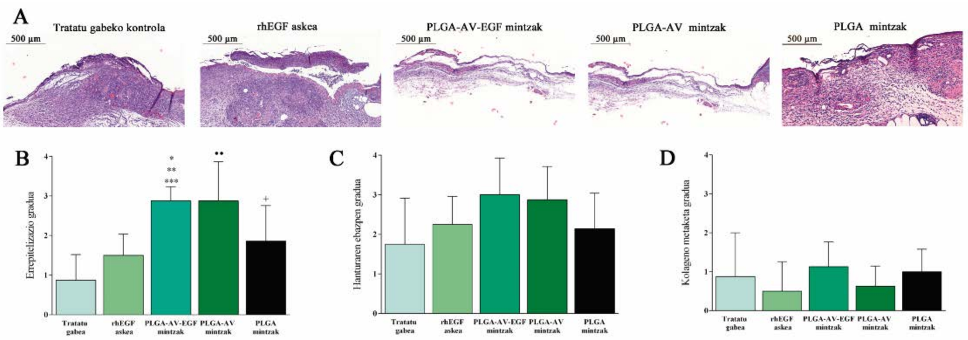


**7. Irudia.** Zaurien analisi histologikoa (n=8). (A) Zaurien irudi histologikoak (H&E) 8. egunean, 10x handipena. (B) Zaurien errepitelizazio gradua 8. egunean. *** p<0,001 PLGA-AV-EGF mintzekin tratatutako taldea tratatu gabeko taldearekin alderatuz. ** p<0,01 PLGA-AV-EGF mintzekin tratatutako taldea rhEGF askearekin tratatutakoarekin konparatuz. * p<0,05 PLGA-AV-EGF mintzekin tratatutako taldea PLGA mintzekin tratatutakoarekin alderatuz. ●● p<0,01 PLGA-AV mintzekin tratatutako taldea rhEGF askearekin eta tratatu gabeko kontrolarekin alderatuz. + p<0,05 PLGA mintzekin tratatutko taldea tratatu gabeko taldearekin alderatuz. (C) Hantura prozesuaren ebazpen maila. (D) Kolageno metaketa maila zaurietan. Emaitzak batazbesteko ± SD moduan adierazita daude.

PLGA-AV-EGF eta PLGA-AV nanozuntzen diametroa ECMko kolageno zuntzen tartean zegoen (50-500 nm). PLGA nanozuntzen diametroa ordea, goiko mugaren apur bat gainetik zegoen. ECMarekin antzekotasun horrek kaltetutako ehunen hemostasia sustatu dezake, zuntzen gainazal azalera altuagatik eta mintzean zehar zirrikitu txikiak daudelako (Abrigo, et al. 2014)

Mintzen ezaugarri mekanikoek haien egokitasuna apositu bezala erabiliak izateko erakutsi zuten, izan ere, lortutako tentsio indarraren balioak giza azalaren balioen antzekoak izan ziren, zeinak 5,7 MPa-tik 12,6 MPa-ra bitartera doazen, Jacquemoud *et al.*-en arabera (Jacquemoud, et al. 2007). Mintzen artean egon ziren desberdintasun txikiak haien osaerarengatik izan ziren. Alde batetik, AVak nanozuntzei malgutasuna eman zien, tentsio indarra handituz eta PLGA-AV mintzaren trakzioari erresistentzia maximoa handituz. Beste aldetik, rhEGFaren hauts liofilizatuak zituen gatzek PLGA-AV-EGF nanozuntzen tentsio indarra txikitu zuten.

Hiru mintzen ur xurgapena antzekoa izan zen arren, PLGA nanotzuntzek balio baxuena izan zuten, PLGA polimero hidrofoboa delako. AVa zuten mintzak, aldiz, hidrofiloagoak ziren, eta beraz ur gehiago xurgatzeko gai izan ziren. Emaitza horiek Son *et al.*-ek (Son, et al 2013) lortutakoekin bat datoz, PLGA nanozuntzetan gelatina kontzentrazio gorakorrak jartzean ur xurgapenaren igoera behatu baitzuten.

Zaurien aposituek ur-lurrunarekiko iragazkortasuna izan behar dute, exudatuak drainatzeko, baina horretaz gain, hezetasuna mantendu behar dute orbaintzea errazteko (Abrigo, et al. 2014; Natarajan, et al. 2000). Hezetasunaren kontrol hori mantendu ahal izateko merkaturatutako mintzek WVPRa balio zehatz batzuen artean daukate (426-2047 g/$m^2$egun) (Tu, et la. 2015). Tarte hori kontuan hartuta, garatutako formulazioek WVPR egokia zeukaten orbaintzean erabiliak izateko.

Mintzen jokabide termikoari dagokionez, PLGA nanozuntzen $T_g$-a PLGA lehengaiarena baino txikiagoa izateak, elektroirundako PLGAn polimeroaren kateek lerrokatze eta orientazio maila handia dutela iradokitzen du. Aldez aurretiko ikerketetan ere, $T_g$-aren antzeko txikipena behatu izan da (Fouad, et al. 2013). Horretaz gain, PLGA-AV eta PLGA-AV-EGF mintzetan eta PLGA-AV nahaste fisikoan tontor termiko berdinak antzeman izanak nanozuntzetan bi osagaiak ez zirela nahasten esan nahi du.

PLGA-AV-EGF nanozuntzetan, EGF aren *in vitro* askapenak profil bifasikoa erakutsi zuen, hasieran eztanda moduko askapena aurkeztuz eta ondoren askapen luzatutako fase bat aurkeztuz. Hasierako askapena nanozuntzen gainazalean zegoen proteinari zegokion, zauriaren ertzetan dauden keratinozitoen aktibazio azkarrarentzako garrantzitsua dena (Schneider, et al. 2009). Ondorengo fase luzatuan, farmakoaren %50 inguru baino ez zen askatu. Dena den, kargatutako farmakoaren askapena bizkorragoa izan daiteke *in vivo*, zaurian dauden entzimek polimeroaren degradazio azkartu dezaketelako (Fredenberg, et al. 2011).

Zauriak mikroorganismoetatik babesteko ahalmena aposituek izan behar duten ezaugarri garrantzitsu bat da, horrela zaurien infekzioak saihestu daitezkelako. Inhibizio gunearen saioan ikusi zen bezala, PLGA-AV nanozuntzak hazkuntza bakterianoa ekiditeko gai izan ziren, AVak eragin antibakterianoa baitu pisu molekular baxuko osagaiei esker. Konposatu horien artean α-bisabolola, lupeola, azido zinamonikoa, azido salizilikoa eta azido urikoa daude, besteak beste. Haien ekintza mekanismoa bakterioen prozesu entzimatikoak oztopatuz haiek hiltzean datza (Ghayempour, et al. 2016; Tummalapalli, et al. 2016). Horretaz gain, aposituek muga fisiko bat eratzen dute bakterioen aurrean, haien poro tamaina txikiak mikroorganismoen sarrera ekiditen baitu (Abrigo, et al. 2014).

AV askea erabiliz, emandako dosi osoa saioaren hasieratik eskuragarri zegoen, nanozuntzetan zegoen AVa, aldiz, haietatik askatu behar zen bakterioen hazkuntza inhibitu ahal izateko. Hori izan liteke AV askearekin inhibizio diametro handiagoa lortu izanaren arrazoia. EGFak eragin antibakterianorik ez duenez, ez ziren PLGA-AV-EGF mintzak aztertu saio honetan, AVaren eragina jadanik frogatuta baitzegoen PLGA-AV mintzen emaitzekin.

*In vitro* entseguekin rhEGFaren eta AV aren bioaktibitatea elektroirute prozesuaren ostean aldatu gabe mantentzen zela frogatu zen. Izan ere, mintzetatik eratorritako erauzkinek fibroblastoen proliferazioa sustatzeko gaitasuna zuten, lehengaiek bezala (Boudreau and Beland 2006; Gainza, et al. 2015a). Hala eta guztiz ere, entsegu honetan lortutako emaitza deigarriena PLGA-AV-EGF nanozuntzekin lortutako proliferazio handia izan zen, AVaren eta rhEGFaren konbinazioa onuragarria dela erakutsi zuena. Gainera, proliferazioa soilik AVaren eta rhEGFaren eraginez izan zela esan daiteke, izan ere, PLGA nanozuntzen erauzkinarekin tratatutako zeluletan ez zen proliferaziorik behatu.

Apposituak tratamenduan zehar aldatzeko diseinatuta zeudenez, zelulen atxikipena edo nanozuntzetan zehar ehunaren hazkuntza ekidin behar ziren, apositua kentzean mina eta eratu berri den ehuna kaltetzea saihesteko. Nanozuntzetan atxikitutako zelulen ehuneko baxua zela eta, garatutako formulazioak aldi baterako apositu modura erabiltzeko baliagarriak zirela ikusi zen.

Orbaintzea *in vivo* ebaluatu zen *db/db* saguetan egindako lodiera osoko zaurietan. Karraskarien orbaintze ereduetan errepitelizazioak ez dauka garrantzia handirik, nahiz eta gizakietan badaukan. Dena den, *db/db* saguetan prozesu horrek garrantzia hartzen du, zaurien uzkurdura oztopatua dagoelako, animalien gizentasunak azalaren malgutasuna txikitzen baitu (Fang, et al. 2010; Tkalcevic, et al. 2009). Horretaz gain, zaurien inguruan silikonazko eraztun bana josi zen, uzkurdura are gehiago eragotziz (Michales, et al. 2007). Errepitelizazioak garrantzia hartzen duenez, animalia hauen orbaintze prozesua gizakienaren antzekoagoa da. Hala eta guztiz ere, kolageno metaketaren emaitzetan ikusi zenez, sagu hauen orbaintzeak aldakortasun altua zeukan, aldez aurretik Trousdale *et al.*-ek deskribatu zuten bezala (Trousdale, et al. 2009).

Orokorrean, PLGA-AV-EGF nanozuntzek, rhEGF askearekin konparatuz, orbaintzea hobetu zezaketela erakutsi zuten, zauriaren itxiera eta errepitelizazioari dagokionez. PLGA-AV-EGF nanozuntzek orbaintzean izan zuten eragina, nanozuntzek kapsularatutako proteinengan duten eragin babesleari atxiki dakioke, izan ere, aldez aurretiko zenbait ikerketetan behatu den modura, nanozuntzek EGFa zaurian dauden proteasen aurrean babesten dute. Ikerketa horien artean, Choi *et al.*-ek eta Lai *et al.*-ek burututakoak daude. Lehenengoan, PCL-PG nanozuntzak EGFarekin konjugatu zituzten (Choi, et al. 2008). Lai *et al.*-ek bi nanozuntz motaz osatutako apositu bat garatu zuten, zeinak, alde batetik bFGFa eta VEGFaz kargatutako gelatina nanopartikulak zituzten azido hialuronikozko zuntzez eta, bestetik, EGFa eta PDGFdun gelatina nanopartikulak zituzten kolagenozko zuntzez osatuta zegoen (Lai, et al. 2014). Horretaz gain, nanozuntzen barne, rhEGFa denbora gehiago mantentzen da zaurian, mintzek luzatutako askapena ahalbidetzen baitute.

PLGA-AV-EGF nanozuntzek baino hein txikiagoan izan arren, PLGA-AV nanozuntzek orbaintzea sustatu zuten ere bai, AVak eta nanozuntzek haiek berak orbaintzea sustatu baidezakete (Abrigo, et al. 2014; Hashemi, et al. 2015). Mintzen egitura arkitektural bereizgarriak, hau da, duten bolumenerako gainazal azalera handia eta nanoporositateak, urari eta gasei iragazkor egiten ditu, zaurian hezetasuna maila egokia mantentzea ahalbidetuz eta arnasketa zelularra sustatuz. Horretaz gain, poroen tamaina txikiak mikroorganismoen sarrera ekiditen du. Aipatutako guztia dela eta, nanozuntzezko mintzek zelulen migrazioa eta proliferazioa sustatzen dute eta orbaintzearen bitartekarien askapena areagotzen dute, hala nola, kolagenoarena, hazkuntza faktoreena eta faktore angiogenikoena, era horretan, errepitelizazioa eta granulazio ehunaren sorrera erraztuz (Abrigo, et al. 2014; Shahverdi, et al. 2014). Honekin batera, errrepitelizazioaren hobekuntzan aukeratutako polimeroa eragina izan dezake, laktatoa, PLGAren degradazio produktu bat, orbaintzea bizkortzen duela ikusi baita (Porporato, et al. 2012).

Ikerketa honen aurretik, bazeuden *Aloe veradun* nanozuntzezko apposituei buruzko beste ikerketa batzuk, baina horietan gainontzeko osagaiekin konparatuz AVaren proportzioa 1:3, 1:6 eta 1:8 zen (Bhaarathy, et al. 2014; Karuppuswamy, et al. 2014; Suganya, et al. 2014). Ikerketa honetan, aldiz, AVren proportzioa handiagoa zen, AV, PLGA eta rhEGF proportzioa

1:1:0,4 baitzen hurrenez hurren. Beraz, ikerketa honetan, lehen aldiz *Aloe veraren* proportzio horren handia zuten nanozuntzak garatu ziren apositu modura erabiltzeko. *Aloe veraren* erabilerak ikerketaren berritasuna azpimarratzen du, bere erabilerak orbaintzea hobetzen duela erakutsi baitu.

Orokorrean, orbaintzearen hobekuntza hiru elementu hauen baturagatik izan zen, rhEGFrena, AVrena eta PLGA nanozuntzena, alegia, izan ere, aldez aurretik hirurek frogatu dute orbaintzea sustatzen dutela.

## 5. Ondorioak

Honako entsegu honetan, *Aloe vera* zeukan fase urtsu bat, azido poli-laktiko-ko-glikolikoarekin (PLGA) emultsionatu zen eta lortutako emultsioa elektroirun zen, rhEGFa kargatuta zuen nanozuntzezko apositu bat garatzeko. Nanozuntzek PLGAren eta AVaren proportzio berdina zuen (1:1), eta gure jakintzaren arabera horren *Aloe vera* kontzentrazio handia ez da orain arte erabili orbaintzean erabiltzeko nanozuntzezko aposituak garatzeko.

Mintzak nanozuntz uniformez osatuta zeuden, haien diametroa 356,03 ± 112,05 nm zen, porositatea % 87,52 zen eta mintzen lodiera 45,92 ± 0,78 µm zen. Elektroirute prozesuak ez zuen osagai aktiboen bioaktibitatean eraginik izan, *in vitro* bioaktibitate entseguak frogatu zuenez.

*Db/db* saguetan burutu zen *in vivo* lodiera osoko orbaintze entseguan, PLGA-AV-EGF nanozuntzek orbaintzearen sustapena eragin zuten, zauriaren itxiera eta errepitelizazioari dagokionez. Orokorrean, lortutako emaitza guztietatik atera daitekeen ondorioa honakoa da: AVaren proportzio handia duten PLGA-AV-EGF nanozuntzezko mintzak zauri kronikoetan erabiltzeko aukera aproposa direla.

## 6. Eskerrak

I. Garcia-Oruek Eusko Jaurlaritzari doktoratu aurreko laguntza eskertzen dio. Egileek UPV/EHU-ko SGIkerren laguntza teknikoa, giza babesa eta Europako finantziazioa (FEDER eta FSE) eskertzen dituzte. Proiektu hau neurri batean Eusko jaurlaritzak (ELKARTEK 2015, Nanoplatform, KK-2015/0000036). Horretaz gain, partzialki Euskal Herriko Unibertsitateak finantziatu du (UFI11/32). Egileek ICTS "NANBIOSIS"-en eta zehazki UPV/EHUan dagoen CIBER-BBNren Farmakoen Formulazio Unitateari (U10) laguntza tekniko eta intelektuala eskertu nahi diote.

**Erreferentzien zerrenda 110-115 orrialdeetan aurkitzen da.**

## 3. KAPITULUA

## Nanopartikula lipidikoak barneratuta dituen PLGA/Aloe veraz osatutako nanozuntz mintz konpositearen garapena, zaurien apositu moduan erabiltzeko.


### LABURPENA

Elektroirutearen bidez ekoitzitako nanozuntzezko aposituek zenbait ezaugarri apropos dituzte orbaintzean erabiliak izateko, hala nola, porositate eta bolumenaren araberako gainazal azalera handia. Hori dela eta, ikerketa honetan PLGA eta *Aloe veraren* erauzkinaz osatutako apositu bat garatu zen. Horretaz gain, nanopartikula lipidikoak (NLCak) gehitu zitzaizkion, osagai lipidikoaren helburua apositua zaurietara atxikitzea ekiditea eta apposituaren maneiua, oklusibitatea eta elastikotasuna hobetzea zirelarik. NLCdun eta NLC gabeko mintzak 1 µm diametro inguru zuten zuntz uniformez osatuta zeuden. Haien porositatea %80 baino altuagoa zen eta lodiera 160 µm, NLCak zituzten apositoak loditasun handiagoa zutelarik. Apositu biek antzeko ur-xurgapena eta ur-lurrunaren iragazkortasun abiadura (WVPR) izan zituzten, haien balioak % 370 eta 1100 g/m$^2$egun izan zirelarik, hurrenez hurren. Ezaugarri mekaniko desberdinak izan zituzten bi mintzek, izan ere NLCak zituen mintza elastikoagoa zen, bere erresistentzia maximoa 2,61 ± 0,46 MPa-koa zelarik. *In vitro*, bi fomulazioek biobateragarriak zirela erakutsi zuten, fibroblasto eta keratinozitoen aurrean. Horretaz gain, zelulen atxikipen entseguan behatu zen bi mintzek itsaspen perfil baxua zutela, NLCdun apositoak baxuagoa zuelarik. Azkenik, mintzen eraginkortasuna *db/db* saguetan egindako lodiera oso zauri eszisionaletan aztertu zen. Orbaintzea antzeko eran hobetu zuten bi formulazioek, zaurien itxierari, errepitelizazioari eta hanturari zegokienez. Ondorioz, PLGA-AV-NLC nanozuntzezko mintzak zauri kronikoen tratamendurako estrategia aproposa izan daitezkeela esan dezakegu, izan ere, NLC gabeko formulazioarekin alderatuz apposituaren maneiua hobetzen zuten.

# 4. KAPITULUA

## Orbaintzea sustatzeko gelatina/kitosano bigeruzadun hidrofilm baten garapena


### LABURPENA

Ikerketa honetan, gelatinan oinarritutako bigeruzadun apositu berri bat garatu genuen. Elkargurutzaketa erreaktibo desberdinak erabiliz geruza bakoitzari ezaugarri bereizgarriak eman genizkion, horrela orbaintzean erabilgarri izan zitekeen hidrofilm multifuntzional bat lortuz. Lehenik, gaineko geruza ekoitzi genuen, zeina laktosaz elkargurutzatutako gelatinaz osatuta zegoen. Geruza hau erresistentea eta ez-degradagarria zen, apositu osoari euskarri mekaniko eta babesa emateko. Azpiko geruza ekoizteko, gelatina azido zitrikoarekin elkargurutzatu zen, ura xurgatzeko ahalmen handia zuen matrize porotsu bat lortuz. Horretaz gain, azpiko geruzari kitosanoa gehitu genion, orbaintzea estimulatzeko duen ahalmenaz baliatzeko. Elkargurutuzatzailearen eragina FTIR eta SEM analisien bidez frogatu zen, izan ere, laktosa gelatinaren bigarren mailako egitura aldatzeko gai zela behatu zen, egitura trinkoago eta lauagoa eraginez. Emaitzek erakutsi zuten bigeruzadun hidrofilma bere pisu lehorraren % 407,3 ± 108,6 ur xurgatzeko gai zela, osotasun mekanikoa mantenduz. Horretaz gain, bere ur lurrunaren transmisio abiadura 1381,5 ± 108,6 g/m$^2$egun zen. *In vitro*, fibroblastoekin biobateragarritasun ona erakutsi zuten garatutako hidrofilmek. Azkenik, haien eraginkortasuna giza azalean burututako *ex vivo* orbaintze saio batean aztertu zen. Hidrofilmek kontrol taldearen antzeko emaitzak lortu zituzten. Beraz, orokorrean esan daiteke garatutako bigeruzadun hidrofilmek apositu moduan erabiliak izateko ezaugarri egokiak izan zituztela.

# Eztabaida

Zauri kronikoen tratamenduak garrantzia handia irabazi du, bere intzidentziaren igoera kezkagarria dela eta. Erronka kliniko bat bilakatzen ari dira, izan ere, AEBtan bakarrik, urtero 5,7 millioi pertsonek (populazioaren % 2 inguru) pairatzen dituzte eta 20 bilioi dolar kostatzen dute zauri kronikoek [1]. Europan, 6000-10000 € xahutzen dira zauriei lotutako gastuetan, hots, erizain denboran, ospitalizazioetan, apposituen aldaketetan eta zaurien infekzioen kudeaketan [2,3].

Zauri kronikoen intzidentziaren igoera zaurien kronizitatearekin lotuta dauden gaixotasunen hazkuntzarekin erlazionatuta dago, gaixotasun horien artean, obesitatea, diabetesa eta gutxiegitasun benosoa daudelarik [4]. Zauri horiek orbaintzearen fase fisiologikoetan (hemostasia, hantura, proliferazioa eta erremodelazioa) zehar igarotzeari huts egiten diote, azalaren integritatearen berreskurapena atzeratuz eta maiz berriro agertuz [5-7]. Oztopatutako orbaintzearen arrazoi nagusia haien etengabeko hantura egoera da, izan ere prozesu osoan zehar neutrofiloak zaurian egoten dira, gehiegizko zitokina proinflamatorioak eta proteasak askatuz. Horiek mikroingurune proteolitiko bat eratzen dute, orbaintzearen bitartekariak eta matrize extrazelularra (*extracellular matrix* edo ECM) degradatzen dituena [8,9].

Gaur egun, zauri kronikoen terapiek ezin dute orbaintze eraginkor bat ziurtatu. Hori dela eta, tratamendu eraginkor baten bilaketak garrantzia handia irabazi du, ahalegin handiak egin direlarik tratamendu berrien garapenean edo egungo tratamenduen hobekuntzan. Orbaintzean parte hartzen duten molekula endogenoen administrazio topikoa tratamendu berri horietako bat da. Zoritxarrez, molekula horietako gehienek egonkortasun oso eskasa dute *in vivo*, haien izaera proteikoa dela eta. Muga hau gainditzeko, sistema desberdinetan kapsularatuak izan daitezke, hala nola, nanopartikula lipidikoetan eta zehazki nanoegituratutako eramaile lipidikoetan (NLCak). NLCak kapsularatutako peptidoa babesteaz gain, orbaintzerako abantaila ugari dituzte: askapen kontrolatua ahalbidetzen dute, haien itsasgarritasun eta oklusibotasunari esker azalaren hidratazioa handitzen dute, eta haien tamaina txikiak azalarekin kontaktu estua ziurtatzen du [10].

Zaurien zainketak dituen eskakizunak betetzeko beste aukera bat nanozuntzezko mintzak dira. Apositu hauek orokorrean elektroirutearen bidez eratzen dira. Teknika honek, indar elektrikoa erabiliz, disoluzio polimeriko batetik zuntz nanometrikoak erauzten ditu [11]. Elektroirutearen bidez lortutako nanozuntzek egitura bereizgarria daukate, zeinak bolumenarekiko gainazal azalera handia eta porositate handia dituen. Ezaugarri horiek orbaintzea sustatzen dute arnasketa zelularra bultzatuz eta exudatuak xurgatzeaz gain zaurian hezetasuna mantenduz, izan ere, gasen iragazkortasuna ahalbidetzen dute eta zauriko hezetasuna kontrolatzen dute [12]. Horretaz gain, haien egiturak ECMaren hiru dimentsioetako egitura imitatzen du, ehun ingeniaritzarako aukera interesgarria bihurtzen dituena [13,14].

Azkenik, bigeruzadun aposituek interes handia jaso dute zaurien orbaintzean erabiliak izateko, haien ezaugarri nabarmenak direla eta. Haien egiturak azalaren bigeruzadun egitura imitatzen du, epidermisa antza duen gaineko geruza babesle batekin eta dermisaren antzekoa den azpiko geruza malgu eta lodiarekin. Hori kontuan hartuz, apposituaren gaineko geruza dentsoa zauria estaltzeko diseinatua dago, aposituari indar mekanikoa emanez. Horretaz gain, hezetasunaren transmisioa kontrolatu behar du, zauriaren deshidratazioa ekiditen duen biartzean, exudatuen garbiketa ahalbidetuz. Horretaz gain, gaineko geruzak bakterioen sarrera ekidin behar du, horrela zaurien infekzioa saihestuz. Beste aldetik, azpiko geruzak egitura porotsua izan behar du, zeinak zauriko exudatua xurgatzeko gai izan behar duen eta zaurira leunki atxiki behar den ehun eratu berriarentzat inguru egokia sortuz [15-17].

Faktore horiek buruan edukita, doktorego honetan orbaintzea sustatzeko formulazio desberdinen garapenean zentratu gara. Lehenengo urrats batean, LL37 giza peptidoan oinarritutako nanopartikula formulazio bat garatzea erabaki genuen, molekula antimikrobiano honek orbaintzea zenbait bidez modulatzen duela frogatu baita, hala nola, angiogenesia aktibatuz [18,19], zelula epitelialen migrazioa eta proliferazioa bultzatuz [20,21] eta monozito, neutrofilo eta zelula dendritikoentzako kimiotaktikoa izanez [22].

LL37ak i*n vivo* egonkortasun eskasa duenez, babesteko asmoz NLCetan kapsula-ratua izan zen. Beraz, tesi honetan garatutako lehen formulazioa LL37a kapsularatuta zuten NLCak izan ziren (NLC-LL37).

NLCak ekoizteko lipido solido (Precirol ATO5) eta likido (Mygliol® 812N) bana zituen urtutako fase lipidiko bat surfaktanteak zituen fase urtsu epel batekin emultsionatu zen. Bi faseak nahastu ondoren, LL37a gehitu eta sonikazioaren bidez emultsionatu ziren. Metodo honen bidez lortutako NLCak 273,6 ± 27,6 nm-ko batazbesteko tamaina zuten eta -31 mV inguruko zeta potentziala. LL37aren kapsularatze eraginkortasuna % 96,4 ± 0,4-koa izan zen eta peptido karga 16,8 ± 0,1 µg LL37/mg NLC.

*In vitro* aktibitate entseguaren aurretik, NLC-LL37en biobateragarritasuna zehaztu zen, haiekin batera inkubatutako fibroblastoen bideragarritasuna neurtuz. Formulazioa zitotoxikoa ez zela frogatu ostean, bere ekintza ebaluatu zen, kapsularatze prozesuak peptidoaren bioaktibitatean eragina zuen aztertzeko. Horretarako, RAW 267.4 makrofago lerro zelularra lipopolisakaridoarekin (LPS) aktibatu zen eta LL37 askearekin, NLC-LL37ekin edo NLC hutsekin tratatu zen. Formulazioak makrofagoen aktibazioa inhibitzeko gai ote ziren kuantifikatzeko, makrofagoek askatutako TNF-α kantitatea ELISA baten bidez neurtu zen. 1. irudian ikus daitekeenez, NLC-LL37ek LL37 askearen antzeko neurrian murriztu zuten TNF-αren ekoizpena, peptidoa kapsularatze prozesuaren ostean aktibo mantentzen zela iradokitzen duelarik. Horretaz gain, NLC hutsek ez zuten efekturik izan, NLC-LL37en eragina kapsularatutako LL37ari esker izan zela nabarmenduz. Makrofagoen neutralizazioa lortzeko, LL37a LPSari elkarrekintza eletrostatiko eta hidrofoboen bidez lotu behar da eta baita makrofagoen CD14 hartzaileari ere lotura selektibo baten bidez [23-25].

Ondoren, NLC-LL37en ekintza antimikrobianoa *E. coliren* aurka aztertu zen, infektatutako zaurietan bakterio arruntenetakoa baita [26]. Laburki azalduta, LL37askea, NLC-LL37ak eta NLC hutsak *E. colirekin* batera inkubatu ziren 4 orduz. Orduan, laginak hartu, agar plaka batean inokulatu, 24 orduz inkubatu eta hazitako koloniak zenbatu ziren. Emaitzek erakutsi zuten LL37 askeak bakterio guztiak hiltzen zituela, NLC-LL37ak hildako bakterioen ehunekoa, aldiz, baxuagoa izan zelarik. Honen azalpena NLCtatik LL37a era luzatuan askatzen zela da, ondorioz, saioaren hasieran eskuragarri zegoen dosia baxuagoa zen. Hori dela eta, NLC-LL37ak ezin izan zituzten bakterio guztiak saioaren hasieran hil, eta geratzen zirenen hazkuntza esponentzialagatik NLC-LL37en ekintza oztopatuta egon zelarik. Hala eta guztiz ere, *in vivo* bakterioak etengabe proliferatzen daude, peptidoaren luzatutako askapena hasieran dosi altua izatea baino beharrezkoagoa egiten duena.

Azkenik, formulazioen eraginkortasuna *in vivo* aztertu zen, *db/db* saguei egindako lodiera osoko zauri eredu batean. Karraskari eredu bat aukeratu zen, animalia txikiekin errazagoa delako lan egitea, nahiz eta txerrien azala gizakienaren antzekoagoa den [27]. Dena den, *db/db* saguek beste karraskari ereduekiko abantaila batzuk erakusten dituzte. Lehenik, leptina hartzailean mutazio bat daukate II motako diabetesaren fenotipoa eragiten diena, horrek orbaintzea atzeratzen die eta ondorioz zauri kronikoen antza handiagoa daukate [28,29]. Bigarrenez, sagu hauek zauriaren uzkurdura oztopatuta

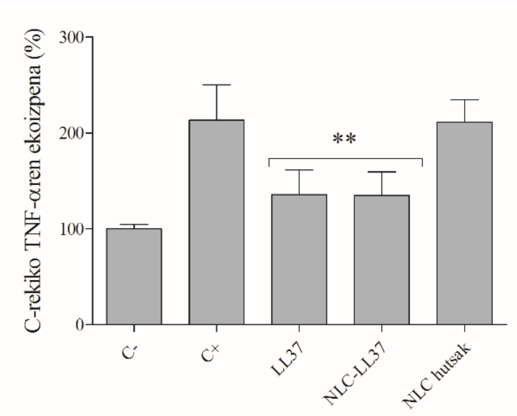


**1. Irudia**. Makrofagoen aktibazioaren inhibizioa. Emaitzak kontrolarekiko TNF-α ekoizpenaren % batezbesteko ± SD bezala adierazita daude. ** NLC eta C+ baino esanguratsuki handiagoa ($p<0,01$). Kontrolak C- (zelulak inolako gehigarririk gabe) eta C+ (zelulak LPSaren gehiketaren ostean) dira.

daukate, haien gizentasunak azalaren malgutasuna murrizten baitu [30,31]. Horren ondorioz, errepitelizazioak garrantzia handiagoa hartzen du, orbaintze prozesua gizakienaren antzekoagoa eginez. Horretaz gain, zaurien uzkurdura are gehiago oztopatu genuen haien inguruan silikonazko eraztun bana josiz [32]. Animaliei NLC-LL37aren bi dosi desberdin administratu zitzazkien bide topikotik, talde bati LL37aren 6 µg-ri zegokion NLC-LL37aren dosia administratu zitzaion eta beste taldeari LL37aren 2 µg-ri zegokiona.

Orbaintzea ebaluatzeko ondorengo parametroak neurtu ziren: (i) zaurien itxiera, zaurien argazkietatik azalerak neurtuz kalkulatu zena; (ii) errepitelizazio gradua, erdi-kuantitatiboki neurtu zen, H&Eren bidez prozesatutako ehun sekzioetan Sinha *et. al.*-ek deskribatutako eskala aplikatuz [33]; (iii) hantura prozesuaren ebazpena, aurrekoa bezala H&Eren bidez tindatutako ehun sekzioak erabiliz ebaluatu zen, kasu honetan Contran *et al.-ek* deskribatutako eskalaren arabera [34]; (iv) kolageno metaketa, Masson trikomiko tindaketaren bidez prozesatutako ehun sekzioak erabiliz aztertu zen, Gal *et al.*-ek ezarritako eskala jarraituz [35], eta (v) angiogenesia, immunohistokimikoki antiCD31 antigorputz monoklonalaz tindatutako ehun sekzioetan odol hodi eratu berriak zenbatuz ebaluatu zen.

2. irudiko emaitzek erakusten dutenez, NLC-LL37en administrazioak zaurien itxiera zein errepitelizazioa orbaintzea bizkortu zuen NLC hutsekin, LL37 askearekin eta tratatu gabeko taldearekin alderatuz. Horretaz gain, NLC-LL37ak hantura prozesuaren ebazpena ere sustatu zuen, baina kasu honetan LL37 askearen neurri berean. Kolageno metaketari eta angiogenesiari dagokienez, ez zen desberdintasunik behatu taldeen artean.

Orokorrean, kapsularatutako peptidoak areagotutako ekintza erakutsi zuen, ziurrenik NLCek degradazio kimiko zein entzimatikoaren aurrean izan zuten efektu babesgarriaren ondorioz. Horretaz gain, NLCek luzatutako askapena ahalbidetzen dute, LL37aren eragina luzatuz [36,37]. Gainera, aurretik garatutako beste LL37dun nanopartikulekin alderatuz [38], NLCek administrazio topikoa alhalbidetzen dute, pazienteentzako bide erraza, eroso eta segurua dena. Aurkikuntza guzti horiek kontuan hartuz, NLC-LL37en administrazio topikoa zauri kronikoen tratamendurako estrategia interesgarria izan daitekeela ondoriozta dezakegu.

Tesi honen bigarren urratsean, hazkuntza faktore epidermikoa (*epidermal growth factor* edo EGF) kapsularatuta zuen nanozuntzezko apositu bat garatu genuen. Faktore trofiko hau orbaintzearen molekula gakoa da, keratinozito eta fibroblastoen proliferazio eta migrazioa estimulatzen dituelako [39]. Bere administrazio topikoak orbaintzea sustatu dezakeela frogatu da jadanik, dena den, duen erdibizitza laburrak bere erabilpen klinikoa zailtzen du [40,41].

Hori dela eta, EGFa nanozuntzezko mintzen barne kapsularatuz muga hori gaindi daitekela hipotetizatu genuen, izan ere, mintzek peptidoa ingurune kaltegarritik babestu dezakete eta gainera haien egiturak orbaintzea sustatu dezake. Nanozuntzezko mintzak

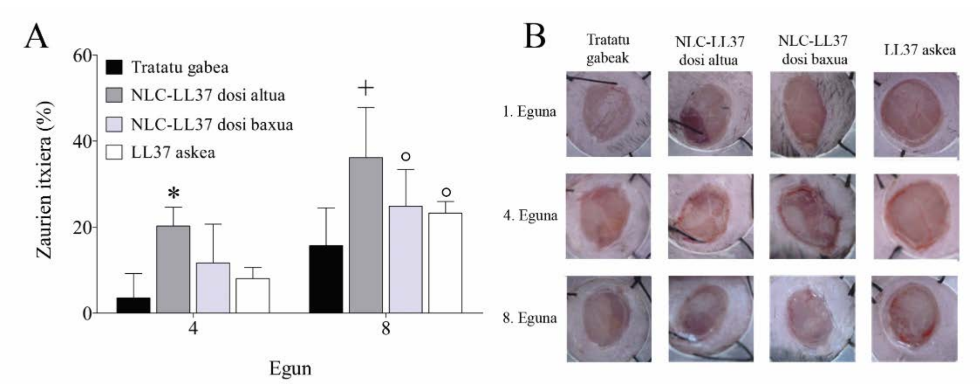


**2. Irudia.** *In vivo* zauriaren itxiera. (A) Zaurien itxiera hasierako gainazal azalerarekiko murrizketa ehuneko bezala adierazita. * Tratatu gabeko taldearekiko esanguratsua ($p<0.05$); ○ Tratatu gabeko taldearekiko esanguratsua ($p<0.05$); + gainontzeko taldeekiko esanguratsua ($p<0.05$). (B) Zaurien irudiak.

ekoizteko hexafluoroisopropanolean disolbatutako PLGA, *Aloe veraren* erauzkina eta EGFa zituen fase urtsu batekin emultsionatu zen. Ondoren, emultsioa elektroirunteko xiringa batean kargatu zen, zeinaren orratza energia iturri batera konektatuta zegoen. Tentsio altuak emultsioa kargatzean, aldarapen indar elektrostatikoak sortu ziren, orratzeko tanta luzatuz eta kolektorera emultsio hari bat jaurtiz. Hari horren barneko disolbatzailea kolektorerako bidean lurruntzen zihoan, kolektorera nanozuntz solidoak helduz [42,43]. Metodo honek EGFa zuten PLGA eta *Aloe veraz* (1:1) osatutako nanozuntzezko mintzen ekoizpena ahalbidetu zuen (PLGA-AV-EGF mintzak). *Aloe vera* formulaziora gehitzearen arrazoia orbaintzea bultzatzen duela frogatuta dagoela izan zen, izan ere, fibroblastoen hazkuntza faktorean eragina dauka, fibroblastoen ekintza, proliferazioa eta kolageno ekoizpena estimulatuz [44,45]. Gure ezagueraren arabera, orbaintzean erabil-

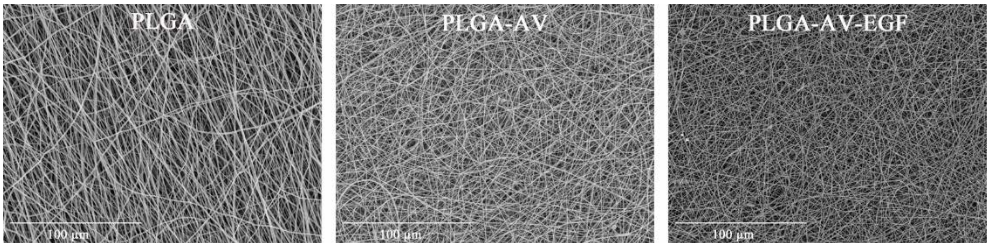


**3. Irudia**. PLGA, PLGA-AV and PLGA-AV-EGF nanozuntzen SEM argazkiak. Irudi bakoitzeko eskalak 100 µm adierazten ditu.

**1. Taula.** Nanozuntzen karakterizazioa: mintzen porositatea (%), mintzen lodiera (µm), nanozuntzen diametroa (nm), tentsio indarra (MPa), ur xurgapena (%), WVPR (g/m$^2$egun) eta peptido karga (µg/cm$^2$). Datuak batazbesteko ± SD modura adierazita daude.

| Nanozuntzen konposaketa | Mintzen porositatea (%) | mintzen lodiera (µm) | Nanozuntzen diametroa (nm) | Tentsio indarra (MPa) | Ur xurgapena (%) | WVPR (g/m$^2$egun) | Peptido karga (µg/cm$^2$) |
|---|---|---|---|---|---|---|---|
| PLGA | 79,50 ±7,42 | 59,17 ±1,83 | 561,61 ±124,28 | 3,06 ±0,35 | 218,17 ±45,03 | 1861,28 ±372,89 | - |
| PLGA-AV | 87,92 ±11,96 | 56,76 ±1,27 | 486,99 ±114,73 | 4,66 ±0,90 | 273,92 ±42,19 | 1690,09 ±190,25 | - |
| PLGA-AV-EGF | 87,52 ±6,62 | 45,92 ±0, 78 | 356,03 ±112,05 | 2,21 ±0,49 | 290,58 ±49,92 | 1907,39 ±228,82 | 9,76 ±1,75 |

tzeko horren *Aloe vera* kontzentrazio handia duten apposituak garatu ziren lehen aldia izan zen hau. Horretaz gain, nanozuntzezko mintz hauek garatu ziren ere: EGFrik ez zutenak (PLGA-AV mintzak) eta EGF zein *Aloe verarik* ez zutenak (PLGA mintzak). Hiru mintz moten karakterizazioa 1. taulan eta 3. irudian laburtuta ageri da. Elektroirute prozesuaren bidez ausaz orientatutako nanozuntz uniformez osatutako mintzak ekoiztu ziren. Egiturak porositate handia zuen (%79 baino altuagoa) eta bolumenarekiko azalera handia ere bai, zelulen arnasketa eta hezetasunaren kontrola baimentzen dituena [11].

Zuntzen arteko desberdintasun handiena haien diametroan eta ur xurgapenean zegoen. *Aloe vera* gehitzeak nanozuntzen diametroa 561,6 ± 124,3 nm-tatik 487 ± 114,7 nm-tara txikitu zuen eta EGFa gehitzeak 356 ± 112 nm-tara. Ur xurgapenean behatutako desberdintasunei dagokienez, *Aloe veradun* mintzek ur gehiago xurgatzeko gaitasuna zutela ikusi zen, konposatu honek mintzen hidrofilotasuna handitzen zuela iradokiz [46].

Mintzen ezaugarri mekanikoak proba desplazamendu kontrolaren arabera aztertu ziren Instron 5848 mikrotestagailu batean. Aipagarria da giza azalaren antzeko balioak izan zituztela, horiek 5,7 MPa 12.6 MPa-ra bitartea doazelarik [47]. Horretaz gain, urlurrunarekiko iragazpen abiadura (*water vapour permeability rate* edo WVPR) apositu komertzialen mailan zegoen (426-2047 $g/m^2$egun), horrek garatutako apositauk hezetasunaren kontrol egokia lortzeko gai zirela iradokitzen duelarik [48]. WVPRa neurtzeko, silika gel lehorgarria zuten ontzien ahoak garatutako mintzekin erabat estali ziren. Ondoren ontziak ganbera klimatiko batean sartu ziren 24 orduz, eta muntaia esposizio denboraren aurretik eta ondoren pisatuz WVPRa kalkulatu zen.

Mintzen jokabide termikoa ekorketazko kalorimetria diferentzialaren (*differential scanning calorimetry* edo DSC) bidez aztertu zen. Emaitzek erakutsi zuten elektroirundako PLGAk polimero kateen lerrokatze eta orientazio maila handia zutela, izan ere, beira-trantsiziozko tenperatura ($T_g$) PLGA mintzetan (49,84 ± 0,23°C) PLGA lehengaian

(53,85 ± 0,16°C) baino baxuagoa zen, aurretik deskribatu den moduan [48]. Horretaz gain, antzeko tontor termikoak antzeman ziren PLGA-AV eta PLGA-AV-EGF elektroirundako mintzetan eta baita PLGA eta *Aloe vera* nahaste fisikoan ere, nanozuntzen barne bi osagaien izaera nahastezina agerian utziz. EGFaren tontorra ez zen inon behatu, ziurrenik mintzetan zegoen proportzio txikia zela eta.

PLGA-AV-EGF mintzetatik EGFaren *in vitro* askapen saioa Franz difusio gelaxketan burutu zen. Hezetutako 1x1 cm-ko mintz zati bana ganbara emailean kokatu zen nylonezko iragazki (0,45 µm-ko poro tamaina) baten gainean eta ganbera hartzailean 5 ml PBS kokatu ziren. Aurretik hautatutako uneetan, ganbera hartzailetik laginak hartu ziren eta askatutako EGFa ELISA komertzial baten bidez neurtu zen. Mintzek askapen profil bifasikoa izan zuten, hasierako eztanda edo *burst* askapena gertatu zen, non lehenengo 8 orduetan farmakoaren % 35a askatu zen eta ondoren askapen fase geldoago bat gertatu zen, 7 egunetan EGF totalaren % 50a askatu zelarik. Hasierako eztanda askapena nanozuntzen gainazalean zegoen EGFari zegokion eta zauri ertzeko keratinozitoen aktibazio azkarra lortzeko balio du [49]. Aipagarri da, EGFaren % 50a soilik askatu zen arren, *in vivo* askapena bizkortu daitekela, zaurian dauden entzimek polimeroaren degradazioa azkartu dezaketelako [50].

Behin aposituak karakterizatu zirela haien bioaktibitatea ebaluatu zen. Alde batetik, *Aloe veraren* aktibibatea aztertu zen [51]. Horretarako PLGA-AV eta PLGA mintzetatik hartutako diskoak *Staphilococcus aureus* eta *S. epidermidisekin* ereindako hazkuntza plaketan jarri ziren, eta inkubatu osean mintzek eratu zuten inhibizio gunea neurtu zen. PLGA mintzen inguruan ez zen inhibizio gunerik agertu, PLGA-AV mintzen inguruan agertutako inhibizio gunea *Aloe veraren* eraginez izan zela nabarmenduz. Hala eta guztiz ere, *Aloe vera* disoluzioa zuten disko komertzialen inguruan inhibizio gune handiagoa agertu zen, ziurrenik bigarren kasu honetan *Aloe vera* dosi osoa hasieratik eskuragarri zegoelako, NLC-LL37 formulazioarekin gertatu zen bezala. Gainera, ekintza antimikrobianoari dagokionez, nanozuntzezko mintzen mikroorganismoen sarrera ekiditen dute, duten poro tamaina txikia dela eta.

Beste aldetik, EGFaren eta *Aloe veraren* efektua fibroblastoen proliferazioan aztertu genuen, elektroirute prozesuak haien ekintzaren gain eragina zuen behatzeko [52,53]. Horren harira, fibroblastoak nanozuntzezko mintzek askatutako ingurunearekin inkubatu ziren, eta haien bideragarritasuna CCK-8 saioaren bidez neurtu zen. Proliferazio zelular altuena PLGA-AV-EGF mintzekin lortu zen, izatez, EGF askearen kontzentrazio berdinarekin inkubatutako zelulena baino altuagoa zen, konbinazioaren efektu onuragarria nabarmenduz. Horretaz gain, PLGA-AV mintzetan proliferazio igoera behatu zen, baina ez PLGA mintzetan. Horrek, ekintza EGF eta *Aloe veraren* eraginez baino ez zela iradokitzen du.

Mintzak tratamenduan zehar aldatzeko diseinatuak zeudenez, zelulen atxikipena edo nanozuntzetan zehar ehunaren hazkuntza ekidin behar dira, apositua kentzean mina eta eratu berri den ehuna kaltetzea saihesteko [11]. Hori dela eta, zelulak mintzetara atxikitzeko gai ziren ebaluatzea erabaki genuen, fibroblastoak haien gainean 24 orduz inkubatuz, eta orduan, atxikitutako zelulak askatuz eta zenbatuz edo haien SEM argazkiak ateraz, 4.A irudian ageri den modura. Grafikoan ikus daitekeenez (4.B irudia), zelulen atxikipena mintzetara oso oztopatuta zegoen hazkuntza plaken hondoarekin konparatuz, aldi baterako apositu bezala haien egokitasuna erakutsiz.

Azkenik, mintzen eraginkortasuna *db/db* saguei egindako lodiera osoko zauri ereduan aztertu zen. Horretarako, aurreko ikerketan bezala, zaurien azaleraren murrizketa, errepitelizazio gradua, hantura prozesuaren ebazpena eta kolageno metaketa aztertu ziren. 4. egunean, PLGA-AV-EGF mintzek zaurien itxiera azkartu zuten gainontzeko taldeekin konparatuta, talde horiek EGF askea, PLGA-AV mintzak, PLGA mintzak eta tratatu gabeko kontrola zirelarik. 8. egunean zaurien itxieraren hobekuntza handiena PLGA-AV-

EGF mintzekin lortu zen ere, nahiz eta kasu honetan PLGA-AV mintzek zaurien itxiera sustatzeko gai izan ziren ere. Horretaz gain, PLGA-AV-EGF eta PLGA-AV mintzak ezarriz, zaurien errepitelizazio gradua hobetu zen. Izan ere, errepitelizazioa ebaluatzeko erabili zen eskalaren arabera zauri osoa errepitelizatuta zuten, baina lodiera irregularrez [33]. Hantura prozesuaren ebazpenari eta kolageno metaketari dagokionez, ez ziren desberdintasunik behatu taldeen artean, dena den, aurreko parametroekin bat zetorren tendentzia arin bat nabari zitekeen.

Orokorrean, *in vivo* entseguan lortutako emaitzek erakutsi zuten zaurietan PLGA-AV-EGF mintzen ezarpena, PLGA-AV mintzen ezarpena eta EGF askearen administrazioa baino abantailatsuagoa zela. Efektu onuragarri hau, neurri batean nanozuntzezko mintzek zauriko proteasen aurka duten eragin babesgarriak azaltzen du, aurretik deskribatu den modura [40,55]. Horretaz gain, mintzetatik gertatzen den askapen luzatuak, EGFaren iraupena luzatzen du, horrela bere eragina hobetuz.

*Aloe vera* eta nanozuntzek haiek berak orbaintzea sustatu zuten. Alde batetik, *Aloe verak* orbaintzea bultzatzen duela frogatua dago, fibroblastoen hazkuntza faktorearengan

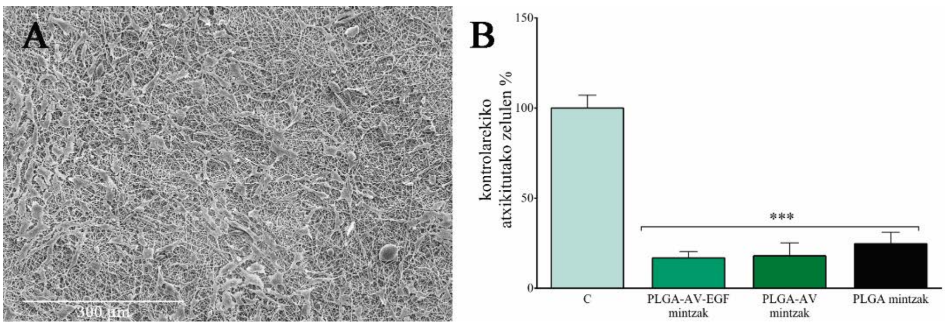


**4 irudia.** *In vitro* atxikipen saioa. (A) Zelulak atxikita dituzten nanozuntzen SEM irudiak. Eskala barrak 300 µm adierazten du. (B) Zelulen atxikipen emaitzak kontrolarekin alderatuz zenbatutako zelulen % batazbestekoa ± SD moduan adierazita daude. *** p<0,001 PLGA-AV-EGF, PLGA-AV eta PLGA mintzak kontrolarekin alderatuz.

eraginez, fibroblastoen ekintza eta proliferazioa sustatzen baitu [53]. Beste aldetik, aurretik azaldu denez, elektroirundako mintzen egiturak zaurien itxieran eragina dauka, gasen eta uraren iragazkortasuna ahalbidetzen baitu [56]. Ondorioz, orbaintzearen hobekuntza EGFaren, *Aloe vera* erauzkinaren eta nanozuntzen baturaren ondorioz izan zen, haien konbinazioz lortutako apositua zauri kronikoen tratamendurako aproposa izan daitekeela erakutsiz.

EGFrik ez zuten nanozuntzezko mintzek ere orbaintzea sustatu zutenez, ondorengo urratsean, PLGA eta *Aloe veran* oinarritutako nanozuntzezko apositu baten garapenari ekin genion. EGFa ez eramateak osasun-produktu baten garapenerako bidea zabaltzen baitu. Mintzen ezaugarrietako batzuk hobetzeko asmoz, elektroirute prozesuan zehar NLCak gehitu ziren, osagai lipidiko horrek mintzak zaurira atxikitzea ekidin eta haien kentzea erraztuko zuelakoan. Horretaz gain, NLCen gehitzeak apposituaren maneiua, elastikotasuna eta oklusibitatea hobetuko zituela ere hipotetizatu genuen.

NLCdun eta NLC gabeko nanozuntzezko mintzak (PLGA-AV-NLC eta PLGA-AV) garatu ziren, NLCak gehitzeak duen eragina ebaluatzeko. Kasu honetan, pisu molekular handiagoko PLGA bat erabili zen, NLCen gehitzea errazten baitzuen. Hori dela eta, mintz hauen karakterizazioa aurrekoenen arinki desberdina izan zen, 2. taulan ikus daiteekenez. Porositatearen balioak aurreko ikerketan lorutako balioen antzekoak izan ziren, % 80 ingurukoak, alegia, horrek gasen iragazketa eta beraz, zelulen arnasketa ahalbidetzen zuelarik. Beste aldetik, nanozuntzen diametroa 500 nm-tatik 1 µm ingurura handitu zuen, ziurrenik pisu molekular handiko PLGArekin prestatutako polimero soluzioaren biskositate handiagoa zela eta, izan zere, soluzioaren biskositatea nanozuntzen morfologia kontrolatzeko faktore kritikoa da [56]. Horretaz gain, mintzen ur xurgapena aurreko ikerketan baino altuagoa izan zen, % 380 ingurukoa, zaurian hezetasuna mantentzen duen bitartean, exudatuak drainatzen laguntzeko baliagarria dena [3,46].

**2. Taula.** Nanozuntzen karakterizazioa: mintzen porositatea (%), mintzen lodiera (µm), nanozuntzen diametroa (nm), tentsio indarra (MPa), ur xurgapena (%) eta WVTR (g/m$^2$egun). Datuak batazbesteko ± SD modura adierazita daude.

| Nanozuntzen konposaketa | Mintzen porositatea (%) | Mintzen lodiera (µm) | Nanozuntzen diametroa (nm) | Tentsio indarra (MPa) | Ur xurgapena (%) | WVTR (g/m2egun) |
|---|---|---|---|---|---|---|
| PLGA-AV mintzak | 1,10 ± 0,42 | 81,55 ± 1,16 | 158,03 ± 17,41 | 1,69 ± 0,35 | 369,06 ± 28,09 | 1128,06 ± 93,23 |
| PLGA-AV-NLC mintzak | 0,96 ± 0,34 | 84,23 ± 0,85 | 178,04 ± 42,05 | 2,61 ± 0,46 | 384,32±35,65 | 1097,6 ± 102,83 |

Mintzen lodiera ere aurreko ikerketan baino altuagoa izan zen, nahiz eta esangura estatistikorik ez zuen, gainera PLGA-AV-NLC mintzetan PLGA-AV mintzetan baino handiagoa izan zen, NLCak gehitzeak mintzen maneiua hobetzeko gai zela iradokitzen zuena. NLCek mintzen oklusibitatea arinki handitu zuen ere bai, izan ere, PLGA-AV-NLC mintzetan ur-lurrunaren transmisio abiadura (*water vapour transmission rate* edo WVTR) PLGA-AV mintzetan baino baxuagoa izan zen. Gainera, Lortutako WVTR balioa (1097,6 ± 102,83 g/m$^2$egun) apositu komertzialen tartearen barne zegoen. Azkenik, tentsio indarrarekiko erresistentzia NLCen gehitzearekin handitu zen, aplikazioan zehar apositua apurtzea zailago egiten duena. Thomas *et al.-ek* behatu zutenez, erresistentziaren igoera nanozuntzen barne nanopartikulen banaketa uniformearen ondorioz izan daiteke, izan ere, horrela indarra uniformeki banatzen da, estresaren kontzentrazio guneak txikituz eta polimerotik NLCetara estresaren zeharkatzea erraztuz [57].

Nanozuntzezko mintzen analisi termikoa DSCaren bidez burutu zen, eta aurreko ikerketan behatu zen bezala elektroirundako PLGAren kateek lerrokatze eta orientazio maila handia aurkezten zuten, $T_g$-aren jaitsierak nabarmentzen zuenez [49]. PLGA-AV-NLC mintzetan eta osagaien nahaste fisikoan PLGA eta NLCei zegozkien tontorrak eta *Aloe verari* zegokion kurba eredua behatu ziren, nahiz eta NLCen tontorraren igoera arina gertatu zen, NLCen eta *Aloe veraren* artean elkarrekintzaren bat egon zitekeela iradokitzen duena.

Aurreko ikerketan, elektroirute prozesuak *Aloe veraren* ekintzan eraginik ez zuela frogatu genuen, bere ekintza antimikrobianoa eta fibroblastoen proliferazioaren gainekoa mantendu baitzen nanozuntzetan. Hori dela eta, ikerketa honetan zuzenean mintzen biobateragarritasuna aztertu genuen, aurreko ikerketan erabilitako metodo berdina jarraituz. Fibroblastoak eta keratinozitoak nanozuntzetatik erauzitako ingurunearekin 48 orduz inkubatu genituen eta, orduan CCK-8 saioa burutu genuen zelulen bideragarritasuna neurtzeko. Emaitzak 5. irudian ageri dira, eta mintzak bi lerro zelularrekin biobateragarriak zirela erakusten dute, kontrolarekin alderatuz bideragarritasuna % 70-a baino altuagoa baitzen. Gainera, fibroblastoetan mintzek bideragarritasuna igo zuten, ziurrenik *Aloe verak* haien gain duen efektu proliferatiboagoa dela eta [45,53].

Apposituaren maneiuan zuten efektuaz gain, NLCak nanozuntzetan barneratzeko arrazoi nagusia, apposituaren kentzea erraztu zezaketela hipotesia zen. Horregatik, zelulen atxikipen entsegua burutu genuen. Mintzak 24 putzutako plaken hondoan kokatu ziren

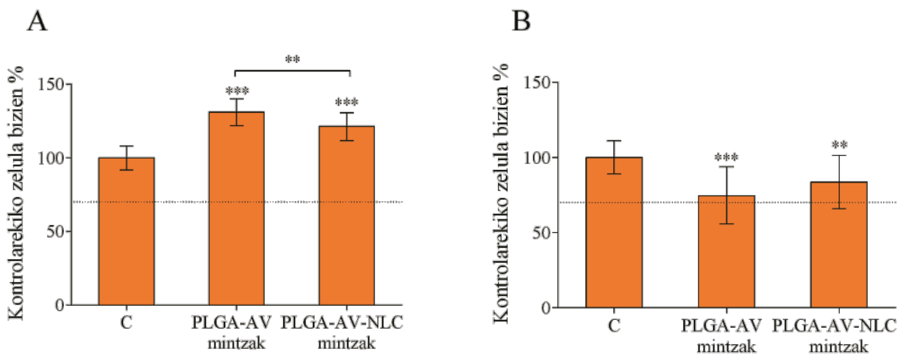


**5 Irudia.** Zelulen bideragarritasun saioa. (A) CCK-8 saioaren emaitzak mintzen erauzkina fibroblastoekin inkubatu ostean. *** p<0.001 PLGA-AV-NLC eta PLGA-AV mintzak kontrolarekin konparatuz; eta ** p<0.01 PLGA-AV mintza PLGA-AV-NLC mintzarekin alderatuz. (B) CK-8 saioaren emaitzak mintzen erauzkina fibroblastoekin inkubatu ostean. *** p<0.001 PLGA-AV mintza kontrol taldearekin alderatuz; eta ** p<0.01 PLGA-AV-NLC mintza kontrol taldearekin alderatuz. Emaitzak kontrolarekiko bizirik dauden zelulen % batezbestekoa ± SD bezala adierazita daude.

eta fibroblastoak edo keratinozitoak haien gainean inkubatu ziren 24 orduz. Orduan, atxikitako zelulak mintzetatik askatu eta zenbatu ziren atxikipena aztertzeko. Horretaz gain, mintzen SEM argazkiak atera ziren, baina irudietan ez zen zelularik behatzen. Zelulen zenbaketak erakutsi zuen bi mintzek zelulen atxikipena oztopatzen zutela, putzuen hondoarekin konparatuz. Fibroblastoen atxikipena antzekoa izan zen bi mintzetan. Keratinozitoetan ordea, NLCak zituen mintzaren gain itsaspen esanguratsuki txikiagoa gertatu zen. Hala eta guztiz ere, ikerketa gehiago burutu beharko lirateke, zauritutako ehunen gain aposituen itsaspena aztertzeko.

Aurreko ikerketetan bezala, aposituen eraginkortasuna *db/db* saguei egindako lodiera osoko zauri ereduan aztertu zen, nahiz eta aurrekoekin alderatuz zenbait aldaketa egin ziren: animaliak 8. eta 15. egunetan sakrifikatu ziren; kolageno metaketa ez zen aztertu, aurreko entseguetan aldakortasun handia baitzeukan; eta hantura zelulen presentzia ikerketa immunohistokimikoen bidez ebaluatu zen.

Orokorrean, bi mintzek antzera hobetu zuten orbaintzea, zaurien itxiera eta errepitelizazioari dagokionez, izan ere biek errepitelizazio osoa lortu zuten 15. egunerako. Hantura prozesuaren ebazpenari dagokionez, 15. egunean PLGA-AV mintzek bakarrik hobetu zuten orbaintzea kontrol taldearekin alderatuz. 8. egunean, aldiz, ez zen desberdintasunik behatu analisi histologikoan, dena den, garatutako mintzek, eta batez ere PLGA-AV-EGF mintzek, zaurietako makrofago infiltrazioa murrizteko gai izan ziren, zeina handituta egon ohi den atzeratutako orbaintzea edo diabetesa duten karraskarien zauri ereduetan [58,59]. Beraz, esan daiteke bi formulazioek zauriaren heltzea sustatu zutela, PLGA-AV-NLC mintzek soilik orbaintzearen fase goiztiarrean eta PLGA-AV mintzek fase berantiarrean. Ezin izan genuen NLCen eragina aposituen kentzean aztertu, izan ere, kendu aurretik PBSarekin hezetu genituen, ehun eratu berriari inolako kalterik ez eragiteko asmotan.

Ondorioz, esan dezakegu PLGA-AV-NLC nanozuntzezko mintzak zaurien zainketarako apositu bezala erabiltzeko estrategia aproposa izan daitezkeela, NLCen gehitzeak mintzen maneiua hobetzen baitu, antzeko eraginkortasunarekin. Dena den, ikerketa gehiago burutu beharko lirateke apposituak kentzerakoan NLCen eragina aztertzeko.

Tesi honen azken urratsean gelatina eta kitosanoz osatutako bigeruzadun apositu bat garatu genuen. Bigeruzadun apposituek alternatiba interesgarri bat aurkezten dute giza azalaren antzeko egitura bat eskaintzen dutelako, epidermisa bezalako gaineko geruza babesgarriarekin eta dermisa bezalako azpiko geruza malguago batekin [16]. Bere elkargurutzaketa mailaren arabera, gelatina bi geruzak osatzeko beharrezko diren ezaugarriak aurkezteko gai da. Polimero natural hau zabalki erabili da erabilera farmazeutikoetan, bere biobateragarritasun eta biodegradazio onak direla eta [60]. Bere kateek zelulen itsaspenaren sustapenerako sekuentzia garrantzitsua daukate, arginina-glizina-aspartiko (RGD) motiboa hain zuzen [61]. Horretaz gain, gelatinak ur kantitate handia xurgatzeko ahalmena du, hidrogelak sortuz, zeinek apositu moduan erabiltzeko abantaila ugari dituzten. Adibidez, zaurietan hezetasun maila egokia mantentzeko gai dira, inguruaren arabera ura xurgatzeko edo askatzeko gai baitira, zaurien azalera freskatzeko gai dira eta mina gutxitzen dute [62].

Horren ondorioz, bi gelatina hidrofilm garatu ziren, bata apposituaren gaineko geruza izateko eta bestea azpiko geruza izateko. Bi geruzak gelatina likidoa molde egokietan isuriz ekoitzi ziren. Gaineko geruza ekoizteko gelatina disoluzioa glizerol eta laktosarekin nahastu zen. Glizerola plastifikatzaile moduan gehitu zen eta laktosa elkargurutzatzaile moduan. Izan ere, gelatina eta laktosa beroaren presentzian nahasten direnean, Maillard erreakzioa deritzona gertatzen da, hau da, gelatinaren proteina kateak glikatzen dira [63]. Lortutako hidrofilma zurruna eta uraren degradazioarekiko erresistentea zen [64]. Zauria estaltzeko eta apposituaren erresistentzia mekanikoa handitzeko diseinatuta zegoen. Horretaz gain, hezetasunaren transmisioa kontrolatu behar zuen eta bakterioen sarrera ekidin [15-17].

Azpiko geruza gelatina disoluzioa, glizerola eta azido zitrikoarekin nahastuz ekoitzi zen. Azido zitrikoak gelatina elkargurutzatzeko gehitu zen, proteina kateen amina taldeekin erreakzionatzen baitu [65]. Lortutako hidrofilma porotsuagoa zen eta ura xurgatzeko gaitasun handia zuen, zauriko exudatuak xurgatzeko ezaugarri egokiak [15-17]. Horretaz gain, azpiko geruzari kitosanoa gehitu genion orbaintzea sustatzeko asmoarekin, izan ere, kitosanoak orbaintzea zenbait mekanismoen bidez bultzatzen du: ekintza hemostatikoa eta antibakterianoa du [66], fibroblasto eta keratinozitoen proliferazioa bultzatzen du [67,68], eta hantura prozesuaren erregulazioan parte hartzen du [69].

Glizerola eta kitosanoa zuten zein ez zuten hidrofilmak ekoiztu ziren eta bi geruzak etanolaren bidez elkarrekin itsatsi ziren. Gelatinaren egituran elkargurutzaketaren eragina Fourieren transformatu bidezko espektroskopio infragorriaren (*Fourier-transform infrared spectroscopy* edo FITR) bidez aztertu zen. Infragorri espektroen artean zeuden aldaketa nabarmenenak 1630 $cm^{-1}$-an (C=O tentsioa, amida I) eta 1530 $cm^{-1}$-an (N-H deformazioa, amida II) ageri ziren tontorren intentsitate erlatiboan ikus zitezkeen. Horretaz gain, amida I-aren azaleraren ehunekoa neurtuz, laktosarekin elkargurutzatutako gelatinan β-orri intermolekularren igoera behatzen zen, azido zitrikoarekin elkargurutzatutakoarekin alderatuz. Aldaketa hau SEM analisian agerikoa zen ere, izan ere elkargurutzaketa laktosaren eraginez gertatzen zenean mikroegitura trinkoago eta leunagoa ikusten zen, 6. irudian irudikatzen den bezala.

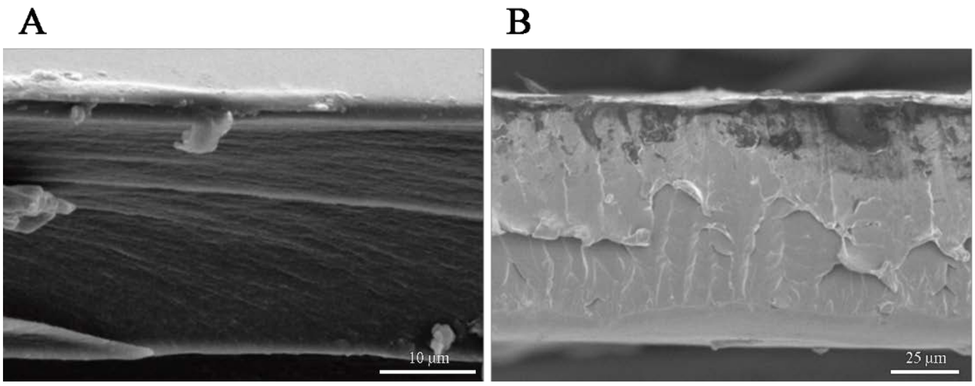


**6. irudia.** SEM analisia. (A) Lac+ HF zeharkako ebaketa. (B) CA+ HF zeharkako ebaketa.

Bigeruzadun apposituaren eta geruza bakoitzaren ur xurgapen ahalmena aztertu genituen, hidrofilm desberdinen portaera konparatzeko (7. irudia). Azalaren tenperaturara egin beharrean, saioa 4 °C-tara burutu zen, azido zitrikoarekin elkargurutzatutako hidrofilmek ur ingurune epeletan haien egituraren osotasuna galtzen baitzuten. Hori dela eta, aurretik pisatutako hidrofilm diskoak PBS hotzean murgildu ziren eta zehaztutako denboretan diskoak PBStik atera, gehiegizko ura lehortu eta berriro pisatu ziren ur xurgapena neurtzeko. Espero zenez, ur xurgapena gelatinaren elkargurutzaketa mailaren araberakoa izan zen. Hau da, laktosarekin elkargurutzatutako hidrofilmek ura xurgatzeko ahalmen baxuena zuten, azido zitrikoarekin elkargurutzatutakoek ahalmen handiena eta bigeruzadun hidrofilmek tarteko ahalmena, izan ere, bi geruzez osatuta zeuden [70].

Hidrofilmen egonkortasun hidrolitikoa aztertzeko, diskoak PBS hotzean murgildu ziren eta orekara heltzean handik atera ziren eta lehortzen utzi. Emaitzek erakutsi zuten glizerola zuten hidrofilmek hasierako pisuaren % 88 inguru mantentzen zutela, glizerol gabeko hidrofilmek pisuaren % 96 inguru mantentzen zuten bitartean. Pisu galera hori glizerolaren eta erreakzionatu gabeko elkargurutzatzailearen disoluzioaren bidez azal daiteke.

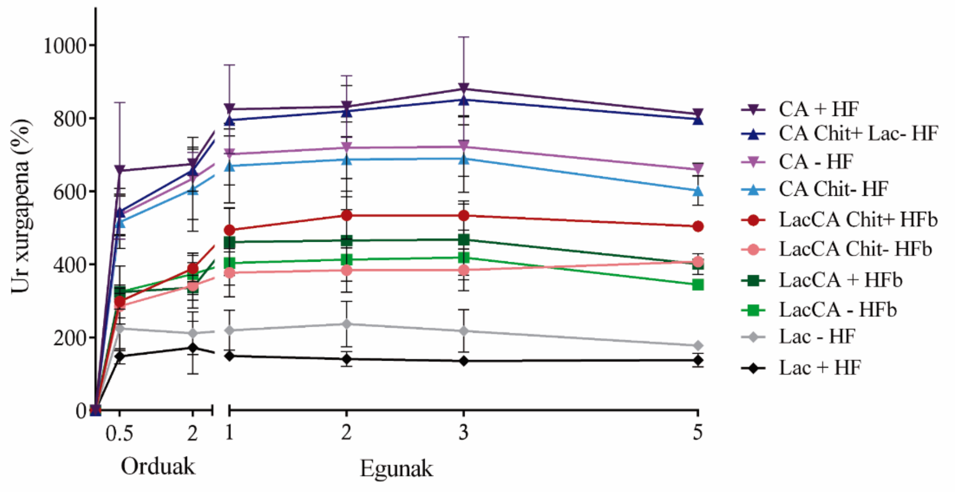


**7. Irudia.** Ur xurgapen kurba. Hidrofilm lehorren pisuarekiko ur xurgapen ehunekoa denbora desberdinetan. Emaitzak batazbestekoa ± SD moduan adierazita daude.

Ondoren, hidrofilmen oklusibitatea ebaluatu zen WVTR zehaztuz, baina erabilitako metodoa nanozuntzezko apposituena neurtzeko erabilitakoaren arinki desberdina izan zen. Franz difusio zelulak urarekin bete ziren eta haien beso hartzailea parafilmarekin estali zen. Hidrofilmak bi ganberen artean kokatu ziren, horrela ur lurruna hidrofilmak zeharkatuz soilik atera zitekeen sistematik. Saioaren hasieran eta 48 ordu ondoren muntaia pisatu zen WVTRa zehazteko. Azido zitrikoarekin elkargurutzatutako hidrofilmen oklusibitatea ez zen neurtu, izan ere hezetutakoan bi ganberen arteko irekidura estaltzeko ahalmena galtzen zuten. Bigeruzadun hidrofilmen emaitzek erakutsi zuten zaurien hezetasuna era egokian kontrola zezaketela, haien WVTRaren balioa aurretik aipatutako apositu komertzialen balioen tartean baitzegoen. Laktosarekin elkargurutzatutako hidrofilmek, ordea, WVTR balio altuagoa izan zuten, oklusibitate baxuagoa adierazten duena. Laktosarekin elkargurutzatutako hidrofilmen iragazkortasun handiagoa, haien lodiera txikiagoagatik azal daiteke [71].

Aurreko ikerketetan bezala, behin formulazioa karakterizatuta zegoela, haien biobateragarritasuna aztertu zen, osasun-produktuen ebaluaketa biologikorako ISO 10992-5:2009 jarraibideen arabera. Jarraibide horiek zitotoxikotasun zuzena eta zeharkakoa neurtzeko saioak proposatzen dituzte. Hala ere, azido zitrikoarekin elkargurutzatutako hidrofilmak 37 °C-tara partzialki disolbatzen zirenez, ezin genituen hidrofilm horiek hazkuntza plaka putzuetatik atera, eta beraz, ezinezkoa izan zitzaigun saio zuzena egitea. Hori dela eta, zeharkako saioa burutu genuen soilik, hidrofilmetatik askatutako ingurunea fibroblastoekin batera 24 orduz inkubatuz, eta orduan haien bideragarritasuna CCK-8 entseguaren bidez neurtuz. Hidrofilm guztiekin bideragarritasuna % 70-aren gainetik zegoen, biobateragarriak zirela frogatuz. Horretaz gain, saio honen bidez frogatu genuen ez zela beharrezkoa aurretiko egokitze pausurik burutzea, saioaren aurretik hidrofilmak 72 orduz dializatuz edo 15 minutuz hidratatuz emaitza berdinak lortu baitziren.

Azkenik, apposituen eraginkortasuna zaurien orbaintzean aztertu zen. Glizerol gabeko hidrofilmetan bakarrik burutu zen, izan ere glizerola hidratazio pausuan disolbatzen zenez, bere erabilera arbuiagarria zen. Bigeruzadun hidrofilmen artean, azpiko geruzan kitosanoa zuena soilik ebaluatu zen, kitosanoa eduki edo ez antzeko ezaugarriak zituztenez, kitosanoaren eragina aztertzeko. Horretaz gain, laktosarekin elkargurutzatutako geruza bakarreko hidrofilmak aztertu ziren, baina ez azido zitrikoarekin elkargurutzatutakoak, azken horiek ez zutelako nahiko egiturazko egonkortasunik haien kabuz apositu moduan erabiliak izateko.

Kasu honetan, eraginkortasuna ez zen *db/db* sagu ereduaren bidez ebaluatu, giza azalean egindako *ex vivo* eredu baten bidez baizik, ikerkuntzan animalien erabilera murrizteko asmoz. Ardura etikoetaz gain, animalia azala erabili beharrean gizakiena erabiliz, espezieen arteko orbaintzean dauden desberdintasunak ekidin daitezke [72]. Laburki, ohiturazko hautazko kirurgietatik lortutako azal biopsiak 6 mm diametroko diskoetan moztu ziren eta haien erdialdean 3 mm-ko lodiera osoko zauri eszisionalak egin ziren. Ondoren, biopsiak 24 putzuetako plaketan kultibatu ziren, *Transwell* sistemetan, epidermisa aire-likido interfasean mantenduz, 8. irudian ikus daitekeenez. Aldez aurretik hidratatutako hidrofilmak 1. eta 4. egunean ezarri ziren eta biopsiak 8 egunez kultibatu ziren.

4. eta 8. egunetan LDH saio bana burutu zen biopsien bideragarritasuna aztertzeko. Kasu guztietan bideragarritasuna % 70 baino handiagoa izan zen, biopsietako zelulak bizirik mantendu zirela esan nahi duena, *ex vivo* entseguan lortutako emaitzen fidagarritasuna erakutsiz. Emaitzek fibroblastoetan egindako zitotoxikotasun entseguan lortutako emaitzak berretsi zituzten, hidrofilmen biobateragarritasuna geruza bakarreko zelula hazkuntza baino egitura konplexuago batean frogatuz.

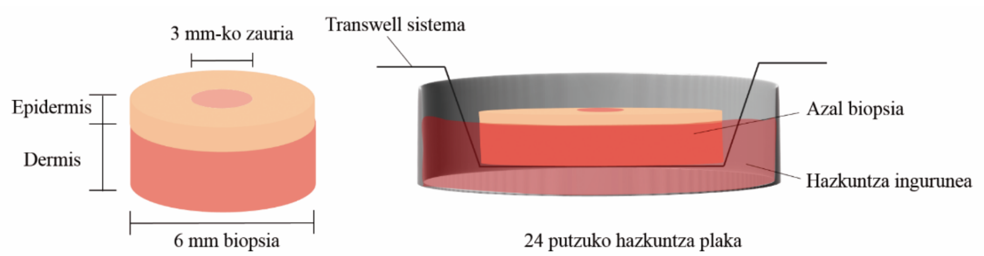


**8. Irudia.** *Ex vivo* saioaren eskema.

Hidrofilmen eraginkortasuna aztertzeko, orbaintzea ebaluatu zen azal laginetan burututako analisi histologiko eta immunohistokimikoen bidez. Orokorrean, antzeko emaitzak lortu ziren hidrofilmekin tratatutako taldeetan eta tratatu gabeko kontroletan, izan ere, ez zen desberdintasunik behatu zauriaren itxieran, zelulen proliferazioan, zauriaren uzkurduran eta keratinozito heldugabeen espresioan. Hala eta guztiz ere, laktosarekin elkargurutzatutako gelatina hidrofilmekin tratatutako taldean kolageno metaketa txikiagoa behatu zen eta bigeruzadun hidrofilmek keratinozito helduen espresioa oztopatu zuten. Inkubagailuaren hezetasun maila altuak eta hazkuntza medioaren poportzio bat xurgatzeko hidrofilmen gaitasunak, zaurian gehiegizko hezetasuna lortzea eragin dezakete, emaitza negatibo horiek azal ditzakeena. Hori dela eta, hidrofilmak eta batez ere, azido zitrikoarekin elkagurutzatutako gelatina hidrofilmak, optimizatu beharko lirateke orbaintzea sustatu dezakeen ingurune aproposagoa lortzeko.

Ondorioz, *ex vivo* entseguak erabilitako ereduaren bailagarritasuna erakutsi zuen *in vivo* entseguak burutu aurretik orbaintzea era orokorrean aztertzeko metodo bezala. Horretaz gain, garatutako hidrofilmek apositu moduan erabilgarri izan zitekeela erakutsi zuen. Haien eraginkortasuna hobetzeko asmoz, etorkizuneko ikerketen helburua azpiko geruzan hazkuntza faktoreen moduko molekula aktiboak kapsularatzea edo immobilizatzea da.

Laburbilduz, tesi honetan lortutako emaitza denak kontuan hartuz, esan dezakegu lan honetan zauri kronikoen tratamendurako estrategia berrien garapenean aurrerapausu bat eman dugula. Urte hauetan, baliabide terapeutiko berriak garatu ditugu zauri kronikoen orbaintzea sustatzeko, hala nola, LL37 peptidoa kapsularatuta duten NLCak, EGF edo NLCak kapsularatuta zituzten PLGA-*Aloe vera* nanozuntzezko mintzak eta gelatina eta kitosanoan oinarritutako bigeruzadun apposituak.

**Erreferentzien zerrenda 202-208 orridaldeetan aurkitzen da.**

# Ondorioak

Doktoretza tesi honetako ikerketa experimentaletan lortutako emaitzetatik honako ondorioak eratorri daitezke:

1. LL37a arrakastaz kapsularatu zen NLCen barne, orbaintzean erabiltzeko ezaugarri egokiak zituen formulazioa lortuz eta peptidoaren ekintza mantenduz kapsularatze prozesuaren ostean.

2. *db/db* saguetan burututako lodiera osoko zauri ereduan, NLC-LL37en administrazio topikoak orbaintzea esanguratsuki hobetu zuen LL37 askearen kontzentrazio berdinarekin alderatuz, zauriaren itxiera, errepitelizazio gradua eta hantura prozesuaren ebazpenari dagokionez.

3. Garatutako EGFdun PLGA eta *Aloe veraz* osatutako nanozuntzezko mintzek apositu moduan erabiltzeko ezaugarri egokiak erakutsi zituzten. Horretaz gain, EGFa zein *Aloe vera* aktibo mantendu ziren elektroirute prozesuaren ostean. Gainera EGFa kapsularatuta zuten mintzek zaurien itxiera eta errepitelizazioa esanguratsuki bizkortu zuten *db/db* saguetan burututako lodiera osoko zaurietan.

4. PLGA/*Aloe vera* nanozuntzezko mintzetan NLCen barneraketak mintzen maneiua hobetu zuen. Gainera, mintz horiek ere orbaintzea sustatzeko gai ziren, nahiz eta hein txikiagoan.

5. Gelatinaz osatutako bigeruzadun aposituak garatu ziren, laktosa edo azido zitrikoa erabiliz elkargurutzatzaile moduan, goiko geruza erresistentea eta beheko geruza porotsua prestatzeko, hurrenez hurren. Garatutako aposituek ezaugarri egokiak zituzten apositu moduan erabiliak izateko eta biobateragarriak ziren, *ex vivo* entseguak frogatu zuen bezala.

# APPENDIX/ IRUZKINA

## APPENDIX 1

# Nanotechnological approaches for skin wound regeneration using drug delivery systems

I. Garcia-Orue[1,2]*, G. Gainza[1,2]*, S. Villullas[3], J.L. Pedraz[1,2], R.M. Hernandez[1,2], Manoli Igartua[1,2,+]

*These two authors contributed equally to this work.

[1] NanoBioCel Group, Laboratory of Pharmaceutics, School of Pharmacy, University of the Basque Country (UPV/EHU).

[2] Biomedical Research Networking Centre in Bioengineering, Biomaterials and Nanomedicine (CIBER-BBN).

[3] Biopraxis Research AIE, Miñano, Vitoria-Gasteiz.

+Corresponding author: Dr. M. Igartua

**ABSTRACT**

The application of nanotechnology in medicine represents a great opportunity to enhance the effectiveness of currently available medical treatments, especially focused on challenging healthcare issues, like skin wound regeneration. Hence, in the last few decades, nanobiomaterials have been extensively studied and optimised for the development of nanoscale drug delivery systems (DDSs) releasing drugs, such as growth factors, cytokines or antimicrobials, for skin wound repair. In this regard, several natural or synthetic materials have been studied due to their similarities to the skin and biocompatible properties, or due to their antibacterial or antiseptic effect. In addition, materials can also be engineered as scaffolds for the development of novel wound dressings. Thus, this chapter presents an overview of the current nanotechnological approaches used for the controlled release of drugs in the field of skin wound regeneration, particularly emphasising on polymeric and lipid nanoparticles, silver nanoparticles, nanofibrous structures, nanosheets and nanohybrids.

**Published in:** Applications of Nanobiomaterials. Volume 5, Nanobiomaterials in Soft Tissue Engineering. William Andrew Publishing. 2016. 31-55

# 1. ERANSKINA

## Farmakoen askatze sistemak erabiliz azaleko zaurien erregenerazio-rako aukera nanoteknologikoak

**LABURPENA**

Nanoteknologiaren aplikazioak aukera paregabea dakar medikuntzan, erabilgarri dauden tratamenduen eraginkortasuna hobetzeko, batez ere, azal zaurien erregenerazioaren moduko arazo kliniko erronkarietan. Hori dela eta, azkeneko hamarkadetan, nanobiomaterialei buruz asko ikertu da, zaurien orbaintzean erabiltzeko nanoeskalan egindako farmakoen askatze sistemak garatzeko, askatzen diztuzten farmakoak hazkuntza faktoreak, zitokinak edo antimikrobianoak izaten direlarik. Horren harira, material sintetiko edo natural ugari ikertu dira, azalarekin duten antzekotasunari, biobateragarritasunari edo haien eragin antibakterial edo antiseptikoari esker. Horretaz gain, materialak bio-aldamioak garatzeko disenatuak izan daitezke zaurien apositu moduan erabiltzeko. Ondorioz, kapitulo honek orbaintzerako egungo aukera nanoteknologikoei buruzko ikuspegi orokor bat ematen du, ondorengo farmakoen askatze sistemetan zentratuz: nanopartikula polimeriko eta lipidikoetan, zilarrezko nanopartikuletank, egitura nanofibrotsuetan, nano-orrietan eta nanohibridoetank.

## 1. Introduction

Non healing wounds have dramatically increased and have become a great problem for health care professionals and patients as pain, diminished quality of life, frequent hospitalisation, and increased morbidity and mortality are associated to chronic ulceration. In developed countries, up to 2% of the population may be affected by a chronic wound at least once in their lifetime, which results in a major health care and economic burden, representing around 2% of the health care expenditure (Menke *et al.* 2007). In fact, chronic wounds are a current and future challenge for health care systems as the demographic change is leading to a much older population. Many other factors than age, associated with a delay in wound healing, can increase the risk of developing chronic wounds such as obesity, smoking and chronic diseases, including diabetes mellitus and vascular disorders (Menke *et al.* 2007). In addition, infection is a common complication that also needs to be addressed when dealing with chronic wounds as it can delay or impair the wound healing process.

Current therapies involve costly and long-lasting treatments that are often insufficient and are associated with high ulcer recurrence (estimated up to 70%). Thus, more effective novel treatments are required to solve this unmet need so that the related tremendous health care costs and resources can be optimised. For that purpose, the scientific community has focused many of its efforts on developing new therapies to promote wound healing and on improving already available treatments to, ultimately, accelerate and achieve wound closure. To this aim, the use of nanotechnology has provided a great tool to develop new drug delivery systems (DDSs) for the sustained release of therapeutic agents in order to achieve more cost-effective therapies.

This chapter will provide a general overview of useful therapeutic agents, such as growth factors (GFs) and antimicrobials, employed in wound healing therapy, and the nanotechnological approaches developed so far to improve treatment effectiveness. A detailed insight of the current advances on DDS development for wound healing therapy will be given, mainly focusing on polymeric and lipid nanoparticles, silver nanoparticles, nanofibrous structures, nanosheets and nanohybrids.

## 2. Cutaneous wound healing and skin lesions

The skin, the outer tissue protecting against the environment, is exposed to chemical, physical and biological harms as well as subject of genetic, inflammatory or metabolic diseases. Aging is associated with a loss or decrease of some of the protective properties of the skin as it becomes dryer, less elastic, thinner, and thus being more likely to suffer damage and infection. Senescent cells accumulated in aging tissues lead to a decline in several functions of the human skin, such as barrier efficacy, sensory perception, wound healing, immune response and DNA repair. Furthermore, changes in collagen formation, flattening of the basement membrane, a reduction in blood supply to the skin and a slower inflammatory response reduce the ability to achieve skin repair (Farage *et al.* 2009).

Cutaneous wound healing is a well-coordinated biological process that involves the integrated interaction of different growth factors, cytokines, enzymes and cell types, such as inflammatory cells, keratinocytes, fibroblasts and endothelial cells. Tissue repair is accomplished by tightly regulated processes that overlap in space and time, including an initial inflammatory response, a proliferative phase and a final remodelling phase (Martin 1997, Singer, Clark 1999). Chronic wounds fail to proceed through those sequential phases, subsequently resulting in delayed or incomplete healing.

Multiple factors contribute to poor wound healing. Among them, a major role has been attributed to an abnormal and persistent inflammatory response, a hallmark of non-healing skin wounds, that leads to an excessive proteolytic activity due to protease inhibitor degradation, and ultimately to inflammation-mediated tissue damage (Trengove *et al*, 1999). A decreased vascular supply is also a common cause of ulcer formation. In addition, a reduction in the amount of available and biologically active growth factors in the wound environment particularly affects wound repair.

One of the most common complications of chronic wounds is infection. In open wounds there is a disruption of the intact skin that is the first mechanical defence line against infection. Elevated levels of bacterial load are typically present on open wounds and can stimulate a proinflamatory environment. Hence, the wound healing process can be impaired partially due to an elongation of the inflammatory phase that suppresses the regenerative phase (Hernandez 2006, Lipsky, Hoey 2009). Bacteria not only compete for the limited oxygen and nutrients present in the wound, they also release toxins and induce an increased production of enzymes that can further lead to cellular failure.

Chronic wounds include pressure, vascular (venous or arterial) and diabetic foot ulcers. A pressure ulcer is defined as an area of localised damage on the skin and/or underlying tissue, usually over a bony prominence, occurred as a consequence of pressure or shear and/or a combination of those (Black *et al.* 2007). Vascular ulcers, usually localised on the lower limbs, are caused by a circulation disorder that leads to a reduction of the arterial blood flow or an impaired venous blood return. Vascular ulcers constitute a group of lesions of particular relevance due to their high prevalence. In addition, these ulcers are a leading cause of morbidity among patients suffering from peripheral vascular disease (Markova, Mostow 2012). Lastly, diabetic foot ulcer (DFU) is a major complication of diabetes because of the high consequences produced on the patients' quality of life. DFUs are caused due to a number of contributing factors, such as mechanical changes in conformation of the bony architecture of the foot, peripheral neuropathy (damaged nerves) and peripheral vascular disease (block arteries), all of which occurred with higher frequency and intensity in the diabetic population (Eldor *et al.* 2004). In addition, DFUs are highly associated with non-traumatic lower extremity amputations in the industrialised world.

On the other hand, major burns produced by heat, chemicals, electricity or radiation, can also became chronic wounds. A burn injury affects the skin integrity leading to fluid loss and being a portal for bacterial infection. Severity of a burn depends on the depth, location and the body surface area injured.

## 3. Therapeutic agents for wound healing therapy

### *3.1 Growth Factors*

Growth factors (GF) are biologically active polypeptides which regulate cell growth, differentiation, proliferation and migration, as well as, protein expression and enzyme production. In addition, GFs have a potential ability to heal wounds by stimulating angiogenesis, modulating the inflammatory response and intervening in the production and degradation of the extracellular matrix and the granulation tissue (Barrientos *et al*. 2008, Bodnar 2013). The main GFs involved in the healing process and skin regeneration are the platelet derived growth factor (PDGF), epidermal growth factor (EGF), basic fibroblast growth factor (bFGF), insulin-like growth factor (IGF) and vascular endothelial growth factor (VEGF) families. Their functions are summarised in Table 1.

The external administration of GFs has become one of the most interesting strategies to promote wound healing and skin regeneration, as a GF level decrease has been reported in chronic wounds (Barrientos *et al.* 2008, Barrientos *et al.* 2014). Nevertheless, the proteases present in the lesion, able to degrade the GFs, along with the low *in vivo* stability of these molecules have limited their clinical application. (Mast, Schultz 1996, Ulubayram *et al.* 2001, Baldwin, Mark Saltzman 1998). In this regard, in the last years the nanotechnological approaches for the release of GFs have been expansively investigated in order to improve the stability of the GFs at the wound site, allowing their sustained release, and ultimately, optimising treatment effectiveness.

### *3.2 Antimicrobial agents*

One of the most common complications in the treatment of chronic wounds are bacterial infections. In fact, 75% of the mortality associated to burn injuries are due to infections, mostly caused by Gram-negative (such as *Pseudomonas aeruginosa*) or Gram-positive bacteria (such as methicillin-resistant *S. aureus*) (Saito *et al.* 2012). Therefore, a suitable strategy for the treatment of chronic wounds involves the administration of antimicrobial agents, such as antibiotics or silver. This section will focus on the latest advances on DDSs devoted to properly formulate antimicrobials for wound infection treatment.

### *3.2.1 Antibiotics*

In the clinical practice, the choice of the antibiotic will depend on the microorganisms present within the wound, the susceptibility to antimicrobials and the patient characteristics. The main broad-spectrum antibiotics effective against the majority of bacteria commonly found in infected wounds are gentamicin, an aminoglycoside that is effective against Gram-

**Table 1.** Summary of the main functions of different GFs involved in wound healing and skin regeneration.

| Growth Factor | Main functions | Reference |
|---|---|---|
| Platelet derived growth factor (PDGF) | Chemotactic for neutrophils, monocytes and fibroblasts.<br>Promotes extracellular matrix production. | (Werner, Grose 2003, Li et al. 2008) |
| Epidermal growth factor (EGF) | Induces reepithelisation by the promotion of keratinocyte proliferation and migration.<br>Promotes angiogenesis.<br>Stimulates wound remodelation and protein production such as fibronectin. | (Barrientos et al. 2008, Tiaka et al. 2012, Hong et al. 2008) |
| basic Fibroblast growth factor (bFGF) | Activates local macrophages up to the remodelling phase. Promotes angiogenesis.<br>Stimulates the extracellular matrix metabolism and growth. | (Robson 1997, McGee et al. 1988, Akita et al. 2008) |
| Insulin-like growth factor (IGF) | Stimulates wound re-epithelisation and fibroblast proliferation.<br>Dampens the local inflammatory response. | (Provenzano et al. 2007, Emmerson et al. 2012) |
| Vascular endothelial growth factor (VEGF) | Promotes angiogenesis, granulation tissue formation and epithelisation. | (Losi et al. 2013, Bao et al. 2009) |

negative bacteria, especially *Pseudomonas* spp and certain Gram-positive (such as *S. aureus*) (Chen *et al.* 2012b); mupirocin commonly used in wound care prophylaxis against *S. aureus* and against some Gram-negative flora (Thakur *et al.* 2008); tetracycline, a broad spectrum antibiotic that, besides being active against a wide range of Gram-positive and Gram-negative bacteria, is effective against *Chlamydia*, *Mycoplasma*, *Rickettsia* and protozoan parasites (Chopra, Roberts 2001); and ciprofloxacin, the most potent fluoroquinolone active against a wide range of bacteria, being the most susceptible the aerobic Gram-negative bacilli (Sharma *et al.* 2010).

Narrow range antibiotics such as penicillin G, vancomycin and lysostaphin, are employed for wound healing treatment. On the one hand, penicillin G is active against non-β-lactamase-producing Gram-positive bacteria, anaerobes and Gram-negative cocci from the *Neisseria* spp (Doi, Chambers 2015). On the other hand, vancomycin is a glycopeptide active against Gram-positive bacteria and is mainly used in recalcitrant staphylococcal infections that are resistant to penicillin or cephalosporin (Chen *et al.* 2012b). Finally, lysostaphin is a cell lytic enzyme secreted by *Staphylococcus simulans* that is highly effective and specific against *S. aureus* (Miao *et al.* 2011).

Another encouraging strategy to overcome wound bacterial infection is the administration of antimicrobial peptides (AMP). AMP are part of the innate immunity providing a first defence line against a wide range of pathogenic or-ganisms (Vandamme *et al.* 2012). Currently, there are more than 600 AMP classified in two families: defensins and cathelicidins (Hancock 2001). The LL37 peptide, also known as hCAP-18, is the only human cathelicidin identified to date. This peptide exerts antimicrobial activity towards various microorganisms, such as Gram-positive and Gram-negative bacteria, fungi, parasites and enveloped virus. Furthermore, LL37 is chemotactic (Vandamme *et al.* 2012), stimulates the production of proinflammatory cytokines, neutralises the immune response through the interaction with the LPS endotoxin (Kai-Larsen, Agerberth 2008), promotes new vessel formation (Koczulla *et al.* 2003) and stimulates the proliferation and migration of epithelial cells (Anderson, Rehders & Yu 2008). Therefore, LL37 is emerging as a potential therapeutic tool for promoting wound healing and inhibiting bacterial growth. However, peptides have shown limited stability *in vivo* due to the proteases present in the wound. Thus, optimisation of the LL37 administration using advanced DDSs can enhance its biological function and thus improve treatment effectiveness (Hancock 2001).

Finally, it should be noted that most of the antimicrobials employed in the treatment of infected wounds are administered through the systemic route. However, this approach can lead to the appearance of undesirable side effects or to an insufficient dosage on the lesion as the antibiotics can barely penetrate into ischemic tissues (Xu *et al.* 2010). In addition, the extensive use and misuse of antibiotics can contribute to the development of antibiotic-resistant bacteria. In order to overcome these disadvantages, antibiotics formulated in advanced DDSs can be locally administered to obtain higher concentrations at the wound site due to a high initial drug release followed by a sustained release that can achieve a long-lasting antimicrobial effect (De Cicco *et al.* 2014).

*3.2.2 Silver*

The use of silver is a widely employed strategy to overcome bacterial infection and prevent wound sepsis. Sil-ver has shown several interesting properties, such as wide spectrum against several microorganisms; multiple mechanisms of action to inhibit bacterial colonisation, which reduces the risk of developing resistance; great effectiveness against multi-drug-resistant organisms and low systemic toxicity (Gunasekaran, Nigusse & Dhanaraju 2011).

Only the soluble form of silver is biologically active, i.e. Ag+ or Ag0 clusters. Ag+ ions are present in silver nitrate, silver sulphadiazine (SSD) and other ionic silver compounds. On the other hand, metallic silver ($Ag^0$) is found in two different crystalline forms, i.e. the nanocrystalline (<20 nm) or the subcrystalline (less than eight atoms of silver) forms (Dunn, Edwards-Jones 2004).

The mechanism of action of soluble silver is still unknown; however, the most widely accepted mode of action is closely related to the interaction of silver with the bacterial cell-wall and cell-membrane that inhibits the bacteria respiration process (Klasen 2000). Further-more, silver is involved in the bacterial DNA condensation, which leads to the loss of the replication ability and therefore, to the cell death (Feng *et al.* 2000). As a result of the multiple bactericidal mechanisms of soluble silver, this noble metal does not produce bacterial resistance; thus, becoming an interesting strategy for the treatment of infected wounds.

## 4. Nanotechnological approaches for the release of therapeutic agents for wound healing

Currently, several research groups have developed different nanotechnological approaches for the release of therapeutic agents as a novel strategy in the wound healing therapy. Due to the distinct characteristics of wounds and healing stages, different wound dressings and therapeutic agents can be employed to meet most of the needs in a particular wound stage. Therefore, in this section, the current nanotechnology based strategies used for the controlled release of drugs involved in skin wound regeneration are summarised (Figure 1).

### *4.1 Nanotechnological approaches for growth factor delivery*

As previously mentioned nanotechnology provides the opportunity to enhance the in vivo effectiveness of GFs, preventing their proteolytic degradation and prolonging their release at the lesion (Kubinová, Syková 2010). A wide type of nanoscale-delivery systems have been designed to promote wound healing, mainly polymeric nanoparticles (NPs), lipid NPs and nanofibrous structures.

#### *4.1.1 Polymeric nanoparticles*

Biocompatible polymeric devices have currently become a promising alternative for the controlled release of active com-

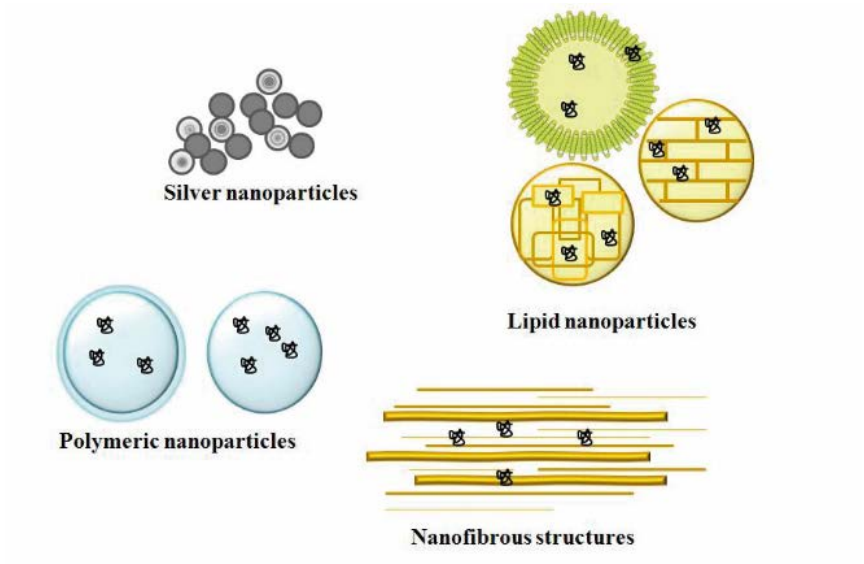


**Figure 1.** Schematic illustration of different DDSs used for the treatment of chronic wounds.

pounds, including GFs. These nanometric colloidal systems can be employed in multiple diseases, administration routes and dosage ranges. Therefore, polymeric carriers have been developed for chronic wound therapy because apart from allowing controlled drug release over time, they may also reduce drug degradation by the prote-ases present in the wound environment (Ulubayram et al. 2001, Gainza et al. 2013), and thus, the administration frequency and dose can be decreased. Nanospheres can be prepared using natural or synthetic biomaterials, as well as other polymer combinations (Makadia, Siegel 2011, Değim 2008, Ye, Kim & Park 2010).

One of the most widely used polymer to prepare nanospheres as DDSs is the synthetic poly lactic-co-glycolic acid (PLGA), because this polymer allows drug sustained release, is biocompatible and biodegradable (Makadia, Siegel 2011). In this regard, Chu and co-workers developed rhEGF-loaded PLGA NPs using a modified double-emulsion method and assessed their effectiveness during 21 days after topical administration in full-thickness wounds created on diabetic rats. The rhEGF-NPs (size around 193.5 nm) showed an encapsulation efficiency (EE) of 85.6% and a rhEGF release for 24 h; therefore, treatments were locally administered once daily. After 7, 14 and 21 days wounds treated with rhEGF-NPs achieved the greatest wound area reduction among all the experimental groups. In addition, the histopathological examination of lesions showed that the rhEGF-NPs promoted the highest level of fibroblast proliferation and PCNA expression. These results support that the controlled release of rhEGF allows continuous contact of the GF with the wound surface to maintain an effective concentration able to promote healing; and suggest a more appropriate administration for rhEGF (Chu et al. 2010).

Latest advances in drug delivery involved the combination of different technological approaches that may improve dressing integration. In this regard, Losi et al. have developed poly-(ether)urethane-polydimethylsilxane/fibrin-based scaffolds containing VEGF and bFGF loaded PLGA NPs that have demonstrated to be effective in enhancing wound closure by day 15 in db/db mice compared with scaffolds not containing GFs. In addition, as observed in the histological evaluation, complete re-epithelisation, improved collagen deposition and more mature granulation tis-sue were observed in scaffolds containing GFs-loaded NPs, even though no difference between scaffolds containing free GFs and GFs-loaded NPs were found. Overall, these results suggest that fibrin-based scaffolds containing GFs-loaded NPs are an interesting strategy for the sustained release of VEGF and bFGF because they acted as a double DDS for GF delivery; and therefore, the initial burst release of the GFs and the leak out of the particles from the wound site after topical administration might be reduced providing a more sustained release of the GFs (Losi *et al.* 2013).

### *4.1.2 Lipid nanoparticles*

Lipid nanoparticles have been intensively studied for dermal application, pharmaceutical and cosmetic uses (Pardeike, Schwabe & Müller 2010). These lipid carriers look promising due to their biocompatibility, ease of preparation and superior efficacy compared with non-encapsulated drugs (Fan, Zhang 2013).

First developed lipid nanocarriers were liposomes, comprising an aqueous core encapsulated by natural or synthetic phospholipids. This structure allows entrapment of hydrophilic drugs in the core, while hydrophobic drugs are entrapped within the lipid bilayers (Fan, Zhang 2013). Since the first liposomal pharmaceutical product, Doxil® [doxorubicin-polyethylenglycol (PEG)ylated liposome] approved in 1995 for Kaposi's sarcoma, ovarian and breast cancer, to date, there are a number of commercially available products. (Allen, Cullis 2013).

Few publications have described the use of liposomes as GF carriers for wound healing. First, Brown and collaborators reported the benefits of locally administered EGF loaded multilamellar liposomes on the tensile strength of experimental incisions on rats. As observed in the measurement of the rate of rhEGF loss from incisions *in vivo*, significant higher levels of the GF were retained by the multilammelar liposomes (62% after 1 day, 48% after 2 days and 11% after 5 days). In addition, a single dose of EGF in liposomes significantly prolonged the exposure of EGF, produc-ing a 200 % increase in wound tensile strength from days 7 to 14, and increasing collagen formation and fibroblast proliferation. These studies clearly proved that the incorporation of the EGF in an appropriate vehicle induced more efficient wound healing than local administration of the free GF, since EGF-loaded liposomes improved early tensile strength and therefore promoted wound remodelation and healing (Brown *et al.* 1988). In a different study published by Pierre and colleagues, very low doses of IGF-I encapsulated in liposomes (0.9 µg/kg/week) administered subcutaneously were as effective improving re-epithelisation as higher doses of IGF-I (5.0 µg/kg/week) administered together with the growth hormone (GH) and more effective than 5.0 µg/kg/week IGF-I without GH administration (Pierre *et al.* 1997). These data suggest that nanoencapsulation may improve treatment effectiveness compared with the free GF administration because this technological approach may protect the GFs from the wound environment and degradation (Almeida, Souto 2007).

However, despite liposomes are well established and extensively investigated, the total number of products in the market is still limited. One of the reasons may be related to the low *in vivo* stability that may induce a rapid uncontrolled release of the drug. Therefore, at the beginning of the 1990s solid lipid nanoparticles (SLN) and later, nanostructured lipid carriers (NLC) were developed as alternative carrier systems to liposomes (Müller, Mäder & Gohla 2000). SLN preparation requires solid lipids as matrix material while NLC are prepared using a blend of solid lipids and oils. In addition, both nanoparticulated formulations are ideal for dermal administration because they are able to remain on the skin, improve skin hydration and release drugs in a sustained manner. However, since SLN have shown drug expulsion during the storage, NLC may be a more suitable alternative for hydrophilic drug encapsulation due to their enhanced stability (Almeida, Souto 2007, Pardeike, Schwabe & Müller 2010).

Based on this nanotechnology, our research group has demonstrated that rhEGF-loaded SLN and NLC topically administered were more effective improving

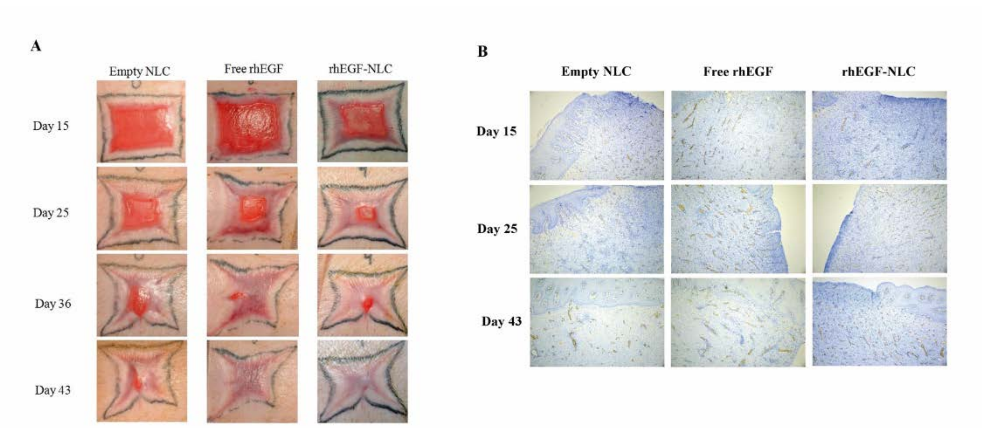


**Figure 2:** rhEGF-loaded nanostructured lipid carriers (rhEGF-NLC) (A) Wound images obtained from each experimental group on days 15, 25, 36 and 43. (B) Representative pictures of endothelial cells marked with anti-CD 31 antibody on days 15, 25 and 43 (x10 magnification). Reproduced and adapted with permission from Gainza *et al.* 2015 (©2014)

healing than a greater dose of free rhEGF intralesionally administered. First, we assessed the effectiveness of both formulations in healing-impaired *db/db* mice. The healing process was improved in terms of wound closure, re-epithelisation and restoration of the inflammatory process in those wounds treated with two weekly doses of topical rhEGF-SLN and rhEGF-NLC over controls, including a significantly higher dose of intralesional free rhEGF (20 µg *vs* 75 µg)) (Gainza *et al.* 2014). Secondly, we assessed the effectiveness of the rhEGF developed nanoformulations in a more relevant preclinical model, such as Large White pigs. Because rhEGF-NLC showed an improved EE compared with rhEGF-SLN, the lack of organic solvent needed for their preparation and the same *in vitro/vivo* effectiveness as rhEGF-SLN; the effect tiveness of two weekly topical administrations of 20 µg rhEGF-NLC was assessed in a full-thickness swine excisional wound model compared with empty NLC and two weekly intralesional administrations of 75 µg free rhEGF. Data obtained from the swine model supported the results previously obtained in rodents, since by day 25, lower doses of rhEGF-NLC increased the wound closure and percentage of healed wounds as much as that exerted by free rhEGF, but more than empty NLC (Figure 2A). In addition, the histopathological examination confirmed that rhEGF-NLC promoted fibroblast migration and proliferation, collagen deposition, resolution of the inflammatory response and, as observed in Figure 2B, neoangiogenesis (Gainza *et al.* 2015). Overall, these findings demonstrated that lower doses of topically administered rhEGF-NLC may stimulate healing of full thickness wounds in rodents and pigs, thereby confirming their potential clinical application for wound management.

### *4.1.3 Nanofibrous structures*

Nanofibrous materials are gaining interest for tissue engineering applications, including skin regeneration. Nanofibrous structures mimic the native extracellular matrix and promote the adhesion of various cells and soluble factors that may promote cell function and tissue regeneration. Nanofibers (NFs) for skin tissue regeneration are mainly developed using the electrospinning technique because it allows the production of micro and nanometric continuous fibres that have shown a uniform adhesion to the lesion without fluid accumulation (Chaudhury *et al.* 2014).

In the last few years several studies have been performed to assess the effect of NFs in the controlled release of GFs for wound repair. Different materials, natural or synthetic, can be used for the fabrication of electrospun NFs. On the one hand, silk fibroin from *Bombyx mori* silkworm, a natural polymer, has demonstrated adequate mechanical strength and excellent biocompatibility for skin regeneration applications. Silk mats containing EGF have shown to maintain their structure during the healing process and to enhance healing by inducing the keratinocyte tongue proliferation and thus, promoting re-epithelisation. Therefore, the silk mats offered not only physical protection of the lesion, but also sustained release of EGF to the wound (Schneider *et al.* 2009). In addition, the effectiveness of silk-protein biomaterials with EGF and silver sulphadiazine has been studied in lesions created on mice. Wound biopsies revealed that those dressings, as well as the other lamellar porous films evaluated in that study, provided the most rapid wound closure, also showing higher healing rate, re-epithelisation, dermis proliferation and collagen synthesis compared with the air-permeable Tegaderm® (Gil *et al.* 2013).

Synthetic biomaterials are also widely employed for the preparation of NFs for wound repair. For example, bFGF-loaded electrospun nanofibers developed using the synthetic poly(ethylene glycol)-poly(DL-lactide) (PELA) polymer for the treatment of diabetic skin ulcers, compared with NFs infiltrated with free bFGF, significantly improved the healing rate by promoting re-epithelisation and regeneration of skin appendages and the ECM remodellation. In addition, the obtained sustained release of bFGF enhanced collagen deposition and improved the density and maturity of capillaries during two weeks (Yang *et al.* 2011).

Due to the practicality, easy fabrication and the successful results NFs have demonstrated, several research groups are currently working on the development of advanced nanofibrous structures combining two or more polymers. In addition, due to the increased recognition of phototherapy to promote wound healing, photosensitive polymers are also used for NF preparation. In this regard, poly(3-hexylthiophene) (P3HT), a photosensitive polymer, and EGF encapsulated in the core-shell-structured gelatin/poly(L-lactic acid)-co-poly-(ε-caprolactone) (PLLCL) NFs (EGF-Gel/PLLCL/P3GF(cs) prepared by coaxial spinning have been evaluated as skin graft. EGF-Gel/PLLCL /P3GF(cs) significantly improved human dermal fibroblast proliferation and wound closure under light stimulation in an *in vitro* wound model compared with fibroblasts treated with those NFs but under dark conditions. Moreover, EGF-Gel/PLLCL/P3GF(cs) treatment in adipose-stem cells under light stimulation induced keratinocyte differentiation (Jin, Prabhakaran & Ramakrishna 2014).

Combinations of poly(ε-caprolactone) (PCL) and polyethylenglycol (PEG) polymers for NF preparation have also been studied. For example, the healing effectiveness of rhEGF surface-immobilised NFs assessed in diabetic burns created on the back of C57BL/6 female mice showed an increased healing rate on days 7 and 14 compared with empty NFs and the untreated control (Choi, Leong & Yoo 2008). Remarkably, wound closure in those wounds treated with rhEGF-NFs was significantly greater than in those treated with a mixture of rhEGF and NFs. These data suggest that the entrapment of rhEGF within NFs may prevent the GF degradation from wound proteases. Moreover, the histological examination also confirmed that lesions treated with rhEGF-conjugated NFs showed increased keratinocyte specific genes and EGF receptor (EGFR) expression; thus, promoting wound healing (Choi, Leong & Yoo 2008). Moreover, two different growth factors, EGF and bFGF, were also incorporated in the coaxial NFs to obtain a bi-phasic release of the GFs (Choi, Choi & Yoo 2011). EGF was surface immobilised and minimal release, related to the NFs mesh degradation, was shown during 7 days while bFGF, immobilised on the core, showed an initial burst and an approximately 30% release of the encapsulated bFGF in the first 12 h. In addition, studies undertaken in diabetic burns created on the back of C57BL/6 female mice clearly demonstrated that controlled release of EGF and bFGF from NFs further accelerated proliferation of epidermal cells and wound closure than the control groups, EGF-NFs and bFGF-NFs. Moreover, animals treated with EGF/bFGF NFs improved collagen and keratin accumulation; confirming the nanofibrous matrix as a promising wound dressing to improve wound healing (Choi, Choi & Yoo 2011).

Combinations of different DDSs have been also used as multifunctional wound dressings. As an example, a biomimetic nanofibrous scaffold containing PDGF-BB loaded PLGA NPs and VEGF loaded chitosan, [poly(ethylene oxide)] (PEO) NFs were developed to achieve dual release of the two GFs (fast and sustained release) (Xie *et al.* 2013). This system allowed the quick release of VEGF to promote new vessel formation and provided PDGF-BB sus-tained release throughout the whole healing process (Figure 3A). Studies performed on a rat full-thickness wound model, depicted in Figure 3B, revealed an accelerated wound closure of

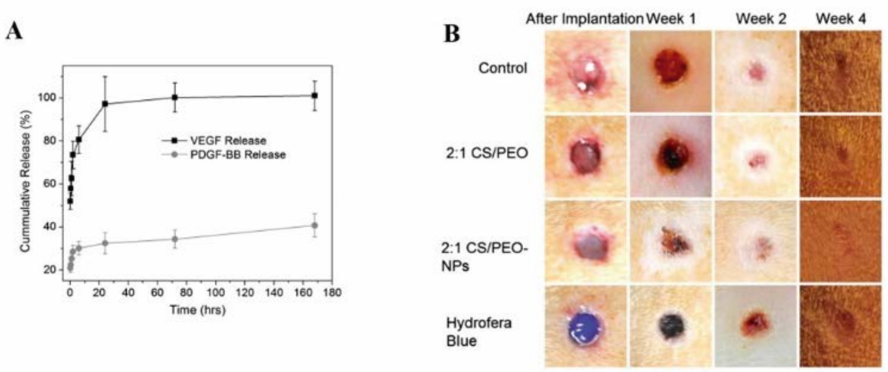


**Figure 3:** Biomimetic nanofibrous scaffold containing PDGF-BB loaded PLGA NPs and VEGF loaded CS-PEO NFs (A) Release kinetics of VEGF from nanofibers and PDGF-nanoparticles within fibers. (B) Representative macroscopic appearance of wound closure on weeks 0, 1, 2, and 4 after wound treatment with two controls (open wound and Hydrofera Blue®) and nanofiber meshes (2:1 CS/PEO) without GFs and nanofiber meshes with nanoparticles and GFs (2:1 CS/PEO-NPs). Reproduced and adapted with permission from Xie *et al.* 2013 (©2013).

those wounds treated with the biomimetic nanofibrous scaffold compared with the untreated group, empty NFs and the commercial dressing Hydrofera Blue®. In addition, as observed in the histological examination, VEGF may be responsible of the increased angiogenesis observed in the early stage of the healing process, while PDFG-BB may improve re-epithelisation, collagen deposition and tissue remodelling (Xie *et al.* 2013).

Finally, a more complex NP in-fiber structures have also been developed using collagen and hyaluronic acid for the programmable multi angiogenic GF release (Lai *et al.* 2014). In this occasion, bFGF and EGF were directly embedded in the nanofibrous skin equivalent and PDGF-BB and VEGF were encapsulated into gelatine NPs and embedded in the NF meshes. Results obtained from lesions created on STZ-diabetised rats treated with this complex structure revealed that the initial delivery of bFGF and EGF may mimic the early stage of healing by accelerating epithelisation and angiogenesis, while the sustained release of PDGF and VEGF may promote tissue remodelation, blood vessel maturation and collagen deposition. Overall, these findings demonstrated that this advanced DDS could be a promising bioengineered construct for wound therapy (Lai *et al.* 2014).

### *4.2 Nanotechnological approaches for antimicrobial agents delivery*

#### *4.2.1 Antibiotics*

Among the current nanotechnological approaches for chronic wound treatment, nanoparticles, nanofibers and nanosheets to release antibiotics can be highlighted.

#### *4.2.1 Polymeric nanoparticles*

Polymeric NPs are one of the most promising DDSs for antibiotics (Cortivo *et al.* 2010). As previously mentioned, it is widely assumed that drug nanoencapsulation can improve the drug stability within the wounded area. In this regard, penicillin G loaded polyacrylate NPs have proven to protect penicillin against β-lactamase, since they present an equipotent *in vitro* antibacterial activity against methicillin-susceptible and methicillin-resistant strains of *S. aureus* (Turos *et al.* 2007). Furthermore, the application of the NP emulsion directly to skin abrasions in mice accelerated wound healing com-pared with saline administration and showed no discernible toxicity, i.e. no redness, irritation or inflammation. In addition, the polymeric film formed by the NP emulsion applied over the wound protected the lesion from microorganisms; so that these wound dressings appeared to be an integral part of the forming skin layers, maintaining the skin mechanical properties, preserving the moisture and allowing oxygenation of the lesion (Greenhalgh, Turos 2009).

A different wound dressing based on an *in situ* gelling nanoparticulated dry-powder composed of alginate-pectin loaded with gentamicin sulphate has been developed. Remarkably, due to the rapid gelation of the nanoparticulated powder, this nanoformulation was able to absorb large quantities of wound fluid and therefore microorganism colonisation could be reduced. Moreover, since the formed hydrogel exhibited proper adhesiveness, easy dressing removal from the wound was allowed. The antimicrobial activity of the gentamicin-sulphate loaded NPs incorporated into the hydrogel was tested against *S. aureus* and *P. aeruginosa* the most common bacteria present in infected wounds, revealing a higher antibacterial activity compared with the free drug (De Cicco *et al.* 2014).

Finally, regarding the controlled delivery of AMPs, Chereddy and collaborators incorporated LL37 in PLGA nanospheres in order to improve the *in vivo* stability of the peptide. As observed in the *in vitro* studies, both PLGA-LL37 and free LL37 showed to be no cytotoxic and to improve wound healing in the HaCaT cell line; and presented anti-inflammatory activity by downregulating TNF-α in macrophages. However, no significant increase of proliferation was observed in HaCaT and in the fibroblast cell line BJ. In addition, PLGA-LL37 nanospheres improved the wound healing rate compared with free LL37 in a full-thickness wound model in mice, and presented a similar wound closure than wounds treated with the plasmid encoding hCAP18. Moreover, PLGA-LL37 promoted angiogenesis and diminished the inflammatory infiltration, since IL-6 and VEGF were upregulated and the myeloperoxidase activity decreased (Chereddy *et al.* 2014).

*4.2.1.2 Nanofibrous structures*

Wound dressings based on antibiotic-loaded nanofibrous scaffolds are another encouraging approach for wound treatment.

In a study published by Miao and collaborators, NFs were prepared by electrospinning cellulose, cellulose-chitosan or cellulose-poly(methylmethacrylate) (PMMA). NFs were then functionalised by conjugation with lysostaphin. In addition, the method of conjugation, which depends on the polymer used, may have a great impact on the antibacterial activity of the antibiotic-loaded NFs. In this regard, the conjugation of lysostaphin and cellulose-nanofibers by covalent bonds produced the most bioestable formulation and the best anti-infective properties, as this formulation showed complete neutralisation of *S. aureus*. Furthermore, minimal cytotoxicity in the keratinocyte cell line HaCaT was shown in biocompati-bility assays and antimicrobial activity was revealed in a skin-like model consisting of a monolayer cultured keratinocytes infected with *S. aureus* (Miao *et al.* 2011).

Additionally, NFs prepared with sodium alginate have also shown to be suitable for wound treatment due to the biocompatible and biodegradable properties of alginate. Sodium alginate NFs have been prepared by the electrospinning technique, incorporating PVA into the polymer solution in order to avoid the early gelation of sodium alginate. In this occasion, ciprofloxacin, loaded during the electrospinning process, was employed as the active compound of the wound dressing. Studies carried out in a full thickness model in rabbits demonstrated that ciprofloxacin loaded PVA-sodium alginate NFs enhanced wound epithelisation compared with PVA-NFs and a commercial ciprofloxacin formulation (Kataria *et al.* 2014).

As previously mentioned, NFs can also be prepared using synthetic polymers. For that purpose, a PEG-PLLA nanofibrous membrane loaded with tetracycline had been successfully developed, showing no loss of the tetracycline bioactivity, since the membranes were effective inhibiting *S. aureus* for 5 days (Xu *et al.* 2010).

Electrospun scaffolds can also be loaded with several drugs. As an example, a PLLA scaffold containing an antibiotic, mupirocin, and an anesthetic, lidocaine hydrochloride had been developed. In order to achieve a different release for each drug, a dual spinneret electrospinning apparatus was used to prepare a single scaffold composed of two types of NFs, i.e. mupirocin-loaded NFs and lidocaine hydrochloride-loaded NFs. The resulting wound dressing presented an initial burst release of lidocaine, for immediate pain relief, and a sustained release of mupirocin, for continuous antibacterial activity. Furthermore, as observed in the *in vitro* activity assays, the antibiotic remained active in the scaffold for at least 3 days (Thakur *et al.* 2008).

NFs, besides being used as DDSs, can also act as a scaffold for cellular growth and proliferation. In this regard, a sandwich-structured membrane was developed comprising a core layer of PLGA for the release of vancomycin, gentamicin and lidocaine; and an outer layer of PLGA and collagen, devoted to act as a scaffold for cellular growth and differentiation. As observed in the *in vitro* antibacterial studies performed in *S. aureus* and *Escherichia coli*, gentamicin and vancomycin NFs had above 30% and 37%, respectively, of the maximum activity of each free antibiotic after 3 weeks. Moreover, as observed in the MTT assay, the viability of human fibroblasts was not affected in 21 days (Chen *et al.* 2012b). The sandwich-structured nanofibrous membranes were effective for the treatment of *S. aureus* and *E. coli* infected wounds in a full-thickness wound model in rats, especially in the early stages of healing. As described by authors, two and three weeks after grafting, wounds treated with the developed sandwich-structured membrane presented a newly synthesised fibrous tissue with small infiltration of inflammatory cells, covered by a re-epithelised epidermis, in contrast with the incomplete re-epithelisation and prominent inflammatory cells infiltration shown in those wounds treated with drug free scaffolds (Chen *et al.* 2012a).

Similar sandwich-structured membranes had also been developed for antibiotic release, such as NFs prepared using a needleless electrospinning technology (Nanospider™). Those NFs were composed of a core layer of PVA loaded with gentamicin and cover layers of polyurethane (PUR). The *in vitro* antibacterial assay conducted to prove the bioactivity of the gentamicin-loaded NFs did not show any loss of the gentamicin activity after its incorporation in the nanofibrous structure (Sirc *et al.* 2012).

#### *4.2.1.3 Nanosheets*

Nanotechnology has also allowed the development of nanosheets. Remarkably, these polymeric ultra-thin two dimensional films have demonstrated to be useful as wound dressing. In this regard, Saito and collaborators developed a nanosheet consisting of three functional layers; a layer-by-layer nanosheet composed of chitosan and sodium alginate, a tetracycline layer and a poly(vinyl acetate) (PVAc) layer, that acted as a hydrophobic protecting layer. The nanosheets improved the survival rate of *P. aeruginosa* infected burn injured mice up to 100%. Moreover, as observed by the viable bacterial count in the wound site and in the liver biopsies, the *P. aeruginosa* infection was suppressed 3 days after wound induction. Finally, the histopathological examinations revealed the resolution of the inflammatory response as the infiltration of inflammatory cells significantly decreased by day 3 in the tetracycline-loaded nanosheet treated group (Saito *et al.* 2012).

### *4.2.2 Silver NP*

Initially, silver was employed in the ionic form and was directly administered on burns. However, one of the major limitations of ionic silver is that it may be neutralised by anions in the body fluids, limitating its effectiveness, and may show several side effects, such as cosmetic abnormalities and impaired healing after prolonged topical use (Gunasekaran, Nigusse & Dhanaraju 2011).

In order to improve the effectiveness of ionic silver, silver nanoparticles (AgNPs) composed of nanocrystalline metallic silver were developed. Their improved effecttiveness can be attributed to the decreased size of the NP that provides a larger surface area to volume ratio and thus, improve the antibacterial activity (Rai, Yadav & Gade 2009, Gunasekaran, Nigusse & Dhanaraju 2011). Moreover, in order to ease their administration and reduce the side effects associated to an excessive exposure to silver, AgNPs are usually formulated in both, traditional dressings and novel DDSs.

AgNPs can be prepared in different manners, such as wet chemical, physical and biological methods, all of them based on a redox reaction, where silver ions ($Ag+$) are reduced to metallic silver ($Ag^0$). The resulting silver NPs are effective against a wide range of microorganisms, such as Gram-positive and Gram-negative bacteria including methicillin-resistant *S. aureus* and vancomycin-resistant enterococci, yeast and mould (Atiyeh *et al.* 2007).

In order to avoid high concentrations of silver in the lesion and thus, reduce associated side effects, Hebeish and collegues developed silver NPs loaded in cotton fabrics through the pad-dry-cure technique. The 250 ppm AgNP cotton dressing showed antimicrobial activity against *S. aureus, E. coli* and in lesser extent against *Candida albicans*. Furthermore, studies in rats revealed that the dressing presented nearly similar wound healing rate to that induced by the marketed 1% micronised SSD cream (Dermazin®) in a burn injury model. Furthermore, the dressing possessed similar anti-inflammatory activity to indomethacin, since the inhibition of carrageenan-induced oedema was similar in animals that received a single oral dose of either formulations (Hebeish *et al.* 2014).

AgNPs-loaded nanofiber membranes can also be prepared *in situ* using bacterial cellulose, a natural biopolymer, with high water content, high wet strength and chemical purity. Those membranes were biocompatible with epidermal cells, since cell growth was observed microscopically, and were able to inhibit bacterial growth *of S. aureus, E. coli* and *P. aeruginosa* in a similar extent to the commercially available silver containing dressing Coloplast® (Wu *et al.* 2014b). The subsequent *in vivo* studies, performed in a second-degree skin burn wound model in Wistar rats, showed that the membranes reduced bacterial proliferation in the wound, reaching to preoperative levels on day 21, as observed in the culture of swab samples collected from the wound bed. Furthermore, the membrane demonstrated excellent healing effects as complete healing was reached by day 28 (Wu *et al.* 2014a).

Guar gum alkylamine (GGAA), a novel cationic biopolymer, can also be employed to develop an antimicrobial wound dressing embedding AgNPs. This polymer presents great water-absorbing capacity that may facilitate wound exudate absorption. The resulting nanobiocomposite presented an enhanced wound healing rate in a full-thickness wound rat model, compared with a silver alginate cream, as both achieved complete healing on days 10 and 12, respectively. Moreover, the biochemical markers, such as increased total DNA and protein content, indicated an increase of cellular proliferation, and thus, enhanced healing. Remarkably, the AgNPs-GGAA formulation achieved an improved healing quality since the tensile strength and the hydroxyproline content, both directly related to the collagen content of the wound, were higher than that induced by the silver alginate cream. Additionally, a primary skin irritation study conducted in rabbits showed no irritation after 4 hours of dermal exposure to AgNPs-GGAA (Ghosh Auddy *et al.* 2013).

Chitosan is a suitable polymer widely used due to its remarkable properties for wound healing, such as pain reliever, bacterial growth inhibitor, and haemostasis and epidermal cell growth inducer. In this regard, Lu and co-workers developed a novel wound dressing composed of AgNPs and chitosan (SNC), by self-assembly technology. SNC dressing treated wounds, in a deep-partial thickness wound model in Sprague-Dawley rats, were almost recovered 10 days after the injury, whereas wounds treated with SSD presented a pseudo-scar and wounds treated with a chitosan film presented some postoperative infection. Furthermore, the SNC group presented an increased wound healing rate since the average healing time was 3,94 days shorter than in the SSD group. Additionally, the rats treated with SNC presented a lower silver systemic content than those rats treated with SSD at any time, reaching normal levels on day 13, as observed by blood sample determination (Lu, Gao & Gu 2008).

Other chitosan based wound dressings have been developed, such as a nanobiocomposite consisted of chitosan and sargo starch impregnated with AgNPs, with and without gentamicin. In addition, alginate and sago starch dress-ing impregnated with AgNPs and a regenerated cellulose-chitosan biocomposite impregnated with AgNP, both with and without gentamicin, have been developed. The wound dressings were evaluated in an open excision wound in Wistar rats obtaining similar results in the three studies, a faster healing of wounds treated with the tested biocomposites in comparison to the control wounds, as observed in Figure 4 for chitosan and sago starch biocomposites. No significant differences were observed in the gross healing pattern among the dressings containing or lacking gentamicin, and the presence of the antibiotic only reduced the number of inflammatory cells. However, as confirmed by the histological

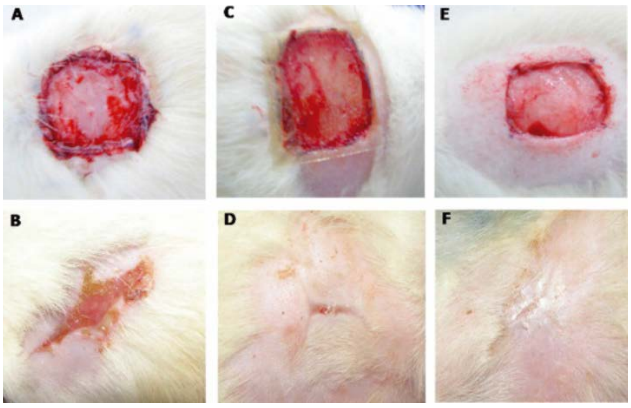


**Figure 4.** Photographic representation of wound contraction rate on different days of healing: A, C & E are control, chitosan-sago starch-AgNP and chitosan-sago starch-AgNP-Gentamicin treated groups on 0th day, respectively. B, D & F are control, chitosan-sago starch-AgNP and chitosan-sago starch-AgNP-Gentamicin treated groups on 16th day, respectively. Reproduced and adapted with permission from Arockianathan et al. 2012 (©2012).

studies, the formulations containing gentamicin achieved complete healing before the control groups (rats treated with a gauze dipped with gentamicin). The biochemical parameters, such as the increase of collagen, DNA, total protein account, hexosamine and uronic acid, demonstrated that the experimental groups presented faster wound healing than the controls (Arockianathan et al. 2012b, Arockianathan et al. 2012a, Ahamed et al. 2015).

AgNPs can be formulated by eco-friendly procedures. Bhuvaneswari and collaborators prepared AgNPs using plant extracts, as the aqueous extract of *N. crenulata*, due to the great affinity of silver to sulphur or phosphorus-containing biomolecules of the plant cells. The resulting AgNPs possessed various phytochemical constituents and were included in an ointment base for topical application in excisional wounds created on Wistar rats. The ointment presented astringent and antimicrobial properties, which enhanced wound contraction and the epithelialisation rate, leading to complete wound healing in 15 days (faster than the standard formulation of betadine) (Bhuvaneswari *et al.* 2014).

AgNPs using either chondroitin sulphate or acharan sulphate had also been produced with a green synthetic route. Both composites showed bactericidal activity *in vitro* against some of the bac teria that usually infect wounds (*S. aureus*, *S. pyogenes*, *P. aeruginosa*, *E. coli*

*Salmonella typhimurium*, *Klebsiella oxytoca*, *K. aerogenes* and *Enterobacter cloacae*). Moreover, in an incisional wound model in mice, these AgNPs showed comparable results with Silmazin® (1% SSD cream) in terms of the wound healing rate and histological findings, achieving normal skin morphology by day 21 in all cases (Im *et al.* 2013).

Nanofibers are another encouraging wound dressing for AgNP incorporation. In that regard, Jin and colleagues developed an electrospun composite of PLLCL containing AgNPs. The scaffolds loaded with 0.25 wt % of AgNPs were not cytotoxic for human skin fibroblasts, and remarkably, maintained the bactericidal activity against *S. aureus* and *Salmonella enterica* after incorporation in the wound dressing (Jin *et al.* 2012).

Li *et al.* published the development of two different wound dressing, the first one consisted of AgNPs-loaded PVA and chitosan-oligosaccharides electrospun NFs (PVA/COS-AgNPs), whereas the second one consisted of $AgNO_3$-loaded in the same type of NFs irradiated with ultraviolet light to form the AgNPs (PVA/COS/$AgNO_3$). Both NFs demonstrated to be effective in a full-thickness wound model in Sprague-Dawley rats; however, the histological examination showed a slightly superior wound healing in the early stages for the PVA/COS-AgNP formulation. Moreover, that scaffold had slightly superior antibacterial activity against *S. aureus* and *E. coli,* and *in vitro* biocompatibility in human skin fibroblasts (Li *et al.* 2013).

Wound dressings can also be prepared using modified clay minerals. Nanohybrids composed of AgNPs and a nanoscale silicate platelet produced from montmorillonite clay presented lower cytotoxicity than commercial SSD in a primary human foreskin fibroblast cell line (Hs68), and no genotoxicity in Chinese hamster ovary cells at concentrations lower than 70 ppm. The effectiveness of those nanohybrids was tested in *S. aureus* infected acute burn wounds and full-thickness wounds created on Balb/C mice. By day 7, the nanohybrid treated groups (both burns and excision wounds) showed similar healing rates and VEGF and TGF-β1 concentrations, than lesions treated with commercially available products (Aquacel®, a silver containing-wound dressing, and a SSD commercial product). Furthermore, it should be noted that those burns treated with nanohybrids showed a cleaner surface, an improved appearance and less scar formation (Chu *et al.* 2012).

## 5. Conclusions

Chronic wounds represent a major health problem from an epidemiologic, economic and social point of view. Current therapies devoted to promote wound healing are often insufficient, showing the great and increasing demand for the improvement of chronic wound management. External administration of therapeutic agents, such as GFs and antimicrobials, to stimulate wound healing and tackle wound infection has shown to be successful enhancing skin regeneration. Nevertheless, stability problems of these agents associated to the presence of proteases in the wound bed needs to be addressed. For that purpose, development of novel DDSs that allow drug protection, controlled release to prolong the drug effect on the wound site, reduction or eradication of the wound bacterial load and improvement of re-epithelisation is a very encouraging strategy to ultimately achieve wound closure.

Different approaches involving the use of polymeric, lipid or silver NPs, nanofibrous structures, nanosheets and nanohybrids have been developed and are promising tools to obtain more cost-effective therapies to improve the wound healing therapy, with the final aim of improving patient quality of life. However, more efforts should be taken as only few of them have reached the use in humans.

## 6. Declaration of interest

The authors report no conflicts of interest. The authors alone are responsible for the content and writing of the paper.

## 7. References

Ahamed, M.I.N., Sankar, S., Kashif, P.M., Basha, S.K.H., Sastry, T.P. 2015. Evaluation of Biomaterial Containing Regenerated Cellulose and Chitosan Incorporated with Silver Nanoparticles. Int J Biol Macromol. 72, 680-686.

Akita, S., Akino, K., Imaizumi, T., Hirano, A. 2008. Basic Fibroblast Growth Factor Accelerates and Improves Second-Degree Burn Wound Healing. Wound Repair Regen. 16(5), 635-641.

Allen, T.M., Cullis, P.R. 2013. Liposomal Drug Delivery Systems: From Concept to Clinical Applications. Adv Drug Deliv Rev. 65(1), 36-48.

Almeida, A.J., Souto, E. 2007. Solid Lipid Nanoparticles as a Drug Delivery System for Peptides and Proteins. Adv Drug Deliv Rev. 59(6), 478-490.

Anderson, R.C., Rehders, M., Yu, P.L. 2008. Antimicrobial Fragments of the Pro-Region of Cathelicidins and Other Immune Peptides. Biotechnol Lett. 30(5), 813-818.

Arockianathan, P.M., Sekar, S., Kumaran, B., Sastry, T.P. 2012a. Preparation, Characterization and Evaluation of Biocomposite Films Containing Chitosan and Sago Starch Impregnated with Silver Nanoparticles. Int J Biol Macromol. 50(4), 939-946.

Arockianathan, P.M., Sekar, S., Sankar, S., Kumaran, B., Sastry, T.P. 2012b. Evaluation of Biocomposite Films Containing Alginate and Sago Starch Impregnated with Silver Nano Particles. Carbohydr Polym. 90(1), 717-724.

Atiyeh, B.S., Costagliola, M., Hayek, S.N., Dibo, S.A. 2007. Effect of Silver on Burn Wound Infection Control and Healing: Review of the Literature. Burns. 33(2), 139-148.

Baldwin, S.P., Mark Saltzman, W. 1998. Materials for Protein Delivery in Tissue Engineering. Adv Drug Deliv Rev. 33(1–2), 71-86.

Bao, P., Kodra, A., Tomic-Canic, M., Golinko, M.S., Ehrlich, H.P., Brem, H. 2009. The Role of Vascular Endothelial Growth Factor in Wound Healing. J Surg Res. 153(2), 347-358.

Barrientos, S., Brem, H., Stojadinovic, O., Tomic-Canic, M. 2014. Clinical Application of Growth Factors and Cytokines in Wound Healing. Wound Repair Regen. 22(5), 569-578.

Barrientos, S., Stojadinovic, O., Golinko, M.S., Brem, H., Tomic Canic, M. 2008. Growth Factors and Cytokines in Wound Healing. Wound Repair Regen. 16(5), 585-601.

Bhuvaneswari, T., Thiyagarajan, M., Geetha, N., Venkatachalam, P. 2014. Bioactive Compound Loaded Stable Silver Nanoparticle Synthesis from Microwave Irradiated Aqueous Extracellular Leaf Extracts of Naringi Crenulata and its Wound Healing Activity in Experimental Rat Model. Acta Trop. 135, 55-61.

Black, J., Baharestani, M., Cuddigan, J., Dorner, B., Edsberg, L., Langemo, D., Posthauer, M.E., Ratliff, C., Taler, G., National Pressure Ulcer Advisory Panel 2007. National Pressure Ulcer Advisory Panel's Updated Pressure Ulcer Staging System. Dermatol Nurs. 19(4), 343-350.

Bodnar, R.J. 2013. Epidermal Growth Factor and Epidermal Growth Factor Receptor: The Yin and Yang in the Treatment of Cutaneous Wounds and Cancer. Adv Wound Care (New Rochelle). 2(1), 24-29.

Brown, G.L., Curtsinger, L.J., White, M., Mitchell, R.O., Pietsch, J., Nordquist, R., Fraunhofer, A., Schultz, G.S. 1988. Acceleartion of Tensile Strenght of Incisions Treated with EGF and TGF-Beta. Ann Surg. 208(6), 788-794.

Chaudhury, K., Kumar, V., Kandasamy, J., RoyChoudhury, S. 2014. Regenerative Nanomedicine: Current Perspectives and Future Directions. Int J Nanomedicine. 9, 4153-4167.

Chen, D.W., Liao, J.Y., Liu, S.J., Chan, E.C. 2012a. Novel Biodegradable Sandwich-Structured Naofibrous Drug-Eluting Membranes for Repair of Infected Wounds: an *in Vitro* and *in Vivo* study. Int J Nanomedicine. 7, 763-771.

Chen, D.W., Hsu, Y., Liao, J., Liu, S., Chen, J., Ueng, S.W. 2012b. Sustainable Release of Vancomycin, Gentamicin and Lidocaine from Novel Electrospun Sandwich-Structured PLGA/Collagen Nanofibrous Membranes. Int J Pharm. 430(1–2), 335-341.

Chereddy, K.K., Her, C., Comune, M., Moia, C., Lopes, A., Porporato, P.E., Vanacker, J., Lam, M.C., Steinstraesser, L., Sonveaux, P., Zhu, H., Ferreira, L.S., Vandermeulen, G., Préat, V. 2014. PLGA Nanoparticles Loaded with Host Defense Peptide LL37 Promote Wound Healing. J Control Release. 194, 138-147.

Choi, J.S., Choi, S.H., Yoo, H.S. 2011. Coaxial Electrospun Nanofibers for Treatment of Diabetic Ulcers with Binary Release of Multiple Growth Factors. J Mater Chem. 21, 5258-5267.

Choi, J.S., Leong, K.W., Yoo, H.S. 2008. In Vivo Wound Healing of Diabetic Ulcers using Electrospun Nanofibers Immobilized with Human Epidermal Growth Factor (EGF). Biomaterials. 29(5), 587-596.

Chopra, I., Roberts, M. 2001. Tetracycline Antibiotics: Mode of Action, Applications, Molecular Biology, and Epidemiology of Bacterial Resistance. Microbiol Mol Biol Rev. 65(2), 232-260.

Chu, C.Y., Peng, F.C., Chiu, Y.F., Lee, H.C., Chen, C.W., Wei, J.C., Lin, J.J. 2012. Nanohybrids of Silver Particles Immobilized on Silicate Platelet for Infected Wound Healing. PLoS One. 7(6), e38360.

Chu, Y., Yu, D., Wang, P., Xu, J., Li, D., Ding, M. 2010. Nanotechnology Promotes the Full-Thickness Diabetic Wound Healing Effect of Recombinant Human Epidermal Growth Factor in Diabetic Rats. Wound Repair Regen. 18(5), 499-505.

Cortivo, R., Vindigni, V., Iacobellis, L., Abatangelo, G., Pinton, P., Zavan, B. 2010. Nanoscale Particle Therapies for Wounds and Ulcers. Nanomedicine. 5(4), 641-656.

De Cicco, F., Porta, A., Sansone, F., Aquino, R.P., Del Gaudio, P. 2014. Nanospray Technology for an in Situ Gelling Nanoparticulate Powder as a Wound Dressing. Int J Pharm. 473(1–2), 30-37.

Değim, Z. 2008. Use of Microparticulate Systems to Accelerate Skin Wound Healing. J Drug Target. 16(6), 437-448.

Doi, Y. & Chambers, H.F. 2015, Penicillins and β-Lactamase Inhibitors in: J.E. Bennett, R. Dolin & M.J. Blaser (Eds.), Mandell, Douglas, and Bennett's Principles and Practice of Infectious Diseases. 8th ed, Elsevier Saunders, Canada, pp. 263-277.

Dunn, K., Edwards-Jones, V. 2004. The Role of Acticoat™ with Nanocrystalline Silver in the Management of Burns. Burns. 30, Supplement 1(0), S1-S9.

Eldor, R., Raz, I., Ben Yehuda, A., Boulton, A.J. 2004. New and Experimental Approaches to Treatment of Diabetic Foot Ulcers: A Comprehensive Review of Emerging Treatment Strategies. Diabet Med. 21, 1161-1173.

Emmerson, E., Campbell, L., Davies, F.C., Ross, N.L., Ashcroft, G.S., Krust, A., Chambon, P., Hardman, M.J. 2012. Insulin-Like Growth Factor-1 Promotes Wound Healing in Estrogen-Deprived Mice: New Insights into Cutaneous IGF-1R/ERalpha Cross Talk. J Invest Dermatol. 132(12), 2838-2848.

Fan, Y., Zhang, Q. 2013. Development of Liposomal Formulations: From Concept to Clinical Investigations. Asian Journal of Pharmaceutical Sciences. 8(2), 81-87.

Farage, M.A., Miller, K.W., Berardesca, E., Maibach, H.I. 2009. Clinical implications of aging Skin: cutaneous Disorders in The elderly. Am J Clin Dermatol. 10(2), 73-86.

Feng, Q.L., Wu, J., Chen, G.Q., Cui, F.Z., Kim, T.N., Kim, J.O. 2000. A mechanistic study of The antibacterial effect Of silver ions on Escherichia Coli and Staphylococcus Aureus. J Biomed Mater Res. 52(4), 662-668.

Gainza, G., Aguirre, J.J., Pedraz, J.L., Hernández, R.M., Igartua, M. 2013. rhEGF-Loaded

PLGA-Alginate Microspheres Enhance the Healing of Full-Thickness Excisional Wounds in Diabetised Wistar Rats. Eur J Pharm Sci. 50(3–4), 243-252.

Gainza, G., Bonafonte, D.C., Moreno, B., Aguirre, J.J., Gutierrez, F.B., Villullas, S., Pedraz, J.L., Igartua, M., Hernandez, R.M. 2015. The Topical Administration of rhEGF-Loaded Nanostructured Lipid Carriers (rhEGF-NLC) Improves Healing in a Porcine Full-Thickness Excisional Wound Model. J Control Release. 197(0), 41-47.

Gainza, G., Pastor, M., Aguirre, J.J., Villullas, S., Pedraz, J.L., Hernandez, R.M., Igartua, M. 2014. A Novel Strategy for the Treatment of Chronic Wounds Based on the Topical Administration of rhEGF-Loaded Lipid Nanoparticles: In Vitro Bioactivity and in Vivo Effectiveness in Healing-Impaired Db/Db Mice. J Control Release. 185(0), 51-61.

Ghosh Auddy, R., Abdullah, M.F., Das, S., Roy, P., Datta, S., Mukherjee, A. 2013. New Guar Biopolymer Silver Nanocomposites for Wound Healing Applications. Biomed Res Int. 2013, 912458.

Gil, E.S., Panilaitis, B., Bellas, E., Kaplan, D.L. 2013. Functionalized Silk Biomaterials for Wound Healing. Adv Healthc Mater. 2(1), 206-217.

Greenhalgh, K., Turos, E. 2009. In Vivo Studies of Polyacrylate Nanoparticle Emulsions for Topical and Systemic Applications. Nanomedicine. 5(1), 46-54.

Gunasekaran, T., Nigusse, T., Dhanaraju, M. 2011. Silver Nanoparticles as Real Topical Bullets for Wound Healing. J Am Coll Clin Wound Spec. 3(4), 82-96.

Hancock, R.E. 2001. Cationic Peptides: Effectors in Innate Immunity and Novel Antimicrobials. Lancet Infect Dis. 1(3), 156-164.

Hebeish, A., El-Rafie, M.H., EL-Sheikh, M.A., Seleem, A.A., El-Naggar, M.E. 2014. Antimicrobial Wound Dressing and Anti-Inflammatory Efficacy of Silver Nanoparticles. Int J Biol Macromol. 65, 509-515.

Hernandez, R. 2006. The use of Systemic Antibiotics in the Treatment of Chronic wounds. Dermatol Ther. 19, 326-337.

Hong, J.P., Kim, Y.W., Lee, S.K., Kim, S.H., Min, K.H. 2008. The Effect of Continuous Release of Recombinant Human Epidermal Growth Factor (Rh-EGF) in Chitosan Film on Full Thickness Excisional Porcine Wounds. Ann Plast Surg. 61(4), 457-462.

Im, A.R., Kim, J.Y., Kim, H.S., Cho, S., Park, Y., Kim, Y.S. 2013. Wound Healing and Antibacterial Activities of Chondroitin Sulfate- and Acharan Sulfate-Reduced Silver Nanoparticles. Nanotechnology. 24(39), 395102.

Jin, G., Prabhakaran, M.P., Nadappuram, B.P., Singh, G., Kai, D., Ramakrishna, S. 2012. Electrospun Poly(L-Lactic Acid)-Co-Poly(Varepsilon-Caprolactone) Nanofibres Containing Silver Nanoparticles for Skin-Tissue Engineering. J Biomater Sci Polym Ed.

Jin, G., Prabhakaran, M.P., Ramakrishna, S. 2014. Photosensitive and Biomimetic Core-Shell Nanofibrous Scaffolds as Wound Dressing. Photochem Photobiol. 90(3), 673-681.

Kai-Larsen, Y., Agerberth, B. 2008. The Role of the Multifunctional Peptide LL-37 in Host Defense. Front Biosci. 13, 3760-3767.

Kataria, K., Gupta, A., Rath, G., Mathur, R.B., Dhakate, S.R. 2014. In Vivo Wound Healing Performance of Drug Loaded Electrospun Composite Nanofibers Transdermal Patch. Int J Pharm. 469(1), 102-110.

Klasen, H.J. 2000. A Historical Review of the use of Silver in the Treatment of Burns. II. Renewed Interest for Silver. Burns. 26(2), 131-138.

Koczulla, R., von Degenfeld, G., Kupatt, C., Krötz, F., Zahler, S., Gloe, T., Issbrücker, K., Unterberger, P., Zaiou, M., Lebherz, C., Karl, A., Raake, P., Pfosser, A., Boekstegers, P., Welsch, U., Hiemstra, P.S., Vogelmeier, C., Gallo, R.L., Clauss, M., Bals, R. 2003. An Angiogenic Role for the Human Peptide Antibiotic LL-37/hCAP-18. J Clin Invest. 111(11), 1665-1672.

Kubinová, S., Syková, E. 2010. Nanotechnologies in Regenerative Medicine. Minim Invasive Ther Allied Technol. 19(3), 144-156.

Lai, H., Kuan, C., Wu, H., Tsai, J., Chen, T., Hsieh, D., Wang, T. 2014. Tailored Design of Electrospun Composite Nanofibers with Staged Release of Multiple Angiogenic Growth Factors for Chronic Wound Healing. Acta Biomater. 10(10), 4156-4166.

Li, C., Fu, R., Yu, C., Li, Z., Guan, H., Hu, D., Zhao, D., Lu, L. 2013. Silver Nanoparticle/Chitosan Oligosaccharide/Poly(Vinyl Alcohol) Nanofibers as Wound Dressings: A Preclinical Study. Int J Nanomedicine. 8, 4131-4145.

Li, H., Fu, X., Zhang, L., Huang, Q., Wu, Z., Sun, T. 2008. Research of PDGF-BB Gel on the Wound Healing of Diabetic Rats and its Pharmacodynamics. J Surg Res. 145(1), 41-48.

Lipsky, B.A., Hoey, C. 2009. Topical Antimicrobial Therapy for Treating Chronic Wounds. Clin Infect Dis. 49, 1541-1549.

Losi, P., Briganti, E., Errico, C., Lisella, A., Sanguinetti, E., Chiellini, F., Soldani, G. 2013. Fibrin-Based Scaffold Incorporating VEGF- and bFGF-Loaded Nanoparticles Stimulates Wound Healing in Diabetic Mice. Acta Biomater. 9(8), 7814-7821.

Lu, S., Gao, W., Gu, H.Y. 2008. Construction, Application and Biosafety of Silver Nanocrystalline Chitosan Wound Dressing. Burns. 34(5), 623-628.

Makadia, H.K., Siegel, S.J. 2011. Poly Lactic-Co-Glycolic Acid (PLGA) as Biodegradable Controlled Drug Delivery Carrier. Polymers (Basel). 3(3), 1377-1397.

Markova, A., Mostow, E.N. 2012. US Skin Disease Assessment: Ulcer and Wound Care. Dermatol Clin. 30, 107-111.

Martin, P. 1997. Wound Healing--Aiming for Perfect Skin Regeneration. Science. 276(5309), 75-81.

Mast, B.A., Schultz, G.S. 1996. Interactions of Cytokines, Growth Factors, and Proteases in Acute and Chronic Wounds. Wound Repair Regen. 4(4), 411-420.

McGee, G.S., Davidson, J.M., Buckley, A., Sommer, A., Woodward, S.C., Aquino, A.M., Barbour, R., Demetriou, A.A. 1988. Recombinant Basic Fibroblast Growth Factor Accelerates Wound Healing. J Surg Res. 45(1), 145-153.

Menke, N.B., Ward, K.R., Witten, T.M., Bonchev, D.G., Diegelmann, R.F. 2007. Impaired Wound Healing. Clin Dermatol. 25(1), 19-25.

Miao, J., Pangule, R.C., Paskaleva, E.E., Hwang, E.E., Kane, R.S., Linhardt, R.J., Dordick, J.S. 2011. Lysostaphin-Functionalized Cellulose Fibers with Antistaphylococcal Activity for Wound Healing Applications. Biomaterials. 32(36), 9557-9567.

Müller, R.H., Mäder, K., Gohla, S. 2000. Solid Lipid Nanoparticles (SLN) for Controlled Drug Delivery – a Review of the State of the Art. Eur J Pharm Biopharm. 50(1), 161-177.

Pardeike, J., Schwabe, K., Müller, R.H. 2010. Influence of Nanostructured Lipid Carriers (NLC) on the Physical Properties of the Cutanova Nanorepair Q10 Cream and the in Vivo Skin Hydration Effect. Int J Pharm. 396(1–2), 166-173.

Pierre, E.J., Perez-polo, J.R., Mitchell, A.T., Matin, S., Foyt, H.L., Hernfon, D.n. 1997. Insuline-Like Growth Factor-I Liposomal Gene Transfer and Systemic Growth Hormone Stimulate Wound healing. J Burn Care Rehabil. 18(4), 287-291.

Provenzano, P.P., Alejandro-Osorio, A.L., Grorud, K.W., Martinez, D.A., Vailas, A.C., Grindeland, R.E., Vanderby, R.J. 2007. Systemic Administration of IGF-I Enhances Healing in Collagenous Extracellular Matrices: Evaluation of Loaded and Unloaded Ligaments. BMC Physiol. 7, 2.

Rai, M., Yadav, A., Gade, A. 2009. Silver Nanoparticles as a New Generation of Antimicrobials. Biotechnol Adv. 27(1), 76-83.

Robson, M.C. 1997. The Role of Growth Factors in the Healing of Chronic Wounds. Wound Repair and Regen. 5(1), 12-7.

Saito, A., Miyazaki, H., Fujie, T., Ohtsubo, S., Kinoshita, M., Saitoh, D., Takeoka, S. 2012. Therapeutic Efficacy of an Antibiotic-Loaded Nanosheet in a Murine Burn-Wound Infection Model. Acta Biomater. 8(8), 2932-2940.

Schneider, A., Wang, X.Y., Kaplan, D.L., Garlick, J.A., Egles, C. 2009. Biofunctionalized Electrospun Silk Mats as a Topical Bioactive Dressing for Accelerated Wound Healing. Acta Biomater. 5(7), 2570-2578.

Sharma, P.C., Jain, A., Jain, S., Pahwa, R., Yar, M.S. 2010. Ciprofloxacin: Review on Developments in Synthetic, Analytical, and Medicinal Aspects. J Enzyme Inhib Med Chem. 25(4), 577-589.

Singer, A.J., Clark, R.A. 1999. Cutaneous Wound Healing. N Engl J Med. 341(10), 738-746.

Sirc, J., Kubinova, S., Hobzova, R., Stranska, D., Kozlik, P., Bosakova, Z., Marekova, D., Holan, V., Sykova, E., Michalek, J. 2012. Controlled Gentamicin Release from Multi-Layered Electrospun Nanofibrous Structures of various Thicknesses. Int J Nanomedicine. 7, 5315-5325.

Thakur, R.A., Florek, C.A., Kohn, J., Michniak, B.B. 2008. Electrospun Nanofibrous Polymeric Scaffold with Targeted Drug Release

Profiles for Potential Application as Wound Dressing. Int J Pharm. 364(1), 87-93.

Tiaka, E.K., Papanas, N., Manolakis, A.C., Georgiadis, G.S. 2012. Epidermal Growth Factor in the Treatment of Diabetic Foot Ulcers: An Update. Perspect Vasc Surg Endovasc Ther. 24, 37-44.

Trengove, N.J., Stacey, M.C., Macauley, S., Bennett, N., Gibson, J., Burslem, F., Murphy, G., Schultz, G. 1999. Analysis of the Acute and Chronic Wound Environments: The Role of Proteases and their Inhibitors. Wound Repair and Regen. 7(6), 442-452.

Turos, E., Reddy, G.S.K., Greenhalgh, K., Ramaraju, P., Abeylath, S.C., Jang, S., Dickey, S., Lim, D.V. 2007. Penicillin-Bound Polyacrylate Nanoparticles: Restoring the Activity of B-Lactam Antibiotics Against MRSA. Bioorg Med Chem Lett. 17(12), 3468-3472.

Ulubayram, K., Cakar, A.N., Korkusuz, P., Ertan, C., Hasirci, N. 2001. EGF Containing Gelatin-Based Wound Dressings. Biomaterials. 22(11), 1345-1356.

Vandamme, D., Landuyt, B., Luyten, W., Schoofs, L. 2012. A Comprehensive Summary of LL-37, the Factotum Human Cathelicidin Peptide. Cell Immunol. 280(1), 22-35.

Werner, S., Grose, R. 2003. Regulation of Wound Healing by Growth Factors and Cytokines. Physiol Rev. 83(3), 835-870.

Wu, J., Zheng, Y., Wen, X., Lin, Q., Chen, X., Wu, Z. 2014a. Silver Nanoparticle/Bacterial Cellulose Gel Membranes for Antibacterial Wound Dressing: Investigation in Vitro and in Vivo. Biomed Mater. 9(3), 035005.

Wu, J., Zheng, Y., Song, W., Luan, J., Wen, X., Wu, Z., Chen, X., Wang, Q., Guo, S. 2014b. In Situ Synthesis of Silver-Nanoparticles/Bacterial Cellulose Composites for Slow-Released Antimicrobial Wound Dressing. Carbohydr Polym. 102, 762-771.

Xie, Z., Paras, C.B., Weng, H., Punnakitikashem, P., Su, L., Vu, K., Tang, L., Yang, J., Nguyen, K.T. 2013. Dual Growth Factor Releasing Multi-Functional Nanofibers for Wound Healing. Acta Biomater. 9(12), 9351-9359.

Xu, X., Zhong, W., Zhou, S., Trajtman, A., Alfa, M. 2010. Electrospun PEG–PLA Nanofibrous Membrane for Sustained Release of Hydrophilic Antibiotics. J Appl Polym Sci. 118, 588-595.

Yang, Y., Xia, T., Zhi, W., Wei, L., Weng, J., Zhang, C., Li, X. 2011. Promotion of Skin Regeneration in Diabetic Rats by Electrospun Core-Sheath Fibers Loaded with Basic Fibroblast Growth Factor. Biomaterials. 32(18), 4243-4254.

Ye, M., Kim, S., Park, K. 2010. Issues in Long-Term Protein Delivery using Biodegradable Microparticles. J Control Release. 146(2), 241-260.